NOTICE

The quality of this microform is heavily dependent upon the quality of the original thesis submitted for microfilming. Every effort has been made to ensure the highest quality of reproduction possible.

If pages are missing, contact the university which granted the degree.

Some pages may have indistinct print especially if the original pages were typed with a poor typewriter ribbon or if the university sent us an inferior photocopy.

Reproduction in full or in part of this microform is governed by the Canadian Copyright Act, R.S.C. 1970, c. C-30, and subsequent amendments:

AVIS

La qualité de cette microforme dépend grandement de la qualité de la thèse soumise au microfilmage. Nous avons tout fait pour assurer une qualité supérieure de reproduction.

S'il manque des pages, veuillez communiquer avec l'université qui a conféré le grade.

La qualité d'impression de certaines pages peut laisser à désirer, surtout si les pages originales ont été dactylographiées à l'aide d'un ruban usé ou si l'université nous a fait parvenir une photocopie de qualité inférieure.

La reproduction, même partielle, de cette microforme est soumise à la Loi canadienne sur le droit d'auteur, SRC 1970, c. C-30, et ses amendements subséquents.

ISBN 0-315-56328-1

PHYSICAL STUDIES OF DIPHYTANYLGLYCEROL PHOSPHOLIPIDS

by
Laura Stewart

Department of Biochemistry,
University of Ottawa;
Division of Biological Sciences,
National Research Council of Canada

Ottawa, Canada

UNIVERSITÉ D'OTTAWA
UNIVERSITY OF OTTAWA

Acknowledgements

I would like to acknowledge the support, encouragement and advice of my supervisors, Dr. Ian C.P. Smith and Dr. M. Kates.

I would also like to acknowledge the assistance of the following people:

Dr. Clem Kazakoff	CI/MS and FAB/MS
H. Seguin	Elemental analysis
Dr. R. Bittman	Osmometry
Dr. Paul Yang, Dr. H.H. Mantsch	FTIR
E. Szabo	Drafting
Harry Turner	Photography
Raj Capoor	^{13}C and ^{1}H NMR
Dr. I.H. Ekiel	^{2}H NMR
Paulette Fejer and Ian Fachnie	Technical assistance

The financial assistance of the Natural Science and Engineering Research Council of Canada was greatly appreciated.

Abstract

The structures of the diphytanylglycerol phospholipids and glycolipids of Halobacterium cutirubrum have been well characterized by synthetic and degradative methods; however, little information exists on the molecular order and dynamics of this class of lipids within model membrane systems.

Physical techniques such as ^{2}H and ^{31}P NMR, FTIR, potentiometric titration and osmometry have been applied to the study of synthetically and biosynthetically deuterated diphytanylglycerol lipids as well as chain and headgroup analogues, including dihexadecylglycerol phospholipids and diphytanylglycerol derivatives of PA, deoxy PG, phosphatidyl-propanol and deoxy and methylated PGP

^{2}H NMR segmental quadrupolar spittings and spin-lattice relaxation measurements provided quantitative information on the phytanyl chain order and dynamics. Comparison of the data from phytanyl lipids with those derived from n-alkyl lipids and data previously reported for n-acyl lipids indicated that the presence of the branched methyl groups has a marked effect on the physical properties of the hydrocarbon chains: the lipid chains are much more disordered than the conventional n-acyl lipids (as evidenced by narrower quadrupolar splittings, < 25 kHz) although the rates of motions are much slower (T_1 values of 5.2 to 11.1 ms at 17°C). In effect, the presence of the methyl groups produces a bilayer which is remarkably similar to that of n-acyl phospholipid/

cholesterol mixtures with respect to segmental dynamics; however, the methyl groups have a disordering effect, in contrast to the well known ordering effect of cholesterol.

^{2}H and ^{31}P NMR studies with oriented bilayers prepared from both total polar lipids and purified PGP indicated that the axis of motional averaging for the PGP headgroups and phytanyl chains are both parallel to the bilayer normal. In addition, the bilayer normals of both PGP and GLS appear to be identical as determined by this technique despite the large difference in the size of the headgroups. These results are consistent with previous studies of n-acyl phospholipids and glycosyl dialkylglycerol lipids, implying that the molecular motional axes for all lipid types are the same. This may arise as a consequence of rapid overall motion which masks subtle differences in the character of the local motions.

Osmometric studies of aqueous dispersions of the total polar lipids and lipid fractions from H. cutirubrum, as well as DPPC and DPPC/cholesterol mixtures, indicated that the diphytanylglycerol lipid bilayers are considerably less permeable to nonelectrolytes such as urea than bilayers comprised of n-acyl phospholipids. For example, the permeability value derived for bilayers of PGP, the predominant membrane phospholipid [$(61.0 \pm 2.4) \times 10^{-3}$ sec^{-1})], is much lower than that of DPPC bilayers [$(94.8 \pm 6.2) \times 10^{-3}$ sec^{-1})] but is comparable to that derived from DPPC bilayers containing relatively high concentrations of cholesterol. Thus, diphytanylglycerol lipid bilayers are less "fluid" in the conventional sense than straight-chain lipids.

Comparison of the pK values for PGP and the deoxy analogue in sonicated, aqueous dispersions indicated a significant difference in the highest pK (pK_2). In both compounds, the value of pK_1 (which corresponds to two equivalents,) is 2.4 - 3.6. The presence of the free headgroup hydroxyl leads to a marked increase in the value of pK_2 (>11) in comparison with the deoxy analogue (8.5 - 8.8) or with previously reported values for PA (8.6) or headgroup analogues such as β-phosphoglycerol (6.6). The abnormally high pK value could be due to the presence of intra- and/or intermolecular hydrogen bonding involving the P-OH group which would stabilize it in the protonated form. This is consistent with FTIR data indicating the presence of hydrogen-bonding in PGP involving the headgroup P-OH and C-OH groups.

^{31}P NMR studies of the effect of such factors as temperature pH, salt forms and the presence of other polar lipids on the chemical shift and CSA values of PGP have shown that the headgroup structure is remarkably stable to environmental changes. This, too, is consistent with the formation of intra- and/or intermolecular hydrogen bonding involving the PGP headgroup as suggested by potentiometric titration and FTIR studies.

Table of Contents

PART I

Isolation, Purification and Characterization of Natural Lipid Samples

PART II

Synthesis

PART III

Physical Studies

List of Tables

List of Figures

Abbreviations

A_i	initial absorbance value
ATPase	ATP dephosphorylase
BR	bacteriorhodpsin
CI/MS	chemical ionization mass spectrometry
CS	chemical shift (ppm)
CSA	chemical shift anisotropy
dPG	deoxy PG; sn-2,3-diphytanylglycerol-1-phosphoryl-1',3'-propane-diol
dPGP	deoxy PGP; sn-2,3-diphytanylglycerol-1-phosphoryl-1',3'-propane-diol-3'-phosphate
DHPA	sn-1,2-dihexadecylglycerol-1-phosphate
DHPC	sn-1,2-dihexadecylglycerol-1-phosphatidcylcholine
DMPC	dimyristoyl phosphatidylcholine
DOPC	dialeoyl phosphatidylcholine
DPhPA	2,3-diphytanylglycerol-1-phosphate
DPPC	dipalmitoyl phosphatidylcholine
D_q	^2H quadrupole splitting, $\Delta\nu_Q$
EM	dection microscopy
ESR	electron spin resonance spectroscopy
GC	gas-liquid chromatography
GC/MS	gas-liquid chromatography/mass spectroscopy
GLS	glycolipid sulphate
FAB/MS	fast atom bombardment mass spectroscopy
FTIR	Fourier transform infrared spectroscopy
FW	formulas weight

Hz	hertz, sec^{-1}
IR	infrared spectroscopy
m.p.	melting point
NMR	nuclear magnetic resonance spectroscopy
PA	2,3-diphytanylglycerol-1-phosphate
PC	phosphatidylcholine
PE	phosphatidylethanolamine
PG	sn-2,3-diphytanylglycerol-1-phosphoryl-3'-glycerol
PGP	sn-2,3-diphytanylglycerol-1-phosphoryl-3'-glycerol-1'-phosphate
PGS	sn-2,3-diphytanylglycerol-1-phosphoryl-3'-glycerol-1'-sulphate
proPG	sn-2,3-diphytanylglycerol-1-phosphoryl-1'-propanol
$PGP(CH_3)_2$	dimethyl ester of PGP
$PGP(CH_3)_3$	trimethyl ester of PGP
$PGP(CH_3)_4$	tetramethyl ester of PGP
pK	refers to apparent pK, pK_a, unless otherwise noted
PM	purple membrane of H. cutirubrum
ppm	parts per million
RM	red membrane of H. cutirubrum
r.p.m.	revolutions per minute
5-SASL, 12-SASL	5-stearic acid spin label, 12-stearic acid spin label
S_{CD}	^2H NMR segmental order parameter
S_{mol}	^2H NMR molecular order parameter
$S_{\alpha,\beta}$	^1H NMR order parameter
S_{meas}	ESR order parameter

TEMED	tetramethyl ethylene diamine
TPS	triisopropylbenzenesulphonyl chloride
TMS	trimethylsilane
TPL	total polar lipids from *H. cutirubrum*

Dedication

To my family, without whose patience, support and encouragement the work for this thesis could never have been completed.

1. General Introduction

1.1 Background on Membrane Structure and Function

The bilayer structure is an integral part of biological membranes; therefore, a detailed knowledge of the structural and dynamic properties of the lipids which comprise these membranes is essential for an understanding of the properties of membranes as a whole. The chemical structures of the major membrane lipids of most organisms, including both prokaryotes (eubacteria and archaebacteria) and eukaryotes, have been determined previously (Ansell et al., 1973). The basic structure is constant: a hydrophobic region comprised primarily of alkyl or acyl chains of varying chain lengths, linked via ether or ester bonds to a glycerol backbone, and a hydrophilic region which is usually phosphorylated or glycosylated. Structural factors, including chain length, degree of unsaturation, and class of headgroup have been shown to affect bilayer characteristics such as the phase transition temperature and extent of lateral diffusion, and therefore such factors as the activity of membrane-bound proteins, permeability and elasticity (Boggs, 1984).

The lipids studied here are the major polar lipids of the archaebacterium Halobacterium cutirubrum (H. cutirubrum). The archaebacteria are so named because they grow under conditions that were thought to be prevalent on the primitive earth: extremes of pH, high salinity, high temperatures and anaerobic conditions (Fox et al., 1980). Thus, the extreme halophiles require saturated salt for growth, methanogens require anaerobic

conditions and thermoacidophiles grow at high temperatures and low pH (Woese and Wolfe, 1985). The membranes of the organisms in this kingdom are markedly different from those of eukaryotes or eubacteria with respect to hydrocarbon-glycerol linkages, the presence of branched methyl or cyclopentyl groups in the hydrocarbon chains and the nature of the headgroups. The structures and relative concentrations of the major polar membrane lipids of H. cutirubrum (TPL) have been determined and are shown in Figure 1 and Table 1 (Kates et al., 1978; Kushwaha et al., 1975). The predominant polar lipid species are diphytanyl analogues of phosphatidylglycerol phosphate (PGP; 58 mol%) and sulphated triglycosyl diphytanylglycerol (glycolipid sulphate, GLS; 17 mol%), together with smaller amounts of the diphytanyl analogues of phosphatidylglycerol (PG; 4 mol%), phosphatidylglycerol sulphate (PGS; 4 mol%) and trace amounts of other glycolipids. It is interesting to note that the sulphated glycolipid and PGS are found only in the purple membrane, whereas the red membrane contains a mixture of as yet unidentified non-sulphated glycolipids.

The membranes of H. cutirubrum are also unusual in that they consist of two functionally and morphologically different fractions: the red and purple membranes. The red membrane, which is red in colour due to the presence of high concentrations of C_{50} bacterioruberins, carries out most of the normal cell membrane functions including oxidative phosphorylation, transmembrane transport, etc. The purple membrane, which is

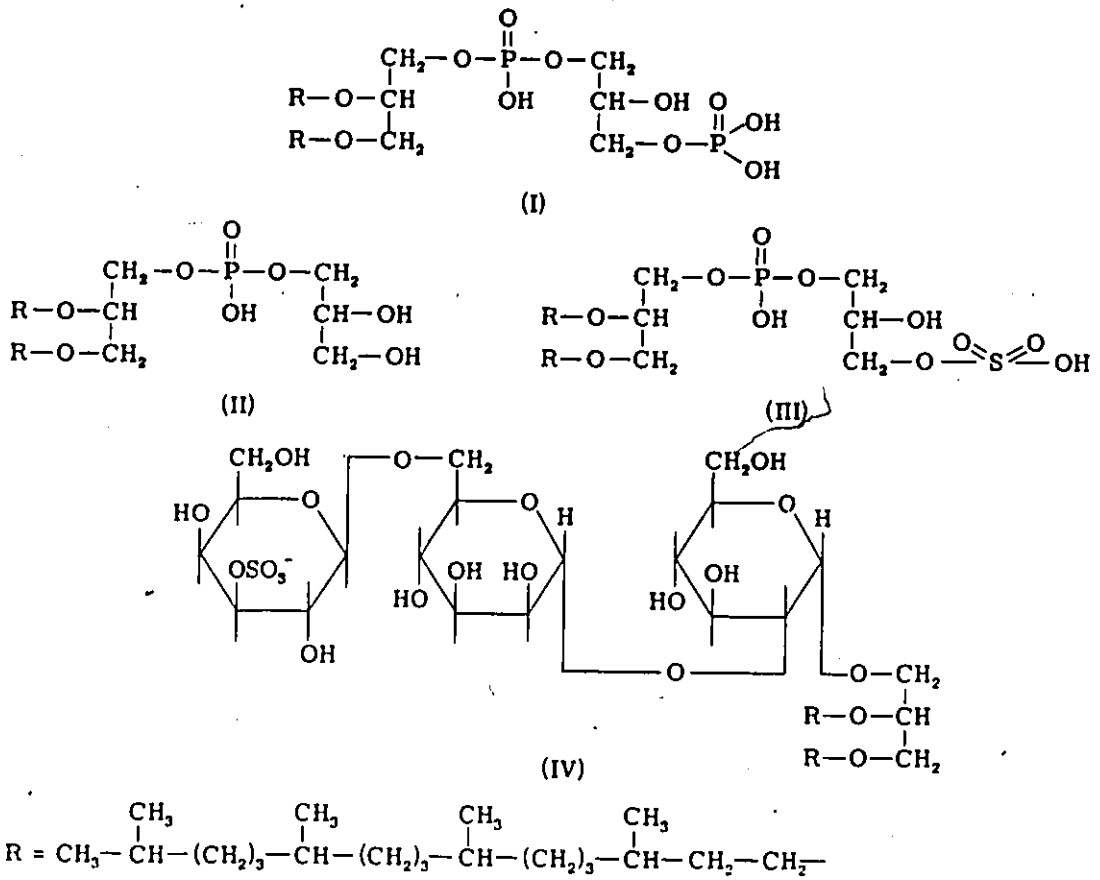

Figure 1

Structures of the major polar lipids in Halobacterium cutirubrum: I, phosphatidylglycerophosphate (PGP); II, phosphatidylglycerol (PG); III, phosphatidylglycerosulphate (PGS); and, IV, glycolipid sulphate (GLS). In all compounds, the alkyl group is 3R, 7R, 11R, 15-tetramethylhexadecyl (phytanyl).

(From Kates et al., 1982)

Table 1

Lipid composition of H. cutirubrum membrane fractions

Lipid component	Mol %					
	Whole cells[a]		PM[b]		RM[c]	
	total lipids	polar lipids	total lipids	polar lipids	total lipids	polar lipids
Neutral lipids						
squalenes	9		10		12	
Vit MK-8	1		2		2	
retinal	0.3		8		0	
C_{50} bacterio-ruberins	2		0		0.5	
Polar lipids						
PG	4	5	5	6	3	3
PGP	58	70	49	61	56	62
PGS	4	4	5	5	-	-
GLS	17	21	7 (22)	(28)	trace	-
TGD[d]	tr	tr	15		trace	-
GL(X_1 + X_2)[e]	-	-	-	-	31	34

a. From Kates, 1978, Kates et al., 1982.

b. From Kushwaha et al., 1975.

c. Discrepancies between whole cell, PM and RM probably arise from different growth conditions for cells grown under normal conditions and those grown specifically for the production of PM.

d. triglycosyldiether

e. unidentified glycolipids

found in patches within the red membrane, is purple in colour due to the presence of an integral membrane protein-retinal chromophore complex called bacteriorhodopsin (BR). BR, present as a single protein in a high concentration within the purple membrane (80% w/w), functions in light-induced trans-membrane proton translocation (Stoeckenius, 1976; Stoeckenius et al., 1979).

The question then arises as to whether these lipids possess unique characteristics arising from their unique structures, and to what characteristics the lipids impart to the cell membranes. The adaptive significance of some of the structural features are obvious. The presence of ether rather that ester bonds leads to greater chemical stability at extreme pH's. The highly charged headgroups may aid in selectivity of cation permeability and/or charge shielding, both of which are of particular importance for the halophilic bacteria. The function of the branched-chain phytanyl groups is presumably to ensure membrane structural integrity over a wide range of environmental conditions. Studies of membrane lipids of halotolerant and moderately halophilic bacteria have shown that growth in media of increasing salt concentration leads to increases in the percentage of branched chain (and cyclopropanoid) containing fatty acids (Kates, 1986a; Kanemasa et al., 1972). The mechanism by which the branched chain lipids stabilize the bilayer at high salt concentrations is unknown as there have been only a limited number of studies directed towards the characterization of the conformation and dynamics of these lipids.

A wide variety of techniques, including EM, neutron scattering, X-ray diffraction, ESR and NMR, have been used to study the properties of diphytanylglycerol lipids. These techniques have provided complementary and, in some cases, contradictory information as they differ with respect to the degree of resolution, the degree of perturbation of the system under study and the sensitivity of the technique with respect to the different frequencies of molecular motion.

Nuclear magnetic resonance spectroscopy (NMR) avoids many of the problems inherent in other physical techniques since information on both the order and dynamics can be obtained using compounds containing naturally abundant atomic species or by isotopic enrichment of otherwise chemically identical molecules. In the present study, deuterium, phosphorus and proton NMR have been used in conjuction with FTIR, osmometry and potentiometric titrations, to provide information on the characteristics of diphytanylglycerol lipids in aqueous dispersion and sonicated vesicles.

1.2 Physical Properties of Phytanyl, Phytanoyl and Phytyl Lipids

1.2.1 EM, Neutron Scattering and X-ray Diffraction

Electron microscopy of PM preparations have provided three dimensional structural information on the molecular organization of PM at a resolution of 7 Å (Henderson and Unwin, 1975). A high degree of resolution was made possible by the unusual molecular organization of the PM. The regular, periodic arrays formed by the BR proteins within the PM and the high protein density (see

Figure 2) allowed for the accumulation of electron diffraction patterns with minimum sample damage.

Analyses of PM preparations have shown a lipid to protein mole ratio within the range of 4-13 (Blaurock and Stoeckenius, 1971; Kushwaha et al., 1975; Blaurock, 1975, Stoeckenius et al., 1975) and the lipid molecules are thought to be located both within the center of the ring of 3 proteins and surrounding them.

The protein conformation and arrangement of the proteins in the PM as been confirmed by neutron scattering studies (King and Schoenborn, 1982). In addition, the location of the retinal chromophore (23° to the membrane plane and 19 Å from the cytoplasmic side) has been determined.

A limited number of high resolution X-ray crystallographic studies have been done on saturated n-acyl lipids such as PC (Hauser et al., 1981; Hitchcock et al., 1974; Pearson and Pascher, 1977). However, high resolution X-ray information on diphytanylglycerol lipids is unobtainable since branched chain lipids do not form crystals of sufficient quality for X-ray studies. In addition, no information on the molecular dynamics can be determined through this technique and the question remains as to the relevance of crystallographic results to the actual lipid conformation in aqueous dispersions.

In contrast, low resolution X-ray diffraction techniques have been used successfully in the study of both the PM and aqueous dispersion of total polar lipids. X-ray diffraction studies on the PM (Blaurock and Stoeckenius, 1971; Henderson and Unwin, 1975; Henderson, 1975) not only confirmed the protein

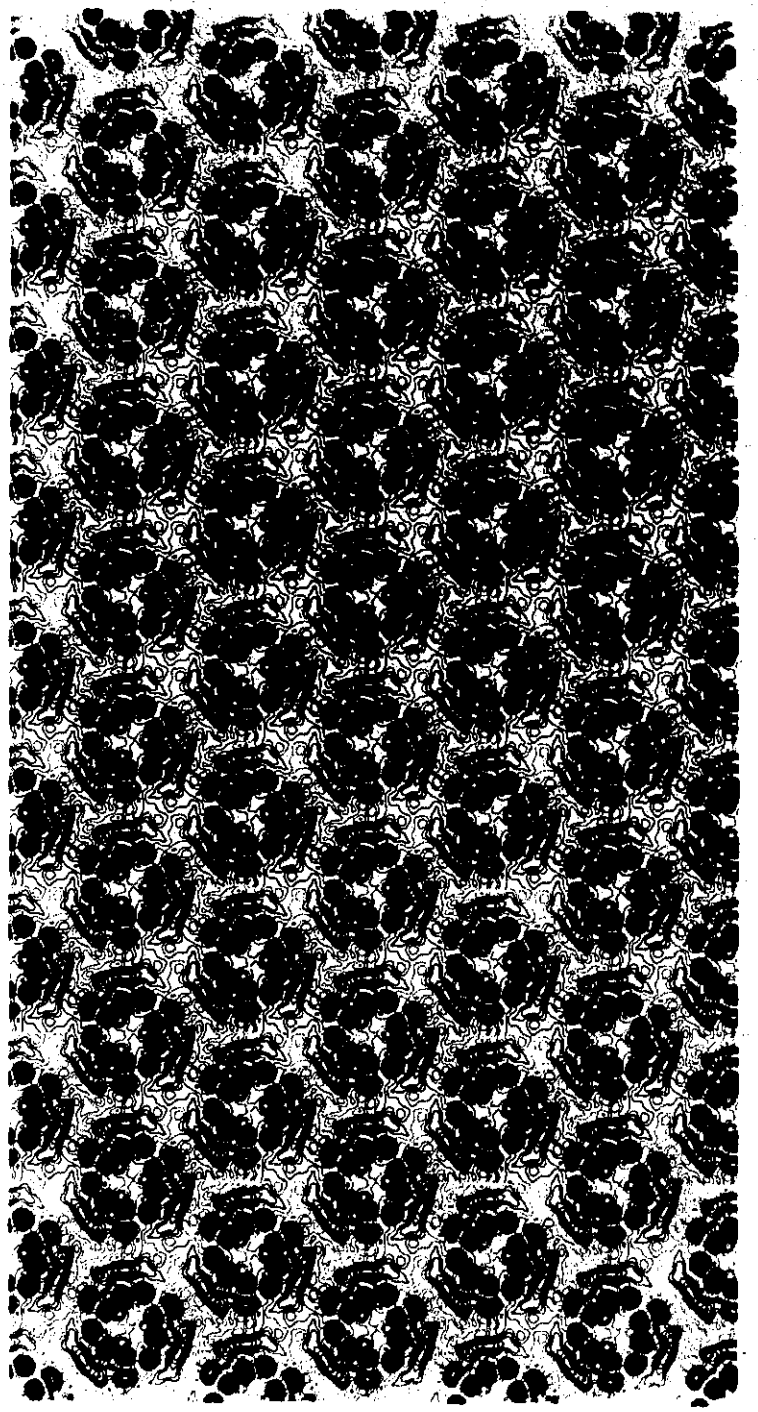

Figure 2

Contour map of the purple membrane lattice derived from X-ray diffraction studies showing three bacteriorhodopsin molecules per unit cell, each containing 7 α-helices.

conformation (7 α-helical segments) but provided some information on the lipid organization within the PM. Despite the low lipid to protein ratio (25% w/w), the diffraction patterns obtained are characteristic of lipids in a bilayer configuration. Treatment with uranyl acetate, which binds acidic groups, leads to marked intensity changes in the diffraction pattern suggesting that up to 30 uranyl acetate ions bind to each unit cell. These ions cannot be positioned accurately, implying that the membrane lipids are rather disordered and can move from one unit cell to the next.

Although the PGP to glycolipid mole ratio in both the PM and red membrane fractions is approximately 2:1, recent EM work by Henderson (Henderson et al., 1978) with a ferritin/avidin/biotin labelling procedure has shown that in the PM, and presumably in the red membrane as well, all of the glycolipid is found in the outer bilayer of the PM (21 mol% or 42% of the outer leaflet).

Although EM and X-ray or neutron scattering studies provide information on the organization of the components (protein, lipid and chromophore) within the PM, they provide more information on the structure of the proteins than of the lipid molecules. This is due, in part, to the presence of lateral diffusion and intramolecular motion of lipid molecules in a bilayer arrangement. However, some high resolution information has been provided by ESR and NMR as will be discussed below.

1.2.2 ESR

Preliminary ESR work (Butler and Smith, unpublished) on the

PM and aqueous dispersions of PGP using 5-SASL (N-oxyl-4',4'-dimethyloxazolidine derivative of 5-ketostearic acid) showed the phytanyl lipids to be highly ordered (S=0.5 for PGP, 1.0 for PM). These results support previous work by Chignell and Chignell (1975) in which 12-SASL exhibited large hyperfine splittings in purple membrane preparations which were interpreted by the authors as being indicative of highly ordered systems with a large proportion of the lipids tightly bound to the protein.

Cell envelope vesicles, prepared by freeze-thawing H. cutirubrum cells, as well as total lipid dispersed in 3.4 M NaCl were studied by ESR using fatty acid spin labels (Esser and Lanyi, 1973). For the cell envelope vesicles at 22°C, the order parameter, S, was found to be unusually high and relatively constant for the first 10 carbon atoms (0.72 - 0.79), decreasing markedly for the last carbon atom (0.24) (See Figure 3). The values were lower at higher temperature (0.62 - 0.70 for positions 1-10 and <0.24 for position 14; 37°C). For total lipid dispersions, the value of S again varied linearly with carbon number for the first 10 positions (0.59 to 0.76) then decreased markedly for the last position (<<0.24). These values are lower at higher temperatures (0.46 - 0.62 for positions 1-10 and <<0.24 for position 14 at 37°C). The higher order parameters for membrane vesicles as compared with liposomes prepared from total polar lipids is due to the presence of a protein matrix in the membrane. The same effect is seen for purple membrane preparations (Butler and Smith, unpublished).

More detailed ESR studies of total polar lipids, individual

polar lipids and polar lipid-squalene mixtures were reported by Plachy et al. (1974) and Lanyi et al. (1974). Within a physiological temperature range (20 - 40°C) and in 3 M NaCl, the value of S for 5-SASL in GLS (0.70 - 0.83) was higher than for TPL (0.59 - 0.74). Probe motional correlation times were also calculated by Plachy and coworkers. The value for τ increases with temperature and and decreases towards the terminal carbon. However, these calculations assume that the paramagnetic N-oxyloxazolidine ring of the SASL experiences rapid motion ($\tau < 3 \times 10^{-9}$ sec) and essentially isotropic reorientational motion (Schreier et al., 1978), neither of which is necessarily true for the diphytanylglycerol lipids (vide infra).

The calculated τ values for all samples vary from 8×10^{-10} to 3×10^{-9} sec with activation energies of 4.9 - 6 kcal/mol. In comparison, the activation energy for n-acyl lipids has been estimated by ^2H NMR to be 3.5 kcal/mol (Brown et al., 1979). The activation energy refers to the rotation about C-C bonds and is a combination of two factors: intrachain activation energy for bond rotation ($\sim$3 kcal/mol) and a structural factor due to interchain interaction (Esser and Lanyi, 1973; Brown et al., 1979). This second term is expected to be greater for branched-chain lipids. Plachy and coworkers (1974) have postulated that the predominant type of motion in diphytanylglycerol lipids would involve "cooperative kinking", resulting in clusters of lipid chains with single kinks at the same position.

Similar findings were obtained in a detailed study of spin-label ESR and saturation transfer ESR of dibiphytanyldiglycerol

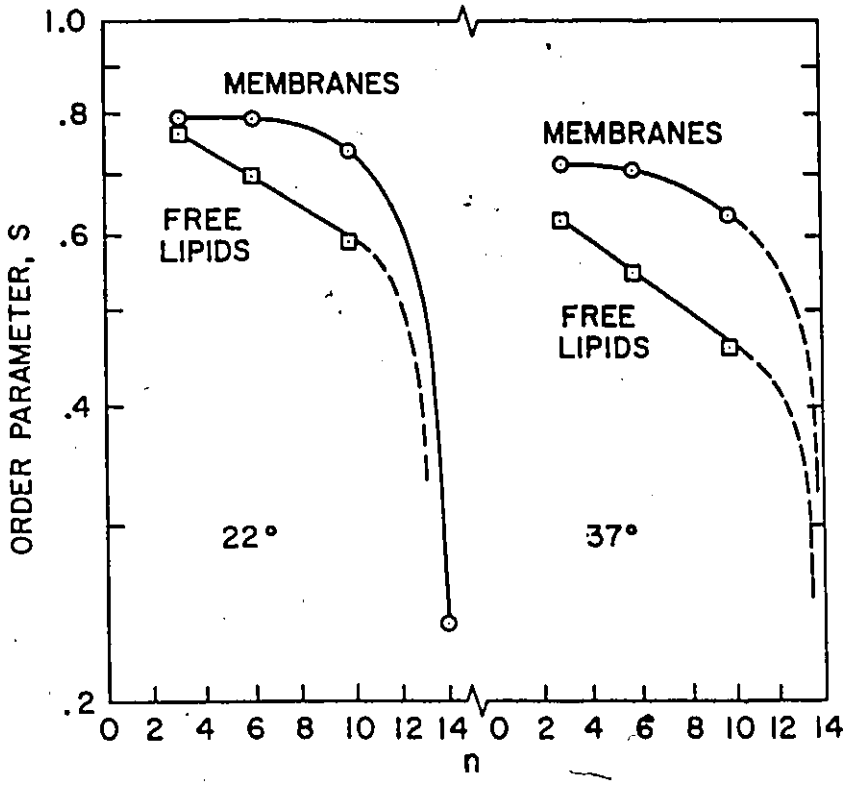

Figure 3

The ESR order parameter as a function of position of the spin-label within H. cutirubrum membrane envelope vesicles and vesicles prepared from TPL.

(From Esser and Lanyi, 1973)

tetraethers derived from the archaebacterium Sulfolobus sulfataricus (Bruno et al., 1985). As was seen for diphytanylglycerol lipids, the tetraether lipids have highly ordered structures (S= 0.97, 0.95 and 0.52 for 5-, 12- and 16-SASL), as indicated by high values of the hyperfine splitting for 5-SASL in dispersions of the diglycerol di-biphytanyl tetraether (60.5 gauss at 31°C) as compared with egg PC (49.5 gauss in 31°C). In addition, rotational correlation times at different portions of the hydrocarbon chains range from 10^{-8} to 10^{-5} s. Saturation transfer at 30°C showed a motional correlation time of approximately 10^{-8}s for 5-SASL and even lower for 16-SASL.

The order parameter for 5-, 12- and 16-SASL shows a non-linear temperature dependence over the range studied (10-90°C) (Bruno et al., 1985). In addition, the values of the order parameter calculated at 30°C for positions 5 and 12 (S=0.7) and the shapes of the curve of S versus temperature are virtually identical for the two positions (see Bruno et al., 1985). The value of S (0.45), as well as the shape of the curve for 16-SASL are significantly different. The variation of S with carbon number of branched chain lipids is different from the order parameter profile determined by ESR for n-acyl lipids which shows a roughly linear decrease in S with carbon number, or from the ^{2}H NMR profile in which there is a plateau for the first eight positions only, followed by a sharp decrease for the remaining positions. Whether the extension of the plateau region to at least carbon 12 is a feature characteristic of phytanyl chains or

just of glycerol dialkylglycerol tetraether-derived lipids is yet to be determined.

The values of the ESR order parameters which have been interpreted as being indicative of very high degrees of order in both PM and aqueous dispersion of diphytanylglycerol lipids may be misleading. ^{2}H NMR (vide infra) has shown that the molecular correlation time for diphytanylglycerol lipids is approximately 10^{-9} sec. In the calculations of the ESR order parameter from the hyperfine splittings, the assumption is made that the motion of the probe is fast on the ESR timescale (i.e., $\tau < 10^{-9}$ sec). Slower rates of motion affect the position of the inner and outer extrema of the spectra and lead to overestimation of the value of S unless complex spectral simulation techniques are used (Schreier et al., 1978).

In addition, if the degree of order is low as has been shown for diphytanylglycerol lipids (^{2}H NMR, vide infra) the outer extrema of the spectra are not well resolved, leading to erroneous calculations of $T_{\parallel}$ and $T_{\perp}$ and therefore of S.

Thus, in retrospect, ESR may not be the technique of choice for the analysis of the lipids of H. cutirubrum because the combination of the low degree of order and low rates of motions of these lipids could lead to erroneously high values of the order parameters.

In addition, as previously discussed, studies based on the use of fluorescence or spin-labelled probe molecules suffer from the inherent uncertainty of location, distribution, conformation and perturbation effects of these probe molecules relative to the

unlabelled molecules in the membrane (Schreier et al., 1978).

1.2.4 NMR

^{1}H, ^{13}C and ^{2}H NMR have also been used to provide both conformational and dynamic information on the phytanyl, phytanoyl and phytyl lipids.

A motional model developed by Peterson and Chan (1977) was used in the study of dispersions of diphytanoyl glycerol analogue of phosphatidylcholine (Lindsey et al., 1979). In this model, the measured ^{1}H NMR order parameter, S_{meas}, may be expressed as the product of two components,

$$S_{meas} = S_{\alpha} \cdot S_{\beta}$$

where S_{β} is a measure of the intrachain order and is related to the fraction of gauche rotamers present in the chain, and S_{α} reflects the amplitude of chain reorientation relative to the director axis. The value of S_{β} would be expected to be smaller in the diphytanoyl glycerol analogue of PC in comparison with n-acyl PC due to a decrease in the energy difference between gauche and trans conformers. The looser packing in diphytanoyl chains should decrease the cooperativity of the chain fluctuations. This would result in a decrease in the low frequency, high amplitude motions and subsequently an increase in the value of S_{α}. Thus, although the amplitude and type of motion of the branched-chain lipids is different than that of the straight chain analogues, the ^{1}H NMR order parameter, S_{meas}, is approximately the same. Studies of the temperature dependence

of the order parameter from -120 to +120°C indicated the absence of a gel to liquid-crystalline phase transition in diphytanoyl PC, confirming previous DSC and X-ray diffraction studies (Ekiel et al., 1981; Jackson and Sturtevant, 1978; Hiraki et al., 1981) as well as X-ray diffraction studies of the PM (Blaurock, 1975), indicating that the lipids are in the liquid-crystalline phase at physiological temperatures.

Goodman and coworkers (1973) measured the ^{13}C NMR spin-lattice relaxation times (T_1) of neat phytol as a function of carbon number along the chain. Although the absolute rates and amplitudes of molecular motions may differ between phytol and the phytanyl chains of phospholipids, it is reasonable to assume that the motional constraints imposed by the branch methyl groups would be qualitatively similar.

To facilitate comparison between positions, the T_1 values were corrected for the number of attached protons as the predominant relaxation mechanism for ^{13}C is dipole-dipole. Thus, NT_1 (where N is the number of attached protons) was used as a measure of the rate of rotational reorientation ($NT_1 \propto 1/\tau_{eff}$).

A plot of NT_1 versus carbon number is shown in Figure 4. It is obvious that the relaxation behavior of the branch methyl group carbons (C-7 and C-11) differs from that of the adjacent methylene carbons (C-6 and C-10), probably due to increased restrictions to internal rotation resulting from the presence of the branch methyl groups. This effect is similar to that seen for ^2H NMR T_1 values of unsaturated lipids at the position of the double bond as shown in Figure 4. It should be noted,

Figure 4

Comparison of the dependence of T_1 values on chain position for unsaturated and branch chain lipids.

A. ^2H NMR spin-lattice relaxation time profile for A. laidlawii enriched in $C_{18:1}$ (From Rance et al., 1980).

B. ^{13}C NMR spin-lattice relaxation time profile for neat phytol. (From Goodman et al., 1973)

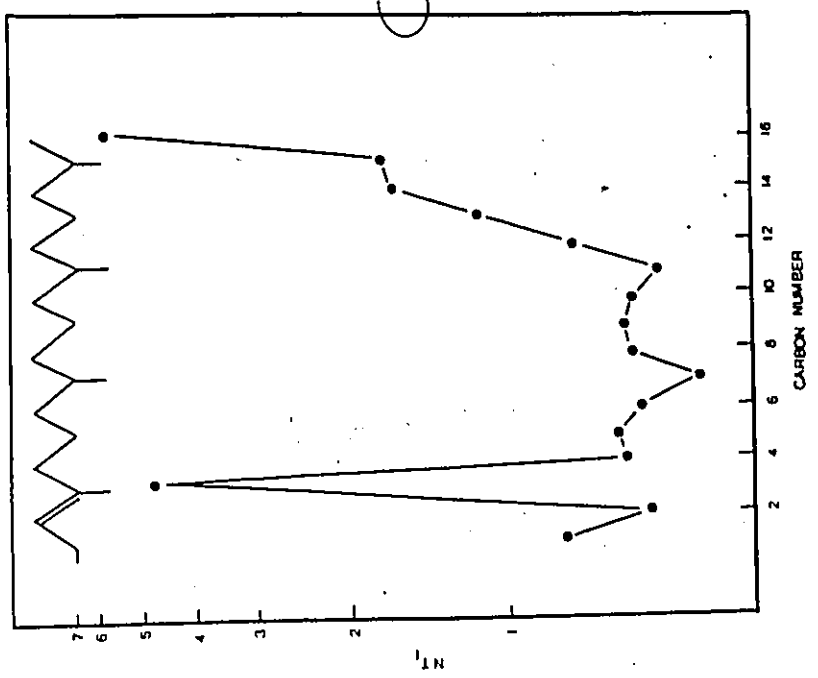
CARBON NUMBER
NT1

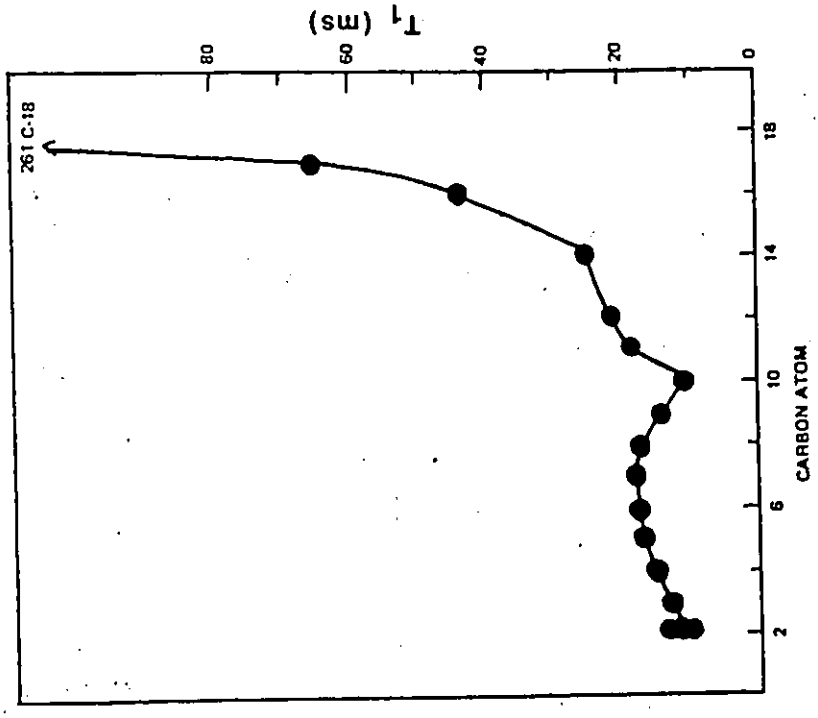
261 C-18
T1 (ms)
CARBON ATOM

however, that ^{13}C spin-lattice relaxation, which depends on both ^{13}C and ^{1}H resonance frequencies, is sensitive to higher frequency motions than ^{2}H NMR (Brown et al., 1982).

In natural and model membrane systems, interpretation of the ^{13}C NMR spin-lattice relaxation times is hampered by the fact that both the rates of molecular motions and the extent of molecular order contribute to relaxation. Therefore, a decrease in the T_1 values can be attributed to a combination of decreased rates of segmental motions and/or increased order (fluctuations of the C-H dipole with respect to the director).

The presence of branch methyl groups may also impose restrictions on the extent of molecular motions although the magnitude or sign of the contribution from the molecular order parameter at each position along the branched phytanyl chains is not known.

1.3 Research Outline

This thesis presents the results of a study of deuterium quadrupole splittings and relaxation times and phosphorus chemical shift and chemical shift anisotropy values of natural and synthetically or biosynthetically deuterated diphytanylglycerol lipids. These parameters have been correlated with similar results obtained for n-alkyl lipids and previously published data on n-acyl lipids. In addition, natural membrane diphytanylglycerol phospholipids and headgroup analogues have been studied by FTIR spectroscopy, osmometry and potentiometric titration techniques.

The research is divided into three sections: sample

preparation of natural and membrane lipids (Part I), synthesis of deuterated and non-deuterated lipids and lipid analogues (Part II), and physico-biochemical studies (Part III).

For ^{2}H NMR studies, ^{2}H-labelled compounds were prepared either by chemical synthesis, biosynthesis or a combination of both. For comparison, straight chain (dihexadecylglycerol) analogues were synthesized as model compounds.

For ^{31}P NMR, FTIR and titration studies, both naturally occurring diphtanylglycerol phospholipids, as well a series of diphytanylglycerol phospholipid analogues, including PA, deoxy PG, deoxy PGP, phosphatidylpropanol and methylated PGP were used.

2. Materials and Methods

2.1 Materials

All solvents were glass distilled prior to use. Anhydrous benzene and pyridine were prepared by keeping freshly distilled solvents over fresh potassium hydroxide pellets for at least 24 hours and were used without distillation. Anhydrous carbon tetrachloride and chloroform were prepared by keeping solvents over phosphorus pentoxide for up to 24 hours followed by decanting and distilling prior to use. Anhydrous ethyl ether for $LiAlH_4$ and $LiAl^2H_4$ reductions was prepared by keeping distilled ether over phosphorus pentoxide, then decanting and distilling it over $LiAlH_4$.

The term "petroleum ether" refers to light petroleum, with a boiling point between 60 and 80°C.

All other materials were of at least reagent grade and were used without further purification.

Platinum oxide catalyst from Anachemia, Montreal, Canada was found to cleave phenyl blocking groups more efficiently than the catalyst obtained from Aldrich Chemical Co., although both were equally efficient at reduction of double bonds.

Palladium on charcoal was purchased from Aldrich (10% Pd on activated carbon) or prepared as previously described (Hessel et al., 1954). A mixture of palladium chloride (1.21 g) and active charcoal (Norit A, 4 g) in 0.25 M aqueous HCl were stirred vigorously under an atmosphere of hydrogen for approximately 1 hour (290 ml of hydrogen taken up). The catalyst was then

filtered through 2 sheets of Whatman #1 filter paper, washed repeatedly with water and air dried for 10 minutes to activate the catalyst.

The catalyst was then washed well with freshly distilled ethanol (35 ml) and was used as soon as possible after preparation.

2.2 Chromatography

2.2.1 Analytical TLC

For purity determination and for monitoring of reactions, analytical TLC was carried out on 20 cm x 20 cm commercial silica gel G plates (0.25 mm, Baker) or on microplates cut from the commercial plates. Following development and drying of the TLC plates, the spots were usually visualized by spraying with 50% sulfuric acid and charring or with phosphate reagent prepared as described in the following section.

2.2.2 Preparative TLC

Preparative TLC was carried out on 20 cm x 20 cm plates coated with silica gel G or H (0.25 - 0.75 mm, Whatman). The plates were prewashed by ascending chromatography in chloroform/methanol (1:1) , air dried and activated at 120°F for 30 - 60 minutes.

Plates were generally streaked with a solution of the compound in chloroform (25 - 50 mg/ml; 30 - 60 mg/plate) using a Pelick Streaker (Applied Science Labs, State College, PA). The plates were developed in rectangular tanks lined with Whatman 3 MM filter paper.

2.2.3 Elution of Compounds from TLC Plates

Following development, the TLC plates were left to dry at room temperature until there was no detectable odour of solvent. The

bands were visualized with iodine and scraped into Erlenmeyer flasks; chloroform/methanol (1:1) was added and the mixture filtered through sintered glass filters and the residual silica washed well with solvent. The extract was concentrated under reduced pressure and the lipids converted to the ammonium salt form as follows through a modification of the technique of Bligh and Dyer (1959) (Kates, 1986b). The lipids were dissolved in chloroform/methanol (1:1; 10 ml) and 0.2 N aqueous HCl (4.5ml) was added. The sample was vortexed and centrifuged if necessary to ensure complete phase separation. The methanol/water phase was removed and washed twice with chloroform (4-5 ml total). The pooled chloroform phases were washed with methanol/water (10:9) and neutralized with 0.2 N methanolic NH_4OH. The sample was diluted with benzene and dried under a stream of nitrogen. Providing the ratios of chloroform/methanol/water are maintained at 1:1:0.9, this procedure can be scaled to accomodate any sample size.

2.2.4 Detection and Identification of Lipids

All TLC plates were air dried prior to staining (at least 2 hours if the solvent system contained acetic acid). The following stains were used to locate and identify lipids.

Ethanol-Sulfuric acid spray was prepared by slowly adding concentrated sulfuric acid (50 ml) to cold 95% ethanol (50 ml). TLC plates were lightly sprayed and slowly heated on a hot plate. Phospholipids give brown spots and glycolipids give pink spots.

Phosphate spray was prepared as previously described (Kates, 1986b). Ammonium molybdate (16 g) was dissolved in water (120

ml) and an aliquot of this solution (80 ml), together with mercury (10 ml), was added to concentrated hydrochloric acid (40 ml). The solution was shaken well for 30 minutes and then filtered. The filtered solution and concentrated sulfuric acid (200 ml) were added to the remainder of the ammonium molybdate solution. This stock solution could be stored for months and was diluted with water to an amber colour (1:3) immediately before use. Plates were sprayed lightly with the reagent and phosphate containing compounds appeared as blue spots on a white background after 2-5 minutes at room temperature.

For non-destructive staining, TLC plates were placed in a closed container which had been pre-saturated with iodine vapour until yellow or brown spots appeared. This stain is non-specific although aromatic and unsaturated compounds stain more readily than saturated.

2.2.5 Column Chromatography

Neutral synthetic intermediates or natural compounds were purified on columns of BioRad Biosil A (100-200 mesh) silicic acid. The silica was activated for an hour prior to use. The silicic acid to sample weight ratio was 50 to 100:1.

2.3 Analytical Procedures

The sample for analysis was diluted, usually with chloroform, to a known volume in a volumetric flask (approximately 1% solution). This solution served as a stock solution from which aliquots were removed for one or more of the following analyses.

Dry weights and phosphorus analysis were done according to the methods described by Kates (1986b). For cation (Na^+, K^+, Mg^{2+})

analysis, samples were either digested with perchloric acid prior to analysis or an aqueous solution containing the cations from a known amount of sample was prepared. In the latter method, the samples were diluted with chloroform/methanol (1:1; 10 ml) and made biphasic by the addition of 0.5N HCl (4.5 ml). The chloroform phase was washed well with methanol/water (1:0.9) and the pooled washings were diluted with benzene and concentrated under reduced pressure. The residue was diluted to a known volume for analysis via flame photometry (minimum concentration of 2 mM, minimum volume of 5 ml).

2.4 Physical Methods

2.4.1 Infrared spectroscopy (IR)

IR spectra were obtained on thin films between NaCl plates or KBr pellets containing 2% w/w sample using a Beckman IR-20 double-beam spectrophotometer. FTIR spectra were obtained in collaboration with Dr. P. Yang and Dr. H.H. Mantsch as described in PART III, section 4.

2.4.2 NMR

High resolution spectra for compound identification and characterization were obtained on a Bruker CXP-300 or MSL-300 spectrometer.

^{13}C NMR spectra were obtained in C^2HCl_3, $C^2HCl_3/C_6{}^2H_6/C^2H_3O^2H$ (1.1:0.2) or $C^2HCl_3/C^2H_3O^2H/{}^2H_2O$ (5:5:1.5) using TMS as an internal standard.

^2H NMR spectra were obtained in $CHCl_3$. Chemical shift values were calculated from the chloroform peak (7.25 ppm).

^{31}P spectra were obtained in $CHCl_3$ or $C_6{}^2H_6/C^2H_3O^2H$

(1.1:0.2). A capillary containing a 85% H_3PO_4 or a solution of aminoethyl phosphate (AEP; 100 mM; CS 18.688 ppm relative to H_3PO_4) was used as an internal standard.

2.4.3 Mass Spectrometry

All MS data (CI and FAB) were obtained by Dr. Clem Kazakoff, Department of Chemistry, Univer sity of Ottawa.

A FAB source fitted to a VG 7070E mass spectrometer (VG Analytical, Manchester, England) was operated at an accelerating potential of 6 kV. A potential of 9 kV at 1.5 mA was applied to the xenon gun used to form the fast atom beam. The samples were dissolved in approximately 1 µl of glycerol and the probe tip was inserted into the source. The spectra were acquired with a DEC DPP8 data system (Digital Equipment Co.). Negative FAB was used for the analysis of most of the anionic phospholipids. Samples were prepared as ammonium salts and the major peak usually corresponded to $(M - H)^-$ or $(M - H_2O - H)^-$

The same spectrometer and data system were used as for CI and both positive and negative FAB/MS. Diethyl ether was used as the ion source. The major peak usually corresponded to MH^+. in positive FAB and M - 1 in negative FAB.

2.4.4 Elemental Analysis

C, H, N and, in some cases P, analysis were carried out by Hector Seguin, Analytical Chemistry, National Research Council of Canada.

2.4.5 Gas-Liquid Chromatography

GLC was carried out using a Pye Unicam GCD gas chromatograph equipped with a flame ionization detector (detector, 210°C; injector port, 220°C). Separation of alcohols, alkyl halides etc. was carried out at 180°C on a 1.8 m x 0.4 cm (I.D.) glass column packed with 10% SP 2330 (100/120 Chromosorb WAW; Supelco). The carrier pressure was set at 0.7-1.0 kg/cm^2, air at 0.4 kg/cm^2 and the hydrogen at 1.1 kg/cm^2.

All retention times are reported relative to methyl palmitate ($RT_{16:0}$).

PART I

Isolation, Purification and Characterization of Natural Lipid Samples

1. Lipid Extraction and Purification

1.1 Growth of Halobacterium Cutirubrum

Halobacterium cutirubrum (NRCC strain 34001) was used as a source of both lipids and purple membrane. The cells were cultured in the standard growth medium which contained, per liter, sodium chloride (250 g), oxoid bacteriological peptone (10 g), potassium chloride (2 g), trisodium citrate (3 g), magnesium sulfate heptahydrate (20 g) and ferric sulfate (50 mg $FeSO_4 \cdot 7H_2O$ in 1 ml of 0.01M HCl). The pH was adjusted to 6.7 and the medium was autoclaved for 15 minutes at 121°C prior to the addition of the peptone extract.

For preparation of cells to be used for extraction of lipids, primary inocula were prepared by transferring cells from stock culture slants to culture medium (50 ml) in a 250 ml flask and incubating in the dark at 39°C at 190 r.p.m. for 48 hours. Cells were normally grown in 1.5 - 2 liter batches in 4 liter Erlenmeyer flasks (39°C at 120 r.p.m. for 4 days), harvested by centrifugation at 9,000 xg and washed with 4 M NaCl.

1.2 Biosynthetic Labelling of Lipids

Cells were grown as described above except that the medium was supplemented with 1 g of deuterated sodium acetate per liter of culture. Deuterated sodium acetate was prepared by titrating perdeuterated acetic acid ($C^2H_3CO_2{}^2H$) with 10% aqueous NaOH to

neutrality and lyophilizing the resultant mixture. The resulting lipids were labelled at the carbons adjacent to the methine groups of the phytanyl chains (Ekiel et al., 1986).

1.3 Extraction of Polar and Neutral Lipids

The cell pellet from 8-12 liters of culture (30-70 g wet weight) was suspended in 4 M NaCl to 200 ml. Methanol (500 ml) and chloroform (250 ml) were added to yield a final solvent ratio of chloroform/methanol/water, 1:2:0.8). The mixture was stirred for approximately 3 hours and filtered through a bed of pyrex wool on Whatman #1 filter paper in a Buchner funnel. The residue was washed with chloroform/methanol/water (1:2:0.8, 475 ml) and the pooled supernatants were transfered to a two liter separatory funnel and diluted with chloroform (375 ml) and water (375 ml). The chloroform phase, containing the total lipids, was withdrawn, diluted with benzene and concentrated under reduced pressure. The residual total lipids were dissolved in chloroform/benzene (1:1, 20 ml), centrifuged to remove salts and particulate matter and concentrated under reduced pressure to dryness and the residue redissolved in chloroform.

1.4 Acetone Precipitation of Polar Lipids

A solution of the total lipids from a 12 liter culture (350-500 mg) in a minimum of chloroform (3-5 ml) was diluted with 20-30 ml of acetone. The mixture was shaken well, cooled on ice and centrifuged. The supernatant was decanted and the precedure repeated on the pellet until the supernatant was colourless. The tan coloured precipitate was dried <u>in vacuo</u> yielding 300-500 mg

polar lipids per 12 liter culture. The pooled acetone supernatants, containing the non-polar lipids, were concentrated under reduced pressure yielding approximately 50 mg per 12 liter culture.

1.5 Purification and Characterization of Lipids

1.5.1 Purification and Characterization of PGP

Lipids were fractionated according to procedures previously described (Smallbone, 1982). A solution of the acetone-precipitated polar lipids (600 mg) in chloroform (4 ml) was diluted to 30 ml with methanol, mixed well and allowed to stand at room temperature for 2 hours and overnight at 4°C. The initial methanol precipitate was centrifuged and washed twice with cold methanol. A solution of 20% aqueous barium chloride was added dropwise to the pooled methanol supernatants until no further precipitation occurred (1-2 ml), and the mixture was allowed to stand overnight at 4°C. The barium precipitate was centrifuged, washed with cold methanol and dissolved in chloroform (12.5 ml). The solution was made biphasic by the addition of methanol (12.5 ml) and 0.2 N HCl (11.25 ml). The chloroform phase was washed with methanol/water (10:9), neutralized with 2 N methanolic NH_4OH, diluted with benzene and concentrated under reduced pressure to yield PGP, contaminated with GLS and traces of other polar lipids. The crude PGP was purified by repeated barium chloride precipitation and the final product was chromatographically pure.

TLC of PGP in chloroform/90% acetic acid/methanol (30:20:4) or chloroform/methanol/NH_4OH (65:35:5) showed one spot with R_f= 0.51

Figure I.1

TLC of total polar lipids (TPL), PG, PGP, PGS and GLS isolated from H. cutirubrum. The solvent system was chloroform/90% acetic acid/methanol (30:20:4) and the spots were visualized by spraying with sulphuric acid and charring as described in section 2 (Materials and Methods).

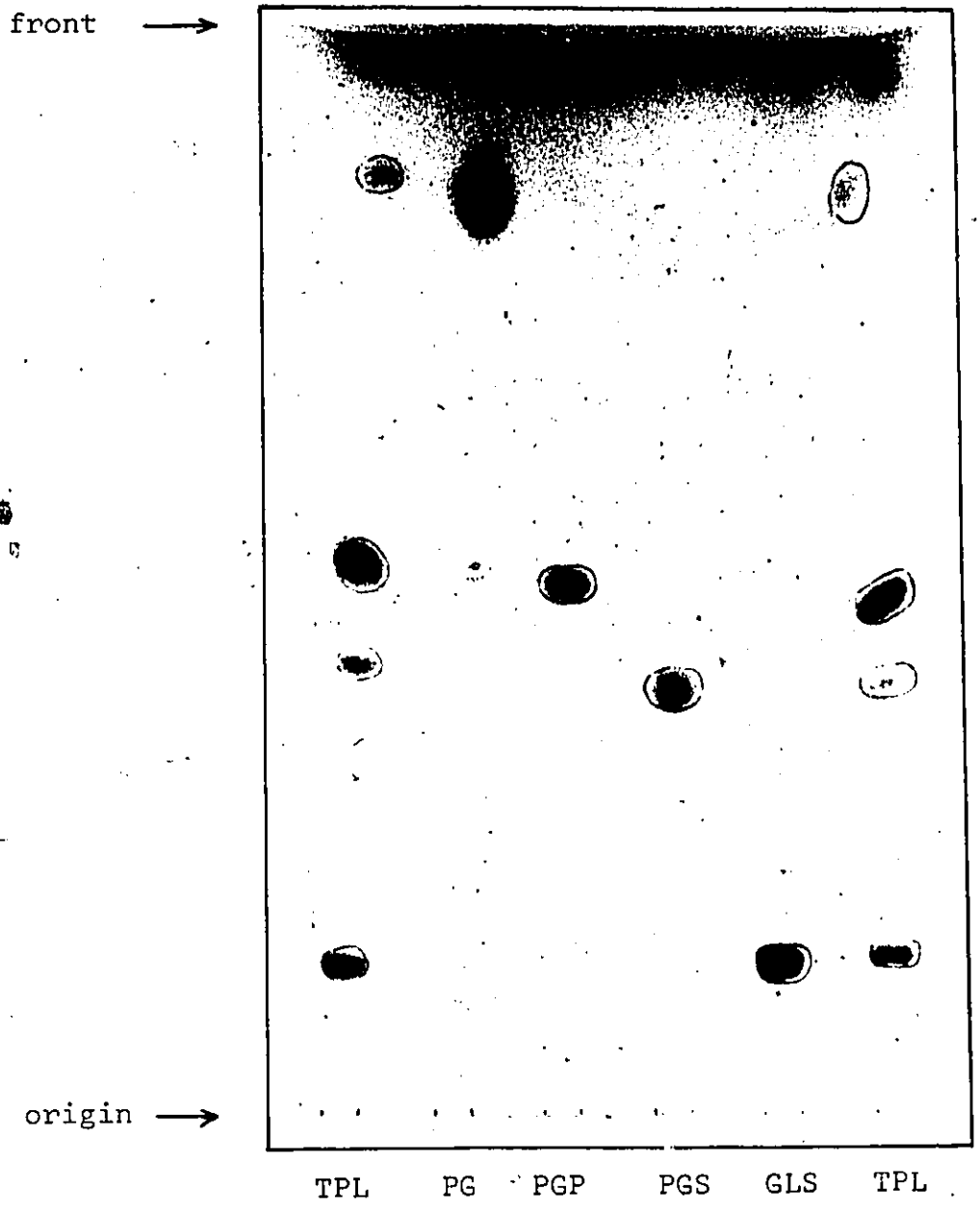
front
origin
TPL
PG
PGP
PGS
GLS
TPL

or 0.14, respectively (see Figure I.1).

Negative FAB/MS ($PGP(NH_4)_2$; $C_{46}H_{102}O_{11}P_2N_2$, FW=920): m/z, 902 $(M - NH_4)^-$.

Elemental analysis ($PGP(NH_4)_2 \cdot H_2O$; $C_{46}H_{102}O_{11}P_2N_2\ H_2O$):

calculated: 6.61% P

found: 6.65% P

NMR (See Table I.1)

1.5.2 Purification and Characterization of PGS

PGS was isolated from the PGP-depleted methanol supernatants by preparative TLC in chloroform/ 90% acetic acid/ methanol (30:20:4). The resultant product was converted to the ammonium salt form and precipitated from chloroform by the addition of a tenfold excess of acetone. The product contained traces of glycolipids but no PGP or PG as indicated by phosphate reagent staining of TLC plate.

Negative FAB/MS ($PGS-H_2$; $C_{46}H_{95}O_{11}SP$; FW= 886): m/z, 885 $(M - 1)^-$.

TLC in chloroform/90% acetic acid/methanol (30:20:4) showed one spot with R_f= 0.41.

1.5.3 Purification of PG

PG was isolated from the methanol supernatant by preparative TLC in chloroform/methanol/NH_4OH (65:35:5) and showed one spot with R_f=0.45 in this solvent system. TLC in chloroform/90% acetic acid/methanol (30:20:4) showed one spot with R_f= 0.88.

Positive FAB/MS (PG-H; $C_{46}H_{95}O_8P$, FW=806): m/z, 807 (MH^+); 808 (MH_2^+).

Table I.1

^{13}C NMR Chemical shift values for natural diphytanylglycerol phospholipids

PG		PGP	
CS (ppm)	Assignments	CS (ppm)	Assignments
19.6-19.8	CH_3 18,19	19.6-19.8	CH_3 18,19
22.6-22.7	CH_3 16,17	22.6-22.7	CH_3 16,17
24.4-24.8	CH_2 5,9,13	24.4-24.8	CH_2 5,9,13
27.99	CH 15	27.99	CH 15
29.9-32.9	CH 3,7,11	29.8-29.9	CH 3,7,11
36.6-36.7	CH 2,4	36.6-36.7	CH 2,4
37.1-37.7	CH 6,8,10 12,14	37.1-37.7	CH 6,8,10 12,14
39.4	CH_3 20	39.4	CH_3 20
63.2	G-1'	65.9	G-1
65.9	G-1	66.9	G-1', G-3'
67.5	G-3'	69.3	C-1 (sn-2)
69.3	C-1(sn-2)	70.4	C-1'(sn-3), G-2'
70.4	C-1'(sn-3)	71.5	G-3
71.4	G-2'	78.8	G-2
71.72	G-3		
78.74	G-2		

Assignment of carbons as indicated on page 42.

Negative FAB/MS (PG-H): m/z, 805 (M^-)

Elemental analysis (PG-NH_4; $C_{46}H_{98}O_8PN$; FW= 824)

calculated: 3.76% P

found: 3.78% P

NMR (See Table I.1)

1.5.4 Purification of GLS

GLS was isolated from the initial methanol precipitate by preparative TLC in chloroform/90% acetic acid/methanol (30:20:4) and showed one spot with R_f= 0.14.

Negative FAB/MS (GLS-NaH_2; $C_{61}H_{117}O_{21}SNa$, FW=1240): m/z, 1217 ($M^- - 23$); 1239 ($M^- - 1$).

1.6 Preparation of Salt Forms of PGP

Mono-, di- or tri- salts of purified PGP were prepared by titrating the free acid forms of the lipids with 1, 2 or 3 equivalents of a 0.2 N methanolic solution of NaOH, KOH or NH_4OH.

Barium and magnesium salts were prepared by titrating the free acid form of the lipids with one equivalent of 20% aqueous barium acetate or magnesium acetate.

All compounds were purified by acetone precipitation and dried in vacuo.

The purity of mono-, di- and trisodium and potassium salt forms of PGP was assayed by phosphorus analysis and flame photometry on aliquots of the same samples. K/P ratios were calculated to be 0.48, 0.96 and 1.41, respectively.

Specific salt forms of PG and PA were also prepared by this method.

2. Preparation of Purple Membrane

2.1 Growth of Halobacterium cutirubrum

For the preparation of purple membrane, primary inocula were prepared as described above. Secondary inocula were prepared by adding the primary inocula (100 ml) to medium (0.8 liters) in a 2 liter Erlenmeyer flask and incubating under the same conditions for 72 hours. The main cultures were prepared by adding secondary inocula (400 ml) to 4 liter Erlenmeyer flasks containing 1 to 1.5 liters of culture medium. These were incubated in the light (39°C at 190 r.p.m. for 72 hours) then for an additional 72 hours in the light (39°C at 100 r.p.m.). Cells were harvested by centrifugation (8000 g; 10 minutes), the pellet was washed 3 times with 4 M NaCl yielding 6.5 g cells (wet weight) per liter of culture.

2.2 Isolation and Purification of the Purple Membrane

Cells from 12 liters of culture grown as described above for purple membrane were suspended in salt solution (25%; 200 ml) containing deoxyribonuclease (10 mg) and stirred for approximately 2 hours at room temperature. The suspension was dialysed overnight against distilled water at 4°C, centrifuged at 10,000 xg for 20 minutes and the supernatant decanted and recentrifuged at 50,000 xg for 1 hour. Resuspension and recentrifugation of the pellet was repeated until the final supernatant was colourless.

The crude purple membrane pellet was resuspended in distilled water (approximately 50 ml) and layered onto six 40 ml

nitrocellulose tubes containing discontinuous sucrose gradients (10 ml 1.5 M; 20 ml 1.3 M). The tubes were centrifuged (100,000 xg for 48 hours at 10°C) using a Beckman SW-28 rotor. The purple membrane, which was found at the interface between the sucrose layers, was collected, pooled and dialysed against distilled water (18 hours; 4°C). The dialysate was then centrifuged (50,000 xg; 1 hour) and the pellet resuspended in a minimum volume of 1 mM aqueous sodium azide and stored at 4°C.

2.3 Analysis of the Purple Membrane

The amount of protein in a sample was determined by a modification of the procedure use by Lowry and coworkers (Lowry et al., 1951) as previously described (Smallbone, 1982). Average yield: 0.7 - 1 gram of protein per 12 liter culture.

The purity of the samples was determined using sodium dodecyl sulfate polyacrylamide gel electrophoresis. The gel buffer was prepared by combining 1.0 M pH 7.1 phosphate buffer (100 ml), 10% sodium dodecyl sulfate (10 ml) and water (290 ml). The gel was prepared by combining the gel buffer (30 ml), aqueous 20% acrylamide with 5% bis-acrylamide (21 ml), water (6 ml), TEMED (90 µl) and freshly prepared 1.5% aqueous ammonium persulfate (3 ml).

Samples were applied at varying protein concentrations (approximately 20 - 100 ug protein per gel). Gels were run at 20 mA for 6 hours and 10 mA for 10 hours and stained with Coomassie Blue (1.25 g dye, 454 ml methanol/water 1:1, 250 ml acetic acid) for two days. All samples tested showed a single protein band at all concentrations.

PART II

Syntheses

1. Introduction

The need for synthesis was threefold: firstly, to synthesize deuterated compounds for ^2H NMR; secondly, to synthesize model compounds such as headgroup analogues of PG and PGP; and, thirdly to synthesis compounds such as PG present only in small amounts in the membranes of H. cutirubrum.

^2H NMR has been used to determine the conformation and dynamics of the phytanyl chains adjacent to the glycerol backbone, necessitating the preparation of a series of deuterated compounds. These compounds were prepared through modifications of previously published techniques for the synthesis of both ^2H-labelled (Tulloch, 1977, 1979) and unlabelled (Kates et al., 1965; Joo et al., 1969; Aneja and Chadha, 1971; Aneja et al., 1970) phospholipids. Deuterium-labelled and unlabelled chains were synthesized from phytol or isolated from total polar lipids of H. cutirubrum resulting in R/S,R,R and R,R,R chains, respectively. These were linked to the backbone glycerol to produce either rac-2,3-diphytanylglycerol which was deuterated in both chains, or sn-2,3-diphytanylglycerol which was deuterated in only the sn-2 chain. The general schemes for the synthesis of labelled phytanyl chains, hexadecyl chains and headgroup analogues are shown in Figures II.1-3 and the structures are shown in Figure II.4.

Figure II.1

Synthesis of (R,R,R)- and (R/S,R,R)diphytanylglycerol phospholipids deuterated in the phytanyl chains

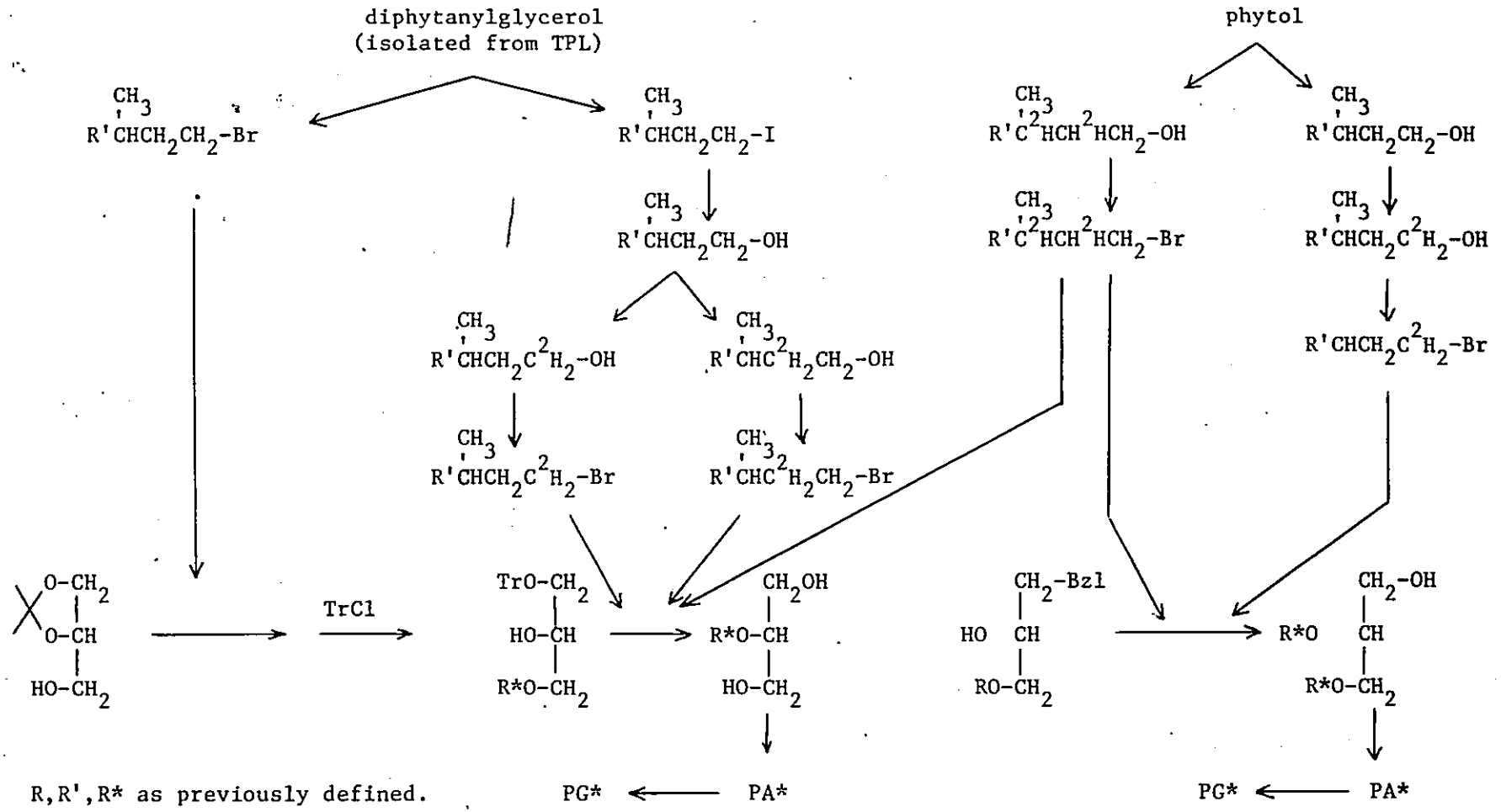

Figure II. 2

Synthesis of deuterated dihexadecylglycerol phospholipids

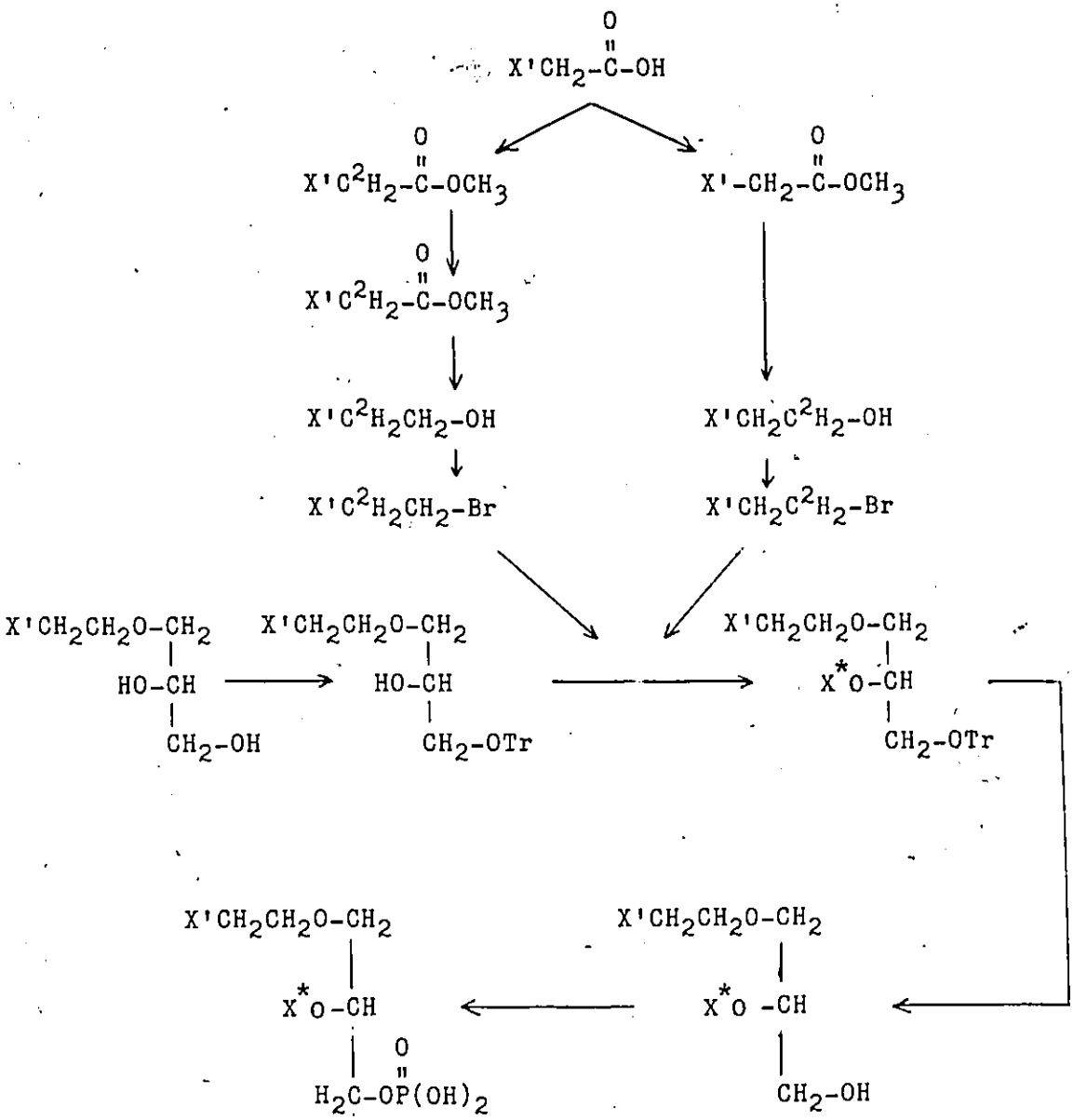

X*= $CH_3(CH_2)_{15}$-; deuterated

X'= $CH_3(CH_2)_{13}$-

Figure II.3

Synthesis of headgroup analogues

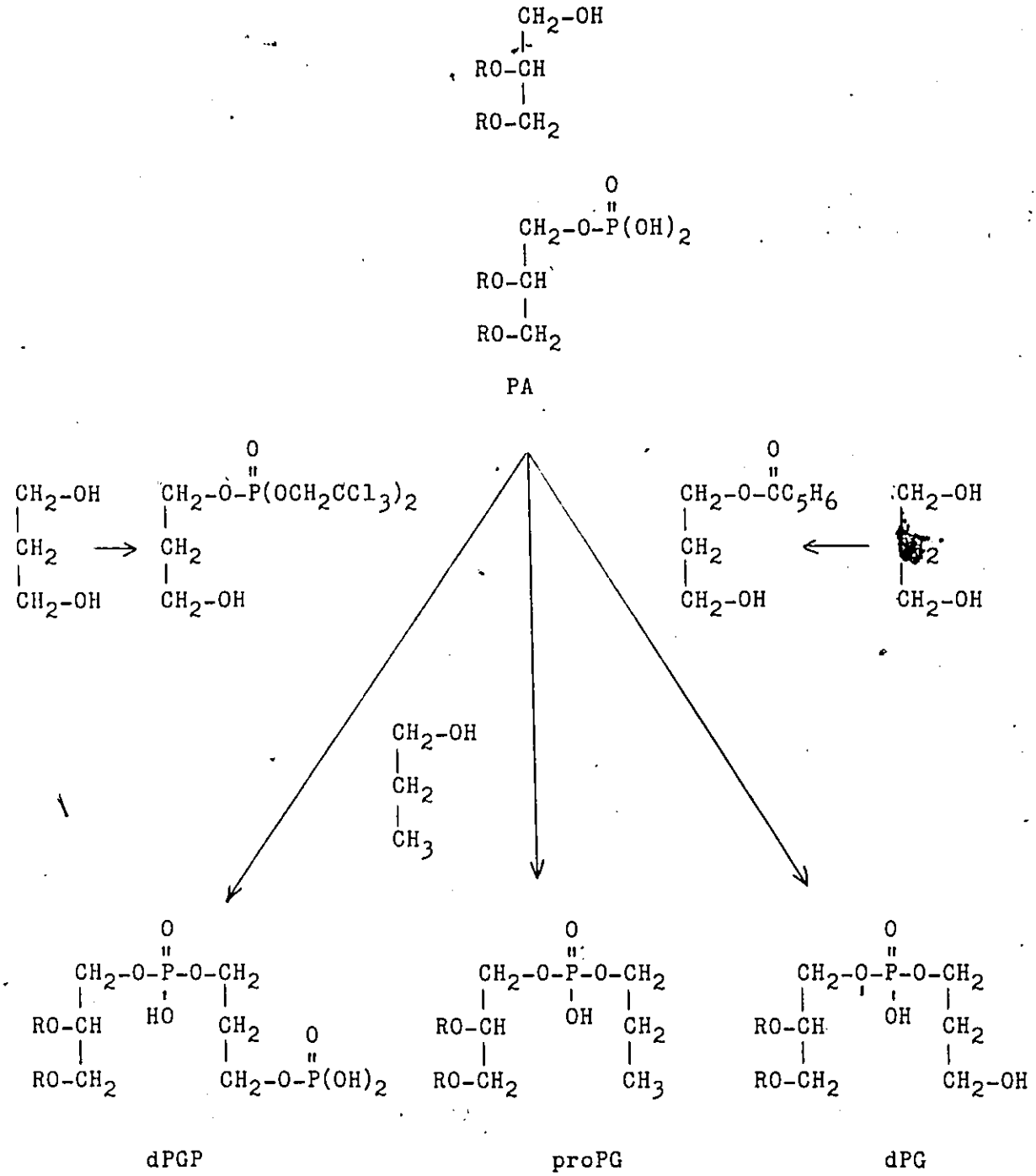

Figure II.4

Structures of the deuterated diphytanylglycerol phospholipids.

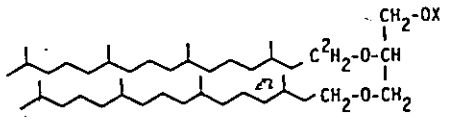

[1,1-$^2H_2$]DPhPA

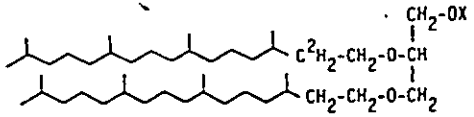

[2,2-$^2H_2$]DPhPA

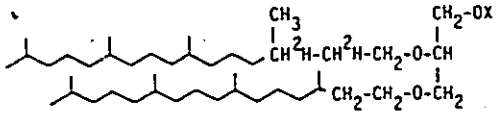

[2,3-$^2H_2$]DPhPA

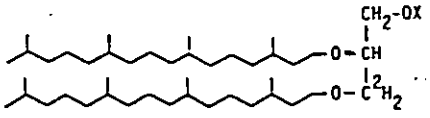

rac-[3,3-$^2H_2$]DPhPA

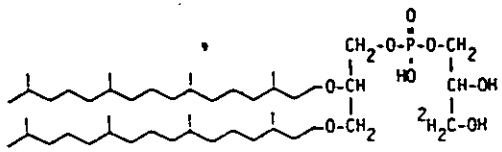

sn-[1,1-$^2H_2$]DPhPA

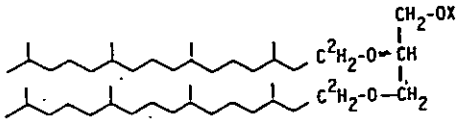

[1,1,1',1'-$^2H_4$]DPhPA

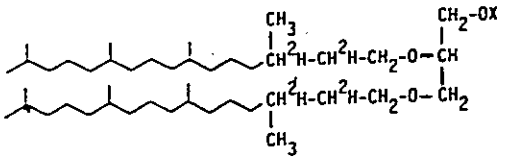

[2,3,2',3'-$^2H_4$]DPhPA

X = $\overset{O}{\overset{\|}{P}}(OH)_2$

The following deuterium-labelled diphytanylglycerol phospholipids have been synthesized:

a. sn-2-[1,1-$^2H_2$]-(R,R,R)-phytanyl-3-(R,R,R)-phytanylglycerol analogues of PA and PG;

b. sn-2-[2,2-$^2H_2$]-(R,R,R)-phytanyl-3-(R,R,R)-phytanylglycerol analogues of PA;

c. sn-2-[2,3-$^2H_2$]-(R/S,R,R)-phytanyl-3-(R,R,R)-phytanylglycerol analogues of PA and PG;

d. rac-2,3-[1,1,1',1'-$^2H_4$]-(R/S,R,R)-diphytanylglycerol analogues of PA;

e. rac-2,3-[2,2',3,3'-$^2H_4$]-(R/S,R,R)-diphytanylglycerol analogues of PA;

f. sn-2,3-(R,R,R)-diphytanylglycerol-1-phosphoryl-sn-3'-([1,1-$^2H_2$]glycerol); and,

g. rac-2,3-(R/S,R,R)-diphytanylglycerol-1-phosphoryl-sn-3'-([1,1-$^2H_2$]glycerol-1'-phosphate).

The following deuterated n-alkyl lipids were synthesized:

a. sn-1-hexadecyl-2-[1,1-$^2H_2$]hexadecylglycerol phosphatidic acid; and,

b. sn-1-hexadecyl-2-[2,2-$^2H_2$]hexadecylglycerol phosphatidic acid.

A number of headgroup analogues of PG and PGP were also prepared for ^{31}P NMR and FTIR experiments. These include the following compounds:

a. sn-2,3-diphytanylglycerol-1-phosphoryl-3'-(1',3'-propanediol);

b. sn-2,3-diphytanylglycerol-1-phosphoryl-3'-(1'-3'-propanediol)-1'-phosphate;

c. sn-2,3-diphytanylglycerol-1-phosphoryl-3'-propanol; and,

d. di-, tri- and tetramethylated PGP

Nomenclature for the hydrocarbon and glycerol backbone regions of n-alkyl and n-acyl lipids is relatively straightforward. For phytanyl lipids, the presence of additional chiral centers makes unambiguous naming of compounds more difficult.

The naturally occurring diphytanylglycerol is sn-2,3-[(3'R,7'R,11'R,15)-tetramethylhexadecyl]glycerol. The stereochemistry of the hydrocarbon chains is specified by the R/S nomenclature and the glycerol backbone by the sn/rac nomenclature. This nomenclature can be shortened to sn-2,3-(R,R,R)-phytanylglycerol, or, where the stereochemistry is not specified, diphytanylglycerol.

A number of different types of compounds were synthesized, including those containing mixtures of stereoisomers: for example, sn-2,3-(R/S,R,R)-diphytanylglycerol contains a mixture of stereoisomers at the third carbon of the phytanyl chains.

The carbons of the backbone glycerol are labelled G-1, G-2 and G-3 and the carbons of the headgroup glycerol, G'-1, G'-2 and G'-3. The carbons of the sn-3 or rac-3 chain of diphytanylglycerol are labelled 1'-20' and those of the 2 chain are labelled 1-20.

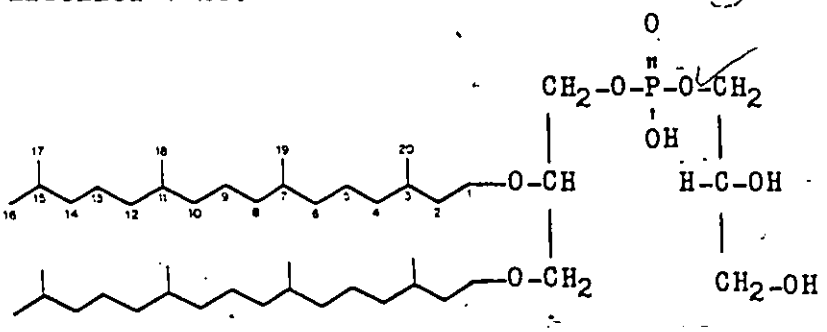

For comparison purposes, the carbons of the headgroup carbons of the headgroup analogues are labelled α, β and γ beginning at the carbon adjacent to the phosphodiester. This nomenclature avoids confusion between, for example, the sn-3' carbon of PGP and the 1' carbon of deoxy PGP, which in both cases refers to the carbon adjacent to the phosphodiester group.

Each synthetic compound has been assigned a number indicating the section number, compound number and position of the deuterium label. The label designation a-c corresponds to [1,1-$^2H_2$] or [1,1,1',1'-$^2H_4$], [2,2-$^2H_2$] and [2,3-$^2H_2$] or [2,3,2',3'-$^2H_4$], respectively. Therefore, 2.5a refers to the fifth compound of section 2 which is labelled in the first position of the phytanyl chain.

Deuterium labels in the glycerol backbone and headgroup are designated by d and e, respectively.

2. (R,R,R)-Diphytanylglycerol Phospholipids

2.1 Undeuterated Starting Materials

The detailed schemes for the synthesis of labelled phytanyl chains are shown in Figures II.5 and 6 and the structures in Figure II.4. The diagnostic ^{13}C NMR chemical shift data are summarized after each step and complete spectra are shown in Appendix A.

2.1.1 sn-2,3-(R,R,R)-Diphytanylglycerol (2.1) (Kates et al., 1965a)

Total polar lipids (2.5 g) extracted from cells of H. cutirubrum were heated under reflux with methanolic HCl (0.6 N, 200 ml) for 5 hours. After dilution with 10% water, the resultant diphytanylglycerol was extracted with several portions of petroleum ether. The pooled ether fractions were washed well with water and concentrated under reduced pressure. The residue was fractionated by chromatography on a column of silicic acid (5 g) by elution with petroleum ether (100 ml) and petroleum ether/ethyl ether (4:1; 100 ml). The second fraction, containing the pure diphytanylglycerol was concentrated under reduced pressure and dried in vacuo, yielding 1.55 g (95%) diphytanylglycerol (2.1) (colourless oil). TLC in petroleum ether/ethyl ether (4:1) showed one spot with R_f=0.32 (R_f of authentic diphytanylglycerol=0.3).

IR: 3450 cm^{-1} (OH); 2860-2960, 1465 cm^{-1} (CH_2, CH_3); 1380 cm^{-1} doublet (isopropyl); 1120 cm^{-1} (C-O-C), 1050 cm^{-1} (C-OH alcohol).

Figure II.5

Synthesis of deuterated (R,R,R)-phytanyl bromides

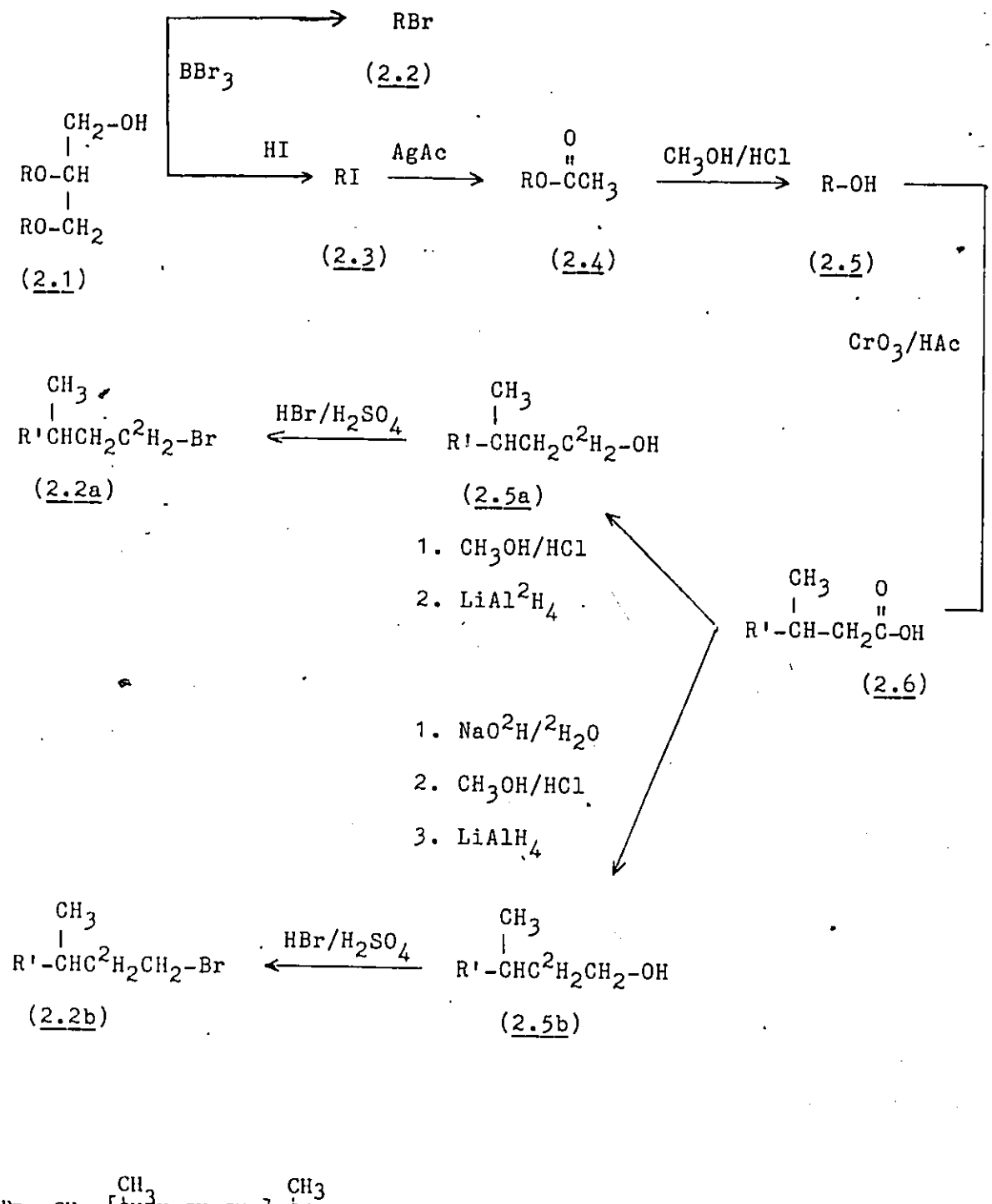

R= $CH_3-[CH(CH_3)CH_2CH_2CH_2]_3CH(CH_3)CH_2CH_2-$

Figure II.6

Synthesis of sn-2,3-(R,R,R)-diphytanylglycerol phospholipids deuterated in the sn-2 chain.

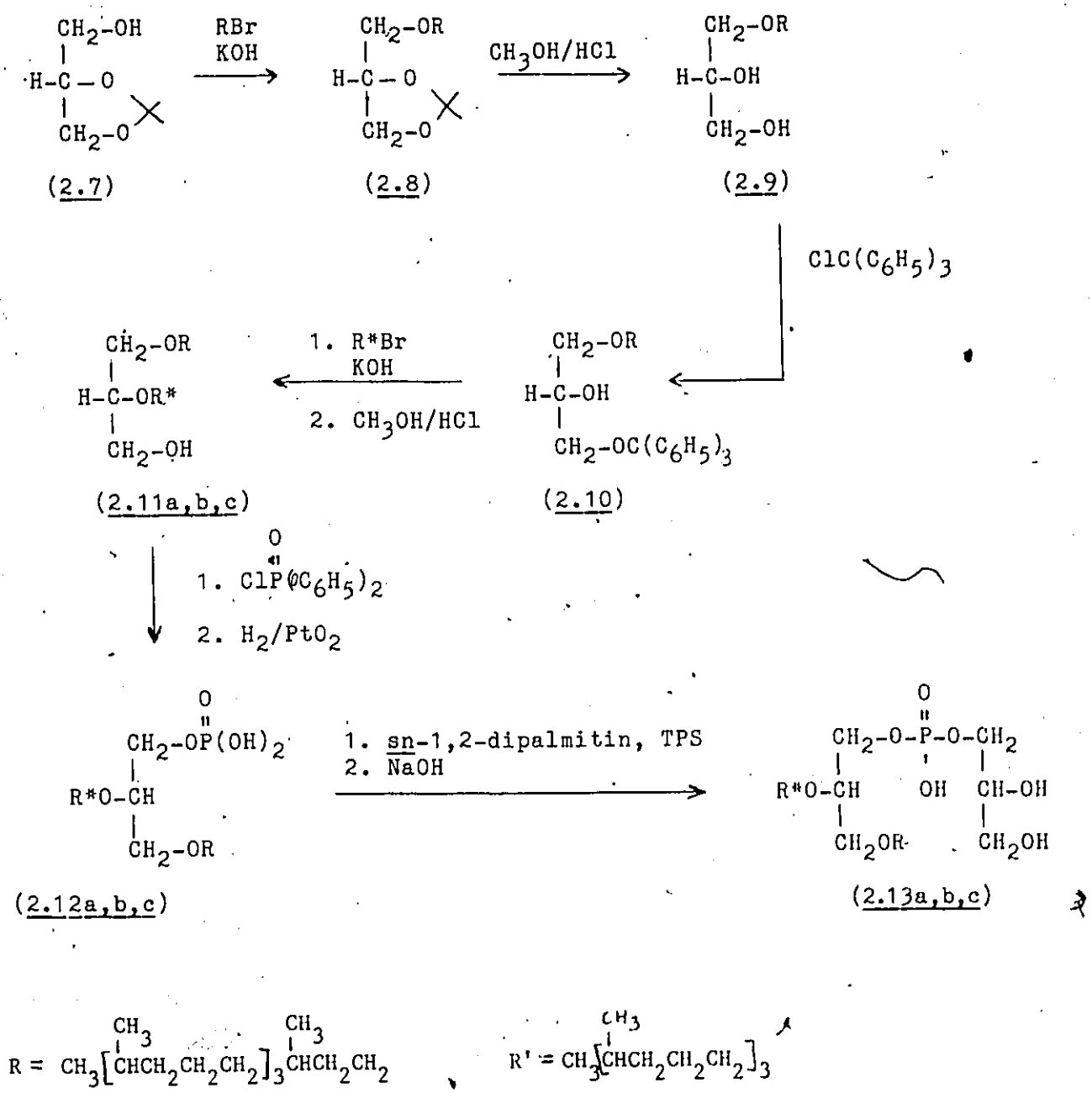

$$R = CH_3\left[CH(CH_3)CH_2CH_2CH_2\right]_3CH(CH_3)CH_2CH_2$$

$$R' = CH_3\left[CH(CH_3)CH_2CH_2CH_2\right]_3$$

Table II.1

^{13}C NMR Chemical shift values for diphtanylglycerol phospholipids

phytanol		diphytanylglycerol		PA		PG	
CS (ppm)	Assignments	CS (ppm)	Assignments	CS (ppm)	Assignments	CS (ppm)	Assignments
19.6-19.8	CH_3 19,20						
22.6-22.7	CH_3 16,17						
24.4-24.8	CH_2 5,9,13						
27.99	CH 15	as phytanyl		as phytanol		as phytanol	
29.8-32.9	CH 3,7,11						
36.6-36.7	CH_2 2,4						
37.1-37.7	CH_2 6,8,10 12,14						
39.4	CH_3 20						
61.9	CH_2-OH	61.4	G-1	64.9	G-1	63.6	G-1'
		67.7	C-1 (sn-2)	68.8	C-1 (sn-2)	65.9	G-1
		68.7	C-1' (sn-3)	69.9	C-1' (sn-3)	67.5	G-3'
		70.2	G-3	71.3	G-3	69.3	C-1 (sn-2)
		78.4	G-2	78.4	G-2	70.4	C-1'(sn-3)
						71.3	G-2'
						71.7	G-3
						78.7	G-2

^{1}H NMR: 0.8 ppm (doublet, CH_3); 1.2 ppm (CH_2); 3.4-3.8 ppm (multiplet; CH_2O, R_2CHO, CH_2OH).

^{13}C NMR: See Table II.1, Appendix A1.

CI/MS ($C_{43}H_{88}O_3$; FW=652): m/z, 653 (MH^+).

2.1.2 (R,R,R)-Phytanyl bromide (2.2) (Kates et al., 1965b)

A solution of boron tribromide (5 ml; 53 mmol) in anhydrous chloroform (50 ml) was added dropwise with stirring to a solution of diphytanyl glycerol (2.49 g; 3.8 mmol) in chloroform (200 ml). The reaction mixture was stirred at room temperature under anhydrous conditions for 24 hours then concentrated under reduced pressure. The oily residue was extracted with petroleum ether and the solution washed well with water and concentrated under reduced pressure to yield 2.4 g (87%) of phytanyl bromide (2.2) (yellow oil). TLC in petroleum ether showed one spot with R_f=0.8 and no residual diphytanyl glycerol (R_f=0.10).

IR: 2820-3005 cm^{-1} (CH_2, CH_3); 1480 cm^{-1} doublet (CH_2, CH_3); 1395 cm^{-1} doublet (isopropyl).

CI/MS ($C_{20}H_{41}Br$; FW=361): m/z, 281 $(M - Br)^+$, 359 $(M - 2)^+$, 361 $(M)^+$.

GC: $RT_{16:0}$=1.29 (synthetic phytanyl bromide standard, $RT_{16:0}$=1.29).

2.1.3 (R,R,R)-Phytanyl iodide (2.3) (Kates et al., 1965a)

A solution of diphytanylglycerol (1.14 g; 1.74 mmol) in 47% HI (40 ml) was heated under reflux for 24 hours. Care was taken to protect the reaction mixture from light. The reaction mixture was diluted with ethyl ether and the ether phase washed with

water, 10% KH_2CO_3 and water to neutrality and dried *in vacuo*. The phytanyl iodide was fractionated by column chromatography (50 g silicic acid) by elution with petroleum ether (200 ml). The petroleum ether eluates containing the desired product were concentrated under reduced pressure yielding 1.22 g (86 %) phytanyl iodide (2.3) (colourless oil). TLC in petroleum ether/ethyl ether (9:1) showed one spot with R_f=0.8 (phytanyl bromide standard, R_f=0.85).

IR: 2860-3000 cm^{-1}, 1480 cm^{-1} (CH_2, CH_3); 1390 cm^{-1} (doublet, isopropyl); 1190 cm^{-1} (isopropyl skeletal).

CI/MS ($C_{20}H_{41}I$; FW=408): m/z, 409 (MH^+).

2.1.4 (R,R,R)-Phytanyl acetate (2.4) (Kates et al., 1965a)

A mixture of phytanyl iodide (2.0 g; 5.5 mmol) and silver acetate (10 g; 5.9 mmol) in glacial acetic acid (150 ml) was heated under reflux for 72 hours. The reaction mixture was diluted with ethyl ether (100 ml), filtered, and the ether phase washed with water, saturated K_2HCO_3 and water to neutrality. The ether phase was concentrated under reduced pressure yielding 1.74 g (93%) phytanyl acetate (2.4) (colourless oil).

TLC in petroleum ether/ethyl ether (9:1) showed complete conversion to phytanyl acetate (R_f=0.38).

IR: 2830-2870 cm^{-1}, 1470 cm^{-1} (CH_2, CH_3); 1750 cm^{-1} (C=O ester); 1380 cm^{-1} (doublet, isopropyl); 1055 cm^{-1} (CH_2-O); 1245 cm^{-1} (C-O, acetate).

2.1.5 (R,R,R)-Phytanol (2.5)

A solution of phytanyl acetate (1.74 g; 5.3 mmol) in

methanolic HCl (0.6 N; 25 ml) was heated under reflux for 2 hours. The reaction mixture was diluted with water (3 ml) and the product extracted with petroleum ether. The ether extract was concentrated under reduced pressure and fractionated by column chromatography (30 g silicic acid) by eluting with petroleum ether (200 ml; fraction 1) and chloroform/methanol (1:1; 250 ml; fraction 2). Fraction 1 contained nonpolar impurities. Fraction 2, containing the desired product, was concentrated under reduced pressure yielding 1.4 g (89%) phytanol (2.5) (colourless oil). TLC in petroleum ether/ethyl ether (9:1) showed one spot with R_f=0.07 (synthetic phytanol standard, R_f=0.09) and no remaining acetate (R_f=0.4).

IR: 3360 cm^{-1} (OH); 2800-2880, 1472 cm^{-1} (CH_2, CH_3); 1385 cm^{-1} (doublet, isopropyl); 1060 cm^{-1} (C-O, alcohol).

^{13}C NMR: See Table II.1.

GC: $RT_{16:0}$= 1.02 (synthetic phytanol standard, $RT_{16:0}$= 1.04)

2.1.6 (R,R,R)-Methyl Phytanate (2.6) (Kates et al., 1967; Joo and Kates, 1969)

A solution of chromium trioxide (1.2 g; 12 mmol) in water (1.5 ml) was added dropwise with stirring to a solution of phytanol (R,R,R) (1.32 g; 4.4 mmol) in glacial acetic acid/acetone (1:2; 60 ml). The mixture was stirred at room temperature for one hour, diluted with water (100 ml) and solid sodium bisulfite was added until the mixture was green in colour. Sulfuric acid (10 %; 20 ml) was added to strongly acidify the reaction mixture and the phytanic acid was extracted with ethyl ether. The ether phase

was washed well with water until neutral and concentrated under reduced pressure. The crude product was taken up in a mixture of methanol (22.5 ml) and 5 N NaOH (2.5 ml) and the neutral byproducts (mostly phytanyl acetate and unreacted phytanol) were extracted with petroleum ether. The methanol phase was acidified and the desired acidic product extracted with petroleum ether. This fraction was concentrated under reduced pressure. The pure phytanic acid was converted to its corresponding methyl ester by heating under reflux in methanolic HCl (0.6 N; 5 ml) and extracting with petroleum ether as previously described, yielding 630 mg (44%) methyl phytanate (2.6) (colourless oil). TLC in petroleum ether/ethyl ether (9:1) showed one spot with R_f= 0.20 (acetate standard, R_f=0.60).

IR: 2850-2960 cm^{-1}; 1460 cm^{-1} (CH_2, CH_3); 2620 cm^{-1} (carboxyl); 1705 cm^{-1} (C=O); 1375 cm^{-1} (doublet, isopropyl).

GC/MS (methyl phytanate, $C_{21}H_{32}O_2$, FW=326): m/z, 325 $(M - 1)^+$, 326 $(M)^+$.

GC: $RT_{16:0}$= 1.99

2.2 Deuterated Intermediates

2.2.1 (R,R,R)-[1,1-$^2H_2$]phytanol (2.5a)

A solution of (R,R,R)-methyl phytanate (550 mg; 169 mmol) in anhydrous ethyl ether (20 ml) was added dropwise with stirring to a solution of $LiAl^2H_4$ (100 mg) in ethyl ether (20 ml) and the reaction mixture was stirred under anhydrous conditions at room temperature overnight. Excess $LiAl^2H_4$ was hydrolysed by the addition of isopropanol and the reaction mixture was diluted with

ethyl ether (100 ml) and washed successively with water, 0.2 N HCl, 2.5 % K_2HCO_3 and finally water to neutrality. The ether phase was concentrated under reduced pressure yielding 530 mg (95%) phytanol (2.5a) (colourless oil). TLC in petroleum ether/ethyl ether (2:1) showed one major spot with R_f=0.35 (phytanol standard R_f=0.34; phytanic acid methyl ester standard, R_f=0.70).

IR: 3350 cm^{-1} (OH); 2880-2980, 1475 cm^{-1} (CH_2, CH_3), 1390 cm^{-1} (doublet, isopropyl).

GC/MS ($C_{20}H_{40}{}^2H_2O$; FW=300): m/z, 282 $(M - NH_4)^+$; 252 $(M - (CH_2C^2H_2OH))^+$.

GC: $RT_{16:0}$= 1.01 (synthetic phytanol standard, $RT_{16:0}$= 1.04)

2.2.2. (R,R,R)-[1,1-$^2H_2$]phytanyl bromide (2.2a) (Kates et al., 1965a)

A mixture of (R,R,R)-[1,1-$^2H_2$]phytanol (530 mg, 1.77 mmol) in 47% HBr (5 ml), water (5 ml) and concentrated sufuric acid (0.5 ml) was heated under reflux for 24 hours. The reaction mixture was diluted with water and extracted with several portions of ethyl ether. The pooled ether fractions were washed with water to neutrality, diluted with benzene and concentrated under reduced pressure. The crude brown oil was fractionated by column chromatography (25 g silicic acid) by elution with petroleum ether. The fractions containing the desired compounds were pooled, concentrated under reduced pressure and dried *in vacuo* yielding 544.5 g (85 %) of (R,R,R)-[1,1-$^2H_2$]phytanyl bromide (2.2a) (pale yellow oil).

IR: 2850-2960 cm^{-1} (CH_2), 2900, 1480 cm^{-1} (CH_3); 1385 cm^{-1} (isopropyl).

CI/MS ($C_{20}H_{39}{}^2H_2Br$, FW= 363): m/z, 281 $(M - Br - 2)^+$, 361 $(M - 2)^+$, 363 $(M)^+$.

GC: $RT_{16:0}$= 1.31 (non-deuterated (R/S,R,R)-phytanyl bromide standard, $RT_{16:0}$=1.29).

2.2.3 (R,R,R)-[2,2-$^2H_2$]Phytanol (2.5b) (Tulloch, 1977)

(R,R,R)-Phytanic acid (840 mg; 2.69 mmol) was converted to the sodium salt by titration in chloroform with 0.2N methanolic NaOH. Sodium phytanate and 1% NaO^2H in ^2H_2O (25 - 30 ml) were heated at 200°C for 3 days in a sealed ampule. The reaction mixture was acidified with concentrated HCl and the product was extracted with chloroform. The extract was washed well with methanol/ water (1:0.8), diluted with benzene and concentrated under reduced pressure yielding 670 mg (79.9% from the corresponding methyl ester) phytanic acid (colourless oil).

An aliquot of the residual [2,2-$^2H_2$]phytanic acid (300 mg; 0.920 mmol) was converted to the corresponding methyl ester and reduced with $LiAlH_4$ as described above for methyl-[1,1-$^2H_2$]phytanate. The reduced product was purified by column chromatography yielding 210 mg (76.7%) of [2,2-$^2H_2$]phytanol (2.5b).

TLC in petroleum ether/ethyl ether (2:1) showed one spot with R_f=0.35 (phytanol standard, R_f=0.34; methyl phytanate standard, R_f=0.7).

IR: 3450 cm^{-1} (OH); 2850-2960, 1485 cm^{-1} (CH_2, CH_3); 1395 cm^{-1} (isopropyl).

GC/MS ($C_{20}H_{40}{}^2H_2O$; FW=300): m/z, 282 $(M - H_2O)^+$, 252 $(M - C^2H_2CH_2OH)^+$

GC: $RT_{16:0}$= 1.01 (synthetic phytanol standard, $RT_{16:0}$= 1.04)

^2H NMR: 2.205, 2.046 ppm (theoretical, 2.0 - 2.2).

2.2.4 (R,R,R;)-[2,2-$^2H_2$]phytanyl bromide (2.2b)

[2,2-$^2H_2$]phytanol (210 mg; 0.705 mmol) was converted to the corresponding bromide as described above yielding 230 mg (91%) [2,2-$^2H_2$]phytanyl bromide (pale yellow oil).

CI/MS ($C_{20}H_{35}{}^2HBr$, FW= 363): m/z, 363 $(M)^+$, 361 $(M - 2)^+$.

GC: $RT_{16:0}$= 1.31 (R/S,R,R)-phytanyl bromide standard, $RT_{16:0}$= 1.29)

2.2.5 sn-3-phytanylglycerol (2.9) (Joo and Kates, 1969)

A mixture of sn-1,2-isopropylidene glycerol (2.7) (1.25 g; 9.5 mmol), phytanyl bromide (R,R,R; 1.72 g; 4.78 mmol) and powdered KOH (10 g) in anhydrous benzene (25 ml) were heated under reflux under anhydrous conditions for 48 hours. A Dean-Stark phase separating head was used to remove water produced in the reaction. TLC of the reaction products in petroleum ether/ethyl ether (9:1) showed complete conversion to phytanylisopropylidene glycerol (2.8) (R_f=0.2). The reaction mixture was diluted with ethyl ether, washed successively with water, 0.2N HCl, 10% KH_2CO_3 and water, and concentrated under reduced pressure. The crude product was purified by column chromatography (20 g silicic acid) by elution with petroleum ether (200 ml; fraction 1), petroleum ether/ethyl ether (9:1; 75 ml, fraction 2; 125 ml, fraction 3; 125 ml, fraction 4) and petroleum ether/ethyl ether

(4:1; 200 ml, fraction 5). Fractions 1 and 2 contained non-polar impurities. Fractions 4 and 5 contained polar impurities, primarily excess isopropylidene glycerol. Fraction 3, containing pure phytanylisopropylidene glycerol, was concentrated under reduced pressure. TLC in petroleum ether/ethyl ether showed one spot with R_f=0.5.

The phytanyl isopropylidene glycerol was heated under reflux for 3 hours in methanolic/HCl (0.2 N; 200 ml). After dilution of the reaction mixture with 10% water, the product was extracted with several portions of petroleum ether and the pooled ether extracts were washed with water and concentrated under reduced pressure, yielding 1.06 g (60% from isopropylidene glycerol) of phytanylglycerol (colourless oil). Thin layer chromatography in petroleum ether/ethyl ether (1:1) showed one spot (R_f=0.12) corresponding to monophytanylglycerol (2.9) (diphytanyl glycerol standard, R_f=0.50).

IR: 3495 cm^{-1} (OH); 2980-3200, 1480 cm^{-1} (CH_2, CH_3); 1395 cm^{-1}, 1135 cm^{-1} (C-O-C, ether).

2.2.6 sn-1-Trityl-3-phytanylglycerol (2.10) (Chaudhary and Hernandez, 1979)

A mixture of sn-3-phytanylglycerol (1.06 g; 2.85 mmol), trityl chloride (1.0 g; 3.58 mmol), dimethylaminopyridine (DMAP) (17 mg; 0.14 mmol) and triethylamine (12 ml) in dimethylformamide (15 ml) was stirred at room temperature under anhydrous conditions for 1.5 days. The reaction mixture was diluted with methylene chloride and washed successively with water, 0.2 N HCl, 10%

KH_2CO_3 and water and concentrated under reduced pressure. TLC of the reaction products in petroleum ether/ethyl ether (9:1) showed complete conversion to tritylphytanylglycerol (R_f=0.15) (phytanylglycerol, R_f=0.35). The crude product was purified by column chromotography (25 g) by elution with petroleum ether (100 ml, fraction 1), petroleum ether/benzene (2:1; 200 ml, fraction 2; 1:2; 200 ml, fraction 3) and benzene (100 ml, fraction 4). Fraction 1 contained non-polar material, fraction 2 contained the desired compound as well as tritanol and ditrityl ether and fractions 3 and 4 contained tritanol and polar impurities. Fraction 2 was concentrated under reduced pressure and dissolved in chloroform (5 ml). A tenfold excess of petroleum ether was added to precipitate the tritanol. After cooling at 4°C for 24 hours, the tritanol was removed by centrifugation and the supernatant was concentrated under reduced pressure. This precipitation step was repeated until TLC indicated that no tritanol remained in the sample. The supernatant was concentrated under reduced pressure yielding 0.66 g (38 % from phytanyl glycerol) of tritylphytanylglycerol (2.10) (yellow oil). TLC in petroleum ether/ethyl ether (9:1) showed one trityl-containing spot (R_f=0.18) and no free tritanol (R_f=0.22).

IR: 3480 cm^{-1} (OH); 3060 , 1600, 1500 cm^{-1} (aromatic); 2880-2970, 1485 cm^{-1} (CH_2, CH_3); 1385 cm^{-1} (isopropyl), 1105 cm^{-1} (C-O-C; ether).

CI/MS: ($C_{42}H_{62}O_3$; FW=614): m/z, 615 (MH+); 537 $(M - C_6H_5)^+$; 371 $(M - C_{19}H_{15})^+$; 243 $(C_{19}H_{15})^+$.

2.2.7 sn-2,3-Diphytanylglycerol (2.11a,b or c)

A solution of sn-1-trityl-3-phytanylglycerol (285 mg; 0.46 mmol), phytanyl bromide ([1,1-$^2H_2$]-, 220 mg; 0.34 mmol; [2,2-$^2H_2$]-, 180 mg; 0.28 mmol; or [2,3-$^2H_2$]-, 280 mg; 0.43 mmol) and powdered KOH (0.5 g) in anhydrous benzene (15 ml) was heated under reflux for 36 hours with a phase separating head. The product was extracted as described above. TLC of the reaction mixture in petroleum ether/ethyl ether (8.5:1.5) showed almost complete conversion of the 1-trityl-3-phytanylglycerol (R_f=0.25) to the 1-trityl-2,3-diphytanylglycerol (R_f=0.8). The mixture was fractionated by column chromatography (10 g silicic acid) by eluting with petroleum ether (100 ml; fraction 1), petroleum ether/benzene (4:1; 150 ml; fraction 2), petroleum ether/benzene (1:1; 100 ml; fraction 3) and chloroform (100 ml; fraction 4). Fractions 1 and 2 contained the desired 1-trityl-2,3-diphytanylglycerol together with smaller amounts of unreacted phytanylbromide, ditrityl ether and tritanol. Fractions 3 and 4 contained tritanol and unreacted tritylphytanylglycerol. Fractions 1 and 2 were pooled and concentrated under reduced pressure and detritylated by heating under reflux in methanolic HCl (0.6 N) overnight. The mixture was extracted with petroleum ether and the pooled extracts were washed well with water and concentrated under reduced pressure. TLC in petroleum ether/ethyl ether (8.5:1.5) showed complete conversion to diphytanylglycerol (R_f=0.26), (natural diether standard, R_f=0.28)

The crude reaction mixture was purified by column

chromatography (15 g silicic acid) by eluting with petroleum ether (100 ml; fraction 1), petroleum ether/benzene (4:1; 400 ml; fraction 2) and chloroform (300 ml; fraction 3). Fraction 1 contained unreacted phytanylbromide and fraction 2 contained dityrityl ether and tritanol. Fraction 3, containing the desired compound and trace amounts of tritanol, was concentrated under reduced pressure, dissolved in chloroform and a ten-fold excess of petroleum ether was added to precipitate the tritanol. After cooling to 4°C for 24 hours, the tritanol was removed by centrifugation and the supernatant was concentrated under reduced pressure.

Yields:

sn-2-[1,1-$^2H_2$]-(R,R,R)-phytanyl-3-(R,R,R)-phytanylglycerol

190 mg (85% from tritylphytanylglycerol) (2.11a)

sn-2-[2,2-$^2H_2$]-(R,R,R)-phytanyl-3-(R,R,R)-phytanylglycerol

80 mg (44% from tritylphytanylglycerol) (2.11b)

sn-2-[2,3-$^2H_2$]-(R/S,R,R)-phytanyl-3-(R,R,R)-phytanylglycerol

260 mg (93% from tritylphytanylglycerol) (2.11c)

TLC of the products in petroleum ether/ethyl ether (4:1) showed one spot with R_f= 0.31-0.33 (natural undeuterated standard, R_f= 0.30)

IR: 3450 cm^{-1} (OH); 2860-2960, 1465 cm^{-1} (CH_2, CH_3); 1380 cm^{-1} (doublet, isopropyl); 1120 cm^{-1} (C-O-C); 1050 cm^{-1} (C-OH, alcohol).

CI/MS ($C_{43}H_{86}{}^2H_2O_3$; FW=654): m/z, 655 (MH^+), 373 $(M - 281)^+$.

2.2.8 Diphytanyl PA (2.12a,b or c) (Kates et al., 1971)

Deuterated diphytanylglycerols ([1,1-$^2H_2$], [2,2-$^2H_2$] and [2,3-$^2H_2$]) were converted to the corresponding diphytanylglycerolphosphate as described in section 5.

TLC in chloroform/methanol/NH_4OH (65:35:5) showed one phosphorus positive spot with R_f= 0.1

Yields:

sn-2-[1,1-$^2H_2$]-(R,R,R)-phytanyl-3-(R,R,R)-phytanylglycerol phosphate

83 mg (38% from diether) (2.12a)

sn-2-[2,2-$^2H_2$]-(R,R,R)-phytanyl-3-(R,R,R)-phytanylglycerol phosphate

15.2 mg (16% from diether) (2.12b)

sn-2-[2,3-$^2H_2$]-(R/S,R,R)-phytanyl-3-(R,R,R)-phytanylglycerol phosphate

102.2 mg (35% from diether) (2.12c)

Negative FAB/MS (deuterated $PA(NH_4)_2$; FW= 768): m/z, 751 $(M - NH_4)^-$.

2.2.9 sn-2,3-Diphytanylglycerol-1-phosphate-3'-glycerol (2.13a,b or c)

Labelled diphytanylglycerol-1-phosphate was converted to the corresponding PG as described in section 7.

sn-2-[1,1-$^2H_2$]-(R,R,R)-phytanyl-3-(R,R,R)-phytanylglycerol phosphoryl glycerol

17.3 mg (19% from PA) (2.13a)

sn-2-[2,3-$^2H_2$]-(*R/S,R,R*)-phytanyl-3-(*R,R,R*)-phytanylglycerol phosphoryl glycerol

8.7 mg (7.5% from PA) (*2.13c*)

TLC in chloroform/methanol/NH_4OH (65:35:5) showed one phosphorus positive spot for each sample with R_f= 0.51 (PG standard, R_f= 0.50).

Negative FAB/MS (deuterated PG-NH_4; FW= 823): m/z, 805 (M - NH_4OH).

3. (R/S,R)-Diphytanylglycerol phospholipids

3.1 Deuterated Hydrocarbon Chains

The detailed schemes for the syntheses of labelled (R/S,R,R)-phytanyl chains are shown in Figure II.7 and the structures are shown in Figure II.4. The diagnostic ^{13}C NMR chemical shift data are summarized after each step. Spectra are shown in Appendix A.

3.1.1 (R/S,R,R)-Phytanol (3.2) (Kates et al., 1965b)

Phytol (5 g; 17 mmol; Aldrich, 80%) in methanol (75 ml) was converted to phytanol by catalytic hydrogenation with platinum oxide (250 mg). The catalyst was removed by centrifugation and the supernatant was concentrated under reduced pressure yielding 4.3 g (95%) phytanol (3.2) (oil).

IR: 3410 cm^{-1} (OH); 2850-2960, 1485 cm^{-1} (CH_2, CH_3); 1385 cm^{-1} (isopropyl); 1060 cm^{-1} (C-O-H).

CI/MS ($C_{20}H_{43}O$, FW= 298): m/z, 299 (MH^+); 280 $(M - NH_4)^+$.

GC: $RT_{16:0}$= 1.04 (phytanol standard, $RT_{16:0}$= 1.04).

3.1.2. (R/S,R,R) [1,1-$^2H_2$] phytanol (3.2a)

[1,1-$^2H_2$]Phytanol (R/S,R,R) was prepared from phytanic acid (R/S,R,R) as described in section 2, yeilding 4.5 g (86%) (colourless oil).

CI/MS ($C_{20}H_{40}{}^2H_2O$; FW=300): m/z, 301 (MH^+).

GC: $RT_{16:0}$= 1.01 (synthetic phytanol standard 1.04)

GC/MS ($C_{20}H_{41}{}^2H_2O$; FW= 300): m/z, 282 $(M - H_2O)^+$.

3.1.3 (R/S,R,R)-[2,3-$^2H_2$]phytanol (3.2c)

[2,3-$^2H_2$]Phytanol was prepared by catalytic reduction of phytol (5.0 g; 16.8 mmol) with $^2H_2$ and platinum oxide (250 mg) in

Figure II.7

Synthesis of deuterated (R/S,R,R)-diphytanylglycerol phospholipids

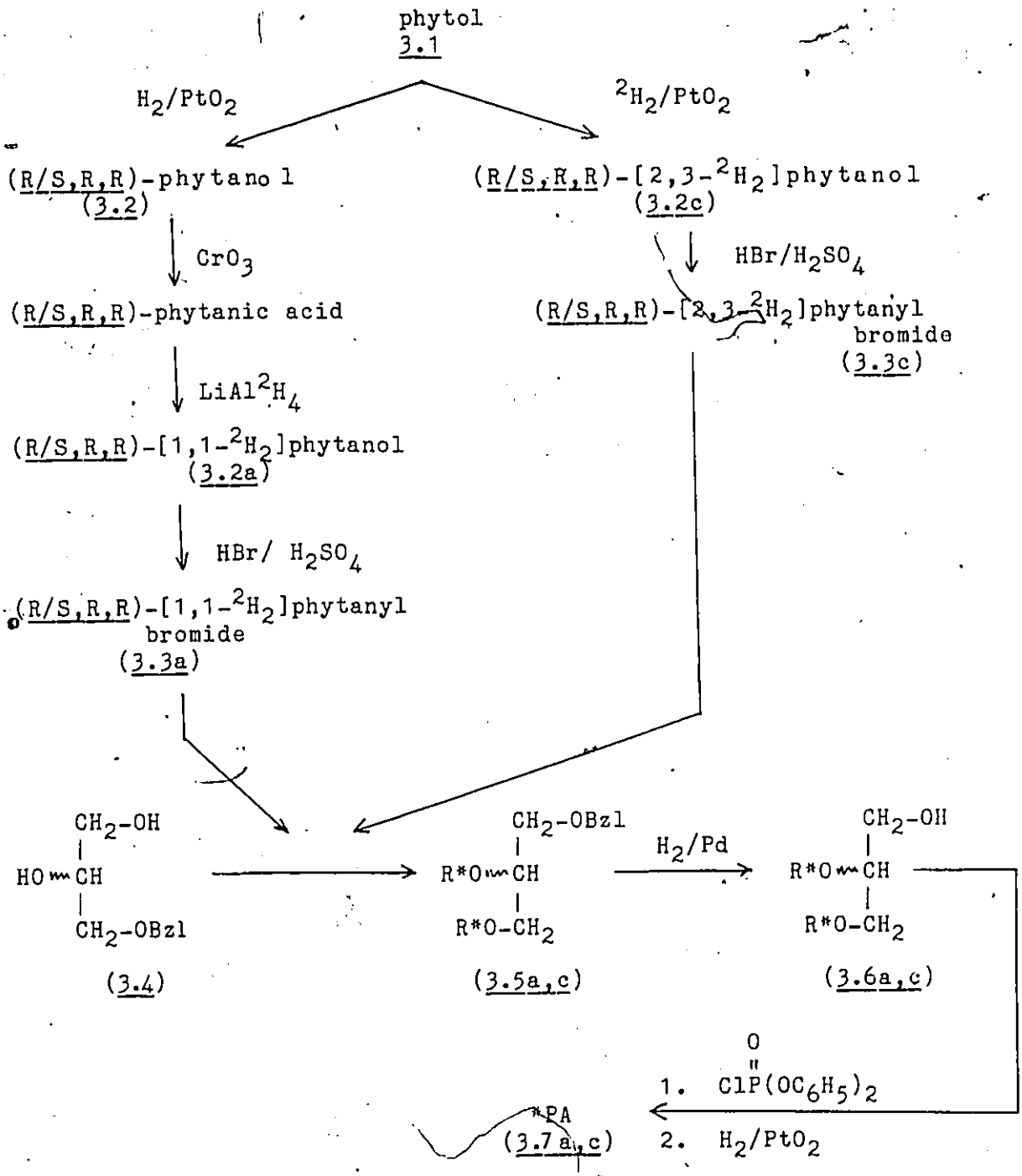

methanol (CH_3O^2H). The catalyst was removed by centrifugation and the supernatant was concentrated under reduced pressure yielding 4.9 g (97%) (colourless oil).

IR: 3450 cm^{-1} (OH); 2870-2980, 1470 cm^{-1} (CH_2, CH_3); 1380 cm^{-1} (doublet, isopropyl); 1050 cm^{-1} (C-OH, alcohol).

CI/MS ($C_{20}H_{40}{}^2H_2O$; FW= 300): m/z, 300 $(M)^+$, 301 MH^+).

GC: $RT_{16:0}$= 1.03 (synthetic phytanol standard, $RT_{16:0}$=1.04).

^{13}O NMR: as for phytanol but with multiplet at 27 ppm ($C^2H_2CH_2$-OH) at long recycle times.

^2H NMR: 1.55 ppm (triplet).

3.1.4 (R/S,R,R)-Phytanyl bromide (3.3a,c, or unlabelled) (Kates et al., 1965b)

A mixture of (R/S,R,R)-phytanol (unlabelled, or [1,1-$^2H_2$]- or [2,3-$^2H_2$]-labelled) (4.3 g; 14.4 mmol) in 47% HBr (50 ml), water (50 ml) and concentrated sulfuric acid (5 ml) was heated under reflux for 24 hours. The reaction mixture was diluted with water and extracted with several portions of ethyl ether. The pooled ether fractions were washed with water to neutrality, diluted with benzene and concentrated under reduced pressure. The crude brown oil was fractionated by column chromatography (25 g silicic acid) by elution with petroleum ether. The fractions containing the desired product were concentrated under reduced pressure and dried in vacuo yielding 3.95 g (76%) phytanyl bromide (3.3) (and 3.3a or c) (yellow oil).

IR: 2950-2960, 1480 cm^{-1} (CH_2, CH_3), 1385 cm^{-1} (isopropyl).

CI/MS ($C_{20}H_{39}Br$; FW=361): m/z, 361 $(M)^+$, 359 $(M - 2)^+$.

($C_{20}H_{38}{}^2H_2Br$; FW=363): 363 $(M)^+$, 361 $(M - 2)^+$.

GC: phytanyl bromide, $RT_{16:0}$= 1.29; [1,1-$^2H_2$]phytanyl bromide, $RT_{16:0}$= 1.31; [2,3-$^2H_2$]phytanyl bromde, $RT_{16:0}$= 1.30 (natural phytanyl bromide standard, $RT_{16:0}$= 1.29).

GC/MS ($C_{20}H_{41}Br$; FW= 361): m/z, 257, 359 $(M - CH_3 - Br)^+$

3.1.5 Diphytanylglycerol

A mixture of (R/S,R,R)-phytanyl bromide (undeuterated) (3.5 g; mmol), rac-1-benzyl glycerol (0.84 g; 4.6 mmol), finely powdered KOH (2.6 g) and anhydrous benzene (50 ml) was heated under reflux under anhydrous conditions for 24 hours. The reaction mixture was extracted with several portions of ethyl ether and the pooled ether extracts were washed successively with water, 0.2 N HCl, 2.5% KH_2CO_3 and water, and concentrated under reduced pressure. The crude diether was fractionated by column chromatography (25 g silicic acid) by elution with petroleum ether (200 ml; fraction 1), chloroform (200 ml; fraction 2), ethyl ether (150 ml; fraction 3) and methanol (100 ml; fraction 4). The pooled fractions containing the benzyl diphytanylglycerol (fractions 2 and 3) were concentrated under reduced pressure yielding 3.32 g (91%) (colourless oil).

The benzyl group was removed by hydrogenolysis in ethyl acetate (20 ml) with 10% palladium on charcoal (250 mg). The catalyst was removed by centrifugation, washed well with ethyl acetate and the pooled supernatants we concentrated under reduced pressure and dried in vacuo. The crude diether was purified by column chromatography (60 g silicic acid) by elution with petroleum ether (150 ml; fraction 1), petroleum ether/ethyl ether

(1:1; 250 ml; fraction 2), ethyl ether (150 ml; fraction 3), chloroform (150 ml; fraction 4) and methanol (150 ml; fraction 5). The fractions containing the desired product (fractions 2-4) were concentrated under reduced pressure, yielding 1.13 g (40% from benzyl diether) diphytanylglycerol (3.6) (yellowish oil).

TLC in petroleum ether/ethyl ether (8:2) showed one spot with R_f=0.3 (natural diether standard, R_f=0.23).

IR: 3440 cm^{-1} (OH); 2910, 1474 cm^{-1} (CH_2, CH_3), 1380 cm^{-1} (isopropyl); 1113 cm^{-1} (C-O-C ether); 1050 cm^{-1} (C-O, alcohol);

CI/MS (FW=652): m/z, 653 (MH^+).

3.1.6 (R/S,R,R)-[1,1,1',1'-$^2H_4$]Diphytanylglycerol (3.6a)

rac-1-Benzyl glycerol (0.54 g; 2.9 mmol), [1,1-$^2H_2$]phytanyl bromide (2.34 g; 6.45 mmol) and powdered KOH (1.5 g) in anhydrous benzene were heated under reflux as described in section 2. After extraction, the crude benzyl diphytanyl glycerol was converted to diphytanylglycerol by hydrogenolysis with 10% palladium on charcoal (150 mg) in freshly distilled ethanol (20 ml), then fractionated by column chromatography as described above, yielding 0.62 grams (29% from benzyl glycerol) of 2,3-[1,11',1'-$^2H_4$]phytanyl glycerol (3.6a) (colourless oil).

TLC in petroleum ether/ethyl ether (4:1) showed one spot with R_f= 0.20 (natural diether standard, R_f= 0.19).

IR: 3500 cm^{-1} (OH); 2880-2960, 1475 cm^{-1} (CH_2, CH_3); 1390 cm^{-1} (doublet, isopropyl); 1050-1140 cm^{-1} (C-O-C, ether; C-OH, alcohol).

CI/MS ($C_{46}H_{51}{}^2H_2O_6$, FW= 656): m/z, 657 (MH^+).

^{13}C NMR: 62.81 ppm (G-1); 71.43 ppm (G-3); 79.75 ppm (G-2). With long recycle times, additional multiplets at 67.91 ppm (C-1) and 69.41 ppm (C-1') were observed (Appendix A3).

3.1.7 rac-1,2-[2,3,2',3'-$^2H_4$]Diphytanylglycerol (3.6c)

rac-1,2-[2,3,2',3'-$^2H_4$]Phytanylglycerol was prepared by reacting benzyl glycerol (0.66g; 3.63 mmol) with [2,3,2',3'-$^2H_4$]phytanyl bromide (0.323 g; 3.23 mmol) as described above, yielding 0.73 g (28% from benzyl glycerol) (3.6c) (colourless oil).

TLC in petroleum ether/ethyl ether (8:1) showed one spot with R_f=0.20 (natural diether standard, 0.19).

IR: 3400 cm^{-1} (OH); 2880-3000 , 1475 cm^{-1} (CH_2, CH_3); 1390 cm^{-1} (doublet, isopropyl)

CI/MS ($C_{46}H_{51}{}^2H_2O_6$, FW= 656): m/z, 657 (MH^+).

^{13}C NMR: 62.10 ppm (G-1); 71.20 ppm (G-3); 79.24 ppm (G-2); 68.4 ppm (C-1), 69.3 ppm (C-1'). Absence of a peak at 29.8 ppm.

3.1.8 rac-1,2-(R/S,R,R)-Diphytanylglycerol-1-phosphate (3.7a or c)

2,3-(R/S,R,R)-[1,1,1',1'-$^2H_4$]Diphytanylglycerol (3.6a) and [2,3,2',3'-$^2H_4$]diphytanylglycerol (3.6c) were converted to the corresponding PA as described in section 5.

Yields:

rac-2,3-(R/S,R,R)-[1,1,1',1'-$^2H_4$]Diphytanylglycerol-1-phosphate: 267.7 mg (37%)

rac-2,3-(R/S,R,R)-[2,3,2',3'-$^2H_4$]Diphytanylglycerol-1-phosphate: 108.8 mg (42%)

TLC in $CHCl_3/CH_3OH/NH_4OH$ (65:35:5) showed one spot for each compound with R_f= 0.25 for [1,1,1',1'-$^2H_4$]DPhPA and 0.21 for [2,3,2',3'-$^2H_4$]DPhPA (0.22 for unlabelled diphytanylglycerol phosphate standard)

Negative FAB (deuterated PA($N\bar{H}_4$); FW= 829): 810 $(MH - NH_4)^-$.

3.2 Deuterated Glycerol Backbone

The scheme for the synthesis of diphytanyl phospholipids labelled in the backbone glycerol is shown in Figure II.8.

3.2.1 rac-[1,1-$^2H_2$]-3-tritylglycerol (3.12d) (Kates et al., 1966)

rac-Glyceric acid hemi-calcium salt (4 g; 14.0 mmol) was converted to the free-acid form by stirring with Dowex 50W-X8 (40 g) in methanol/water (1:1; 150 ml) for 2 hours. The Dowex was removed by centrifugation and the supernatant was diluted with ethanol and benzene and concentrated under reduced pressure.

The free acid was converted to the corresponding methyl ester by heating under reflux in methanolic HCl (0.6 N; 80 ml) for 4 hours. The reaction mixture was diluted with ethyl ether and the ether phase was washed with water and concentrated under reduced pressure, yielding 3.35 g (87%) of methyl glycerate (3.10) (colourless oil).

IR: 3400 cm^{-1} (OH); 1740 cm^{-1} (C=O ester); 1440 cm^{-1} (OCH_3); 1240 cm^{-1} (C-O, ester); 1130 cm^{-1} (sec C-OH); 1070 cm^{-1} (primary C-OH).

A solution of methyl glycerate (3.10) (3.35 g; 2.79 mmol) in anhydrous pyridine (20 ml) was added dropwise with stirring to a mixture of trityl chloride (17 g; mmol) in anhydrous pyridine (20 ml). The reaction mixture was stirred under anhydrous conditions at room temperature overnight. The reaction mixture was then diluted with ethyl ether and the ether phase washed with water, 0.2 N HCl, 2.5% KH_2CO_3 and water to neutrality, and concentrated under reduced pressure. TLC of the reaction products in petroleum ether/ethyl ether (9:1) showed the presence of tritanol

Figure II.8

Synthesis of diphytanylglycerol phospholipids deuterated in the glycerol backbone

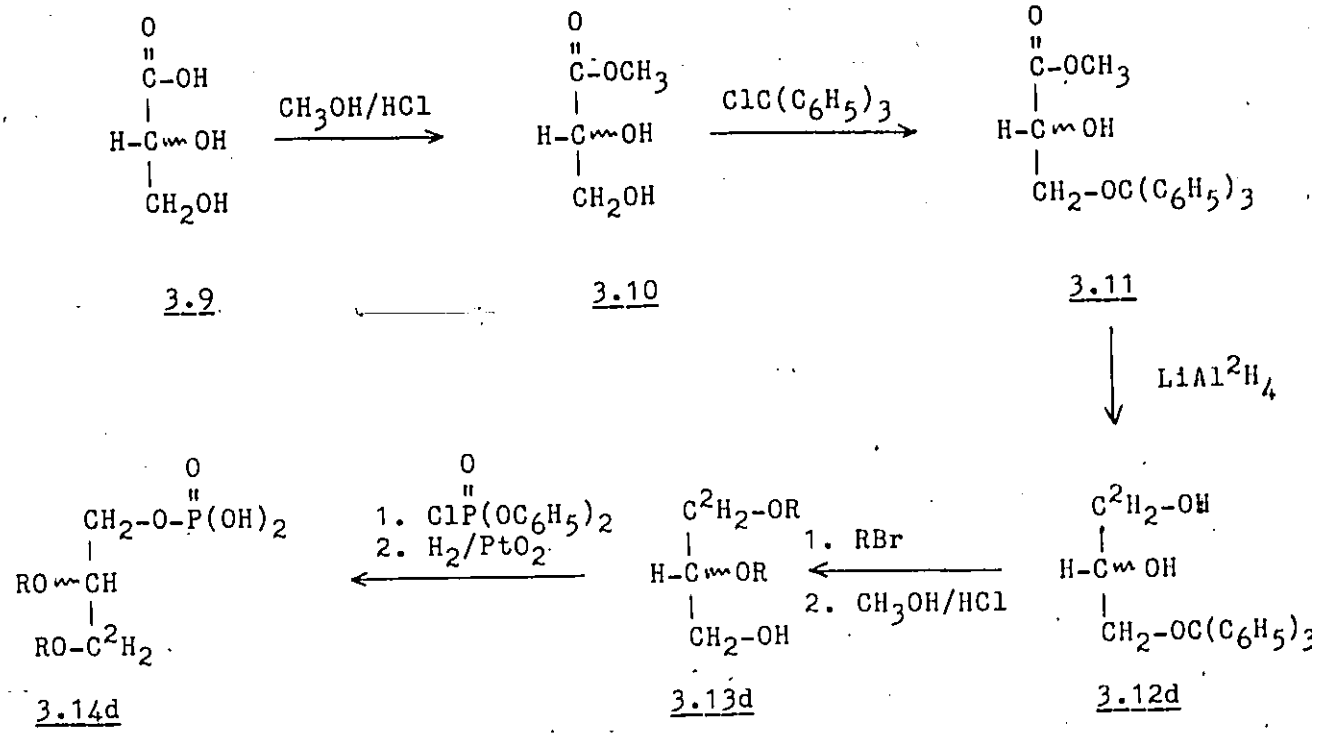

3.9 3.10 3.11 3.12d 3.13d 3.14d

(R_f=0.21) and ditrityl ether (R_f=0.76) as well as the desired product (R_f=0.13). The crude product was dissolved in chloroform/ methanol (5:1; 5 ml), diluted with petroleum ether (5 ml) and kept at 4°C for 3 days to precipitate excess tritanol. The crystallized tritanol was removed by centrifugation and the supernatant was concentrated under reduced pressure. The procedure was repeated until the tritanol no longer precipitated. TLC in petroleum ether/ethyl ether (9:1) showed a trityl-positive spot (3-trityl methyl glycerate) (R_f=0.14) (3.11) as well as traces of tritanol (R_f=0.38) and ditrityl ether (R_f=0.85).
IR: 3510 cm^{-1} (OH); 1760, 1108 cm^{-1} (C=O, C-O, ester); 1610, 1510, 770, 645 cm^{-1} (aromatic); 1455 (OCH_3); 1075 cm^{-1} (C-OH, alcohol).

A solution of the crude 3-trityl methyl glycerate (3.11) in anhydrous ethyl ether (10 ml) was added dropwise, with stirring, to a suspension of $LiAl^2H_4$ (1.0 g) in anhydrous ethyl ether (25 ml) and the mixture was stirred overnight at room temperature. Water-saturated ether was added to hydrolyse excess $LiAl^2H_4$ and the reaction mixture was diluted with ethyl ether (50 ml) and washed successively with water, 0.2 N HCL, 2.5% KH_2CO_3 and water to neutrality and concentrated under reduced pressure yielding 5.8 g (64% from methyl glycerate) of rac-[1,1-$^2H_2$]-3-trityl-glycerol (3.12 d) (colourless solid).
TLC in petroleum ether/ethyl ether (1:1) showed one major trityl-positive spot with R_f=0.2.
IR: 3440 cm^{-1} (OH); 1085 cm^{-1} (sec C-OH); 3080, 1605, 1500, 655,

770 cm^{-1} (aromatic); 1455 cm^{-1} (OCH_3); 1080 cm^{-1} (C-O-C).

3.2.2. rac-1,2-Diphytanyl-[1,1-$^2H_2$]glycerol (3.13d).

rac-[1,1-$^2H_2$]-3-tritylglycerol (800 mg; 2.35 mmol), phytanyl bromide (R/S,R,R) (3.8 g; 10.53 mmol) and powdered KOH (2.9 g) in anhydrous benzene (40 ml) were heated under reflux for 2 days. A Dean-Stark phase separating head was used to remove water formed during the reaction. The reaction mixture was diluted with ethyl ether and the ether phase washed successively with water, 0.2N HCl, 10% KH_2CO_3 and water and concentrated under reduced pressure.

The residual reaction mixture was heated under reflux with 0.6 N methanolic HCl (200 ml) for 16 hours, diluted with water (10%) and extracted with several portions of petroleum ether. The pooled petroleum ether phases were washed well with water and concentrated under reduced pressure.

TLC in petroleum ether/ethyl ether (9:1) showed complete conversion to diphytanylglycerol (R_f=0.15).

The crude mixture was fractionated by column chromatography (80 g silicic acid) by elution with petroleum ether (400 ml; fraction 1), petroleum ether/benzene (1:1; 200 ml; fraction 2), benzene (300 ml; fraction 3) and chloroform (200 ml; fraction 4). Fraction 1 contained non-polar impurities. Fractions 2 and 3 contained tritanol and trace amounts of the diether. Fraction 4, containing the desired diether and trace amounts of tritanol, was concentrated under reduced pressure.

The crude mixture was dissolved in a minimum of chloroform and

the tritanol was precipitated with a tenfold excess of petroleum ether. After cooling at 4°C overnight, the tritanol was removed by centrifugation and the supernatant was concentrated under reduced pressure, yielding 1.0 g (65% from trityl glycerol) of rac-1,2-diphytanyl-[1,1-$^2H_2$]glycerol (3.13d) (colourless oil).

CI/MS ($C_{43}H_{86}{}^2H_2O_3$; FW=654): m/z, 655 (MH^+).

TLC in petroleum ether/ethyl ether (4:1) showed one spot with R_f= 0.31 (natural diether standard, R_f= 0.30).

IR: 3380 cm^{-1}(OH), 2880-3000, 1475 cm^{-1} (CH_2, CH_3), 1385 cm^{-1} (isopropyl), 1070 cm^{-1} (C-O-C).

^{13}C NMR: 62.87 ppm (G-1); 69.02 ppm (C-1); 70.27 ppm (C-1'); 79.73 ppm (G-2) (see Appendix A3).

3.2.3 rac-2,3-Diphytanyl-[3,3-$^2H_2$]glycerol-1-phosphate (3.14d)

rac-1,2-Diphytanyl-[1,1-$^2H_2$]glycerol (1.0 g; 1.53 mmol) was converted to the corresponding PA by reaction with $ClP(O)(OC_6H_5)_2$ as described in section 5. The crude material was purifed by TLC in chloroform/methanol/NH_4OH (65:35:5); overall yield, 180 mg (15.6 %) of rac-2,3-Diphytanyl-[3,3-$^2H_2$]glycerol-1-phosphate (3.14d). TLC in the same solvent system showed one phosphorus-positive spot with R_f= 0.1.

Negative FAB/MS (PA-H_2; FW= 734): m/z, 733 $(M - H)^-$.

^2H NMR spectra are reported in PART III, section 1.

4. Dihexadecylglycerol derivates

Deuterated DHPA was prepared by modification of standard synthetic techniques developed for n-acyl lipids. [1,1-$^2H_2$]Hexadecanol was prepared by $LiAl^2H_4$ reduction of methyl palmitate and [2,2-$^2H_2$]hexadecanol was prepared by $NaO^2H/^2H_2O$ exchange of the C-2 hydrogens of palmitic acid, followed by $LiAlH_4$ reduction of methyl palmitate. Either the [1,1-$^2H_2$]- or [2,2-$^2H_2$]-labelled chains were coupled to 3-trityl chimyl alcohol and the trityl dihexadecylglycerol was detritylated and converted to the corresponding phosphatidic acid. The final compounds were TLC pure and were characterized by NMR, negative FAB and elemental analysis. The compounds and the reaction schemes are shown in Figure III.9.

4.1 [1,1-$^2H_2$]-hexadecanol (4.2a)

Palmitic acid (5.0 g; 19.5 mmol) was converted to the corresponding methyl ester by heating under reflux in 2.5% methanolic HCl (200 ml). The reaction mixture was diluted with water (20 ml) and the product was extracted with several portions of petroleum ether. The pooled ether extracts were concentrated under reduced pressure and dried in vacuo.

A solution of methyl palmitate (5.0g; 18.5 mmol) in anhydrous ethyl ether (30 ml) was added dropwise with stirring to a suspension of $LiAl^2H_4$ (400 mg) in anhydrous ether (50 ml) and the reaction mixture was stirred at room temperature for 24 hours. Water (5 ml) was added to hydrolyse excess $LiAl^2H_4$ and the reaction mixture was diluted with additional ethyl ether (100 ml) and washed successively with water, 0.2N HCl, 2.5% KH_2CO_3 and

Figure II.9

Detailed synthetic scheme for deuterated dihexadecylglycerol phosphatidic acid

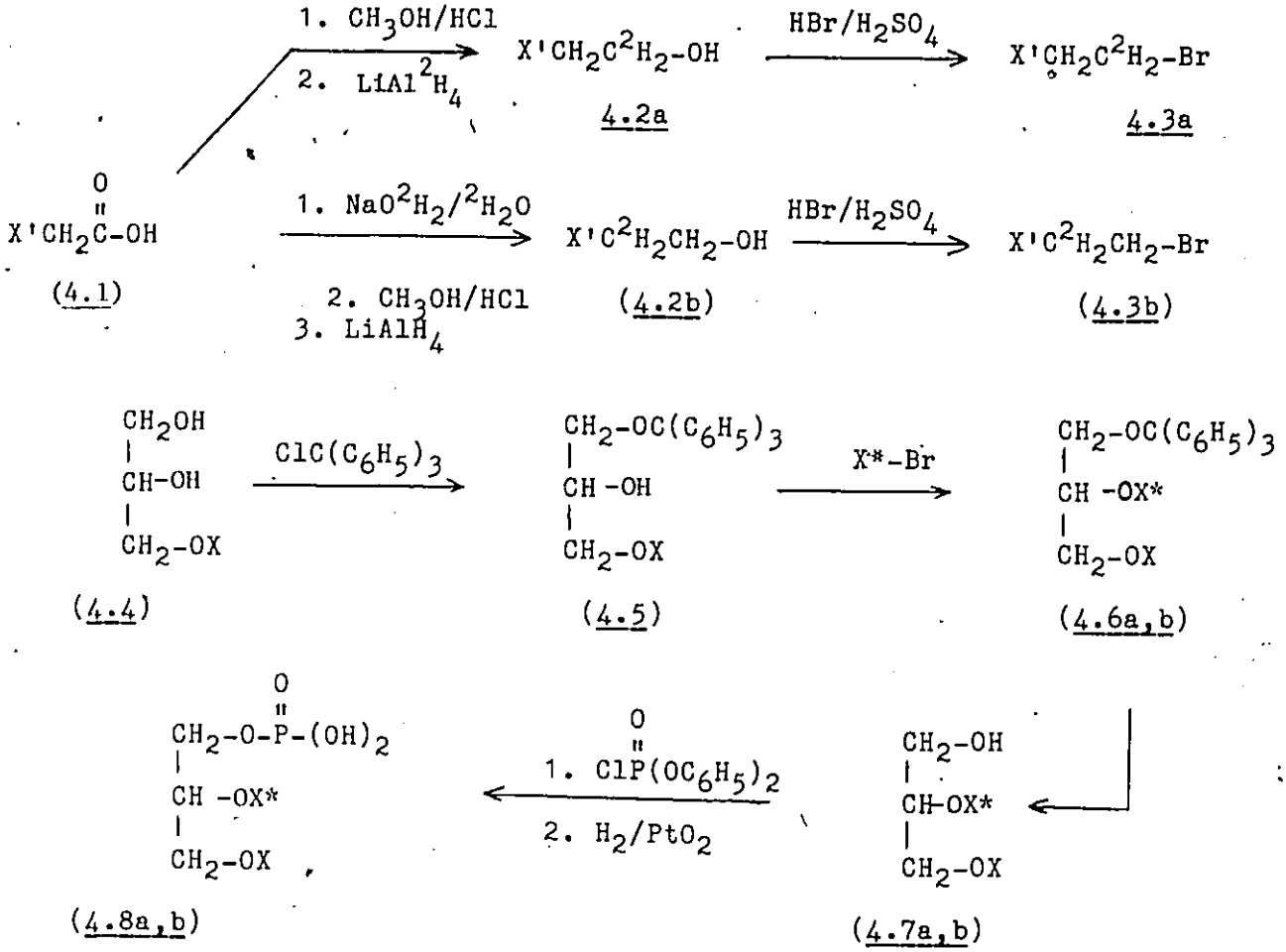

X'= $CH_3(CH_2)_{13}$-

X= $CH_3(CH_2)_{15}$-

X*= as X; deuterated

water then concentrated under reduced pressure. TLC of the residual product in petroleum ether/ethyl ether (4:1) showed a major spot with R_f=0.2 as well as a small amount of unreduced material (R_f=0.8). The crude mixture was fractionated on a silicic acid column (50 g; prepared in petroleum ether) by elution with petroleum ether (800 ml; fraction 1) and petroleum ether/ethyl ether 1:1 (100 ml; fraction 2 and 800 ml; fraction 3). Fraction 1 contained unreacted starting material, fraction 2 contained the desired material as well as a small amount of faster moving material and fraction 3 contained the pure hexadecanol. Fraction 3 was concentrated under reduced pressure, yielding 3.08 g (86%) [1,1-$^2H_2$]hexadecanol (4.2a).

TLC in petroleum ether/ethyl ether (4:1) showed one spot with R_f= 0.2.

IR: 3360 cm^{-1} (OH); 2900-2980, 1485 cm^{-1} (CH_2, CH_3); 1145 cm^{-1} (C-OH, alcohol).

GC/MS ($C_{16}H_{31}{}^2H_2O$-TMS, FW=316): m/z, 301 $(M - CH_3)^+$

GC: $RT_{16:0}$= 0.84 (hexadecanol standard, $RT_{16:0}$= 0.87).

^1H NMR: 1.53 ppm ($C\underline{H}_2$-CH_2-O); 1.28 ppm (CH_2); 0.86 ppm (CH_3). The peak corresponding to CH_2-O was absent. (See Appendix A6)

^{13}C NMR: 32.5 ppm (CH_2-$\underline{C}H_2$-O); 31.9 ppm (CH_2); 29.6 ppm 25.7, 22.7, 14.1 ppm (CH_3). The peak corresponding to CH_2-O was absent. (See Appendix A5)

^2H NMR: 3.58 ppm (C^2H_2-O).

4.2 [2,2-$^2H_2$]-hexadecanol (4.2b) (Tulloch, 1977)

A mixture of sodium palmitate (2.54 g; 0.01 mol) in 1% NaO^2H

in ^2H_2O (15 ml) was heated at 200°C in a sealed ampule for 3 days. After acidification with HCl, the product was extracted as the free acid (Bligh and Dyer, 1959) and converted to the corresponding methyl ester as previously described yielding 2.35 g (96%) [2,2-$^2H_2$]palmitic acid methyl ester (4.2b) (white crystals).

TLC of the product in petroleum ether/ethyl ether (4:1) showed one spot with R_f= 0.54 (methyl palmitate standard, R_f=0.55)

GC: $RT_{16:0}$= 1.0

Methyl-[2,2-$^2H_2$]palmitate was reduced to the corresponding alcohol as described above yielding 2.35 g (96%) [2,2-$^2H_2$]-hexadecanol. TLC in petroleum ether/ethyl ether (4:1) showed a single spot with R_f=0.2 and no unreacted starting material (R_f= 0.8) (hexadecanol standard R_f= 0.2).

GC/MS ($C_{16}H_{31}{}^2H_2O$-TMS, FW=316): m/z, 301 $(M - CH_3)^+$.

GC: $RT_{16:0}$=0.84 (hexadecanol standard, $RT_{16:0}$= 0.83).

^1H NMR: 3.61 ppm (CH_2-O); 1.28 ppm (CH_2); 0.87 ppm (CH_3). Peak at 1.53 ppm corresponding to ($\underline{C}H_2$-CH_2-O) was absent (Appendix A6).

^{13}C NMR: 62.8 ppm (CH_2-O); 31.9 ppm (CH_2); 29.6, 25.5, 22.7, 14.1 ppm (CH_3). The peak at 32.5 ppm corresponding to ($\underline{C}H_2$-CH_2-O) was absent (Appendix A5).

^2H NMR: 1.53 ppm (R_2-$C^2H_2CH_2$-OH).

4.3 [1,1-$^2H_2$]hexadecyl-1-bromide (4.3a)

A mixture of [1,1-$^2H_2$]hexadecanol (1.5 g; 6.14 mmol), concentrated sulfuric acid (1.5 ml), water (5 ml) and 48% HBr (5 ml) ws heated under reflux for 24 hours. The reaction mixture

was cooled and diluted with petroleum ether. The petroleum ether phase was washed well with water and concentrated under reduced pressure. The crude material was purified by column chromatography (10 g silicic acid) by elution with petroleum ether/ethyl ether (9:1; 150 ml) yielding 1.69 g (89.9%) [1,1-$^2H_2$]hexadecyl-1-bromide (4.3a) (golden-yellow oil).

TLC in chloroform showed one spot with R_f= 0.81.

IR: 2900-2980, 1480 cm^{-1} (CH_2, CH_3); 735 cm^{-1} (C-Br).

GC: $RT_{16:0}$=1.17 (hexadecyl-1-bromide standard, $RT_{16:0}$= 1.19).

4.4 [2,2-$^2H_2$]hexadecyl-1-bromide (4.3b)

[2,2-$^2H_2$]hexadecanol (2.35 g; 9.63 mmol) was converted to the corresponding bromide as described for [1,1-$^2H_2$]hexadecanol yielding 1.62 g (86.2%) of [2,2-$^2H_2$]hexadecyl-1-bromide (4.3b).

TLC in chloroform showed one spot with R_f= 0.81.

IR: 2890-2970, 1480 cm^{-1} (CH_2, CH_3); 735 cm^{-1} (C-Br).

GC: $RT_{16:0}$= 1.17 (hexadecylbromide standard, $RT_{16:0}$= 1.19).

4.5 sn-1-Hexadecyl-3-trityl glycerol (4.5) (Chaudhary and Hernandez, 1979)

A mixture of D-chimyl alcohol (sn-1-hexadecyl glycerol) (2.0 g; 6.3 mmol), trityl chloride (2.2 g; 7.9 mmol) and dimethylaminopyridine (40 mg; 0.33 mmol) in dimethylformamide (20 ml) were stirred at room temperature under nitrogen for 48 hours. The reaction mixture was diluted with methylene chloride (100 ml) and washed successively with water, saturated ammonium chloride and water. The methylene chloride phase was concentrated under reduced pressure and dried in vacuo. TLC in petroleum ether/

ethyl ether (1:1) showed the presence of a trityl-containing product (R_f= 0.47) as well as tritanol (R_f= 0.59) and dityrityl ether (R_f= 0.70) but only a small amount of unreacted starting material (R_f=0.04). The crude reaction mixture was fractionated by column chromatography (50 g silicic acid) by elution with petroleum ether (150 ml; fraction 1); petroleum ether/benzene (2:1; 150 ml; fraction 2); and petroleum ether/benzene (1:1; 400 ml; fraction 3). Fraction 1 contained dityrityl ether and fraction 2 contained dityrityl ether, tritanol and some tritylchimyl alcohol. Fraction 3 (200 ml) contained the desired compound (6.5) and a small amount of tritanol. Fraction 3 was concentrated under reduced pressure to a colourless oil which crystallized at room temperature yielding 1.97 g (55%) sn-1-hexadecyl-3-tritylglycerol (4.5) (colourless needles).

TLC in petroleum ether/ethyl ether (1:1) showed a major spot with R_f= 0.28 and trace amounts of tritanol, R_f= 0.45.

IR: 3500 cm^{-1} (OH); 3100, 1615, 1505, 720 cm^{-1} (aromatic); 2900-2980, 1465 cm^{-1} (CH_2, CH_3); 1080-1140 cm^{-1} (C-OH, C-O-C, ether).

4.6 sn-1-hexadecyl-2-[1,1-$^2H_2$]hexadecylglycerol or sn-1-hexadecyl-2-[2,2-$^2H_2$]hexadecylglycerol (4.7a or b)

A mixture of trityl chimyl alcohol (sn-3-trityl-1-hexadecyl glycerol; 0.9 g; 1.49 mmol), 1-bromohexadecane (either [1,1-$^2H_2$]-1-bromohexadecane or [2,2-$^2H_2$]-1-bromohexadecane) (0.55g; 1.88 mmol) and finely powdered KOH (0.75 g) in anhydrous benzene was heated under reflux for 36 hours. A Dean-Stark phase separating

head was used to remove water formed during the reaction. The reaction mixture was diluted with ethyl ether and washed successively with water, 0.2 N HCl, 10 % KH_2CO_3 and water, and concentrated under reduced pressure. TLC of the crude product in chloroform showed complete conversion from trityl hexadecylglycerol (R_f=0.63) to trityl dihexadecylglycerol (R_f=0.19). The crude reaction mixture was heated under reflux in 2.5% methanolic HCl (150 ml) for 18 hours and the product extracted with several portions of petroleum ether. The petroleum ether extract (200 ml) was concentrated under reduced pressure.

TLC of the product in petroleum ether/ethyl ether (4:1) showed complete conversion of trityl dihexadecyl glycerol (R_f=0.70) to dihexadecyl glycerol (R_f=0.23) (hexadecyl glycerol standard R_f=0.25).

sn-1-Hexadecyl-[1,1-$^2H_2$]hexadecylglycerol (4.7a) was obtained in a yield of 430 mg (53% from tritylchimyl alcohol, first crop) (white crystalline solid).

CI/MS ($C_{35}H_{70}{}^2H_2O_3$; FW= 542): m/z, 543 (MH^+).

^{1}H NMR: 0.86 ppm (CH_3); 1.23 ppm (CH_2); 1.53 ppm ($\underline{CH_2}CH_2O$); 3.4-3.75 ppm (R_2CHO, RCH_2O; decreased intensity).

Elemental analysis ($C_{35}H_{66}{}^2H_2O_3$; FW=542.56):

calculated:	77.41% C	13.74% H
found:	77.32% C	13.44% H

m.p.= 44-45°C (nondeuterated sn-1,2-dihexadecylglycerol, m.p.= 48.5-49.5°C; Kates et al., 1963).

sn-1-Hexadecyl-2-[2,2-$^2H_2$]hexadecylglycerol (4.7b) was prepared as described for [1,1-$^2H_2$]hexadecylglycerol yielding 470 mg (58% from tritylchimyl alcohol, first crop) (white crystalline solid).

CI/MS ($C_{35}H_{70}{}^2H_2O_3$; FW=542): m/z, 543 (MH^+).

^1H NMR: 0.861 ppm (CH_3); 1.23 ppm (CH_2-); 1.54 ppm ($\underline{CH_2}CH_2O$; decreased intensity); 3.4-3.75 ppm (R_2CHO, RCH_2O); absence of peaks 7.15-7.25 ppm (aromatic).

Elemental analysis ($C_{35}H_{70}{}^2H_2O_3$; FW=542.56):

calculated:	77.41% C	13.74% H
found:	77.37% C	13.50% H

m.p.= 42-44°C (nondeuterated sn-1,2-dihexadecylglycerol, m.p.= 48.5-49.5°C; Kates et al., 1963).

4.8 Dihexadecylglycerol Phosphate (4.8a and b)

A solution of diphenyl phosphoryl chloride (375mg; 1.4mmol) in anhydrous pyridine (5 ml) was added dropwise with stirring to an ice cold solution of deuterated dihexadecylglycerol (either sn-3-hexadecyl-2-[1,1-$^2H_2$]-hexadecyl glycerol 400 mg, 0.74 mmol; or sn-3-hexadecyl-2-[2,2-$^2H_2$]-hexadecyl glycerol 450 mg; 0.83 mmol) in anhydrous pyridine (5 ml). The reaction mixture was stirred for 1 hour at 0°C under anhydrous conditions, then overnight at room temperature. Water (10 ml) was added to hydrolyse excess diphenylphosphoryl chloride. The reaction mixture was diluted with ethyl ether (200 ml) and washed successively with water, 0.2N HCl, 10% KH_2CO_3 and water. The organic phase was concentrated under reduced pressure and the

residue dried *in vacuo*.

The phenyl groups were removed by repeated hydrogenolysis (2-3 times) with platinum oxide (150-200 mg) in ethanol as described in section 7 and the resultant PA was converted to the ammonium salt form and purified by repeated acetone precipitation.

sn-1-hexadecyl-2-[1,1-$^2H_2$]hexadecylglycerol-3-phosphate (4.8a) was obtained in a yield of 360 mg (78% from diether) (white crystalline solid).

^{13}C NMR: 13.43 ppm (CH_3); 22.10, 25.56 ppm (CH_2); 29.36 ppm (CH_2-CH_2O); 31.37 ppm (CH_2-O; *sn*-1); 63.8 ppm (CH_2-O-P); 70.36 ppm (CH_2O; *sn*-1 position); 71.17 ppm (C-1, *sn*-1 chain). Absence of peak at 69.99 ppm (C-1, *sn*-2 chain) (See Appendix A7).

^1H NMR: 0.553 ppm (CH_3); 0.939 ppm (CH_3); 1.06, 1.23 ppm (CH_2); 3.16 ppm (CH_2O); 3.33, 3.54 ppm (R_2-CHO, CH_2O); 4.11-4.22 (CH_2O-P). The peak 3.25 ppm (CH_2-CH_2-O) was decreased in intensity.

Negative FAB/MS (PA-H_2, FW=622): m/z, 621 $(M-1)^-$.

Elemental analysis ($C_{35}H_{71}{}^2H_2O_6P$; PA-NH_4; FW=637.58):

calculated:	65.88% C	12.02% H	4.86% P	2.20% N
found:	64.20% C	12.06% H	4.41% P	2.39% N

sn-1-hexadecyl-2-[2,2-$^2H_2$]hexadecylglycerol-3-phosphate (4.8b) was obtained in a yield of 438 mg (85% from diether) (white crystalline solid).

^{13}C NMR: 13.33 ppm (CH_3); 22.10, 25.66 ppm (CH_2); 29.60 ppm (CH_2-CH_2-O; decreased intensity); 31.38 ppm (CH_2-O, *sn*-3); 69.99 ppm (CH_2O, *sn*-2); 70.32 ppm (CH_2O, *sn*-1); 71.17 ppm (CH_2-O, *sn*-1 and CH-O, *sn*-1) (See Appendix A7).

^{1}H NMR: 0.94 ppm (CH_3); 1.06, 1.24 ppm (CH_2 decreased intensity); 3.17 ppm ($C\underline{H}_2O$); 3.25 ppm ($C\underline{H}_2$-CH_2-O, reduced intensity in comparison with [1,1-$^2H_2$]DHPA); 3.33, 3.54 ppm (R_2 CHO, CH_2O;, 4.23 (CH_2O-P).

Negative FAB/MS (PA-H_2, FW=622): m/z, 621 $(M - 1)^-$.

Elemental analysis ($C_{35}H_{70}{}^2H_2O_6P$; PA-NH_4; FW=637.58):

calculated:	65.87% C	12.01% H	4.86% P	2.20% N
found:	64.11% C	11.95% H	4.38% P	2.38% N

^{2}H NMR spectra are shown in PART III, section 1.

5. Phospholipids Containing Deuterated and Undeuterated Headgroups

5.1 Undeuterated Headgroups

The scheme for the synthesis of unlabelled diphytanylglycerol phospholipids from diphytanylglycerol is shown in Figure II.10.

5.1.1 sn-2,3-Diphytanyl-1-phosphatide (5.2) (Method a) (Kates et al., 1971)

A solution of diphenylphosphoryl chloride (0.9 g; 3.3 mmol) in anhydrous pyridine (20 ml) was added dropwise, with stirring, over 30 minutes to an ice cold solution of sn-2,3-(R,R,R)-diphytanylglycerol (1.05 g; 1.6 mmol) (5.1, derived from polar lipids of H. cutirubrum as described in section 2) in anhydrous pyridine (20 ml), and the mixture was stirred at room temperature for 24 hours. Water (10 ml) was added to hydrolyse excess TPS and the reaction mixture was diluted with ethyl ether (200 ml), washed successively with water, 0.2 N HCl, 2.5 % KH_2CO_3 and water to neutrality; the ether phase was concentrated under reduced pressure and the residue was dried in vacuo, yielding 1.21 g (98%) diphytanylglycerol analogue of diphenyl phosphatidate (5.2).

TLC in $CHCl_3/CH_3OH/30\%\ NH_4OH$ (65:53:5) showed one spot with R_f=0.87 and in $CHCl_3$/petroleum ether (3:1) R_f=0.75 (diphytanyl glycerol standard, R_f=0.63).

IR: 1380 cm^{-1} doublet (isopropyl); 1100 cm^{-1} (C-O-C ether); 1050 cm^{-1} (P-O-C); 700 cm^{-1} (aromatic).

The crude diphenyl phosphatidate was hydrogenolysed in freshly distilled ethanol (100 ml) with platinum oxide (1.5 g) Usually, the hydrogenolysis was carried out at least twice to ensure

Figure II.10

Synthesis of undeuterated diphytanylglycerol phospholipids from diphytanylglycerol

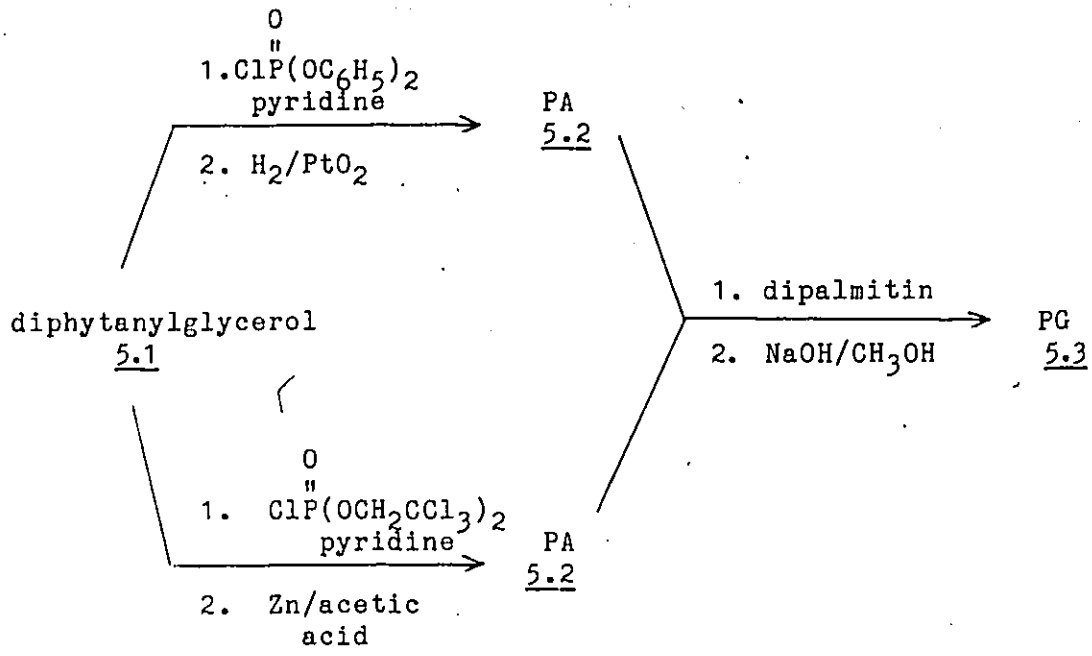

complete conversion to the diphytanylglycerol phosphate. The product was purified by preparatory TLC in $CHCl_3/CH_3OH/30\%\ NH_4OH$ (65:35:5) and eluted from the silicic acid with $CHCl_3/CH_3OH$/0.2 N aqueous HCl (1:1:0.9). The product was converted to the ammonium salt form (Kates, 1986) and purified by acetone precipitation yielding 870 mg (74%) of sn-2,3-diphytanyl-1-phosphate (5.2) (white solid).

TLC in chloroform/methanol/NH_4OH (65:35:5) showed one phosphorus-positive spot with R_f= 0.10.

IR: See PART III, section 4.

^{13}C NMR: 64.91 ppm (G-1); 68.79 ppm (C-1); 69.92 ppm (C-1'); 71.28 ppm (G-3); 78.49 ppm (G-2).

Negative FAB/MS (PA-H_2; FW=732): m/z, 731 $(M - H)^-$.

Positive FAB/MS: m/z, 733 $(MH^+)^+$.

5.1.2 sn-2,3-diphytanyl-1-phosphate (5.2) (Method b) (Ogilvie et al., 1977)

A solution of bis(trichloroethyl)chlorophosphate (1.08 g; 2.84 mmol) in anhydrous pyridine (10 ml) was added dropwise with stirring to an ice cold solution of diphytanylglycerol (370 mg; 0.57 mmol) in anhydrous pyridine (15 ml). The mixture was stirred at room temperature for 48 hours, then the reaction mixture was diluted with ethyl ether then washed with water, 0.2 N HCl, 10% KH_2CO_3 and water to neutrality. The ether phase was concentrated under reduced pressure yielding 710 mg of crude bis(trichloroethyl)-diphytanyl phosphatidic acid. TLC in chloroform/ethyl ether (3:1) showed complete conversion of the diether (R_f=0.65) to the phosphorylated product (R_f=0.78).

The product was dissolved in a minimum of chloroform (5 ml) and diluted with glacial acetic acid (45 ml). Powdered zinc (0.8 g) was added and the reaction mixture was shaken for an hour at room temperature. The zinc was removed by centrifugation and washed well with choroform/methanol (1:1). The pooled supernatants were concentrated under reduced pressure, and the resultant diphytanylglycerol phosphatidic acid was converted to the ammonium salt form and purified by acetone precipitation. The acetone precipitation was repeated once yielding (367 mg) (87%) of sn-2,3-diphytanyl-1-phosphate (5.2) (white solid) with identical R_f values in chloroform/methanol/30% NH_4OH (65:35:5) to the sample prepared by Method a (R_f=0.15). TLC in chloroform/methanol/NH_4OH (65:35:5) also indicated that the acetone supernatants contained primarily unreacted diether (R_f=0.91) with trace amounts of phosphorylated biproducts (R_f=0.73; 0.62 and 0.24).

Positive FAB/MS (PA-H_2; FW= 732): m/z, 733 $(MH^+)^+$.

Negative FAB/MS: m/z, 731 $(M - H)^-$.

This procedure has the advantage over Method a in that the blocking groups are more easily and rapidly removed, minimizing the formation of side products such as the monophenyl and cyclohexyl derivatives of PA.

5.1.3 sn-2,3-Diphytanylglycerol-1-phosphoryl-3'-glycerol (PG) (5.3)

A solution of trisopropylbenzenesulfuryl chloride (TPS; 630 mg; 2.08 mmol) anhydrous pyridine (40 ml) was added dropwise

with stirring to a solution of non-racemic sn-1,2-dipalmitoylglycerol (576 mg, 1.12 mmol) (or rac-dimyristoylglycerol) and the free acid form of sn-1,2-diphytanylglycerol-1-phosphate (495 mg; 0.68 mmol) in anhydrous pyridine (40 ml). The reaction mixture was left at room temperature for 30 hours. The mixture was then cooled (0°C) and stirred with 10 ml water for 40 minutes to hydroyse excess TPS. The reaction mixture was diluted with diethyl ether (300 ml), washed with water, 0.2 N HCl, 10% KH_2CO_3 and water to neutrality and concentrated under reduced pressure. The product was converted to the ammonium salt form and precipitated by the addition of acetone , yielding 776.6 mg of crude diphytanylglycerol phosphatidyl dipalmitoylglycerol.
TLC in $CHCl_3/CH_3OH/30\%$ NH_4OH (65:35:5) showed a major phosphate positive spot with R_f=0.45 as well as some unreacted starting material (diphytanyl phosphatidic acid, R_f=0.05).

Crude diphytanyl phosphatidyl dipalmitoylglycerol (655 mg) was deacylated in $CHCl_3$/methanol (2:1; 13.4 ml) and methanolic NaOH (0.2 N; 10 ml) at room temperature for at least 40 minutes. Chloroform (5 ml) and 0.6 N HCl (13 ml) were then added to make the system biphasic. The chloroform phase was removed and washed twice with CH_3OH/H_2O (10:9), neutralized with methanolic 2 N NH_4OH, diluted with benzene and concentrated under reduced pressure. The residue was precipitated by the addition of a ten-fold excess of acetone and dried in vacuo yielding, 363 mg.
TLC in $CHCl_3/CH_3OH/30\%$ NH_4OH (65:35:5) showed one major phosphate-positive spot (R_f=0.49) as well as some unreacted diphytanylglycerol phosphoryl (dipalmitoylglycerol) (R_f=0.87)

(natural diphytanyl PG standard R_f=0.48).

The crude diphytanylglycerol phosphoryl glycerol was purified by preparative TLC in $CHCl_3/CH_3OH/30\%\ NH_4OH$ (65:35:5) and the pure compound was converted to the ammonium salt form yielding 220 mg of diphytanylglycerol phosphorylglycerol (PG) (6.3) (47% from diphytanyl phosphatidic acid) TLC in chloroform/methanol/NH_4OH (65:35:5) showed one phosphate-positive spot with R_f= 0.49 Negative FAB/MS (PG-NH_4; FW= 823): m/z, 805 $(M - NH_4)^-$.

Elemental analysis ($C_{46}H_{98}O_8PN$; FW= 823.68):

calculated:	67.20 %C	11.92% H	1.70 %N	3.76 %P
found:	66.69 %C	11.64 %H	1.43 %N	3.78 %P

^{13}C NMR: 63.3 ppm (G-1'); 65.9 ppm (G-1); 67.4 ppm (G-3'); 69.2 ppm (C-1); 70.40 ppm (C-1'); 71.40 ppm (G-2'); 71.78 ppm (G-3); 78.70 ppm (G-2) (See Appendix A1 and A2).

5.2 Deuterated Headgroups

The scheme for the synthesis of deuterium-labelled diphytanylglycerol phospholipids from diphytanylglycerol is shown in Figure II.11.

5.2.1 L-(-)-Methyl glycerate

Methyl glycerate was prepared from the calcium salt of glyceric acid essentially as described in section 2.

L-(-)-Glyceric acid (calcium salt; 1.0 g; 8.33 mmol) was heated under reflux in methanolic HCl (0.6 N; 100 ml) for 2 hours. The mixture was concentrated under reduced pressure, diluted with water (10 ml) and extracted with ethyl ether. The ether phase was concentrated under reduced pressure, yielding a colourless oil.

^{13}C NMR: 53.06 ppm (OCH_3); 57.43 ppm (CH-OH); 64.27 ppm (CH_2-OH); 169.58 ppm (C=O).

IR: 3400 cm^{-1} (OH); 1740, 1240 cm^{-1} (C=O, C-O, ester), 1440 cm^{-1} (OCH_3), 1130 cm^{-1} (sec C-OH); 1050 cm^{-1} (primary C-OH).

5.2.2 sn-3-Trityl glyceric acid methyl ester (5.5)

A solution of L-(-)-methyl glycerate (1.0 g; 8.33 mmol), trityl chloride (3.0 g; 8.78 mmol), dimethylaminopyridine (50 mg; 0.43 mmol) and triethylamine (2 ml; 14.3 mmol) in dimethylformamide (10 ml) was stirred at room temperature for 48 hours under anhydrous conditions. The reaction mixture was diluted with ice water (10 ml) and extracted with several portions of methylene chloride. The pooled organic phase was washed successively with saturated ammonium chloride and water and concentrated under reduced pressure to yield a yellow oil.

Figure II.11

Synthesis of diphytanylglycerol PG deuterated in the headgroup

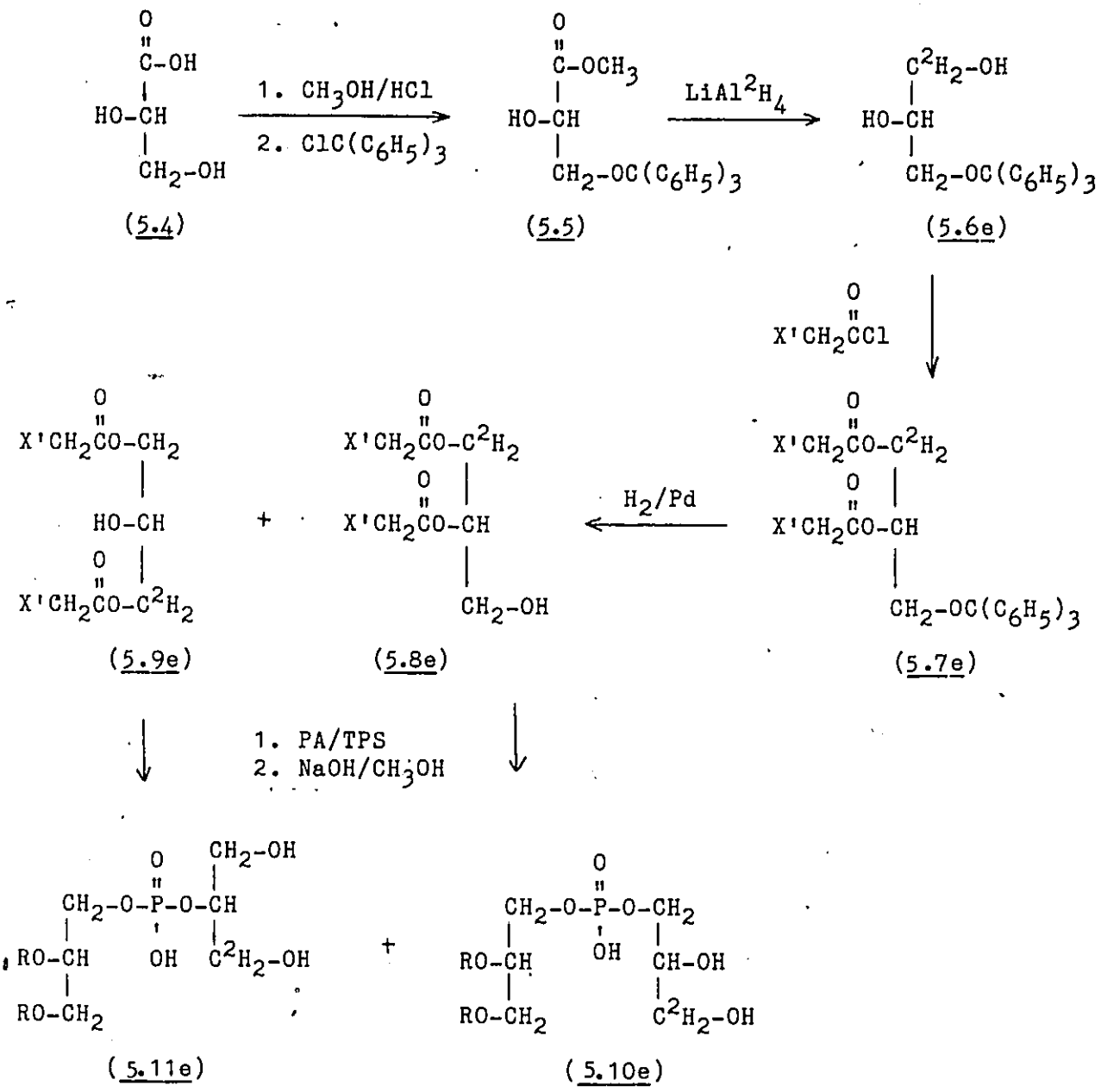

R= CH_3-[CH-$CH_2CH_2CH_2$]$_3$ CHCH_2CH_2 (with CH_3 branches)

X'= $CH_3(CH_2)_{13}$-

The crude reaction mixture was fractionated by column chromatography (50 g silicic acid) by elution with petroleum ether/ethyl ether (9.5:0.5, 150 ml, fraction 1), petroleum ether/ethyl ether (9:1, 200 ml, fraction 2; 150 ml, fraction 3). Fraction 1 contained ditrityl ether and tritanol. Fraction 2 contained tritanol and a small amount of the desired compound. Fraction 3, containing the desired compound plus a small amount of tritanol, was concentrated under reduced pressure and dried in vacuo yielding 1.09 g (36%) of 3-trityl methyl glycerate (6.5) (white crystalline solid).

TLC in $CHCl_3$ showed one major spot with R_f=0.3 and trace amounts of tritanol (R_f=0.5).

CI/MS ($C_{23}H_{22}O_4$; FW= 362): m/z, 362 $(M)^+$; 243 $(C(C_6H_5)_3)^+$.

IR: 3505 cm^{-1} (OH); 3100, 1610, 1505, 775 cm^{-1} (aromatic); 1760, 1190 cm^{-1} (C=O, C-O, ester); 1110 cm^{-1} (C-O-C).

5.2.3 sn-[1,1-$^2H_2$]-3,3-Trityl glycerol (5.6e)

A solution of trityl methyl glycerate (1.09 g; 3.01 mmol) in anhydrous ethyl ether (10 ml) was added dropwise with stirring to a solution of $LiAl^2H_4$ (150 ml) in ethyl ether (10 ml) and the reaction stoppered and left stirring at room temperature overnight. Ethanol and water were added dropwise to hydrolyse excess $LiAl^2H_4$ and the mixture was diluted with 0.2 N HCl and extracted repeatedly with ethyl ether. The pooled ether phases were washed successively with 0.2 N HCl, 2.5% $KHCO_3$ and water and concentrated under reduced pressure. The crude material was purified by column chromatography (50 g silicic acid) by elution

with petroleum ether/benzene (1:1, 300 ml, fraction 1), benzene (100 ml, fraction 2; 100 ml, fraction 3), benzene/ethyl ether (9:1, 200 ml, fraction 4) and benzene/ethyl ether (5:1, 100 ml, fraction 5). Fractions 1 and 2 contained tritanol. Fractions 3-5, containing the desired material as well as a small amount of tritanol, were pooled and concentrated under reduced pressure yielding a viscous, colourless oil. The oil, still containing traces of unreacted starting material, was dissolved in a minimum (2 ml) of chloroform and the tritanol was precipitated with a ten-fold excess of petroleum ether. The tritanol was removed by centrifugation and the petroleum ether supernatant concentrated under reduced pressure. The resulting viscous oil was recrystallized from warm isopropyl ether, yielding 766 mg (76%) tritylglycerol (5.6e) (white crystalline solid); m.p.= 96-97°C (reported valued for non-deuterated sn-1-tritylglycerol, m.p.= 96.5°C; Tattrie et al., 1958).

TLC in petroleum ether/ethyl ether (1:1) showed one major trityl positive spot corresponding to tritylglycerol with R_f=0.15 and trace amounts of tritanol (R_f=0.6).

IR: 3400 cm^{-1} (OH); 3080, 1610, 1500, 715 cm^{-1} (aromatic); 2936, 1465 cm^{-1} (CH_2, CH_3); 1080 cm^{-1} (C-O-C).

CI/MS ($C_{22}H_{20}{}^2H_2O_3$; FW=336): m/z, 336 $(M)^+$; 243 $(C(C_6H_5)_3)^+$

^1H NMR: 1.58 ppm (CH_3); 1.92 ppm (CH_2); 2.44 ppm ($C\underline{H}(C_6H_5)$; 3.24 ppm ($C\underline{H}_2$-OC); 3.86 ppm ($C\underline{H}$-OH) and 7.1-7.8 ppm (aromatic). Absence of peaks at 3.4-4.0 ($C\underline{H}_2$-OH).

^2H NMR: 3.87 ppm (theor. 3.4 - 4.0).

Elemental Analysis ($C_{22}H_{20}{}^2H_2O_3$; FW= 336.37)

calculated: 78.55% C 6.55% H

found: 78.32% C 6.49% H

5.2.4 3-Trityl-[1,1-$^2H_2$]-1,2-dipalmitoylglycerol (5.7e)

A solution of [1,1-$^2H_2$]-3-trityl glycerol (0.39 g; 1.16 mmol), palmitoyl chloride (1.0 g; 3.64 mmol) and pyridine (0.3 ml; 3.6 mmol) in carbon tetrachloride (15 ml) was stirred at room temperature for 48 hours. The reaction mixture was diluted with ethyl ether and washed successively with water, 0.2 N HCl, 10% KH_2CO_3 and water. The ether phase was concentrated under reduced pressure and dried in vacuo, yielding 1.49 g (80.9%) of trityl-dipalmitoylglycerol (5.7e) (white crystalline material).
TLC in $CHCl_3$/ethyl ether (3:1) indicated complete conversion from trityl glycerol (R_f=0.07) to tritylpalmitin (R_f=0.82).

5.2.5 sn-[1,1-$^2H_2$]-1,2-dipalmitoylglycerol (5.8e)

The crude trityl dipalmitin (0.8 g) was hydrogenated with Pd on charcoal (0.2 g; 10% Pd) in freshly distilled ethanol (20 ml). The catalyst was removed by centrifugation and the supernatant was concentrated under reduced pressure. The solid material was recrystallized twice from hexane and once from chloroform/petroleum ether (1:10), yielding 460 mg (82%) of dipalmitoyl glycerol (5.8e) (fluffy white crystalline solid).

Trityl dipalmitoylglycerol was also converted to dipalmitoylglycerol by hydrogenolysis with equal amounts (w/w) 10% palladium on charcoal and $CaCO_3$, yielding, after recrystallization, 460 mg (67.8%). Although both methods lead

to complete detritylation, the final product was a mixture of both the sn-1,2- and sn,-1,3-steroisomers as shown by ^{13}C NMR and optical rotation. TLC in petroleum ether/ethyl ether (9:1) showed complete conversion of trityl dipalmitin (R_f=0.8) to dipalmitin (R_f=0.10) (dipalmitin standard, R_f= 0.09) but TLC in petroleum ether/ethyl ether (3:2, double development) showed two spots with R_f= 0.36 and 0.47 corresponding to the 1,2- and 1,3-isomers, respectively.

Attempts to fractionate the mixture by preparative TLC in petroleum ether/ethyl ether (3:2, double development) were unsuccessful because of isomerization of the 1,2- to the 1,3-isomer during chromatography; therefore, the mixture of diasteriomers was used for further synthesis.

CI/MS ($C_{35}H_{66}{}^2H_2O_5$; FW= 570): m/z, 553 $(MH - H_2O)^+$.

^{13}C NMR: 14.11 ppm (CH_3); 22.69-31.91 ppm (CH_2); 34.12 ppm (CH_2-COOR, acyl C-2); 61.56 ppm (CH_2-OH); 65.04 ppm ($\underline{C}H_2$-OCOR); 68.33 ppm ($\underline{C}$H-OCOR); 72.02 ppm (CH-O$\underline{C}$(O)R); 172 ppm (RC-O, acyl ester carbonyl). Ratio of 61.56 and 72.0 ppm to 65.03 and 68.29 ppm (sn-1,3-diacylglycerol: sn-1,2-diacylglycerol), 2:1 (see Appendix A9).

5.2.6 sn-2,3-Diphytanylglycerol-phosphoryl-[1',1'-$^2H_2$]-glycerol (5.11e)

A solution of TPS (950 mg; 3.13 mmol) in pyridine (20 ml) was added dropwise with stirring to a solution of diphytanyl PA (310 ml; 0.414 mmol) and deuterated dipalmitoylglycerol (0.74 g; 1.3 mmol, a mixture of sn-1,2- and 1,3- stereoisomers) in anhydrous pyridine (20 ml). The reaction mixture was stirred at room

temperature for 72 hours. Water (5 ml) was added to hydrolyse excess TPS and the product was extracted with several portions of ethyl ether. The pooled ether fractions were washed with water, 0.2 N HCl, 10% KH_2CO_3 and water to neutrality and concentrated under reduced pressure.

The crude material was deacylated as described in section 5.2. TLC in chloroform/methanol/NH_4OH (65:35:5) showed four spots with mobilities as follows: R_f=0.15 (PA); 1.0 (fatty acid) and two at 0.48 and 0.51 corresponding to the two steroisomers of PG. These were further purified by preparative TLC, yielding 53.6 mg of sn-2,3-diphytanyl-1-phosphoryl-2'-[1',1'-$^2H_2$]glycerol (upper spot) and 18.6 mg of sn-2,3-diphytanyl-1-phosphoryl-3'-[1',1'-$^2H_2$]-glycerol (lower spot) (72.2 mg total; 72.5%).
Negative FAB/MS (deuterated PG-$(NH_4)_2$; FW= 825): m/z, 807 $(M - NH_4)^-$.

sn-2,3-Diphytanylglycerol-1-phosphoryl-3'-[1'-1'-$^2H_2$]glycerol (5.11e)
^{13}C NMR: 64.31 ppm (G-1); 64.71 ppm (G-3'); 68.37 ppm (C-1); 69.60 ppm (C-1'); 70.26 ppm (G-2); 70.49 (G-3). Peak at 78 ppm (G-2') obscured by $CHCl_3$. The peak for G-1' (63.2 ppm) was absent.

sn-2,3-Diphytanylglycerol-1-phosphoryl-2'-[1'-1'-$^2H_2$]glycerol (5.10e)
^{13}C NMR: 61.80 ppm (CH_2OH); 65.96 ppm (G-1); 68.37 ppm (C-1, CH of headgroup); 69.57 ppm (C-1'); 70.30 ppm (G-2); 70.45 ppm (G-3). Spectra shown in Appendix A10.

6. Headgroup analogues

Chemical structures of the analogues are shown in Figure II.12 and include deoxy derivatives of PG and PGP as well as methylated derivates of PGP. A detailed synthetic scheme for the deoxy compounds is shown in Figure II.13 and ^{1}H and ^{13}C NMR data on the final products are summarized in Tables II.2 and II.3.

Diphytanylglycerol Analogue of dPGP (Method a)

6.1 1-Diphenylphosphoryl-1,3-propane-diol (6.2)

A solution of diphenylphosphoryl chloride (15.75 g; 59 mmol) in anhydrous pyridine (20 ml) was added dropwise with stirring to an ice-cold solution of 1,3-propanediol (5.25 g; 69 mmol) in anhydrous pyridine (25 ml). The reaction mixture was stirred at 0°C for one hour and then at room temperature overnight (18 hours) under anhydrous conditions. Water (5 ml) was added to hydrolyse any unreacted diphenylphosphoryl chloride. The reaction mixture was diluted with ethyl ether and the ether phase was washed successively with water, 0.2 N HCl, 2.5% KH_2CO_3 and water to neutrality, and concentrated under reduced pressure.

Thin layer chromatography in $CHCl_3/CH_3OH$ (9:1) showed two phosphate positive spots with R_f=0.48 (major) and R_f=0.65 (minor) corresponding to the mono- and diphosphorylated compounds, respectively. The crude mixture was purified by column chromatography (50 g, prepared in petroleum ether)by elution with petroleum ether/chloroform 4:1 (200 ml, fraction 1); 2:1 (100 ml, fraction 2); 1:1 (400 ml, fraction 3) and $CHCl_3$ (300 ml, fraction 4). Fraction 1 contained the diphosphorylated compound, fraction

Figure II.12

Structures of headgroup analogues of diphytanylglycerol phospholipids

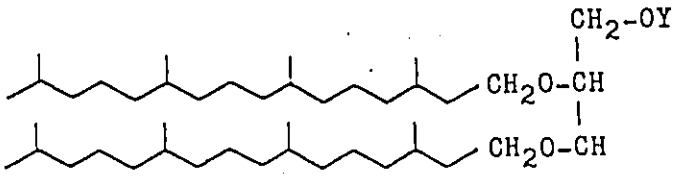

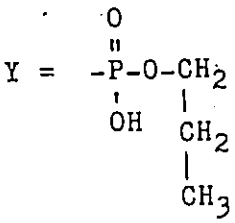

phosphatidyl propanol

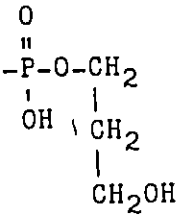

deoxy PG

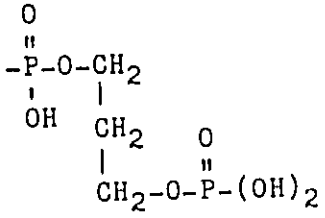

deoxy PGP

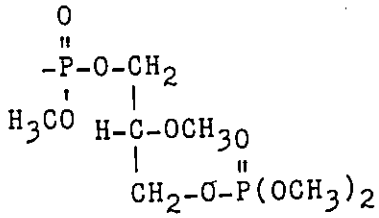

$PGP(CH_3)_4$

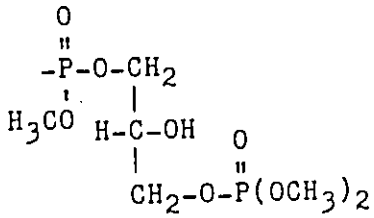

$PGP(CH_3)_3$

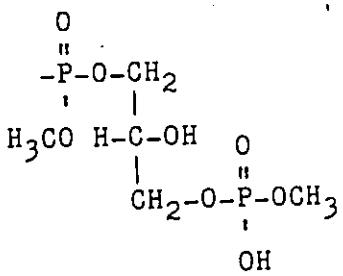

$PGP(CH_3)_2$

Figure II.13

Scheme for synthesis of deoxy analogues of PG and PGP

deoxy PGP (Method a)

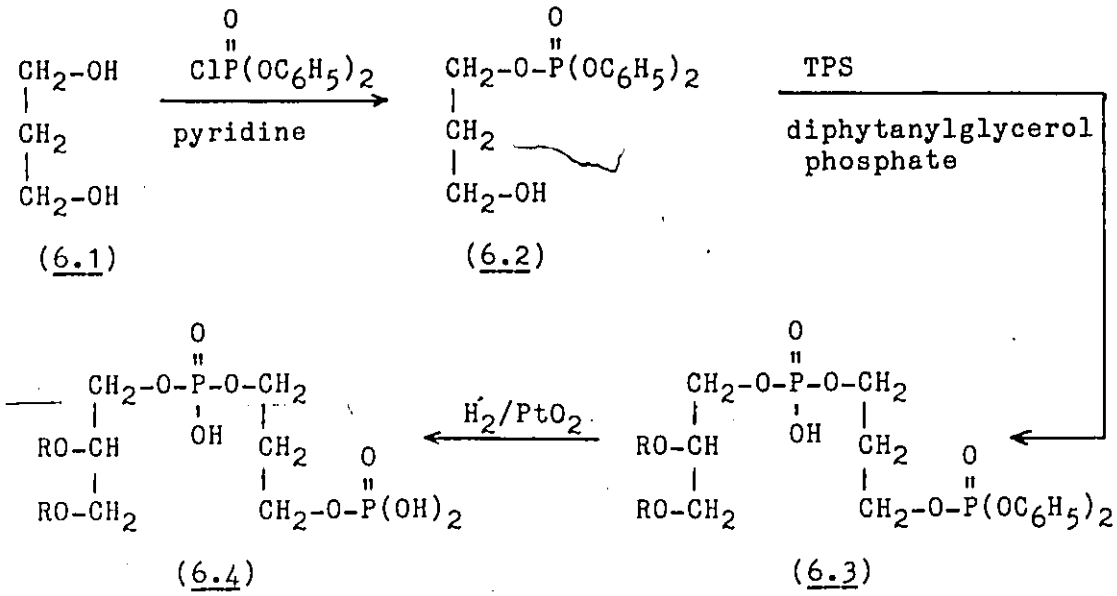

deoxy PGP (Method b)

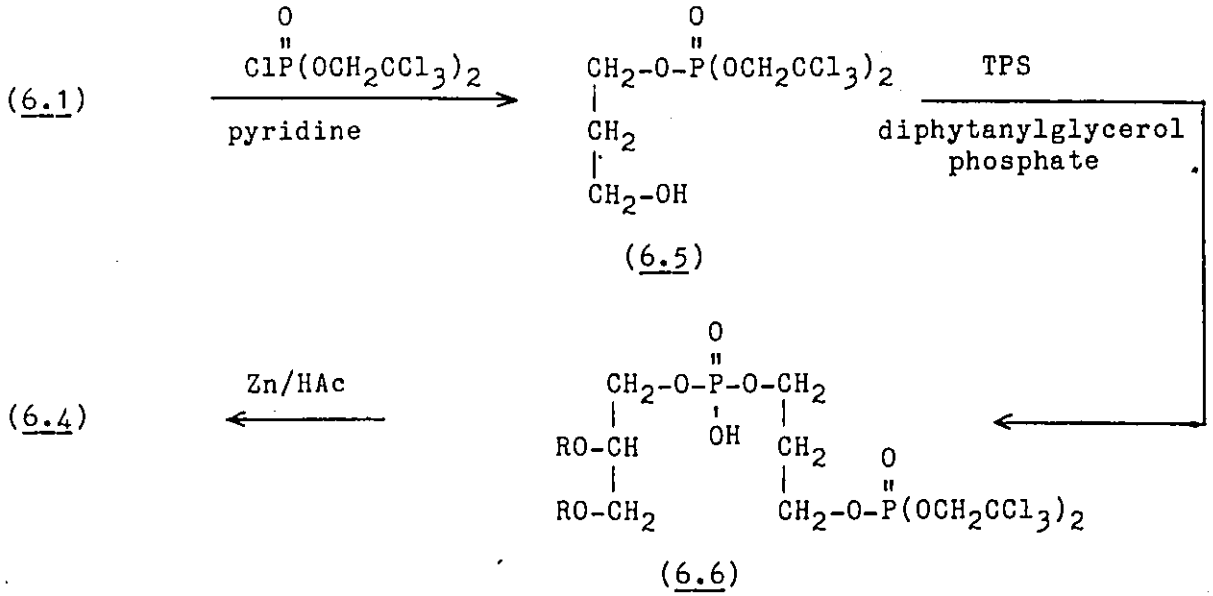

deoxy PG

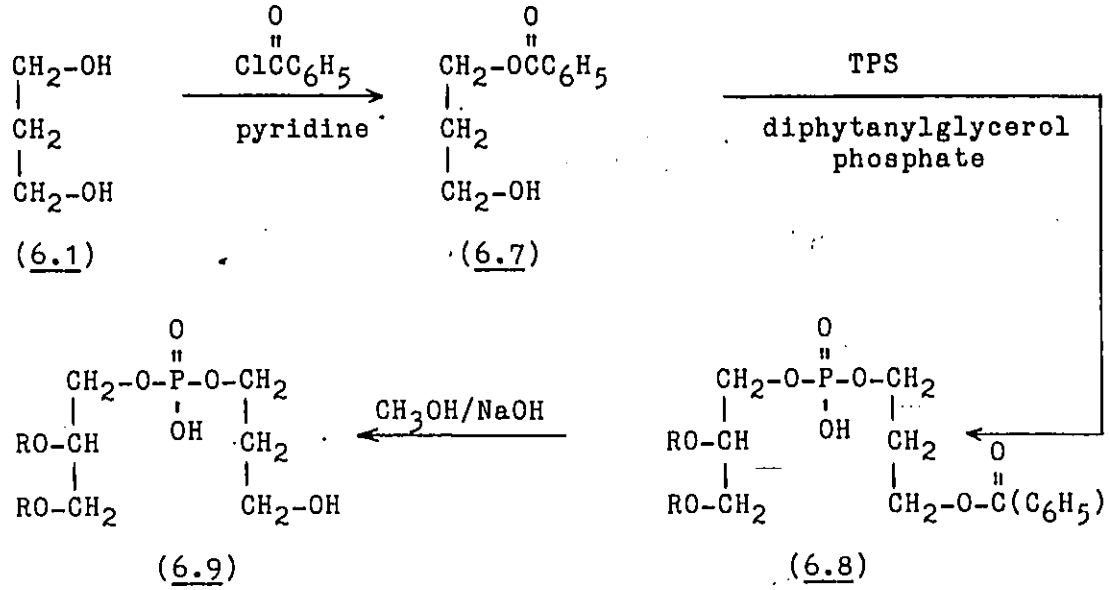

(6.1) (6.7) (6.8) (6.9)

phosphatidyl propanol

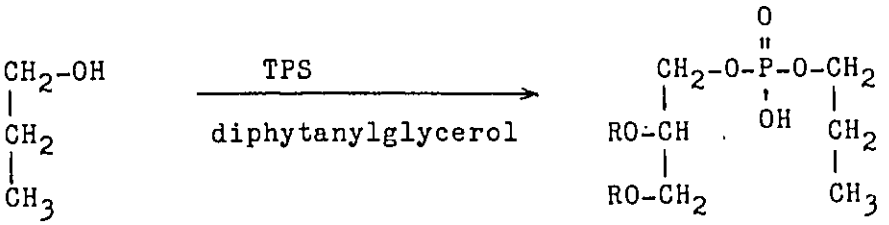

(6.10) (6.11)

Table II.2

^{13}C NMR chemical shift values for deoxy analogues of diphytanylglycerol phospholipids

Position	proPG	dPG	dPGP
C-1, C-1'	68.4, 69.9	68.4, 69.6	68.3, 69.5
G-1	64.5	64.4	64.2
G-2	77.4	77.4	77.4
G-3	70.0	70.2	70.3
G-α	67.2	63.3	61.5
G-β	36-38	36-38	36-38
G-γ	9.52	59.8	61.2

Table II.3

^1H NMR chemical shift values for methylated PGP

	Chemical shift (ppm)	
	PGP $(CH_3)_3$	PGP $(CH_3)_4$
CH, CH_2, CH_3	0.8-1.6	0.8-1.6
$CH-OCH_3$	-	3.55
R_2CH-O-, RCH_2-O-	3.5, 3.6, 4.15-4.35	3.5, 3.6, 4.15-4.35
$P-OCH_3$	3.78, 3.81	3.78, 3.81

2 contained a mixture of mono- and diphosphorylated compounds and fractions 3 and 4 contained the pure, monophosphorylated compound (6.2). The latter fractions were pooled and concentrated under reduced pressure yielding 5.6 g (26 %) 1-diphenylphosphoryl-1,3-propane-diol (colourless oil).

TLC in $CHCl_3/CH_3OH$ (9:1) showed one phosphorus positive spot with R_f=0.48.

IR: 3480 cm^{-1} (OH); 2920-3010 cm^{-1} (CH_2); 3110, 1605, 1505, 780, 705 cm^{-1} (aromatic); 1300 cm^{-1} (P=O); 1210, 980 cm^{-1} (P-O-aromatic); 960-1008 cm^{-1} (P-O-C, C-O-C, P-OH, C-OH).

^{13}C NMR: 33.03 ppm (CH_2); 58.67 ppm (CH_2-OH); 120-130 ppm (aromatic).

CI/MS ($C_{15}H_{17}O_5P$; FW= 308): m/z, 309 (MH^+); 291 $(M - NH_4)^+$; 215 $(M - C_3H_7O)^+$; plus traces of 541, 447 derived from di(diphenyl)phosphopropanol.

Elemental analysis ($C_{15}H_{17}O_5P$; FW 308.27):

calculated:	58.44% C	5.56% H	10.05% P
found:	58.57% C	5.72% H	10.12% P

6.2 2,3-di-O-phytanylglycerol-1-phosphoryl-1'-(propane-1',3'-diol -3'-phosphate)(dPGP) (6.4)

A solution of TPS (TPS; 30 mg; 0.1 mmol) in anhydrous pyridine (10 ml) was added dropwise with stirring to an ice-cold solution of 2,3-diphytanyl-sn-glycerol-1-phosphate (PA, free acid; 130 mg; 0.18 mmol) and 1-diphenylphosphoryl-1,3-propanol (55 mg; 0.2 mmol) in anhydrous pyridine (15 ml). The reaction mixture was stirred at room temperature for 48 hours under anhydrous

conditions. Water (3 ml) was added to hydrolyze any unreacted TPS and the reaction mixture was extracted with ethyl ether. The ether phase was washed with water to neutrality and concentrated under reduced pressure. TLC of the residual oil in $CHCl_3$/CH_3OH/NH_4OH (65:35:5) showed a major phosphate-positive spot (R_f=0.83) as well as minor spots corresponding to unreacted diphenylphosphoryl propanol (R_f=0.95) and unreacted PA (R_f=0.10).

The crude diphenyl-dPGP (6.3) was purified by preparative TLC in $CHCl_3$/CH_3OH/NH_4OH (65:35:5) and the phenyl blocking groups were removed by hydrogenolysis with PtO_2 (75 mg) in freshly distilled ethanol (10 ml). TLC of the product (dPGP, 6.4) in chloroform/methanol/acetic acid (65:35:5) showed the presence of a single phosphorus-positive spot with R_f=0.36 (PGP standard R_f= 0.75).

The dPGP was converted to the ammonium salt form and precipitated from a minimum of chloroform with a 10-20 fold excess of acetone yielding 40.5 mg (24% from starting material) of the desired compound (6.4) (colourless oil).

^1H NMR: 0.8 ppm (CH_3); 1.0-1.87 ppm (CH_2); 3.42-3.70 ppm (RCH_2-O, R_2CH-O) and 3.8-4.16 ppm (CH_2-O-P, CH-OP).

^{13}C NMR: 61.2 ppm (G-γ); 61.5 ppm (G-α); 64.2 (G-1), 68.3 ppm (C-1); 69.5 ppm (C-1'); 70.3 ppm (G-3); 77.4 ppm (G-2) (see Appendix A11 and A13).

Negative FAB (dPGP(NH_4)2, FW=904): 869 (M - 2(NH_4))$^-$.

Elemental analysis dPGP-$(NH_4)_2 \cdot H_2O$:

$(C_{46}H_{104}O_{11}N_2P_2$; FW=922.77)

calculated: 59.84% C 11.31% H 3.03% N

found: 60.24, 60.34% C 11.21, 11.38% H 2.50, 2.44% N

Diphytanylglycerol Analogue of dPGP (Method b)

6.3 1-Bis(trichloroethyl)phosphoryl-1,3-propanediol (6.5)

A solution of bis(trichloroethyl)chlorophosphate (4.9 g; 0.013 mol) in anhydrous pyridine (20 ml) was added dropwise with stirring to an ice-cold solution of 1,3-propanediol (0.9 g; 0.018 mmol) in anhydrous pyridine (25 ml). The reaction mixture was stirred at 0°C for one hour and then at room temperature overnight (18 hours) under anhydrous conditions. Water (5 ml) was added to hydrolyse any unreacted bis(trichloroethyl)-chlorophosphate. The reaction mixture was extracted with ethyl ether and the ether phase was washed successively with water, 0.2 N HCl, 2.5% K_2HCO_3 and water to neutrality and concentrated under reduced pressure.

TLC of the residual product in $CHCl_3/CH_3OH$ (9:1) showed two phosphate-positive spots with R_f=0.55 (major) and R_f=0.70 (minor) corresponding to the mono- and diphosphorylated compounds, respectively. The crude material was purified by column chromatography (25 g silicic acid) by elution with petroleum ether (4:1; 200 ml; fraction 1), petroleum ether/chloroform (2:1; 150 ml; fraction 2), petroleum ether/chloroform (1:1; 250 ml; fractions 3 and 4) and chloroform (500 ml; fraction 5).

Fractions 1 and 3 contained the diphosphorylated and smaller amounts of the monophosphorylated. Fractions 4 and 5, containing the desired compound were pooled and concentrated under reduced pressure, yielding 1.71 grams (32%) of 1-trichloroethylphosphate-propane-3-ol (6.5) (colourless oil).

^{13}C NMR: 32.6 ppm (CH_2); 50.1 ppm (CH_2OH); 57.7 ppm ($O\underline{C}H_2CCl_3$); 66.6 ppm (CH_2-O-P); 77.1 ppm (CCl_3).

Elemental analysis ($C_7H_{11}O_5PCl_6$; FW=418.83)

calculated: 20.07% C 2.65% H

found: 20.30% C 2.73% H

6.4 2,3-diphytanylglycerol-1-phosphoryl-1'-(propane-1',3'-diol)-3'-phosphate (dPGP) (6.4)

A solution of TPS (1.2 grams; 4 mmol) in anhyrous pyridine (10 ml) was added dropwise with stirring to an cooled solution of diphytanylglycerophosphate (PA) (free acid; 255 mg; 0.35 mmol) and 1-trichloroethylphosphate-propane-3-ol (380 mg; 0.907 mmol) in anhydrous pyridine (10 ml). The reaction mixture was stirred at room temperature overnight under anhydrous conditions, then diluted with ethyl ether, and the ether phase was washed sequentially with water, 0.2 N HCl, KH_2CO_3 and water to neutrality, diluted with benzene and concentrated under reduced pressure.

The crude product (6.6) was dissolved in chloroform (4 ml) and acetic acid was added until the compound started to precipitate (8 ml) then an additional 0.5 ml of chloroform was added to re-dissolve the precipitate. Powdered zinc (800 mg) was

added and the mixture shaken well for 90 minutes. The zinc was removed by centrifugation and washed well with chloroform/methanol (1:1). The pooled supernatants (200 ml) was diluted with water (90 ml) to make the system biphasic. The chloroform phase was washed well with methanol/water (10:9), neutralized with 1N NH_4OH and concentrated under reduced pressure.

TLC in $CHCl_3/CH_3OH/NH_4OH$ (65:35:5) showed that the phosphate-positive band (R_f=0.8) had been converted to the desired product (R_f=0). The crude mixture was purified by preparative TLC in chloroform/methanol/NH_4OH (65:35:5). TLC of the crude dPGP in chloroform/methanol/acetic acid (65:35:5) of this band showed the presence of a major phosphate-positive band with R_f=0.3 corresponding to the desired product and a minor phosphate positive band with R_f=0.4 corresponding to PA formed by decomposition during treatment with zinc and acetic acid. The crude dPGP was further purified by preparatory TLC in chloroform/methanol/acetic acid (65:35:5) yielding 68.2 mg (21.6 %) chromatographically pure dPGP (6.4).

^{13}C NMR: 61.2 ppm (G-β); 61.5 ppm (G-α); 64.2 ppm (G-1); 68.3 ppm (C-1); 69.5 ppm (C-1'); 70.3 ppm (G-3); 77.4 ppm (G-2) (see Appendix A11 and A13).

Elemental analysis ($dPGP(NH_4)_2 \cdot H_2O$; FW= 922.78)

calculated:	59.84% C	11.32% H	3.03% N
found:	59.77 %C	11.45 %H	2.98 %N

Negative FAB/MS ($dPGP(NH_4)_2$; FW= 904): m/z, 869 $(MH - 2(NH_4))^-$.

Diphytanylglycerol analogue of dPG (6.9)

6.5 1-Benzoyl-propane-1,3-diol (6.7)

A solution of benzoyl chloride (8.42 g; 60 mmol) in anhydrous pyridine (15 ml) was added dropwise with stirring to an ice-cold solution of 1,3-propanol (5.25 g; 69 mmol) in 20 ml anhydrous pyridine and the reaction mixture was stirred at 0°C for one hour and then at room temperature for 6 hours under anhydrous conditions. Water (10 ml) was added and the mixture was extracted with ethyl ether, the ether phase was washed successively with water, 0.2 N HCl, 2.5% KH_2CO_3 and water to neutrality and concentrated under reduced pressure. TLC in chloroform/methanol/NH_4OH (65:35:5) showed two spots with R_f=0.49 (major) and 0.65 (minor) corresponding to the mono- and dibenzoylated compounds, respectively. The crude mixture was fractionated on a silicic acid column (50 g; prepared in petroleum ether) and eluted with petroleum ether/$CHCl_3$ (2:1; 200 ml, fraction 1); petroleum ether/$CHCl_3$ (1:1; 300 ml; fraction 2); $CHCl_3$ (500 ml, fraction 3). Fraction 1 contained the dibenzoylated compound and fractions 2 and 3 contained the desired product. Fractions 2 and 3 were pooled and concentrated under reduced pressure yielding 2.94 g (27%) of 1-benzoyl-3-propane-diol (6.7) (colourless oil).

TLC in $CHCl_3/CH_3OH$ (9:1) showed one spot with R_f=0.49.

^{13}C NMR: 32 ppm (CH_2); 59, 62 ppm (CH_2-O) ; 129-133 ppm (aromatic) ; 167 ppm (ester C=O).

IR: 3480 cm^{-1} (OH); 1725, 1295 cm^{-1} (C=O, C-O, ester); 3100,

1610, 1590, 1465, 730, 690 cm^{-1} (aromatic); 1295 cm^{-1} (ester C-O); 1075 cm^{-1} (C-OH, primary alcohol)

CI/MS (FW=180): m/z, 181 (MH^+); 163 $(MH - NH_4)^+$

Elemental analysis ($C_{10}H_{12}O_3$; FW 181.20):

calculated:	66.65% C	6.71% H
found:	66.95% C	6.88% H

6.6 2,3-Diphytanylglycerol-1-phosphoryl-1',3'-propanol (dPG) (6.9)

A solution of TPS (TPS; 360 mg; 1.2 mmol) in 20 ml anhydrous pyridine was added dropwise with stirring to a cooled (0°C) solution of PA (free acid; 90 mg; 0.123 mmol) and 1-benzoyl-1,3-propane-diol (6.7) (200 mg; 1.1 mmol) in 15 ml anhydrous pyridine. The reaction mixture was stirred at room temperature for 48 hours under anhydrous conditions. Water (3 ml) was added to hydrolyse excess TPS and the reaction mixture was extracted with ethyl ether. The ether phase was washed well with water to neutrality and concentrated under reduced pressure. TLC of the residual oil in chloroform/methanol/acetic acid (65:35:5) showed a major phosphate-positive spot with R_f=0.83 (PG standard R_f=0.49) together with minor byproducts.

A solution of the residual oil in chloroform (4 ml), methanol (2 ml) and 0.4N methanolic NaOH (10 ml) was left at room temperature for one hour and the reaction mixture was made biphasic by the addition of chloroform (12 ml) and 0.5N HCl (10 ml). The chloroform phase was washed well with methanol-water (10:9), neutralized with methanolic NH_4OH and concentrated under

a stream of nitrogen. The crude deacylated product was purified by preparative TLC in $CHCl_3/CH_3OH/NH_4OH$ (65:35:5) yielding 68 mg (32.3%) of dPG (6.9) (colourless oil).

TLC in $CHCl_3/CH_3OH/NH_4OH$ (65:35:5) showed one phosphate-positive spot with R_f=0.69 (PG standard R_f=0.49)

^1H NMR: 0.8 ppm (CH_3); 1.0-1.87 ppm (CH_2); 3.06-3.72 ppm (RCH_2-O, R_2CH-O) and 4.0-4.22 ppm (CH_2-OP, CH-OP).

^{13}C NMR: 59.8 ppm (G-β); 63.3 ppm (G-α); 64.4 ppm (G-1); 68.4 ppm (C-1); 69.6 ppm (C-1'); 70.2 ppm (G-3); 77.4 ppm (G-2) (see Appendix A12 and A13).

Negative FAB/MS (dPG-NH_4; FW= 807): m/z, 789 $(M - NH_4)^-$.

Elemental analysis for dPG(NH_4) ($C_{46}H_{98}O_7NP$; FW=807.75):

calculated:	68.34% C	12.22% H	1.73 % N
found:	68.60% C	12.39% H	1.58% N

6.7 sn-2,3-Diphytanylglycerol-1-phosphoryl-1'-propanol (Phosphatidyl propanol, proPG) (6.11)

A solution of TPS (350 mg; 2.64 mmol) in anhydrous pyridine (15 ml) was added dropwise with stirring to a cooled (0°C) solution of PA (free acid; 75 mg; 0.068 mmol) and freshly distilled 1-propanol (0.4 ml; 16.7 mmol) in pyridine (15 ml). The reaction mixture was stirred at room temperature under anhydrous conditions for 48 hours and extracted as described for dPG, yielding 18 mg (33%) of diphytanylglycerol phosphatidyl-propanol.

TLC of the residual oil in chloroform/methanol/acetic acid (65:35:5) showed the presence of one phosphate-positive spot

(R_f= 0.85) (PG standard, R_f= 0.90) corresponding to diphytanyl-phosphatidyl propanol (6.11). TLC in $CHCl_3/CH_3OH/NH_4OH$, R_f= 0.75; PG standard, R_f= 0.49)

^{13}C NMR: 9.52 ppm (G-γ); 64.5 ppm (G-1); 67.2 ppm (G-α); 68.4 ppm (C-1); 69.6 ppm (C-1'); 70.0 ppm (G-3); 77.4 ppm (G-2) (see Appendix A13).

Negative FAB/MS (phosphatidyl propanol-NH_4; FW=791): m/z, 773 $(M - NH_4)^-$.

Elemental analysis ($C_{46}H_{98}O_6PN$; FW=791.76):

calculated:	69.72% C	12.48% H	1.77% N
found:	69.65 %C	12.19 %H	1.47 %N

6.8 Methylated PGP (6.12-14) (Kates and Hancock, 1971)

A mixture of PGP-H_3 (50 mg, 0.056 mmol) and freshly washed AgO (150 mg) in freshly distilled CH_3I (6.5 ml) was stirred at room temperature for one hour. The reaction mixture was diluted with ethyl ether and the catalyst was removed by centrifugation and washed with chloroform/methanol (1:1). The pooled supernatants were concentrated under reduced pressure and the residual material was converted to the ammonium salt form as described in PART I.

TLC in $CHCl_3/CH_3OH$ (9:1) showed the presence of 4 components with R_f= 0.54, 0.73, 0.85 and 0.95 corresponding to unreacted PGP, tri- and tetramethylated PGP and methylated diphytanylglycerol, respectively. The latter compound was formed by alkaline-catalysed decompostion of PGP. The crude material was purified by preparatory TLC yielding 25.7 mg

$PGP(CH_3)_3$ (48 %) (6.12) and 6.4 mg of $PGP(CH_3)_4$ (12.3%) (6.13) and small amounts (< 2 mg) of $PGP(CH_3)_2$ (6.14).

^1H NMR: $PGP(CH_3)_3$: 3.78, 3.81 ppm ($P-O-CH_3$); 3.5-4.35 ppm (CHO, CH_2O); 0.8-1.6 ppm (CH, CH_2, CH_3).

$PGP(CH_3)_4$: 3.78-3.81 ppm ($P-O-CH_3$); 3.55 ppm ($C-O-CH_3$); 3.5-4.35 ppm (CHO, CH_2O); 0.8-1.6 ppm (CH, CH_2, CH_3).

Elemental analysis ($PGP(CH_3)_3$; $C_{49}H_{102}O_{11}P_2$; FW= 928.65):

calculated:	63.32 %C	11.07 %H
found:	62.88 %C	10.93 %H

NMR spectra shown in Appendix A14. FTIR spectra shown in PART III, section 4.

PART III

Physical Techniques

1. Deuterium NMR

1.1 Introduction and Theory of ^2H NMR

An understanding of the macromolecular properties of the membranes of the halophilic bacteria requires a more detailed knowledge of the order and dynamics of the lipid molecules which comprise these membranes. ^2H NMR is capable of providing quantitative information on the time-averaged orientations and rates of motions of specific positions within the hydrophobic or headgroup regions of bilayer lipids. The residual quadrupole splittings ($\Delta\upsilon_Q$ or D_q) are directly related to the segmental order parameters and the spin-lattice relaxation times (T_1) provide information on the timescales of molecular motions.

Molecular Order

The deuterium nucleus has a nuclear spin I=1 and therefore a quadrupole moment. In the presence of a magnetic field, the combination of the Zeeman and quadrupolar interaction will result in a 2 line spectrum with a maximum frequency separation which is given by

$$\Delta\upsilon_Q = 3/4\ (e^2qQ/h)\ |S_{CD}|(3\cos^2\phi - 1) = 128\ \text{kHz}$$

where e is the charge on the electron, eq is the electric potential, Q is the quadrupole moment and ϕ is the angle between the externally applied magnetic field and the director or local

bilayer normal (Rance et al., 1983). This equation assumes that the electric field gradient at the deuteron site is axially symmetric (Rance et al., 1983). S_{CD}, the C-^{2}H bond order parameter or segmental order parameter is given by the following equation:

$$\left|S_{CD}\right| = \left\langle \frac{3\cos^2\theta - 1}{2} \right\rangle$$

where θ is the angle between the C-^{2}H bond and the axis of motional averaging (generally assumed to be the bilyaer normal). The angular brackets denote a time average over times short compared with $1/\Delta\upsilon_Q$ (10^{-5}-10^{-6} sec).

Thus, the values of $\Delta\upsilon_Q$ and therefore S_{CD} are determined both by the average orientation of the C-^{2}H with respect to the bilayer normal and by the amplitude of the angular fluctuations about this average orientation.

In liposomes, in which there is a distribution of all orientations with respect to the magnetic field, the spectrum is a superposition of doublets, each with splittings given by the equation shown above. The resultant "powder pattern" , shown in Figure III.1 has two distinct peaks which are separated in frequency by

$$\Delta\upsilon_Q = 3/4\ (e^2qQ/h)\ \left|S_{CD}\right|$$

The powder pattern linshape is termed a "Pake doublet" after G.E. Pake, an early researcher in this field (Pake, 1948). A deconvolution technique, "de-Pake-ing", developed by Bloom and

Figure III.1

^2H NMR powder patterns and corresponding de-Paked spectra for A, one splitting with $\Delta\nu_Q$ = 20 kHz; B, two splittings with the ratio of 3:2 with $\Delta\nu_Q$ = 10 and 20 kHz, respectively.

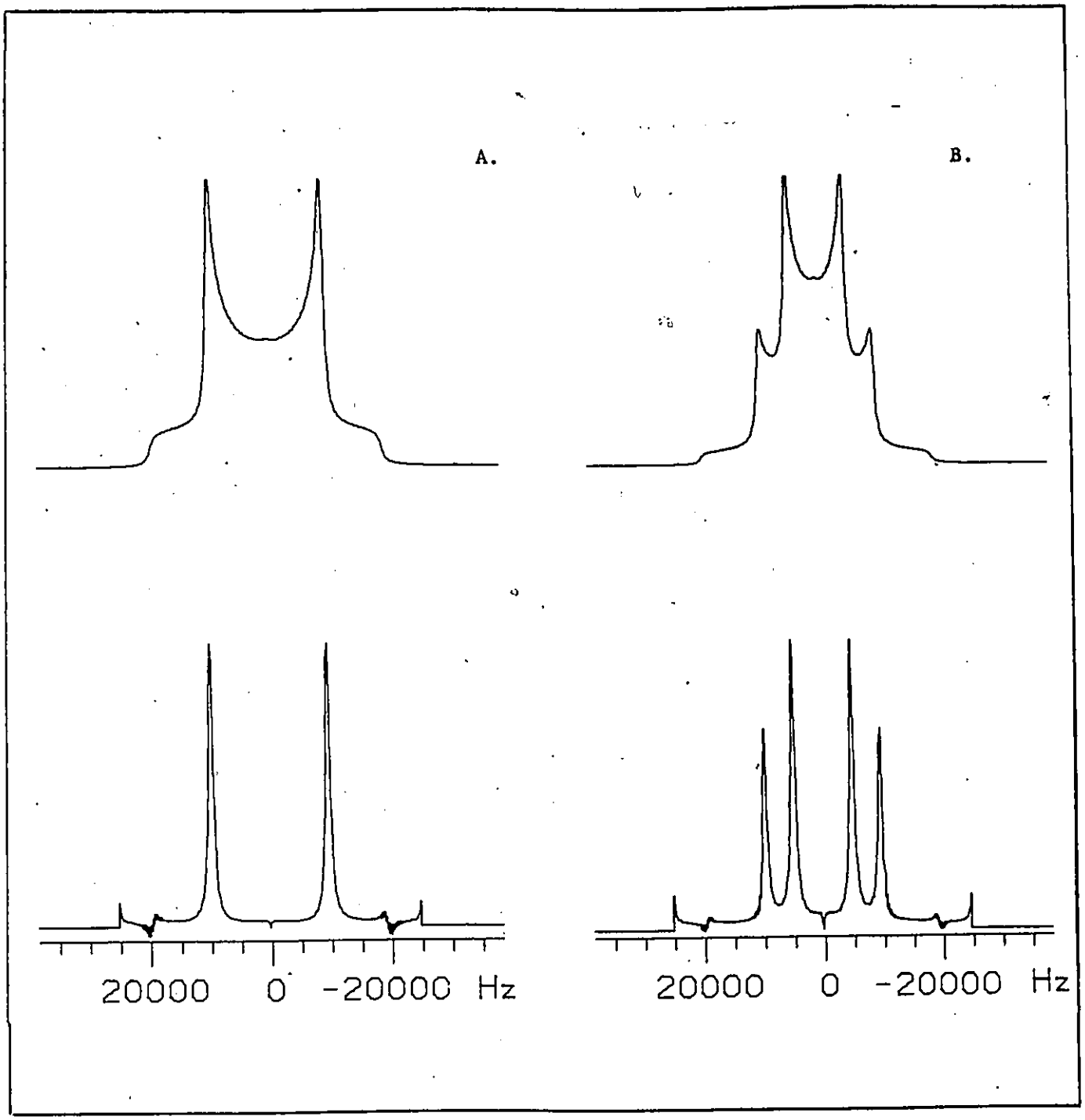
A.
B.
20000
0
-20000
Hz
20000
0
-20000
Hz

coworkers (Sternin et al., 1983) reduces the powder spectrum to the spectrum which would be expected for an oriented bilayer with an angle of 90° between the applied magnetic field and the axis of conformational averaging of the acyl chains (see Figure III.1). Removal of the overlap from subspectra corresponding to other angles usually leads to decreased signal-to-noise but increased resolution of the splittings. This technique is particularly useful for multiply deuterated compounds. The relative intensities of the splittings of the de-Paked spectra correspond well to the relative proportions of the labelled species, allowing for quantitative analysis and facilitating the correlation of sets of splittings and labelled positions.

If there is axial rotation but no disordering of the chain segments, the quadrupolar splitting is reduced to approximately 64 kHz. Disordering of the chains with rapid interconversion between disordered states leads to a further reduction in the value of the splittings. This disordering is due to the presence of intramolecular motion such as gauche-trans isomerization about C-C bonds in the hydrocarbon chains, chain wagging, and wobbling of the molecular axis. These motions lead to reorientations of the C-C bond relative to the axis about which the molecule is rotating within the bilayer.

The bond order parameter is thus a quantitative measure of the ensemble- and time-averaged distributions of gauche and trans conformers and reflects the state of molecular organization. For n-acyl lipids, the bond order parameter can be converted to the molecular order parameter (S_{mol}) with appropriate transformation

to account for the angle between the C-D bond and the long axis of the molecule

$$S_{mol} = S_{CD}\, S_{geo}$$

For the phytanyl lipids and for n-alkyl lipids near the glycerol backbone, S_{geo} is not known and thus results cannot be expressed in terms of S_{mol}. This is a drawback as the value of S_{CD} had both a motional and an orientational dependence and unambiguous interpretation of the data is difficult.

Molecular Dynamics

The currently accepted model for the organization of membrane systems is the fluid mosaic model (Singer and Nicholson, 1972) which postulates that the lipid molecules are arranged predominantly in a bilayer conformation with the hydrophilic headgroups exposed to the aqueous environment and the hydrophobic tails sequestered inside. Membrane stability is then provided by hydrophobic (van der Waals) and hydrophilic interactions as well as hydrogen bonding between polar headgroups.

The absence of covalent interactions allows for mobility of the lipid molecules; anisotropic molecular rotation, lateral diffusion in the plane of the bilayers and, to a lesser extent, intermonolayer lipid exchange. Although the importance of these different types of mobility to the function of biological membranes is not well understood, the ability of lipid molecules to undergo lateral diffusion, for example, allows for phenomena such as membrane flexibility, elasticity, permeability and lateral

phase separation of specific membrane components. It is therefore probable that the other molecular motions play different but equally important roles in membrane structure and function. The molecular motions of lipid bilayers encompass a wide range of frequencies. For example the rates of motions affecting the quadrupole splittings are on the order of 10^{-5} to 10^{-6} sec. In contrast, the spin-lattice relaxation times report on a much higher frequency range (corresponding to 10^{-4} to 10^{-10} sec) even though the T_1 values are on the order of 10 ms (for ^2H NMR) to seconds (^{31}P NMR). ^2H NMR T_1 studies are particulary useful as this frequency range corresponds to that of the intramolecular segmental reorientations of the phospholipid molecules.

Bilayer lipids undergo a number of different motions of distinct amplitudes and timescales. These motions, which are fast on the NMR timescale ($<10^{-6}$ sec), include molecular rotation, chain rotational isomerization, chain torsional oscillation and bond stretching and bending (Brown, 1982). In ^2H NMR, analysis of spin-lattice relaxation times (T_1) has provided a means of obtaining information about the dynamics of membrane lipids.

Following excitation of the ^2H nucleus with a radio-frequency pulse, energy is transferred to the surrounding or 'lattice' via fluctuating local magnetic fields which are induced by molecular motion. In ^2H NMR, the dominant relaxation pathway is via quadrupolar interactions. Because the strength of the fluctuating quadrupolar interaction determines the efficiency of the spin-lattic relaxation, measurement of the T_1 values provides

information on the dynamics of the system.

The rate of relaxation of ^2H-labelled bilayer lipids may be described by the following empirical equation:

$$1/T_1 = A\tau_f + BS_{CD}^2\omega_o^{-\frac{1}{2}}$$

where A and B are constants, τ_f is the correlation time for fast, axially symmetric motions, S_{CD} is the segmental order parameter and ω_o is the resonance frequency. The degree of dependence on ω_o is model-dependent and is still under debate (Sininovitch et al., in press).

This equation implies that the rate of spin-lattice relaxation is determined both by the rapid local motions of the hydrocarbon chain segments (primarily gauche-trans isomerization) and by cooperative fluctuations of the local director axis with respect to the bilayer normal (larger amplitude wave-like motions down the hydrocarbon chain) providing that these motions are within the appropriate frequency range.

Previous ^2H NMR Studies of Synthetically and Biosynthetically Deuterated Lipids

The hydrocarbon chains of phospholipids have been specifically labelled both synthetically and biosynthetically. The value of S_{CD} has been shown to vary as a function of position of the label (carbon atom) along the chains as shown in Figure III.2 (Seelig and Seelig, 1974; Stockton et al., 1977). A variety of saturated lipids have been studied by this method, including PE, PC, PS, PG and cardiolipin as well as *E. coli* and *A. laidlawii* membranes

Figure III.2

Dependence of the quadruple splitting (or order parameter, S_{CD}) on position of labelling of the $C_{16:0}$ chains in the membranes of A. laidlawii at 40°C.

Data from Stockton et al., 1977.

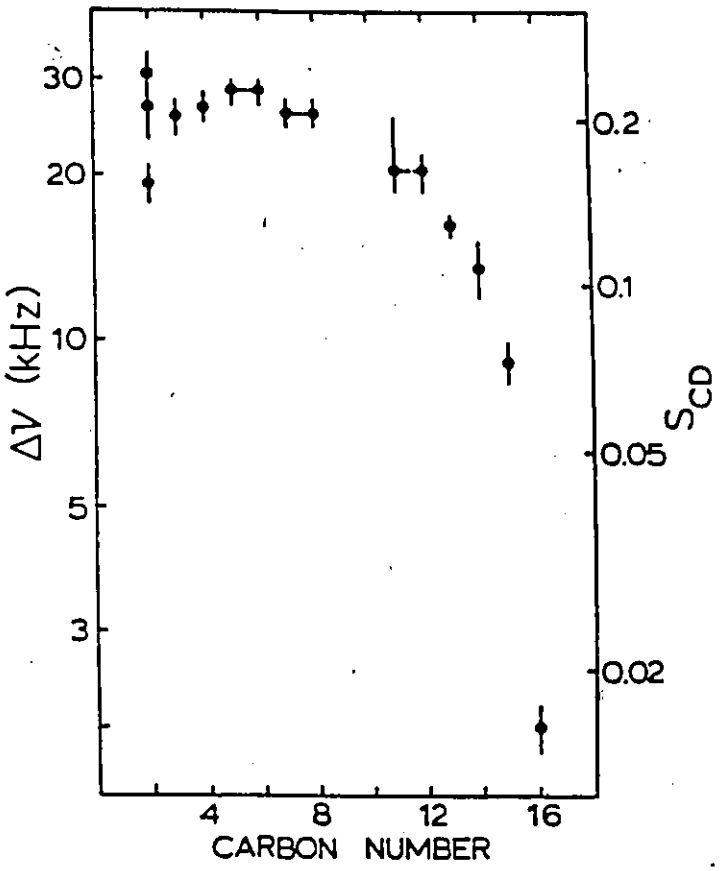
30
20
10
5
3
ΔV (kHz)
0.2
0.1
0.05
0.02
S_{CD}
4
8
12
16
CARBON NUMBER

(see reviews by Smith, 1984; Seelig, 1977; and Davis, 1983). The order parameter profile is virtually the same for all lipids studied and was essentially independent of the headgroup. The profile is roughly constant for the first eight positions then decreases sharply, indicating that the molecular motion is much more restricted adjacent to the glycerol backbone than in the interior of the membrane.

Interestingly, three splittings are seen for the four deuterons on the C-2 positions of the sn-1 (12.0 and 19.2 kHz) and sn-2 (27.2 kHz) chains. The splittings for the two deuterons of the sn-1 position of the backbone glycerol differ by almost a factor of two, not because they differ in their degrees of motions, but because the average orientation with respect to the molecular axis of motion are different for the two deuterons (Engle and Cowburn, 1981). Only one value for the quadrupole splitting is seen for all the remaining positions of the n-acyl chains.

In saturated hydrocarbon chains, the average orientation of the C-D bonds of each methylene segment is essentially the same. Thus, the segmental order parameter measures variations from this average value. For unsaturated lipids, the presence of the double bond leads to a change in the average orientation of the adjacent methylene segments.

The significance of this is shown in Figures III.3 and 4 which compare the dependence of segmental and molecular order parameters on the position of the label along the chain for saturated and unsaturated phospholipids. Incorrect conclusions

Figure III.3

Variation in the quadrupole splittings and order parameters with position of the deuterium label for saturated and unsaturated chains of A. laidlawii membranes.

□ oleate-labelled A. laidlawii membranes at 0°C.

o palmitate-labelled A. laidlawii membranes at 42°C.

(Data from Rance et al., 1980)

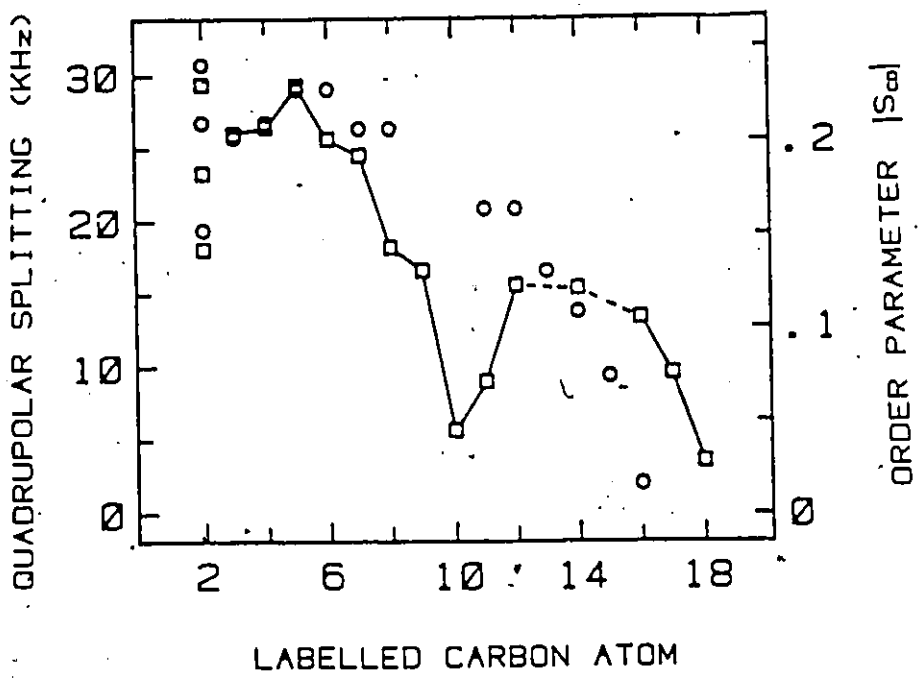
QUADRUPOLAR SPLITTING (KHz)
30
20
10
0
2
6
10
14
18
LABELLED CARBON ATOM
.2
.1
0
ORDER PARAMETER |Scd|

Figure III.4

Comparison of the variation of the molecular order parameter with the position of the deuterium label for saturated (●) and unsaturated (○) lipid probes in membranes and model membranes.

Oleate-labelled chain in A. laidlawii membranes, 25°C, data from Jarrell et al., 1983.

Stearic acid probe in egg PC liposomes at 30°C, data from Stockton et al., 1976.

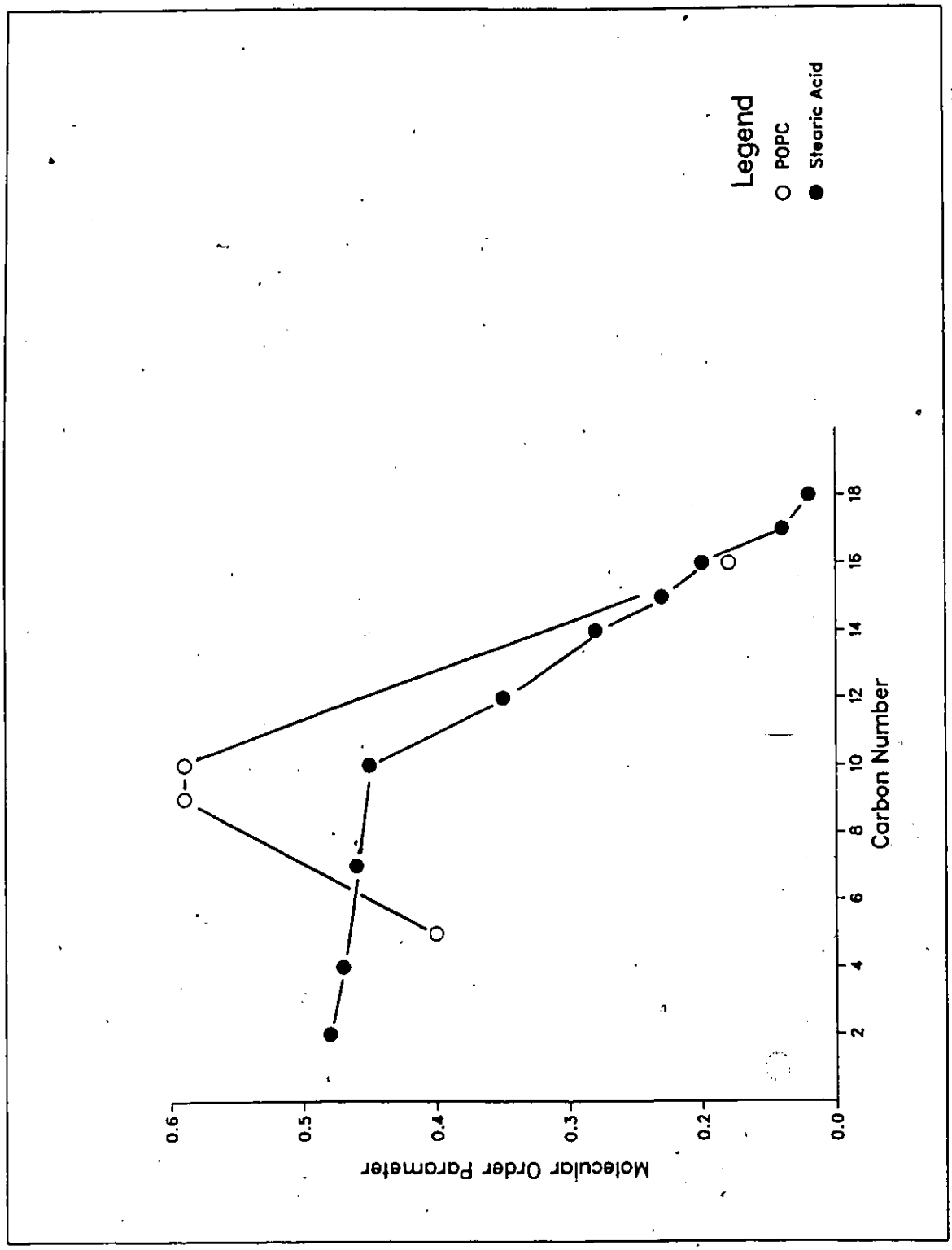
Legend
POPC
Stearic Acid
Molecular Order Parameter
0.0
0.2
0.3
0.4
0.5
0.6
Carbon Number
2
4
6
8
10
12
14
16
18

may be drawn without sufficient attention to the possibility of both motional and orientational contributions to S_{CD}.

Most ^2H NMR studies on the hydrocarbon region of deuterated phospholipids have used saturated, unsaturated or cyclopropyl-containing ester-linked lipids (Seelig, 1977; Griffin, 1981; Jarrell, 1983). Recently, two studies have been completed with ether-linked lipids: dihexadecyl PC (Ruocco et al., 1985) and plasmalogens and related compounds (Malthaner et al., 1987)

^2H NMR spectra from synthetic dihexadecyl PC deuterated in the first positions (C-1) of both chains showed that the four deuterons were magnetically inequivalent (see Figure III.5, Table III.1). Although the splittings were assigned to two groups based on the magnitude of the splittings and the values of the spin-lattice relaxation times, they could not be assigned to a specific chain. Unlike the diacyl lipid, the first labelled positions of both the sn-1 and sn-2 chains of the dialkyl lipids (DHPC) are magnetically inequivalent. The values for DHPC (2.3-16.8 kHz) are also significantly lower than the C-2 position of the diacyl lipids (12.0-27.2 kHz). Although this implies that the conformation and/or amplitudes of motions at the beginning of the ester-linked and ether-linked hydrocarbon chains are different, the same positions were not labelled in the two lipid classes, making comparison difficult.

Phosphatidylethanolamine and phosphatidyl-N-monomethyl-ethanolamine, as well as the corresponding plasmalogens and plasmalogen-glycerolacetals, were isolated from Clostridium

Figure III.5.

^2H NMR spectra of aqueous dispersions of $[2,2\text{-}^2H_2]$ DPPC and $[1,1\text{-}^2H_2]$ DHPC. $T = 45^{\circ}C$; $\omega_o = 45.3$ MHz. (Data from Ruocco et al., 1985).

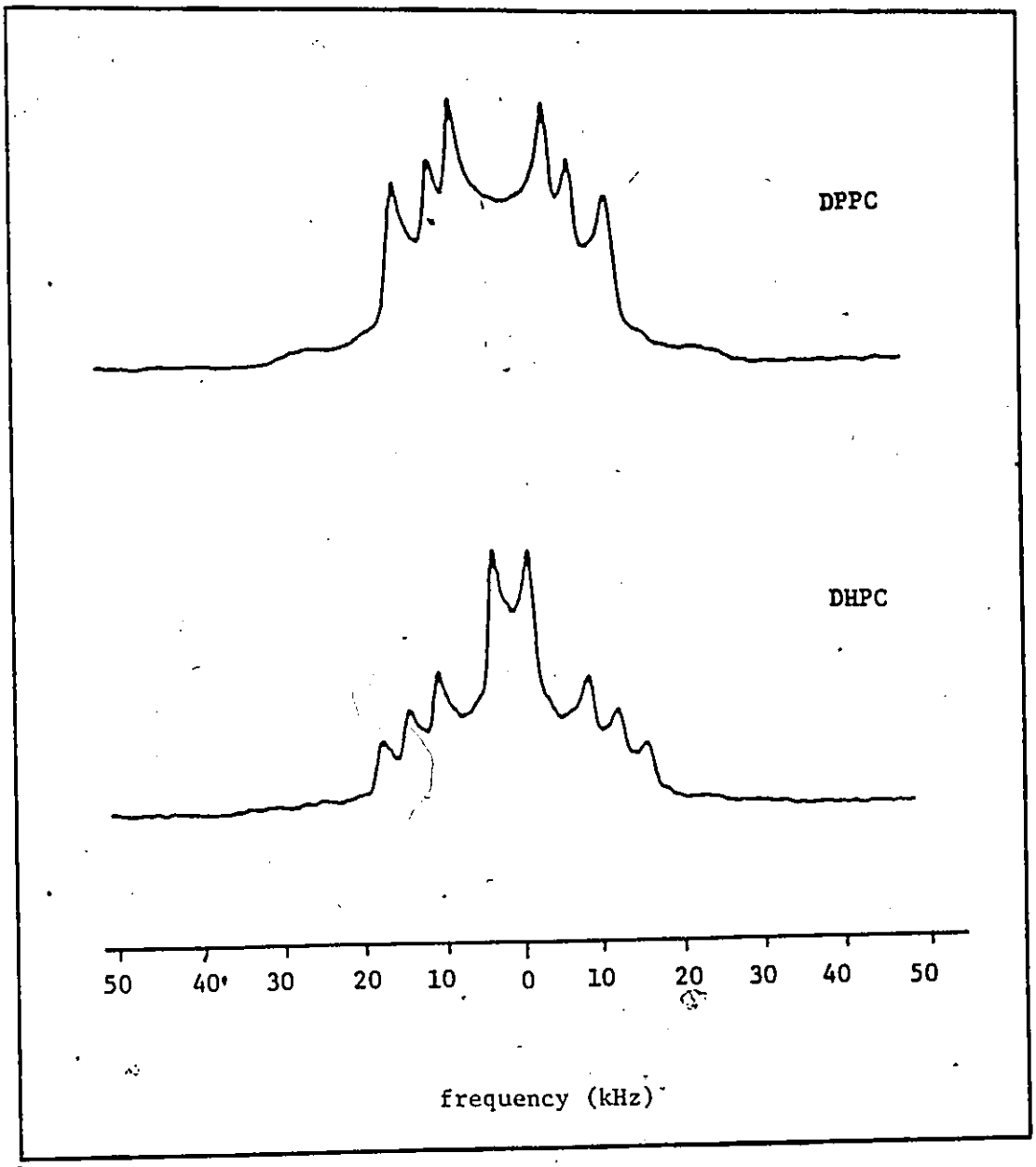
DPPC
DHPC
50
40
30
20
10
0
10
20
30
40
50
frequency (kHz)

Table III.1

Quadrupole splittings and spin-lattice relaxation times for synthetic DHPC and DPPC

Compound	Relative intensity	Quadrupole splittings (kHz)	T_1 (ms)
[2,2,2',2'-$^2H_4$]DPPC			
	1	11.8	15.14
	1	17.6	15.15
	2	27.4	18.61
[1,1,1',1'-$^2H_4$]DHPC			
	1	2.34	18.14
	1	9.45	18.80
	1	13.1	20.93
	1	16.8	21.11

Data from Ruocco et al., 1985, ω_o= 45.3 MHz, T= 46°C.

Table II.2

Quadrupole splittings of phospholipids of *C. butyricum* and *C. beijerickii* grown on [2,2-$^2H_2$]palmitic acid/oleic acid

Compound	Quadrupole splittings (kHz)			
	C. butyricum		*C. beijerinckii*	
	sn-2	sn-1	sn-2	sn-1
diacyl PE	13.0,19.0	25.0	12.7,18.6	25.5
plasmalogen PE	25.0		25.5	
glycerol acetals	18.4,20.9	-	16.4,18.7	-
PG and CL	10.9,16.0	23.8	11.1,15.8	24.0

Data from Malthaner et al., 1987 ω_o = 45.6 MHz, T= 30°C.

butyricum and C. beijerickii grown on either palmitic acid with deuterium labels at C-2, C-3 or C-4 or oleic acid with deuterium labels at C-2 and C-9,10 (Malthaner et al., 1987).

Palmitic acid and oleic acid were preferentially bound to the sn-2 and sn-1 positions, respectively. For all three lipid fractions, the quadrupole splittings were low for C-2 and increased by almost a factor of two for positions 3 and 4 of the palmitoyloleoylglycerol derivatives (Table III.2). In contrast to the diacyl lipids, one set of quadrupole splitings were seen for the C-2 position of the sn-2 chain of the plasmalogens (< 25 kHz) indicating that the presence of the vinyl group results in an unusual orientation of the chain, i.e., similar to that of the sn-1 chain in n-acyl lipids.

1.2 Materials and Methods

1.2.1 Samples and Solvents

Deuterated diphytanylglycerol and dihexadecylglycerol derivatives of PA and PG were synthesized as described in PART II. Biosynthetically-labelled total polar lipids were prepared from Halobacterium cutirubrum grown on medium containing perdeuterated sodium acetate as described in PART I. Growth on perdeuterated sodium acetate-supplemented medium resulted in labelling of at least some of the methylene groups adjacent to the methine groups (Ekiel et al., 1986).

Samples (10-60 mg) were suspended in deuterium-depleted water (0.5-1.0 ml; Aldrich) or buffer (10 mM tris, pH 7.5, 2 mM EDTA, 110 mM NaCl in deuterium-depeleted water) then frozen, thawed and vortexed until the samples appeared homogeneous. Bilayer structures were confirmed by ^{31}P NMR.

1.2.2 Hardware and Software

Solid state ^{2}H NMR spectra were obtained on a Bruker CXP-300 or MSL-300 spectrometer operating at 46.066 MHz or a home-built spectrometer operating at 30.70 MHz using a home-built probe. Spectra were acquired on resonance using the quadrupolar echo sequence (90°_{x}-τ-90°_{y}-acquire) with full phase cycling of the radio-frequency pulses (Griffin, 1981; Solomon, 1958).

Pulse spacings were typically 30-50 us, the 90° pulse length was 3.5-5 us and the recycle time $>5T_1$.

Spin-lattice relaxation times were determined by a modification of the standard inversion-recovery techniques (Vold et al., 1966)

$$180^{\circ}_{y} - \tau - 90^{\circ}_{x} - \tau - 90^{\circ}y \quad \text{-acquire}$$

The intensity, after de-Pake-ing (Sternin et al., 1983) of the quadrupolar splittings as a function of τ is given by

$$M_o = M_t[(1-2\exp(-\tau/T_1)]$$

where M_o is the intensity when $\tau > 5T_1$ and M_t is the intensity at a given τ value.

1.3 Results and Discussion

1.3.1 Dihexadecylglycerol phosphatidic acid

Molecular order

The ^2H NMR spectra obtained from aqueous dispersions of sn-1,2-dihexadecylglycerol-3-phosphate (DHPA) labelled in the first or second position of the sn-2 chain are shown in Figure III.6 and the values of the quadrupole splittings, together with the corresponding previously reported values for DHPC (Ruocco et al., 1985) and DPPC (Seelig et al., 1977) are given in Table III.3. Two quadrupole splittings are seen for each labelled segment: 4.5 and 10.5 kHz for sn-2-[1,1-$^2H_2$]hexadecyl-1-hexadecylglycerol-3-phosphate ([1,1-$^2H_2$]DHPA) and 20.4 and 22.2 kHz for sn-2-[2,2-$^2H_2$]hexadecyl-1-hexadecylglycerol-3-phosphate ([2,2-$^2H_2$]DHPA).

Comparison of these results with previous data on DHPC labelled in the first position (Ruocco et al., 1985) allows for the assignment of the four previously published splittings to the sn-1 (13.1 and 16.8 kHz) and sn-2 (2.3 and 9.5 kHz) chains. The difference in the splittings of DHPA and DHPC may be attributed to headgroup effects similar to those seen for the membrane lipids of A. laidlawii (Rance et al., 1983). Rance and coworkers reported minor differences in the orientation and conformation of the acyl chain at the C-2 position of the various lipid classes although these differences did not persist beyond the second carbon. Similar effects would be expected for the positions adjacent to the glycerol backbone (C-1) in alkyl chains.

As previously mentioned, the presence of multiple splittings for the two deuterons of one methylene group is also seen for the

Figure III.6

^2H NMR spectra of aqueous dispersions of $[1,1-^2H_2]$- and $[2,2-^2H_2]$ DHPA. The shape of the spectra do not vary significantly with decreased interpulse delays and is therefore thought to arise from magnetically oriented samples similar to those reported previously (Seelig et al., 1985).

(T= 80°C; ω_o= 30.70 MHz)

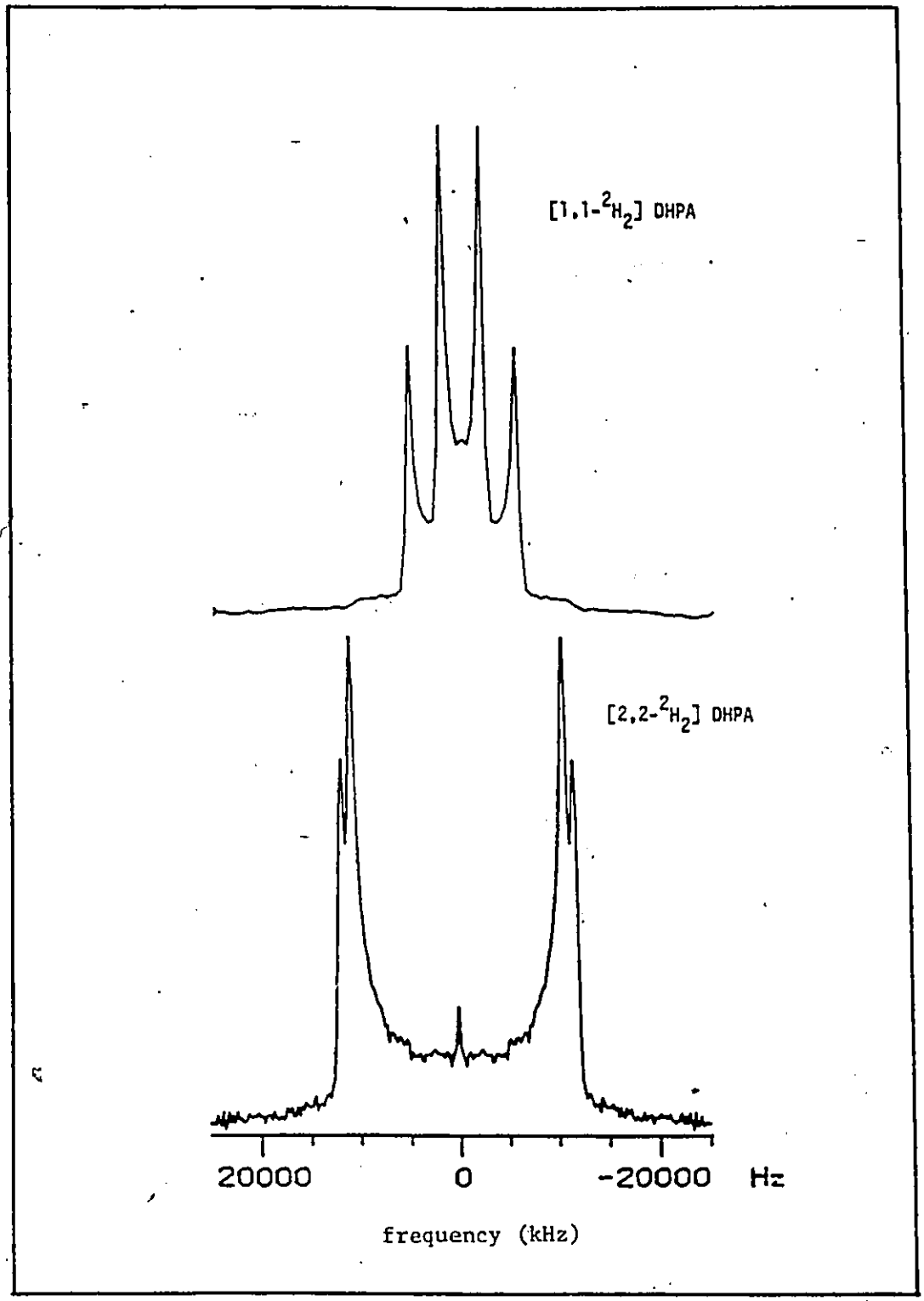
[1,1-$^2H_2$] DHPA
[2,2-$^2H_2$] DHPA
20000
0
-20000
Hz
frequency (kHz)

Table III.3

Quadrupole splittings for n-alkyl and n-acyl phospholipids[a]

Compound	Position of deuterium label					
	C-1		C-2		C-3	
	sn-1	sn-2	sn-1	sn-2	sn-1	sn-2
DHPA[b]		4.5		20.4		
		10.5		22.2		
DPPC[c]			27.2	12.0	26.2	23.2
				19.2		
DHPC[d]	13.1	2.34				
	16.8	9.45				

a. Quadrupole splittings in units of kHz.

b. Present studies, ω_o= 45.3 MHz; T= 80°C; T_c= 72°C.

c. Seelig et al., 1977, ω_o= 13.78 MHz; T= 50°C; T_c= 44°C.

d. Ruocco et al., 1985, ω_o=45.3 MHz; T= 45°C; T_c= 41°C.

second carbon of the sn-2 chain of DPPC (see Table III.3) and can be attributed either to orientational inequivalence of the pro-R and pro-S deuterons or to the presence of two long-lived ($>10^{-5}$ sec) conformers. Stereospecific monodeuteration of the second position of the sn-2 chain of n-acyl lipid has shown that, in this system, each of the splittings arises from one deuteron (Engel and Cowburn, 1981). The magnetic inequivalence was thus attributed to differences in the orientation of the acyl chains at the positions adjacent to the glycerol backbone.

This conclusion is consistent with the crystal structure of diacyl phospholipids determined by X-ray crystallography (Hitchcock et al., 1974; Pearson and Pascher, 1977) and neutron diffraction studies (Büldt et al., 1978; Zaccai et al., 1979; Büldt and Seelig, 1980).

To confirm that this is also the case for DHPA, the temperature dependence of the quadrupole splittings was determined (Figure III.7a). If the two splittings arise from interconversions between two conformations at a rate which is slow relative to the NMR timescale, an increase in the temperature may result in an increase in the rate of interconversion and may lead to one pair of peaks at a frequency separation which is the weighted average of the previous values. Conversely, if the multiple splittings arise from geometric effects (one conformation, but the deuterons are oriented at different angles relative to the director), increasing the temperature would lead only to decreases in the degree of order as reflected by similar decreases in the quadrupole splittings.

Table III.7a

Temperature dependence of quadrupolar splittings of aqueous dispersions of $[1,1\text{-}^2H_2]$DHPA and $[2,2\text{-}^2H_2]$DHPA.

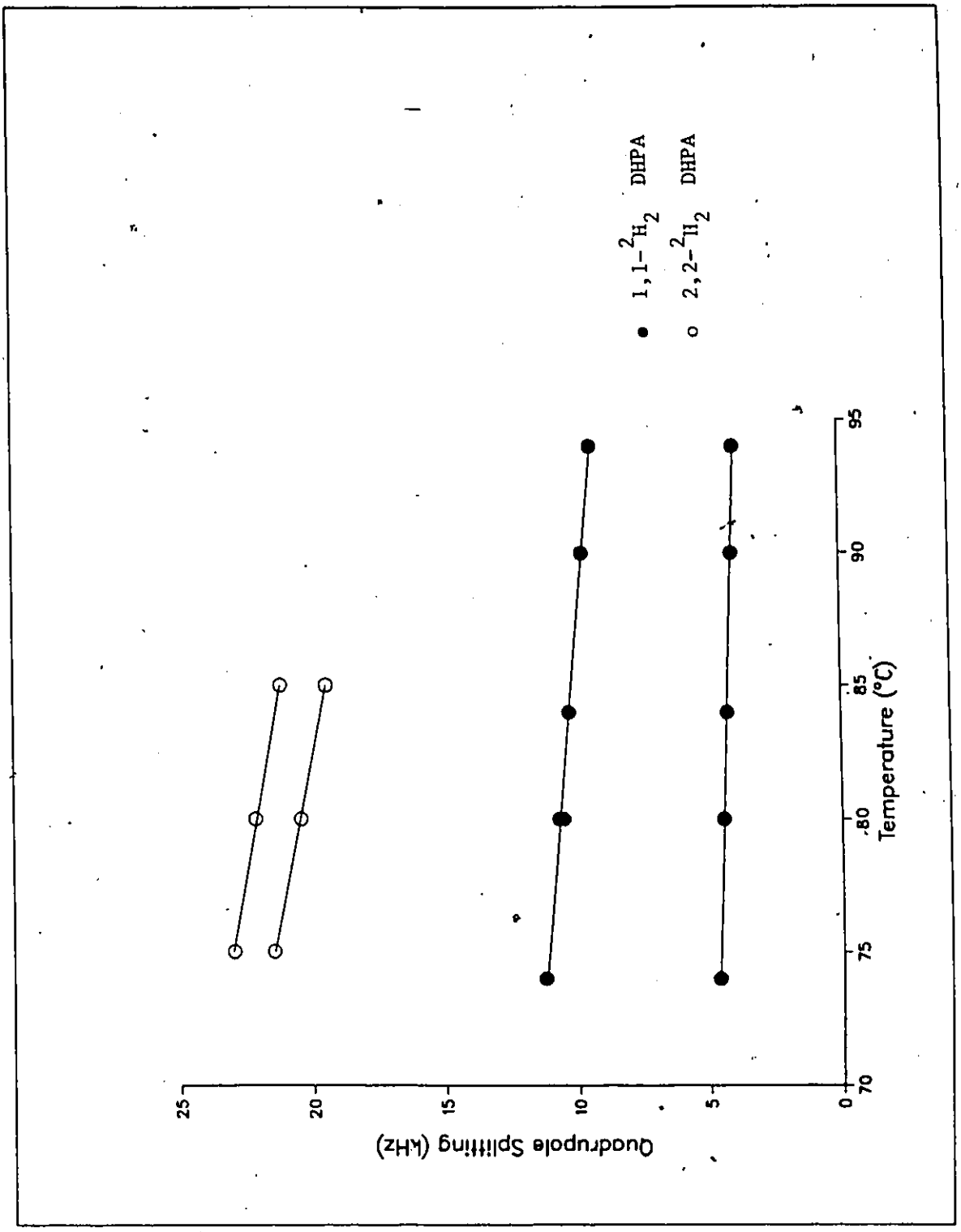
Quadrupole Splitting (kHz)
25
20
15
10
5
0
70
75
80
85
90
95
Temperature (°C)
• 1,1-$^2H_2$ DHPA
o 2,2-$^2H_2$ DHPA

The change in the two splittings of [2,2-$^2H_2$]DHPA as a function of temperature is the same within experimental error (-0.19 and -0.21 kHz/degree) indicating that the two splittings result from magnetic inequivalence due to differences in the average orientations of the C-D bond with respect to the axis of motional averaging. Alternatively, the energy difference between the two conformations may be too high to be affected by changes within this temperature range. However, for [1,1-$^2H_2$]DHPA, the values of the slopes are significantly different (-0.037 and -0.095 kHz/degree) indicating that there may be two conformational states, each giving rise to one set of splittings.

In addition to determining the temperature dependence of the quadrupole splittings, the change in the relative heights of the two peaks were measured as a function of temperature for each labelled position. The rationale for this experiment is as follows: if the multiple splittings arise from conformational effects, the increase in the temperature may cause a shift in the equilibrium between the two conformations. This shift in the relative populations of each conformer would be reflected in the relative peak heights providing that the energy difference between the two conformations is large. Figure III.7b shows that the relative heights of the two peaks of [2,2-$^2H_2$]DHPA are virtually invariant with temperature; however, the relative heights of the two peaks of [1,1-$^2H_2$]DHPA are temperature dependent.

The temperature dependence of both the quadrupolar splittings and the relative peak heights are consistent with the hypothesis that the deuterons attached to the first carbon of the sn-2 chain

Table III.7b

Temperature dependence of the relative heights of the quadrupolar splittings of aqueous dispersions of both $[1,1\text{-}^2H_2]$- and $[2,2\text{-}^2H_2]$ DHPA.

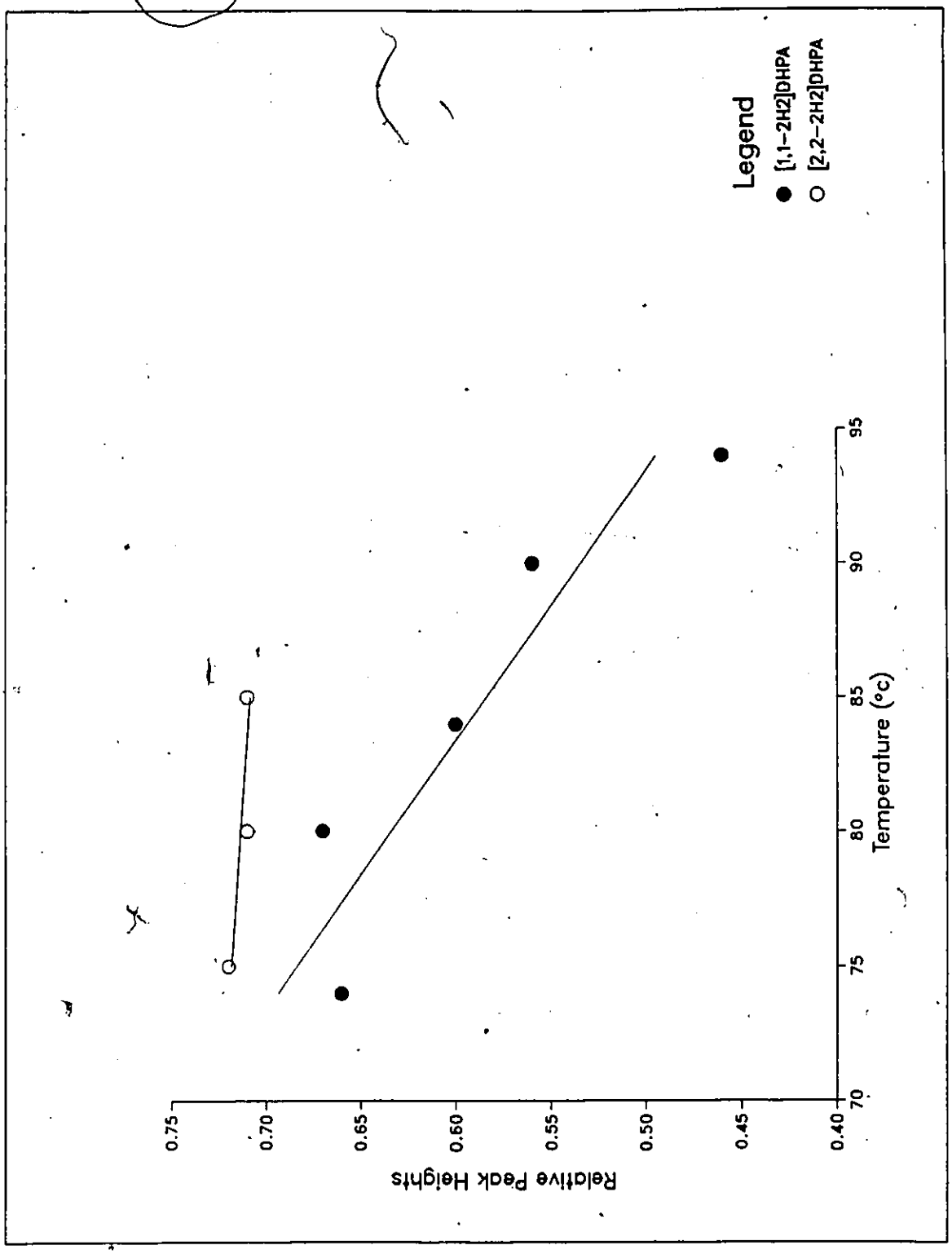
Legend
● [1,1-2H2]DHPA
○ [2,2-2H2]DHPA
Relative Peak Heights
0.75
0.70
0.65
0.60
0.55
0.50
0.45
0.40
70
75
80
85
90
95
Temperature (°c)

give rise to multiple splittings due to the presence of two conformations which are interchanging slowly on the NMR time-scale. Conversely, the multiple splittings arising from the labelled second carbon of the chain may arise from slight differences in the orientation of the deuterons with respect to the director. Alternatively, the energy difference between the two putative conformers of the second methylene segment may be higher than that of the first methylene.

The values of the quadrupolar splittings for the labelled second position in the n-alkyl lipids (C-2, 20.4 and 22.2 kHz) are significantly different from those of the corresponding positions of the n-acyl lipids (C-2, 12.0 and 19.0 kHz). This reflects the conformational differences in the chains between the n-alkyl and n-acyl lipids due to the glycerol-hydrocarbon ether linkage as compared to the ester linkage.

Molecular dynamics

The spin-lattice relaxation times for DHPA, DHPC and DPPC, at comparable reduced temperatures but different field strengths, are shown in Table III.4. The T_1 values for the first carbon (C-1) of the n-alkyl lipids (14.93, 16.25 ms) are comparable, to previously reported values for n-alkyl lipids (Ruocco et al. 1985) (20.93-21.11 ms). The value for the second carbon (C-2) (26.67 ms) is significantly higher than that of the n-acyl lipids (15.14-18.6 ms), indicating that there is a marked effect of the nature of the linkage on the rates of molecular motions of the hydrocarbon chains, at least at positions adjacent to the glycerol backbone.

Table III.4

Spin-lattice relaxation times

of synthetic n-alkyl and n-acyl phospholipids

Compound	position of label	T_1 (ms)	T (°C)	T_c (°C)
DHPA[a]	C-1 sn-2	14.93 16.25	85	71
	C-2 sn-2	26.67		
DPPC[b]	C-2	15.14-18.61	46	41
	C-3	32.3		
	C-4	32.7		
DHPC[b]	C-1 sn-1	20.93-21.11	46	44
	C-1 sn-2	18.14-18.80		

a. Present studies, ω_o= 30.70 MHz

b. Ruocco et al., 1985, ω_o= 45.3 MHz.

1.3.2 Synthetically Deuterated Diphytanylglycerol Phospholipids

The ^2H NMR spectra and the corresponding de-Paked and simulated spectra for rac-(R/S,R,R)-2,3-[1,1,1',1'-$^2H_4$]-diphytanylglycerol phosphate ([1,1,1',1'-$^2H_4$]DPhPA), rac-(R/S,R,R)-2,3-[1,1,1',1'-$^2H_4$]diphytanylglycerolphosphate ([1,1,1',1'-$^2H_4$]DPhPA) and (R,R,R)-2-[2,2-$^2H_2$]phytanyl-3-phytanyl-sn-glycerol phosphate ([2,2-$^2H_2$]DPhPA are shown in Figures III.8 and III.9. The values and the relative intensities of the quadrupolar splittings are given in Table III.5. For comparison, the values of the quadrupolar splittings for phytanyl, n-alkyl and n-acyl lipids are shown together in Table III.6.

The values for the first carbon of the sn-2 chain for both the phytanyl and n-alkyl lipids are comparable (3.14, 16.70 kHz for phytanyl and 4.5, 10.5 kHz for n-alkyl) implying that the orientation and amplitudes of motions which the segments undergo are similar. The two deuterons of the first methylene segment of the sn-3 chain of the phytanyl lipids exhibit three splittings (11.73, 14.16 and 16.70 kHz) in the ratio 0.5:1.0:0.5, respectively. These data are consistent with the presence of two long-lived conformers with splittings of 11.73, 14.16 kHz and 14.16,16.70 kHz. The presence of two conformers may be attributed to the presence of multiple stereoisomers due to the racemic glyceryl and phytanyl starting materials.

Comparison of the splittings from DPhPA labelled in the C-2 carbon of the sn-2 chain ([2,2-$^2H_2$]DPhPA; 7.91, 14.15 kHz) with

Figure III.8

^2H NMR spectra and de-Paked and simulated de-Paked spectra of [1,1,1',1'-$^2H_4$]DPhPA and [2,3,2',3'-$^2H_4$]-DPhPA.

(T=25°C; ω_o=46.07 or 30.70 MHz).

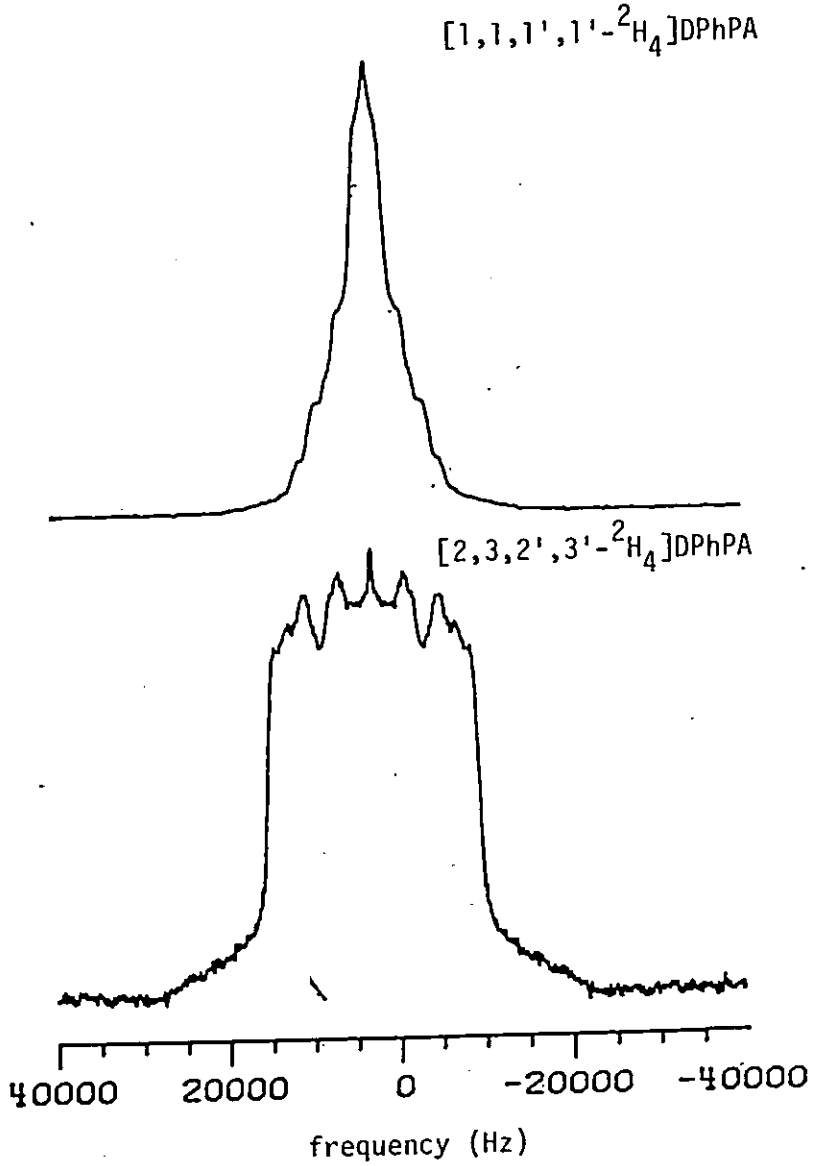
[1,1,1',1'-$^2H_4$]DPhPA
[2,3,2',3'-$^2H_4$]DPhPA
40000
20000
0
-20000
-40000
frequency (Hz)

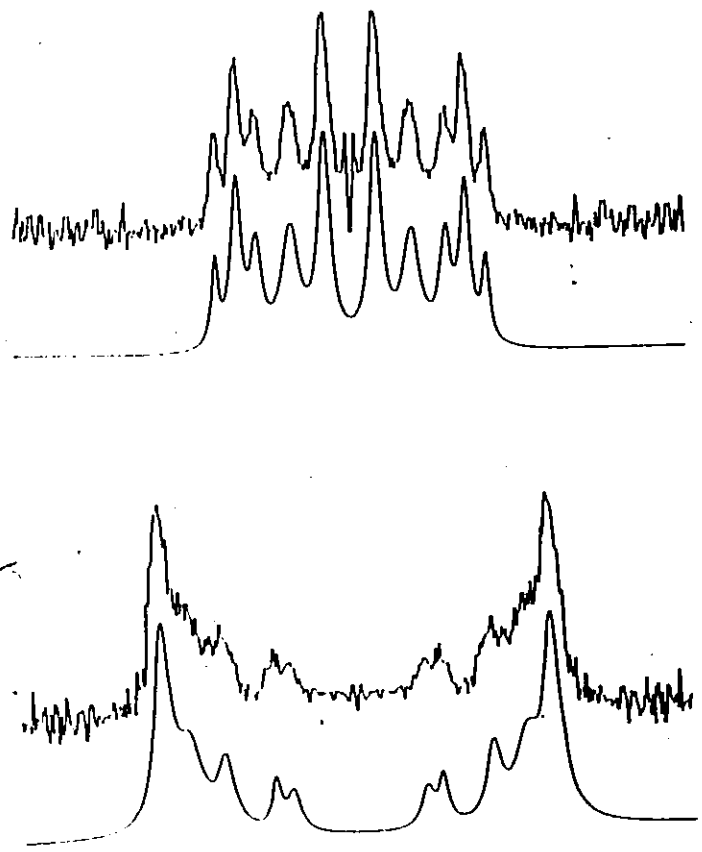

Figure III.9

^2H NMR spectrum and de-Paked and simulated de-Paked spectrum of [2,2-$^2H_2$]DPhPA.
(T=25^{0}C; ω_0=30.70 MHz).

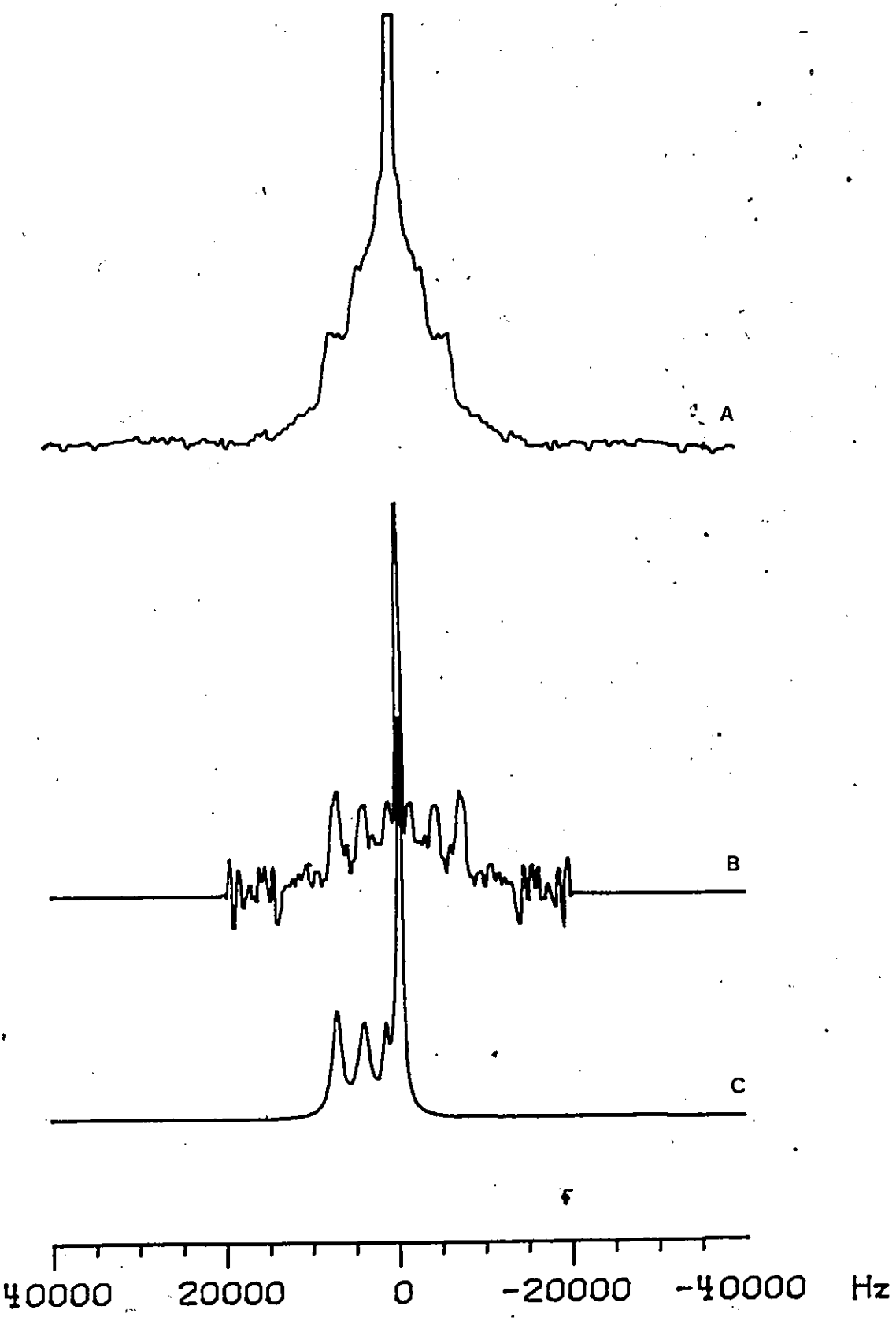
A
B
C
40000
20000
0
-20000
-40000
Hz

Table III.5

Values and relative intensities of quadrupole splittings of diphytanylglycerol phospholipids[a]

Labelled Position	Dq (KHz)	relative intensity
[1,1,1',1'-$^2H_2$]DPhPA	3.14	1
	7.49	1
	11.73	0.5
	14.16	1
	16.70	0.5
[2,2-$^2H_2$]DPhPA	7.91	1
	14.15	1
	2.52[b]	<0.5
[2,3,2',3'-$^2H_2$]DPhPA	8.31	1
	16.57	1
	10.34	1
	20.91	1
	24.17	2

a. Data taken from Figure III.8.

b. Probably arises from scrabling of label to methyl group as indicated by high resolution ^2H NMR.

Table III.6

Comparison of quadrupole splittings from phytanyl, n-alkyl and n-acyl phospholipids

Compound	C-1[a]		C-2[a]		C-3	
	sn-1	sn-2	sn-1	sn-2	sn-1	sn-2
	rac-3	rac-2	rac-3	rac-2		
DHPA[b]	-	4.5 10.5	-	20.4 22.2		
DPhPA[c]	14.16 11.73 16.70	3.14 7.49	10.34 20.91	8.31 16.57	24.17	24.17
DPPC[d]	-	-	27.2	12.0 19.2	26.2	23.2
DHPC[e]	13.1 16.8	2.34 9.45				

a. sn-1 and sn-2 for DPPC, DHPC and DHPA; and rac-2 and rac-3 for DPhPA.

b. T= 80°C; ω_o= 30.7 MHz.

c. T= 25°C; ω_o= 46.07 MHz.

d. Seelig and Seelig, 1974. T= 50°C; ω_o= 13.78.

e. Ruocco et al., 1985. T= 45°C; ω_o= 45.3 MHz.

Figure III.10

Dependence of the quadrupole splittings on position of labelling for n-alkyl, n-acyl and phytanyl lipids. Data given in Table III.6.

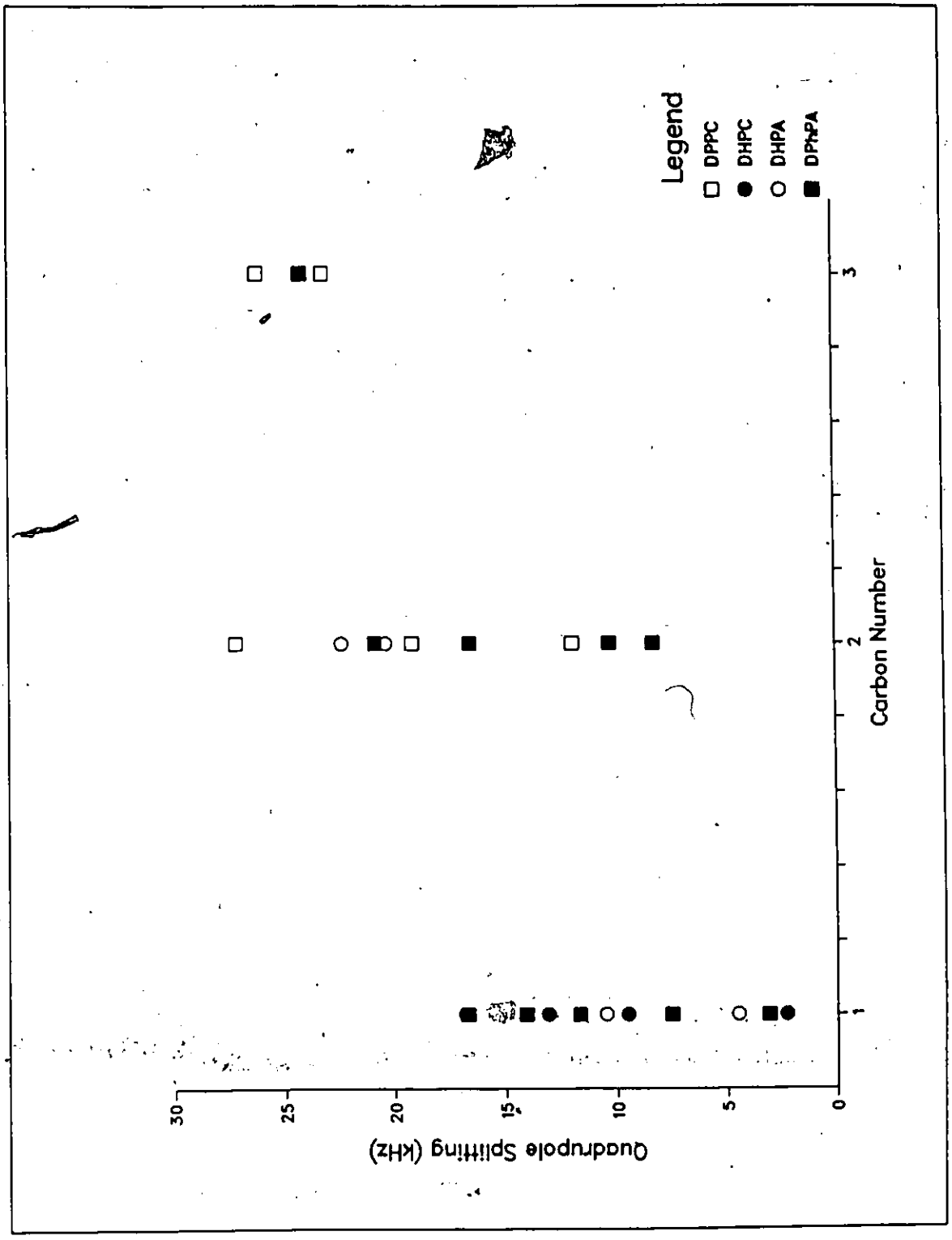
Legend
DPPC
DHPC
DHPA
DPPA
Quadrupole Splitting (kHz)
30
25
20
15
10
5
0
1
2
3
Carbon Number

those from [2,3,2',3'-$^2H_4$]DPhPA allows for unambiguous assignment of the sn-3 chain, C-2 carbons (10.34,20.91 kHz) and C-3 carbons (24.17 kHz). The values for the second position of the sn-2 chain of the phytanyl lipids (8.31, 16.70 kHz), n-acyl lipids (12.0,19.2 kHz) and n-alkyl lipids (20.4,22.2 kHz) are significantly different, reflecting the effect of the presence of both the branch methyl group and nature of the glycerol/hydrocarbon linkage on the conformation of the methylene groups. The splittings of the thrid methylene segmnet of both the phytanyl (24.17 kHz) and n-acyl lipids (23.3, 26.2 kHz) are comparable. The ^2H NMR spectrum and de-Paked and simulated de-Paked spectra from the phytanyl lipids labelled in the third carbon of the glycerol backbone (diphytanyl-rac-[3,3-$^2H_2$]glycerol phosphate; [3,3-$^2H_2$]DPhPA) is shown in Figure III.8. The values and relative intensities of the splittings together with the corresponding values for the n-acyl lipids from E. coli grown on deuterated glycerol (Gally et al., 1981) are given in Table III.7. The magnitudes of the splittings from diphytanylglycerol lipids (3.54-17.84 kHz) are within the same range as those determined for n-acyl lipids (0-17 kHz) (Gally et al., 1981); however, the number of splittings is much larger. Although the compound is labelled at only one position, there are six splittings of varying intensities. It should be noted that the labelled phytanyl compounds studied here are a mixture of eight stereoisomers due to the presence of three chiral centers per chain as well as the chiral center in the glycerol backbone.

Unlike the n-acyl lipids, interaction of the branch methyl groups in the multiple stereoisomers of the phytanyl lipids may to the presence of a number of conformations in which the orientation of the glycerol backbone methylene segment is slightly different. Each orientation would give rise to a different set of quadrupolar splittings with relative intensities corresponding to the relative amounts of each conformer. In addition, in a recent x-ray crystallographic study of rac-1,2-dimyristoyl PG (DMPG) (Pascher et al., 1987), DMPG derived from D-glycerol would not crystallize whereas DMPG derived from D,L-glycerol formed crystals of quality suitable for crystallographic studies. This indicates that different lipid stereoisomers may have different packing properties.

Figure III.11

^2H NMR spectrum, de-Paked and simulated de-Paked spectra of aqueous dispersions of diphytanyl-[3,3-$^2H_2$]glycerol phosphate.

diphytanyl-[3,3-$^2H_2$]glycerol phosphate

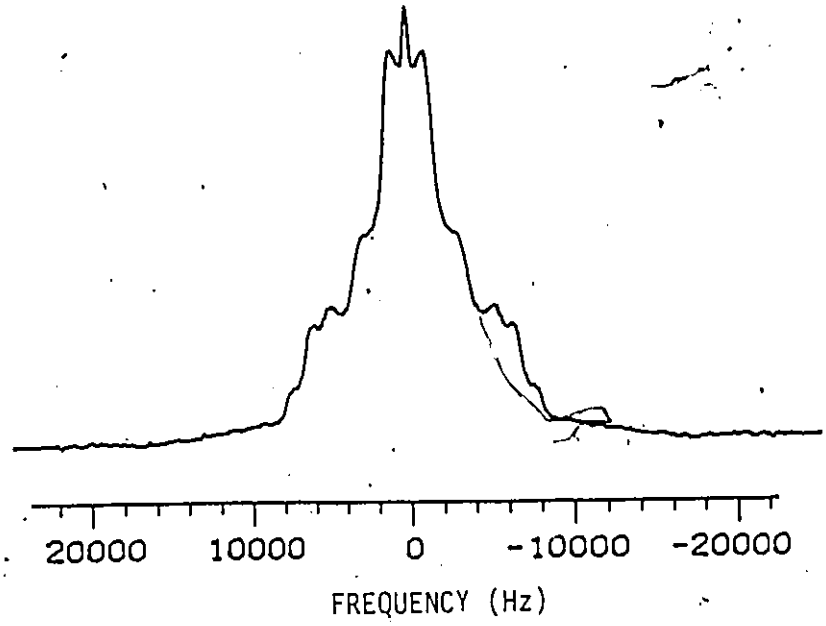

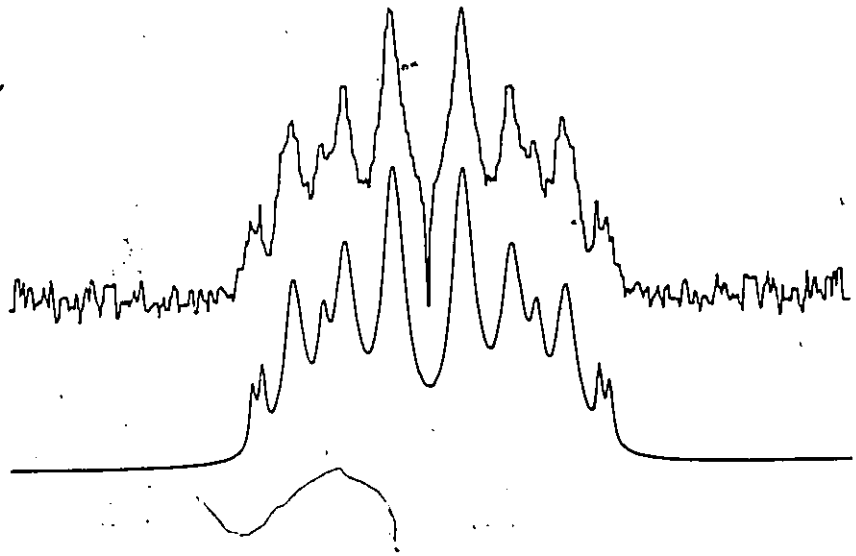

Table III.7

Values and relative intensities

of quadrupole splittings from diphytanylglycerol

and diacyl phospholipids labelled in the backbone glycerol

Compounds	Dq (kHz)	intensity	relative intensity	total intensity
rac-[3,3-$^2H_2$]DPhPA [a]				
	3.54	358	4.5	
	10.79	117	1.5	8.0
	16.94	89	1.0	
	17.84	77	1.0	
	8.38	246	3.0	6.0
	13.68	213	3.0	
sn-[1,1-$^2H_2$]diacyl PG [b]				
	0		1.0	
	17		1.0	

a. T= 25°C; ω_o= 46.07 MHz.

b. Gally et al., 1981. T= 37°C; ω_o= 46.4 MHz.

1.3.3 Biosynthetically Deuterated Diphytanylglycerol Lipids

Molecular order

The wide variations in the quadrupole splitings (3.14 to 16.70 kHz for the C-1 position) for two deuterons on the same methylene group of one phytanyl chain indicates a strong orientational contribution to the segmental order parameter; therefore, the low segmental order parameter does not necessarily imply a low molecular order parameter.

Since high resolution conformational information on phytanyl lipids does not exist, there is no way to correct the values of S_{CD} for possible geometric effects and therefore to differentiate between a low degree of order and an unusual orientation of the C-D bond with respect to the axis of motional averaging.

To distinguish between these two explanations, the effect of the addition of increasing amounts of unlabelled diphytanylglycerol lipids to deuterium-labelled n-acyl lipids was determined. If the low quadrupole splittings of the branched-chain lipids are due solely to orientational effects rather than to low molecular order, it is unlikely that their presence will lead to substantial decreases in the splittings of the straight chain lipids.

The results of the addition of unlabelled TPL to deuterated DMPC are shown in Figure III.12. The splittings are reduced from 5.26 - 31.89 kHz to 2.11 - 20.63 kHz in the presence of approximately 90% TPL. The splittings of DMPC, perdeuterated in the sn-2 chain, at high concentrations of TPL are comparable in magnitude to those of labelled TPL (see Table III.8). The magnitude

Figure III. 12

Effect of the addition of TPL from H. cutirubrum on the quadrupole splittings of deuterated DMPC.

$T = 45^{\circ}C$; $\omega_o = 45.6$ MHz.

Data from Ekiel et al., unpublished.

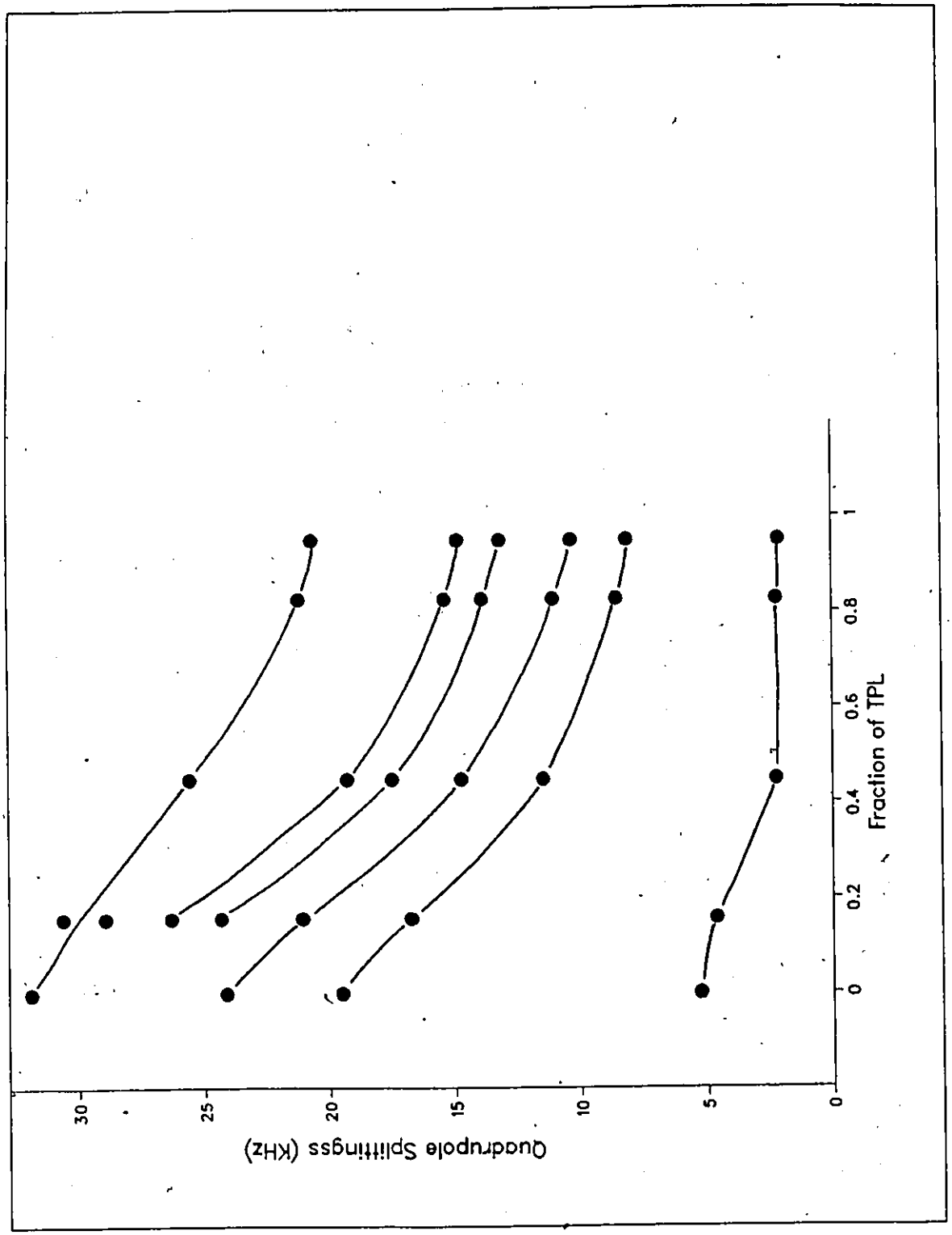
Quadrupole Splittings (KHz)
30
25
20
15
10
5
0
0
0.2
0.4
0.6
0.8
1
Fraction of TPL

of the decrease (up to 50% for some positions) and the fact that the values of the splittings of labelled DMPC in the presence of high concentrations of unlabelled TPL are comparable to those of labelled TPL alone, argue that the splittings are due to decreased motional restriction of the n-acyl chains. Therefore, the low splittings of the labelled diphytanylglycerol lipids are due predominantly to low molecular order rather than orientational effects. This is somewhat suprising as it seems intuitively obvious that the bulky methyl groups of the phytanyl chains would produce a bilayer which is characterized by a higher degree of order (see Fig. III.13).

To determine the effect of the nature of the headgroup on the order and dynamics of the diphytanylglycerol lipids, the quadrupolar splittings and were compared for biosynthetically labelled PGP and total polar lipids of H. cutirubrum. (see Table III.8). Within experimental error, the values for the splittings are the same, indicating no effect of the presence of GLS or other polar lipids on the order of the chains of PGP. This is in agreement with earlier ^2H NMR work by Rance and coworkers (1983) who showed no significant effect of the different headgroups on the quadrupolar splittings of the chains except at the carbon adjacent to the carbonyl group.

The temperature dependence of the quadrupole splittings of biosynthetically deuterated TPL from H. cutirubrum (see Figure III.14) shows no evidence of an obvious, sharp, first-order phase transition between 30 and 45°C. Further experiments with biosynthetically-deuterated TPL, over the temperature range of -25 -

Figure III.13

Space-filling models of PGP (left) and DPPC (right).

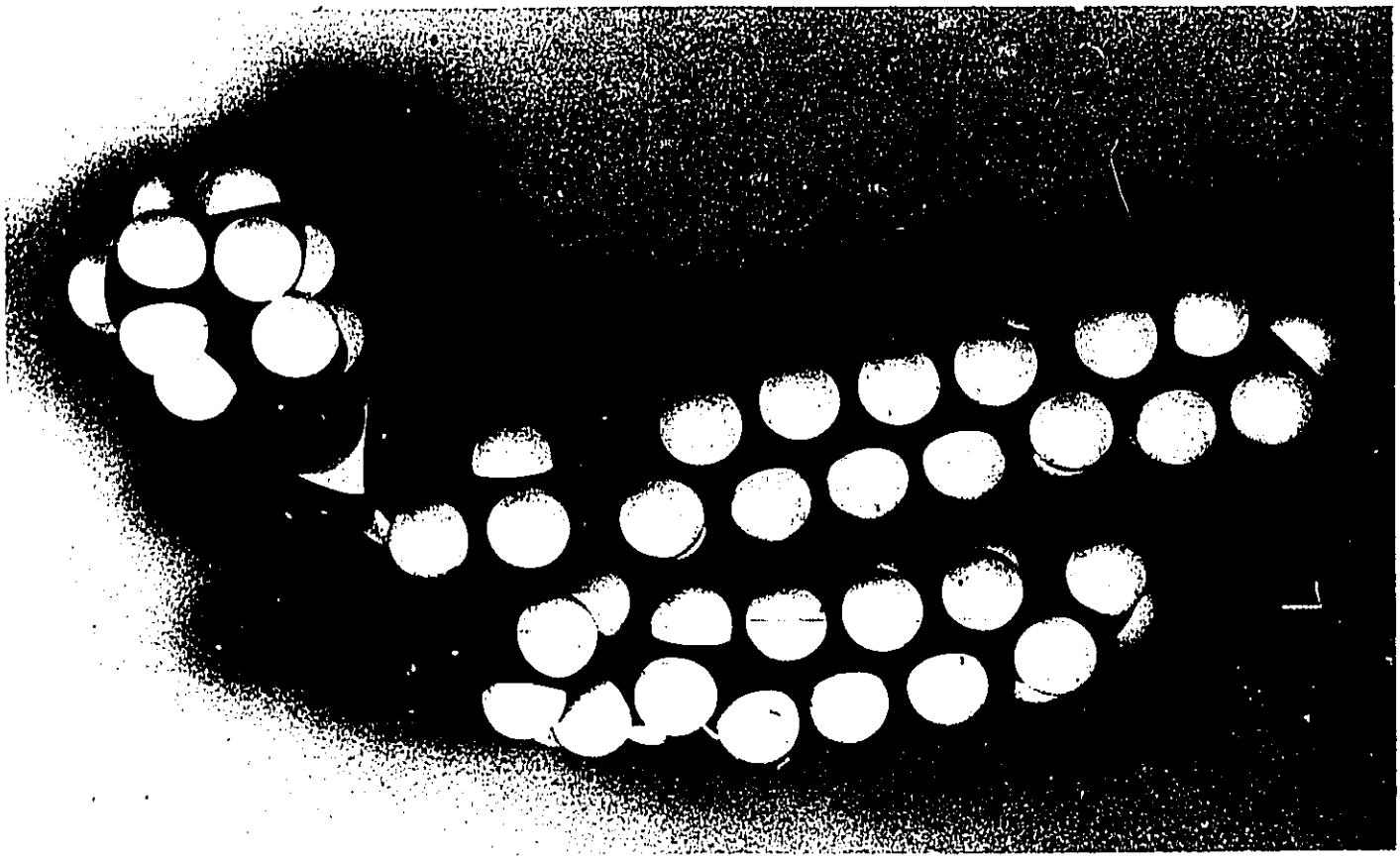

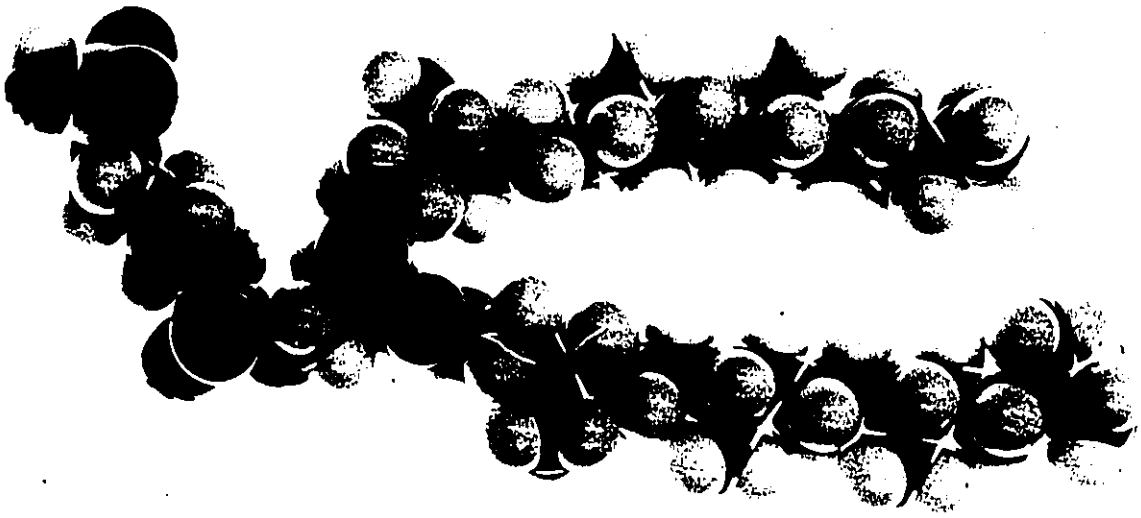

Table III.8

Comparison of quadrupole splittings for biosynthetically labelled PGP and TPL

Quadrupole splittings (kHz)	
PGP	TPL
18.59	18.55
13.67	13.87
6.25	6.45
2.73	2.54
1.95	1.76
0.195	0.195

ω_o= 30.70 MHz; T= 25°C.

The splittings are listed in order of decreasing value and do not necessary reflect the position of the deuterium label within the hydrocarbon chain.

Figure III.14a

Temperature dependence of the quadrupole splittings for biosynthetically deuterated total polar lipids of H. cutirubrum.

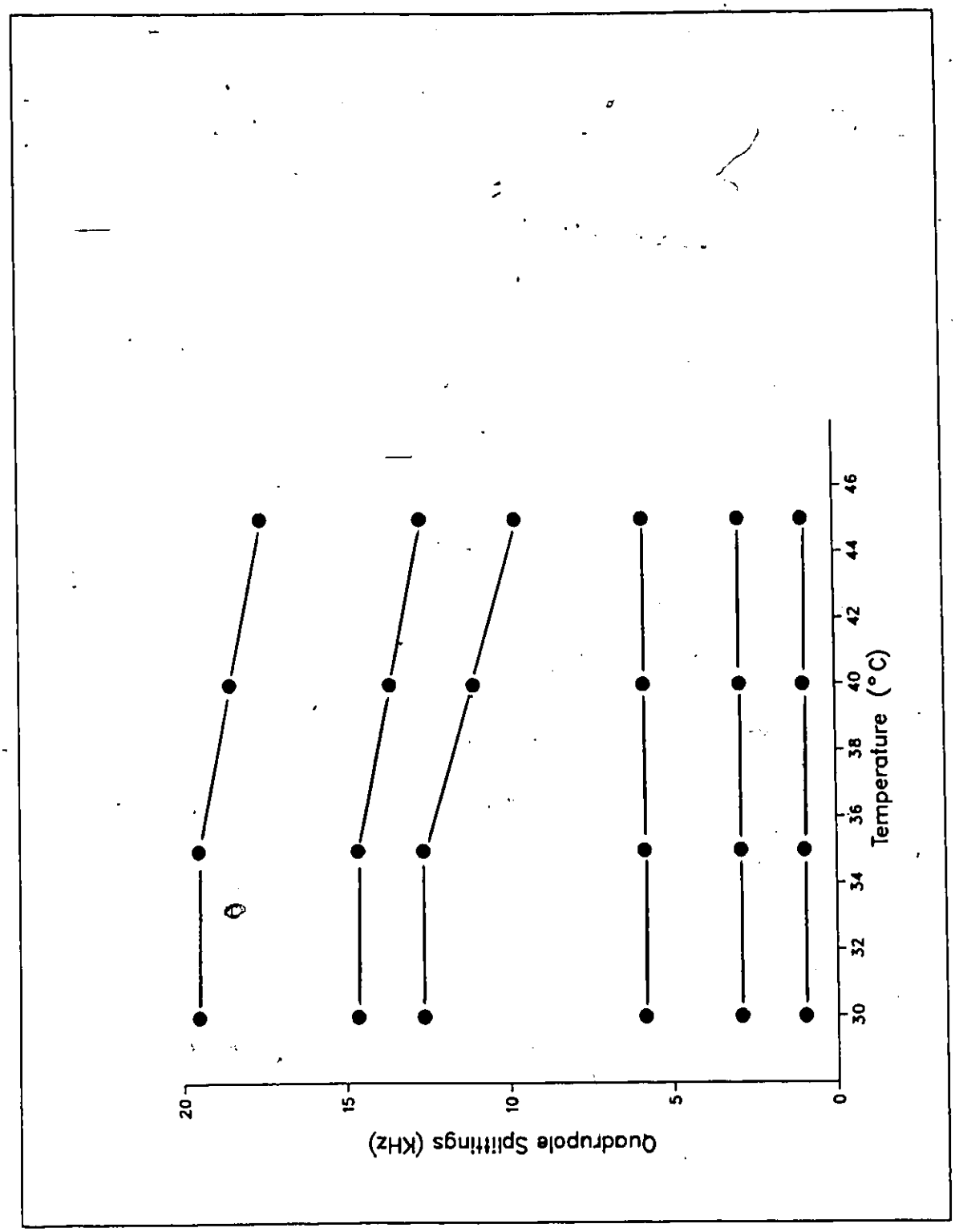
Quadrupole Splittings (KHz)
20
15
10
5
0
30
32
34
36
38
40
42
44
46
Temperature (°C)

Figure III.14b

De-Paked ^{2}H NMR spectra of biosynthetically deuterated TPL of H. cutirubrum at 30, 35.1, 40, 45.1°C.

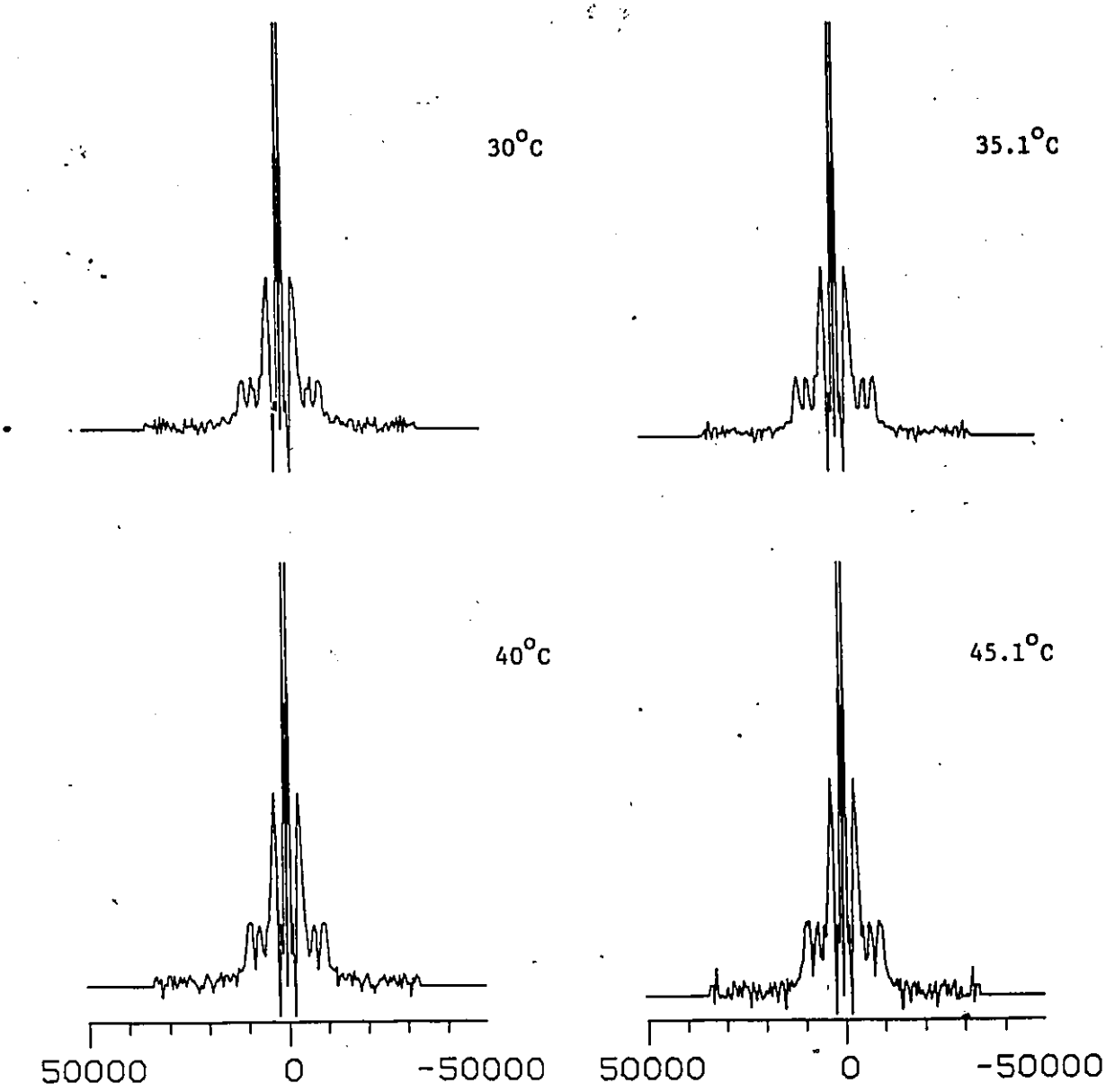
30°C
35.1°C
40°C
45.1°C
50000
0
-50000
50000
0
-50000

44°C (data not shown) confirmed the absence of a transition at lower temperatures. This is consistent with recent high sensitivity DSC (Jackson and Sturtevant, 1978; Ekiel et al., 1981) studies which show that there is no detectable gel to liquid-crystalline phase transition over a broad temperature range (-120 to +120°C, in the case of ^{1}H NMR studies of diphytanoylglycerol phosphatidylcholine; Lindsey et al., 1979). However, a number of other techniques have reported the presence of a temperature-induced discontinuity in the PM or lipids isolated from the halobacteria at 25-30°. These studies include a change in the ^{13}C NMR linewidths at various positions along the chain (Degani et al., 1980), ESR hyperfine splittings (Chignell and Chignell, 1975), coefficient of thermal expansion (Tristam-Nagle et al., 1986) and the rate of photo-transient decay of excited-state BR (Sherman, 1976).

In the acyl chains of phospholipids, the order-disorder (gel-liquid crystalline) phase transition is associated with the onset of the formation of kinks and similar chain conformations involving gauche-trans isomers of the hydrocarbon chains (Träuble, 1971; Nagle, 1973). Consequently, the temperature and enthalpy of the phase transition will be affected by the sum of the potential energies associated with the various molecular conformational states.

In straight-chain lipids, the combination of the relative stabilities of the trans versus gauche conformers and the high lateral packing densities is responsible for the large enthalpies (approximately 10 kcal/mol) and high temperatures (approximately

300 K) of the phase transition.

In comparison, the presence of the branch methyl groups in the phytanyl (or phytanoyl) chains causes the gauche and trans conformers to be energetically more equivalent. In addition, the steric interaction probably prevents efficient lateral packing. As a result, the gel to liquid-crystalline phase transition is expected to be a low-temperature, low-enthalphy transition.

This effect is seen in the comparison of the phase transition temperatures of straight-chain, iso-branched and anteiso-branched chain lipids (Keough and Davis, 1984) where the presence of a branch methyl group leads to a 20-40C° reduction in the value of T_c.

The temperature-dependent discontinuity in the ^2H NMR quadrupole splittings, as well as in the other physico-biochemical parameters, must be due not to a gel to liquid-crystalline phase transition but to the fact that the chains are undergoing a number of different types of motions at different rates, each of which contributes to the overall chain dynamics to a degree which is temperature-dependent. ^{31}P NMR studies of changes in the CSA of aqueous dispersions of TPL as a function of temperature (vide infra) indicate cessation of axial rotation at -20°C which may account for the low temperature behaviour previously attributed by some authors (Chen et al., 1974) as a gel to liquid-crystalline phase transition.

Molecular dynamics

Spin-lattice relaxation times were calculated for aqueous dispersions of biosynthetically deuterated H. cutirubrum total

Figure III.15

Temperature dependence of the spin-lattice relaxation times for biosythetically deuterated TPL from H. cutirubrum. Each curve corresponds to a different, deuterated position.
Data from Ekiel et al., unpublished.

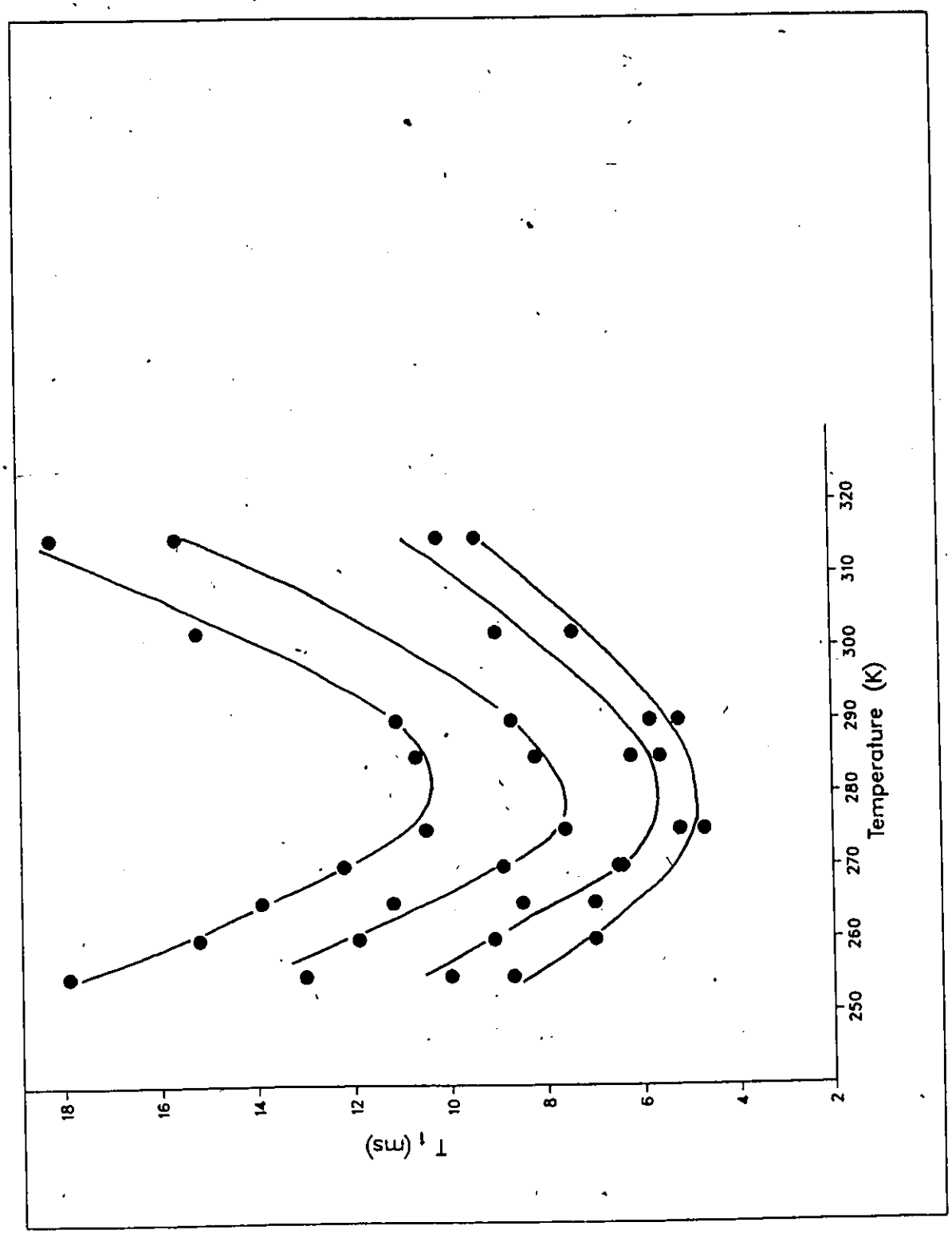
T 1 (ms)
18
16
14
12
10
8
6
4
2
250
260
270
280
290
300
310
320
Temperature (K)

polar lipids as a function of temperature. Figure III.15 shows low overall values for the T_1 in comparison with n-acyl lipids and a temperature minimum at 8-10°C. At the temperature minimum of the curve, the effective segmental correlation time (τ_c) can be calculated from the following formula:

$$\tau_c = 0.62\ \omega_o^{-1}$$

where ω_o is the deuterium Larmor frequency (in this case, 46.07 MHz). Therefore, at 8°C, the segmental correlation time for all labelled positions is 3.5×10^{-9} sec. Although the deuterons exhibit different T_1 values, the fact that they have the same temperature-dependence; i.e., they all show a minimum at 8-10°, indicates that they possess similar rates of motions. The T_1 values of [2,2,3,4,4,6-$^2H_6$]cholesterol in cholesterol/DPPC mixtures also exhibit a similar temperature dependence, with a minimum at 32-35°C for all labelled positions, leading to $\tau_c = 3.5 \times 10^{-9}$ sec at 46.07MHz (see Figure III.16; Dufourc and Smith, 1986).

The biphasic behaviour of the temperature dependence of the spin-lattice relaxation time seen for both the diphytanylglycerol lipids and cholesterol-DPPC mixtures is best understood in terms of the distribution of molecular rotational frequencies (Farrar and Becker, 1976). The efficiency of the T_1 relaxation processes increases (T_1 becomes shorter) with an increase in the density of motional frequencies in the region of the ^2H resonance frequency. The density is greatest for cholesterol at 32-35°C and for diphytanylglycerol lipids at 8-10°C. At higher

Figure III.16

Variation in the spin-lattice relaxation times with temperature for three labelled positions of cholesterol.

(From Dufourc and Smith, 1986).

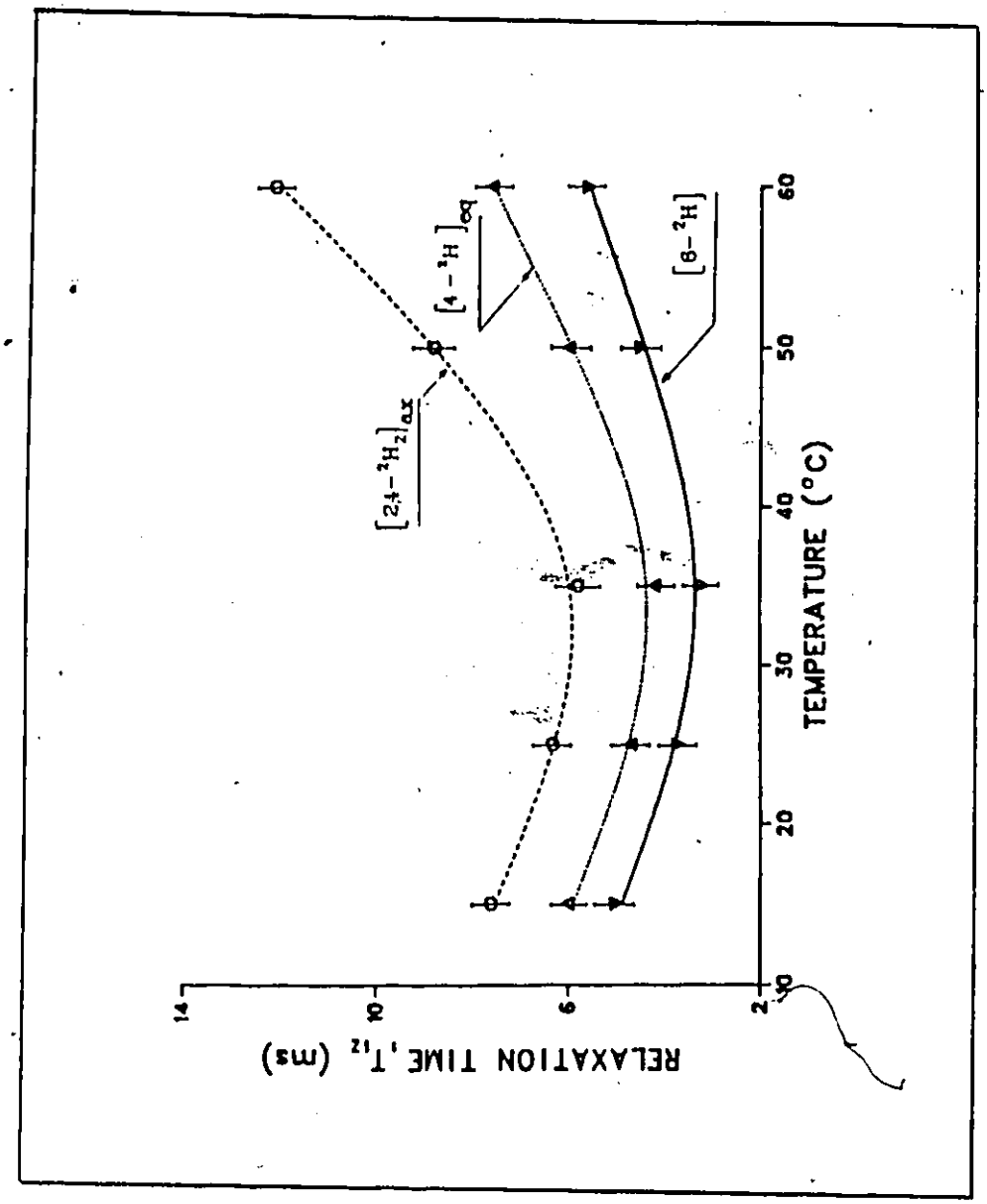
RELAXATION TIME, T_{1z} (ms)
14
10
6
2
0
20
30
40
50
60
TEMPERATURE (°C)
$[\alpha,\alpha-^2H_2]_{ax}$
$[4-^2H]_{eq}$
$[\beta-^2H]$

temperatures, the distribution of frequencies of molecular motions increases. Similarly, at lower temperatures, the processes again become less efficient due to a shift in the density to lower frequency values.

Because the 4 quadrupole splittings have not yet been assigned to specific positions along the chain, a T_1 profile has not been determined. However, for cis-unsaturated lipids, there is a decrease in the spin-lattice relaxation times (NT_1) at the position of the double bond due to a change in the types and/or rates of motions which the segments undergo. Similarly, it is reasonable to assume that the presence of the branch methyl groups in the phytanyl chains would lead to a decrease in the frequency of molecular motions due to steric interactions. This, in fact, is seen for the ^{13}C NMR relaxation times of neat phytol in which the T_1 values of the methine groups are significantly lower than the adjacent methylene groups (Goodman et al., 1974; see Figure 4).

1.4 Summary of ^2H NMR results

The physical and biological properties of membranes are determined by the physical properties of the lipids of which they are composed. ^2H NMR has been used to study synthetically and biosynthetically deuterated diphytanylglycerol lipids and the corresponding synthetically deuterated straight-chain lipids in order to better understand the properties of the membranes of Archaebacteria such as H. cutirubrum. ^2H NMR provides a non-perturbing method of determining the segmental order (extent of molecular motion) and dynamics of the hydrocarbon chains.

Data provided from studies with the model compound, dihexadecylglycerol phosphatidic acid, labelled in the first and second positions of the sn-2 chain, aided in the comparison of data obtained from phytanyl lipids with that previously obtained from n-acyl lipids.

The splittings for the deuterons on the second carbon of the sn-2 chain of DHPA (20.4 and 22.2 kHz) are slightly higherthan those of the corresponding position of DPPC, indicating a slight effect of the ether linkage on the orientation or amplitude of motion of the methylene group. The splittings of the sn-2 chain of DHPA (4.5 and 10.5 kHz) are comparable to those of DHPC (2.34 and 9.45 kHz) and are lower than those of the sn-1 chain of DHPA (13.1 and 16.8 kHz) (Ruocco et al., 1985) indicating that the orientation and order are different for the sn-1 and sn-2 chains. Different conformations of the sn-1 and sn-2 chains at the

positions adjacent to the backbone glycerol are also seen for n-acyl lipids.

The temperature dependence of both the splittings and the relative heights of the splittings is consistent with the hypothesis that the magnetic inequivalence of the two deuterons of the first methylene group of the sn-2 chain of DHPA results from interconversion between two distinct conformations. This does not seem to be true for the second methylene group, where the two splittings have a similar temperature dependence and the ratios of the heights do not vary appreciably. However, this may be due to a small energy difference between the two conformations.

As expected, the spin-lattice relaxation times determined for the first position of the sn-2 chain are comparable to those previously obtained by Ruocco et al. (1985) for DHPC. The T_1 values determined for the second methylene segment of DHPA are significantly lower than that of the second position of the n-acyl lipids indicating a substantial effect of the glycerol-hydrocarbon linkage on the dynamics of the chains at positions adjacent to the glycerol backbone.

Both synthetically and biosynthetically deuterated compounds were used to provide information on the conformation and dynamics of the hydrocarbon region of diphytanylglycerol lipids. Biosynthetic labelling proved to be a facile method for selectively deuterating several positions along the chain. At least some of the methylene groups adjacent to the methine groups are labelled. Synthetic labelling provided information on

specific positions adjacent to the backbone glycerol (C-1, C-2 and C-3 of both the sn-2 and -3 chains). At the first carbon, the quadrupole splittings of the phytanyl lipids were comparable in magnitude to those of the n-alkyl lipids, indicating that the branch methyl group had virtually no effect on the order or orientation at this position, although an effect was seen at the second methylene segment. Further along the chain, the branched groups lead to significant effects on both the order ($\Delta\nu_Q$ <19 kHz) and dynamics ($\tau_c \cong 10^{-9}$ sec) in comparison with the n-acyl lipids ($\Delta\nu_Q$ 25-35 kHz for the first 8-10 position, $\tau_c \cong 10^{-10} - 10^{-11}$ sec). This data indicates that the phytanyl chains are relatively disordered but that the rates of motions which the chains are undergoing are slow relative to n-acyl lipids.

The magnitude of the reduction in the quadrupole splittings of deuterated DMPC following the addition of unlabelled TPL from H. cutirubrum, argue that the narrow quadrupole splittings for high ratios of TPL to labelled DMPC, as well as in the labelled TPL, resulted primarily from low molecular order rather than from unusual orientations of the methylene segments with respect to the axis of motion or "fluidity" effects resulting from different reduced temperatures. The temperature dependence of the quadrupolar splittings for biosynthetically deuterated phytanyl lipids confirmed the absence of a abrupt gel to liquid-crystalline phase transition in the physiological range (optimum growth temperature for H. cutirubrum is 39°C).

2. Phosphorus NMR

2.1 Introduction and Theory

Phosphorus NMR has been used extensively in the study of both model and biological membrane systems as a non-perturbing probe of lipid conformation and dynamics (see reviews by Smith and Ekiel, 1984; Seelig, 1978). Changes in the residual chemical shift anisotropy (CSA) reflect changes in the extents of motions and/or a change in the orientation of the headgroup phosphorous group with respect to the axis of motional averaging. The spin-lattice relaxation time (T_1), which is a measure of the rate of relaxation of a spin system following excitation by a radio frequency pulse, provides information on the rates of molecular motions which are prevalent on the NMR timescale.

In phosphorus NMR, the chemical shift of a rigid phosphate group is dependent upon the orientation of the group with respect to the magnetic field of the spectrometer (Smith and Ekiel, 1984). The chemical shifts along the three principal directions are arbitrarily labelled δ_{11}, δ_{22} and δ_{33}, as shown in Figure III.17. These values correspond to the components of the chemical shift or shielding tensor which describes the Zeeman interaction between the phosphorus nucleus and the magnetic field.

In a randomly oriented sample, all orientations of the phosphate group (and therefore of δ_{ii}) with respect to the magnetic field are possible. The spectrum is the sum of spectra for all possible orientations and the values of the principal

Figure III.15

Possible motional states of the phosphodiester groups of a phospholipid and the expected ^{31}P NMR spectra: A. static phosphodiester; B. ordered phosphodiester undergoing rapid axial rotation; and, C. disordered phosphodiester.
(From Smith and Ekiel, 1984)

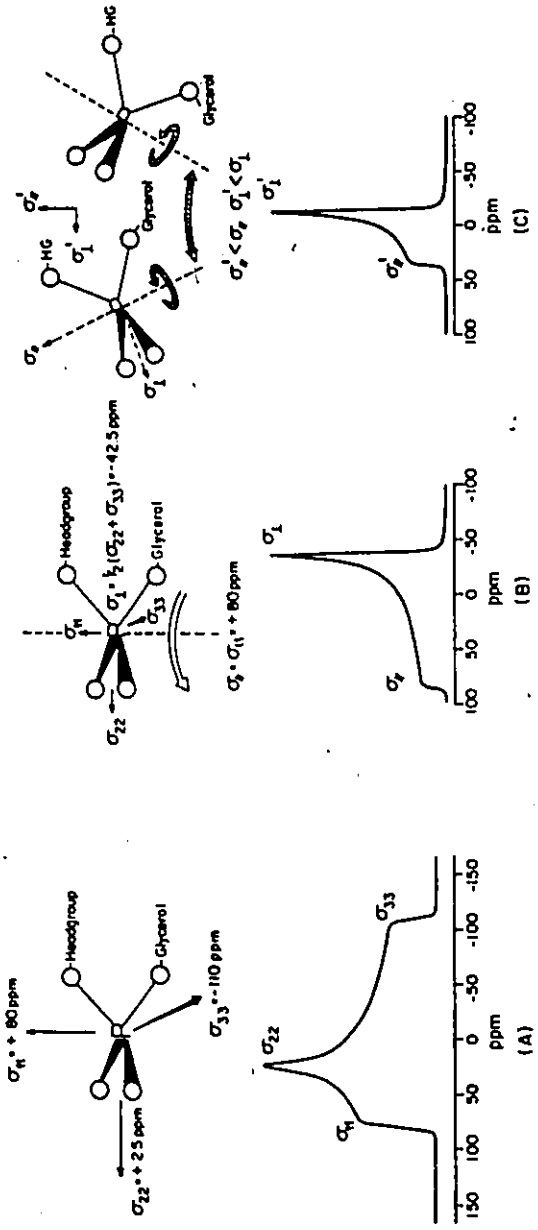
HG
Glycerol
Headgroup
Glycerol
ppm
(A)
(B)
(C)

tensor components can be estimated directly from the spectrum.

The value of σ_{22} is determined from the chemical shift of the peak of maximum intensity in the static phosphodiester spectrum and δ_{11} and δ_{33} are determined from the midpoints of the downfield and upfield shoulders.

In a membrane or model membrane system, rapid axial rotation of the phospholipids leads to partial averaging of the tensor components. The new values of the chemical shift tensor ($\delta_{\perp} = (\delta_{22} + \delta_{33})/2$ and $\delta_{11} = \delta_{//}$) can again be determined directly from the spectra. Increasingly disordered motion with rapid interconversion between allowed conformations leads to further averaging of the tensor components so that the total chemical shift anisotropy (CSA) ($\Delta\delta' = \Delta\delta'_{//} - \Delta\delta'_{\perp}$) is again reduced. Note that the lineshape depends on the type of motion and not the rate of motion providing that the motions are fast on the NMR timescale. The limit of total disorder is a single resonance ($\delta_{isotropic}$) with a CSA identical to within 5 ppm of that found in a non-viscous medium ($\delta_{iso} = (\delta'_{//} + 2\sigma'_{\perp})/3$).

The value of the observed CSA, $\Delta\sigma$, is therefore dependent upon both the degree of order of the phosphate group, or the amplitude of angular excursion during motional averaging, and the orientation of the axis of motional averaging with respect to the principal tensor components. The extent of the contributions from each of these two parameters to the observed CSA cannot be accurately assessed. This information may be determined from solid (non-hydrated) samples from which the static CSA, which reflects only orientational effects, can be determined.

For small molecules in solution the asymmetry in the charge distribution which leads to the orientational dependence of the chemical shift is averaged by rapid reorientation. The resulting spectrum is a narrow peak whose chemical shift is determined by changes in bond overlap and hybridization, changes in atomic charge and changes in the energy differences between the ground and excited states (Gorenstein, 1984). For phosphoryl compounds such as phosphomono- and diesters, electrostatic effects (P-O bond and torsion angles) (Gorenstein and Kar, 1975; Gorenstein, 1975) contribute significantly to the chemical shift although electronegativity effects (including degree of esterification and degree of ionization) predominate (Letcher and van Wazer, 1967). Association with hydrogen bonding donors has little effect on the chemical shift other than that attributed to a shift in the pK.

In addition to the CSA, another parameter which has been used to provide information on the headgroup region is the spin-lattice relaxation time (T_1). Relaxation times have been used in high resolution NMR spectroscopy to gain information regarding the rates of molecular and intramolecular motions. They have also been used in the study of membranes and model membrane systems; however, because of the anisotropic nature of the motion, it is more difficult to correlate relaxation times with the various motional correlation times. Interpretation of ^{31}P data is further complicated by the fact that the relaxation mechanism is a mixture of chemical shift and dipolar, in contrast

to the ^{2}H NMR where relaxation is almost exclusively quadrupolar. In addition, the relative contributions of each mechanism varies with the spectrometer field strength. The complex temperature and field dependence of ^{31}P relaxation for DOPC and sarcoplasmic recticulum enriched with DOPC (Seelig et al., 1981) illustrates the drawbacks of simple numerical comparison of T_1 values.

Preliminary experiments by Smith and coworkers (Ekiel et al.,1984) on both the purple membrane and pure PGP bilayers indicated that the rather unusual shape of the phosphorus spectrum arises from the superposition of two patterns with different values of the CSA. The two subspectra can be separated through spectral simulation or through the use of the DANTE sequence (Morris and Freeman, 1978) and were attributed to the phosphomono- and diester groups of PGP (see Figure III.18). Comparison of the purple membrane and PGP samples also showed a marked increase in the CSA of the purple membrane (60 and 17.5 ppm) in comparison with PGP (18 and 41 ppm) due to a change in the amplitude of motion of the headgroup and/or in the headgroup conformation of PGP in the presence of bacteriorhodopsin, neutral lipids and other polar lipids. The change is significantly greater for the phosphodiester (32% increase) than the phosphomonoester (14%) (see Figure III.19).

In addition to an increase in CSA, an increase in the linewidth, and hence in the spin-spin relaxation time (T_2) was seen in the presence of bacteriorhodopsin ($\Delta\nu_{1/2} = 1/\pi T_2^{*}$) (Ekiel et al., 1981). This indicates an increase in the molecular

Figure III.18

^{31}P NMR spectrum of the purple membrane at 15°C and the simulated spectrum showing the contributions from the phosphomonoester and phosphodiester groups of PGP.
(From Ekiel et al., 1981)

Figure III.19

Temperature dependence of ^{31}P NMR CSA for the phosphomonoester and phosphodiester groups of PGP in aqueous dispersions of PGP (o) and in the PM (•).
(From Ekiel et al., 1981)

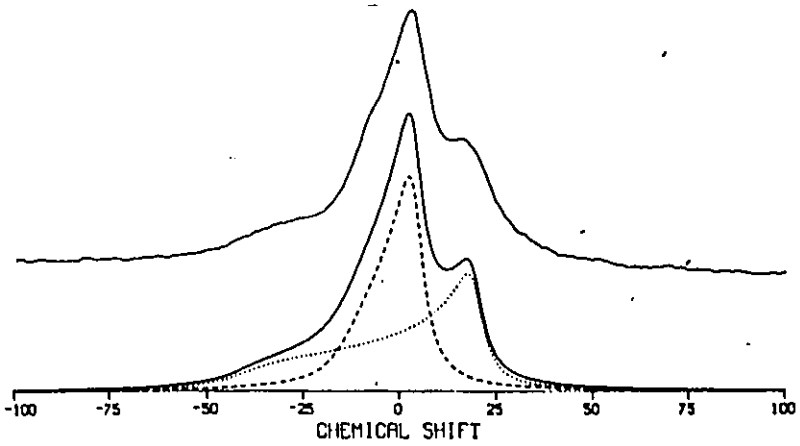
-100
-75
-50
-25
0
25
50
75
100
CHEMICAL SHIFT

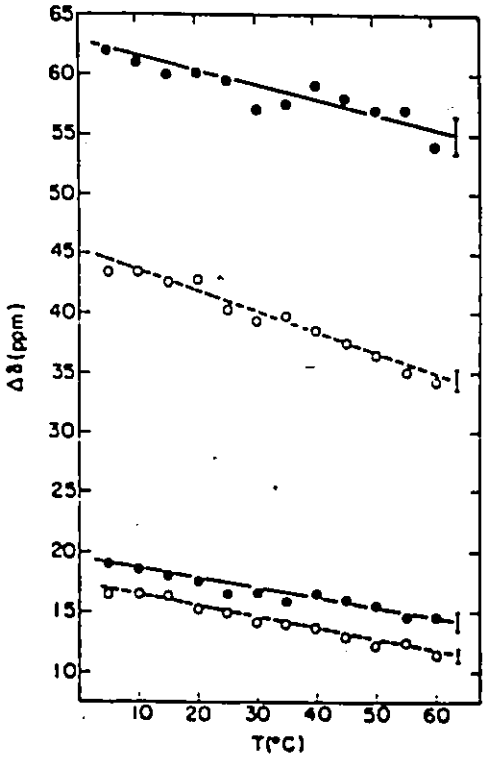
65
60
55
50
45
40
35
30
25
20
15
10
Δδ(ppm)
10
20
30
40
50
60
T(°C)

correlation time (τ_c) which corresponds to slower frequency motions in the time scale of 10^5 to 10^6 sec^{-1}.

In the present studies, the values for the ^{31}P chemical shifts and chemical shift anisotropies were determined for diphytanylglycerol derivatives of PA, PG, PGP and PGS. The purpose of the measurements was to unambiguously assign the two subspectra of the high power spectrum of PGP to the phosphomono- and diester. This was done by comparing the values for the diphytanylglycerol phospholipids. In addition the pH dependence of both the CS and CSA of the two subspectra were measured. The effect of the presence of other polar lipids and/or bacteriorhodopsin on the chemical shift anisotropy (CSA) of PGP was also studied.

2.2 Materials and Methods

2.2.1 Apparatus

Solid state ^{31}P NMR spectra were obtained on a Bruker CXP-300 or MSL-300 spectrometer operating at 121.466 MHz using a 10 mm home-built high power probe. Spectra were acquired using the Hahn spin-echo technique ($90^\circ_x - \tau - 180^\circ_y - \tau$-acquire) with full phase cycling of the radiofrequency pulse (Rance and Byrd, 1983 , Hahn 1950; Fukushima and Roeder, 1981). Pulse spacings were typically 35-45 μs, the 90° pulse length was 4-8 μs and the recycle time was greater than $5xT_1$. T_1 values were determined using an inversion recovery sequence (Fukushima and Roeder, 1981) and were averaged over the entire spectrum.

Alternatively, a Bruker VSP 3000 high resolution probe (300 watts) was used in place of the homebuilt probe. The 90° pulse width was longer than with the high power probe (8-10 μs).

Samples were ^{31}P-^{1}H decoupled using either standard broadband or WALTZ decoupling techniques (Skaka et al., 1983).

Spectra were acquired at ambient temperatures (25°C).

CS are reported relative to H_3PO_4 and spectra were determined relative to an external capillary of 80% phosphoric acid (H_3PO_4) or 100 mM amino-ethyl phosphonate (-18.7 ppm relative to H_3PO_4)

2.2.1 Sample preparation

Total polar lipid and purified PG, PGS and PGP were prepared as described in PART I, section 1. Lipid dispersions were prepared as follows: lipids (50 - 100 mg) were dissolved in chloroform and dried under a stream of nitrogen to a thin film on the sides of a 15 ml stoppered centrifuge tube and dried in vacuo. Distilled water or buffer (1-2 ml) was added and the suspension was vortexed, frozen, thawed and vortexed repeatedly until it appeared homogeneous.

Purple membrane samples were prepared as described in PART I, section 2 and finally pelleted by centrifugation (43,000 g; 80 minutes) prior to use.

Sonicated, aqueous dispersions were prepared as follows: $PGP(NH_4)_2$ (60-100 mg) was diluted with 1.5 ml deuterated water ($^{2}H_2O$) and sonicated with a Branson Sonifier Cell Disrupter 350 for 45 minutes (50% duty cycle, 20% power). The sample was

centrifuged to remove particulate matter generated from the sonicator tip during sonication. The sample was virtually transparent throughout the experiment. The pH of the sample was adjusted with either 2 N aqueous HCl or NH_4OH, sonicated again and the final pH determined with a pH meter.

PGP samples (60-80 mg) were also dissolved in organic solvents (benzene/methanol; 1.1:0.2, 1.3 ml). For measurement of the ^{31}P spectrum at different apparent pH's, the solutions were titrated with 2 N methanolic HCl or NH_4OH over the pH_a range of 2.1-4.6 and 7.2-7.8 as determined with a pH meter.

2.3 Results and Discussion

2.3.1 Assignment of subspectra

Before studies could be undertaken to assess the effects of external parameters on the phosphorus spectra of PGP, it was necessary to assign each of the subspectra to the phosphomono- and diester groups. Previously, the subspectra with the narrow CSA has been attributed to the phosphomonoester and the wide CSA to the diester. This assignment was based on the assumption that the expected greater motional freedom of the terminal phosphate would lead to a greater degree of motional averaging resulting in a narrower pattern. In addition, the CSA of the subspectrum attributed to the phosphodiester (41 ppm) and the monoester (16 ppm) of PGP were similar to those of other systems (40 to 60 ppm and 18 to 20 ppm for the phosphodiester and monoester,

respectively).

The ^{31}P NMR chemical shift has been found to be sensitive to the degree of esterification, increasing from -2.3 to -0.8 to 0.4 ppm in monoethyl phosphate to di- and triethyl phosphate (Gorenstein, 1984). On this basis, the upfield peak of PGP (0.48 ppm) should be attributed to the terminal phosphate (phosphomonoester) and the downfield peak (1.45 ppm) to the phosphodiester. Based on calculations of the isotropic chemical shift from the solid state spectra ($\sigma_{iso} = \sigma_{//} + 2\sigma_{\perp})/3$) (0.80 ppm and 1.91 ppm from the narrow and broad subspectra, respectively) the downfield and upfield peaks can be assigned to the broad (phosphodiester) and narrow (phosphomonoester) subspectra, respectively.

However, it is not sufficient to assign the subspectra solely on the basis of degree of esterification as the ^{31}P NMR CS has also been shown to be strongly affected by the degree of ionization, O-P-O bond angle, etc. (Gorenstein, 1984). Similarly, the CSA reflects a combination of both motional and geometric effects.

Therefore, in an attempt to confirm the assignment of the subspectra of PGP, a comparison was made of both the CSA and CS values for a series of diphytanylglycerol phospholipids, including PGP, PGS, PG and synthetic PA (see Table III.9).

Neither the CSA (25.4-31.3 ppm) nor the chemical shift (1.081 ppm) values of PG corresponded to either of the two subspectra of PGP (CSA, 18 and 41 ppm; CS, 0.48 and 1.45 ppm) (See Table III.9). The absence of a terminal phosphate probably results in

a change in the conformation of the diester phosphate, and therefore a change in the orientation of the principal tensor components with respect to the axis of motional averaging. This could result in a change in the effective CSA as previously discussed. The CSA difference may be explained by electrostatic effects resulting from the absence of a charged phosphate group at the sn-1' position of the headgroup glycerol.

The values for the CSA of PA (49.3 ppm) corresponds roughly to CSA value attributed to the phosphodiester of PGP (41 ppm) and the CS value (2.05 ppm) corresponds most closely to the downfield peak of PGP (1.45 ppm) attributed to the phosphodiester from σ_{iso} calculations (1.91 ppm). Again, differences between the two compounds can be explained in terms of conformational effects which predominate in the solid state spectra and electrostatic effects (due to the increased degree of ionization) which predominate in the high resolution specta.

Similarly, the CSA of PGS (47 ppm) was greater than that of the phosphodiester of PGP (41 ppm) and the CS value (1.57 ppm) corresponds most closely to the downfield peak of PGP (1.45 ppm). Both the CS and CSA values of PGS are expected to correspond most closely to PGP because of the structural similarities.

Comparison of these results, particularly those of PA and PGS, indicates that the phosphate adjacent to the backbone glycerol, the phosphodiester in the case of PGP, gives rise to a wide spectrum (PA, 49.3 ppm; PGS 47 ppm; PGP 41 ppm). This assignment was corroborated by the similarity of the CS value of PGS and the high resolution peak tentatively assigned to the phosphodiester

Table III.9

Comparison of ^{31}P NMR CS and CSA values of diphytanylglycerol phospholipids

Compound	CS (ppm)[a.]	CSA (ppm)[b.]
PA	2.05	49.3
PGS	1.57	47.0
PG	1.08	25.4 - 31.1
PGP	0.48 , 1.45	18.0, 41.0
	0.80 , 1.91[c]	
Total polar lipids		18.0, 41.0

a. solution in $C_6{}^2H_6/C^2H_3O^2H$ (1.1:0.2); 50-100 ml/ml. CS relative to H_3PO_4.

b. sonicated, aqueous dispersions; 50-00 mg/ml.

c. σ_{iso} values calculated from ^{31}P (see text for more detailed description). All other values determined from high resolution spectra.

of PGP and the σ_{iso} value calculated for the broad component (see Table III.9).

2.3.2 Effect of pH

The rationale for studying the effects of pH on ^{31}P NMR spectra was two-fold. The first was an attempt to use the pH dependence to determine which subspectrum arose from which phosphate moiety. As stated in the theory section, the phosphorus chemical shift can vary with changes in electronegativity induced by ionization of the phosphate groups. As well, if ionization leads to changes in the headgroup conformation, there may be concomitant changes in the CSA. The second reason for studying the effect of pH on the CSA, and therefore on the headgroup conformation, was to determine if there was a conformational change in the lipids in response to pH. Gradient changes of the up to 3.5 pH units have been measured in cell envelope vesicles (Kouyama et al., 1987) following light-induced proton translocation.

^{31}P NMR chemical shift values (high resolution NMR) are sensitive to electrostatic effects; and, titration of inorganic phosphate or phosphate-containing compounds usually leads to a upfield shift of up to 5 ppm as the degree of ionization increases. Previous studies had determined the pK's of PGP in methanol/water (1:1) to be 3.25, 3.25 and 7.45-7.95 (Kates et al., 1965). The high resolution phosphorus spectrum of PGP has two resonances corresponding to the phosphomono- and phosphodiester groups, and assignment of these resonances, and therefore of the solid state subspectra, should be possible by

Table III.10

pH Dependence of ^{31}P NMR chemical shift values of PGP in organic solvents[a]

pH	chemical shift (ppm)[b]
2.10	-0.125, 0.960
2.72	0.277, 1.362
3.40	0.438, 1.521
4.58	0.719, 1.885
7.23	0.840, 2.005
8.89	0.799, 2.005

a. Solution in $C_6{}^2H_6/C^2H_3O^2H$ (1.1: 0.2); 50-75 mg/ml.

b. Relative to H_3PO_4.

c. Data shown in Figure III.20.

Figure III.20

pH dependence of ^{31}P NMR chemical shift values of PGP in organic solvents.

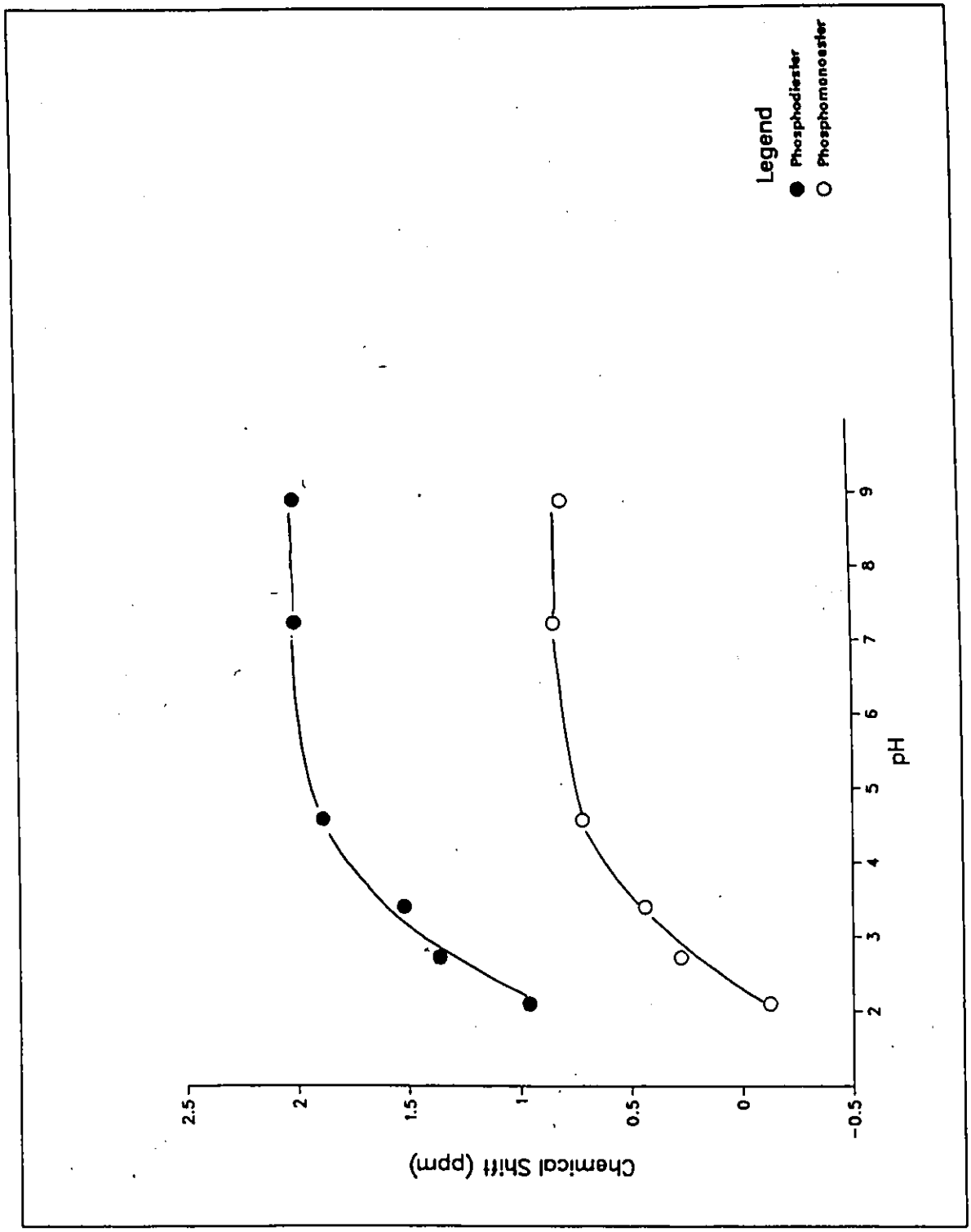
Legend
Phosphodiester
Phosphomonoester
Chemical Shift (ppm)
2.5
2
1.5
1
0.5
0
-0.5
2
3
4
5
6
7
8
9
pH

Table III.11

pH Dependence of ^{31}P chemical shift of sonicated aqueous dispersions of PGP

pH	chemical shift (ppm)[a]
3.95	1.548, 0.201
4.05	1.618, 0.230
4.55	1.660, 0.343
5.40	1.668, 0.412
6.05	1.719, 0.432
9.60	1.744, 0.442
10.08	1.739, 0.442
10.35	1.734, 0.442
10.35	1.749, 0.437
10.95	1.739, 0.432
11.08	1.739, 0.472
11.70	1.703, 0.442
11.95	1.744, 0.432
12.30	1.729, 0.442

a. Relative to H_3PO_4.

b. Data shown in Figure III.21

Figure III.21

pH dependence of ^{31}P NMR chemical shift values of aqueous, sonicated dispersions of PGP.

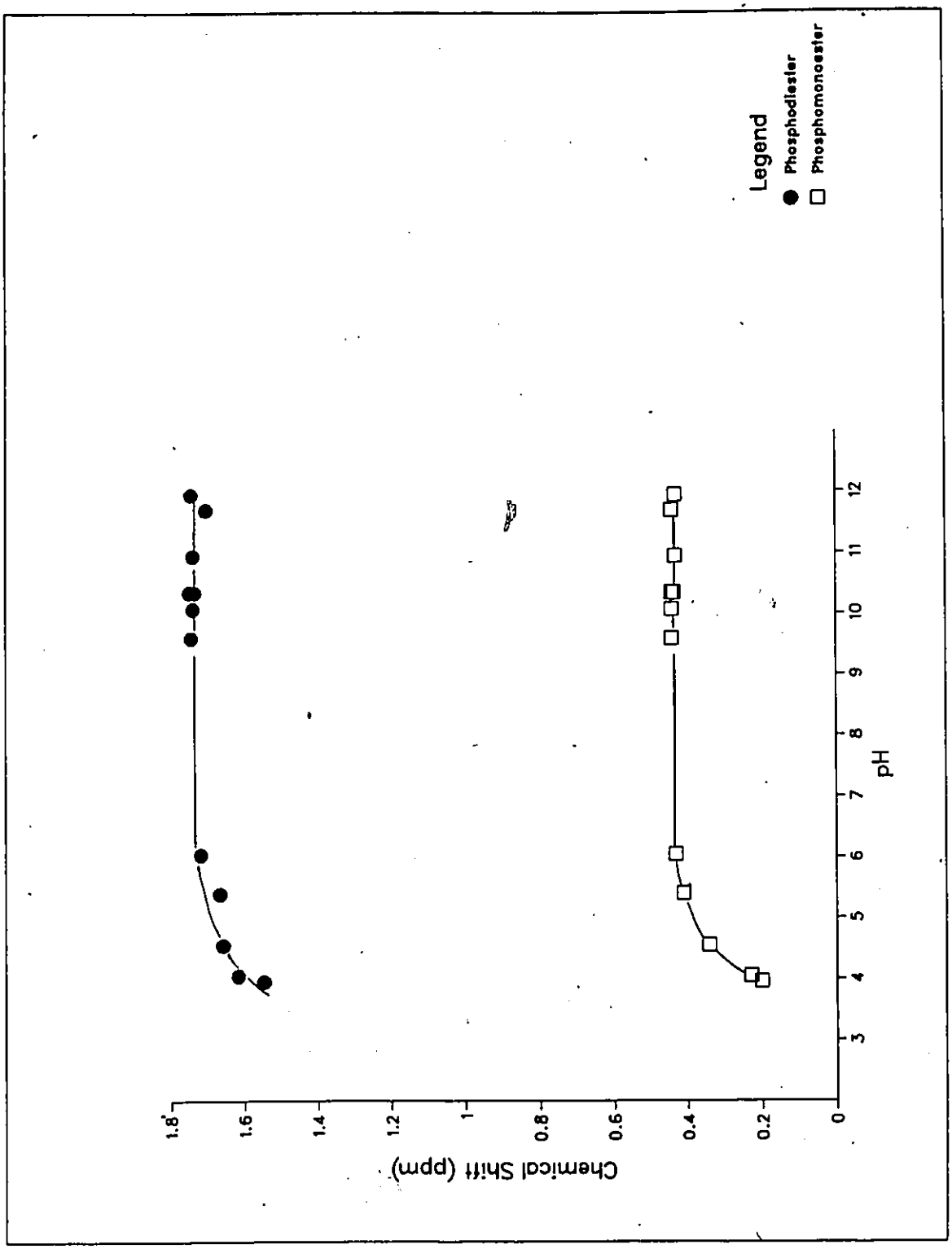
Legend
Phosphodiester
Phosphomonoester
Chemical Shift (ppm)
1.8
1.6
1.4
1.2
1
0.8
0.6
0.4
0.2
0
3
4
5
6
7
8
9
10
11
12
pH

determining which resonance is sensitive to pH near the pK or the third ionizable group. The titration curve of PGP in organic solvents and as aqueous, sonicated dispersions is shown in Figures III.20 and III.21 and Tables II.10 and III.11. Both resonances show marked frequency shifts in the pH range 2.0-4.5; however, neither show a pH-dependent shift at higher pH values (5-11). This experiment was repeated by high power ^{31}P NMR and the CSA of both subspectra of PGP were determined as a function of pH. Previous ^{31}P NMR experiments with DPPC (Phillips et al., 1972; Michaelson et al., 1974; Seelig and Gally, 1976) have shown a marked dependence of the value of the CSA on pH. Since the effective CSA is dependent upon both the average orientation of the ^{31}P chemical shielding tensor with respect to the axis of motional averaging and the extent of angular fluctuations around the axis of rotation, either a conformational change or more disordered motion (or a combination of both) could account for the observed CSA changes. Phillips and Michaelson have postulated that at pH's above the pK of the primary amine, the positively charged trimethylamino group can interact with the negatively charged phosphate to stabilize the headgroup conformation.

In the case of PGP, both subspectra showed a marked change in the CSA at pH 4.25 but no further change in the pH range 5-8 (See Figure III.12, Table III.22). Since these results seem to be in contradiction to previous pK determinations (Kates et al., 1965b), the potentiometric titration was repeated on sonicated samples of aqueous PGP in duplicate, under nitrogen atmosphere

Table III.12

pH dependence of ^{31}P NMR CSA values of aqueous dispersions of TPL from H. cutirubrum[a,b]

pH[c]	CSA (ppm)
3.00	10.291, 35.401
3.70	10.291, 35.401
4.55	16.054, 42.810
4.80	15.231, 43.634
5.20	15.642, 44.045
8.00	16.466, 44.045

a. 75 mg/ml; tris or citrate buffer (25 mM); ammonium salt forms.

b. Data taken from Figure III.22.

c. Final pH of lipid/buffer suspension.

Figure III.22

pH dependence of ^{31}P NMR CSA values of aqueous dispersions of TPL from H. cutirubrum (experimental details given in text).

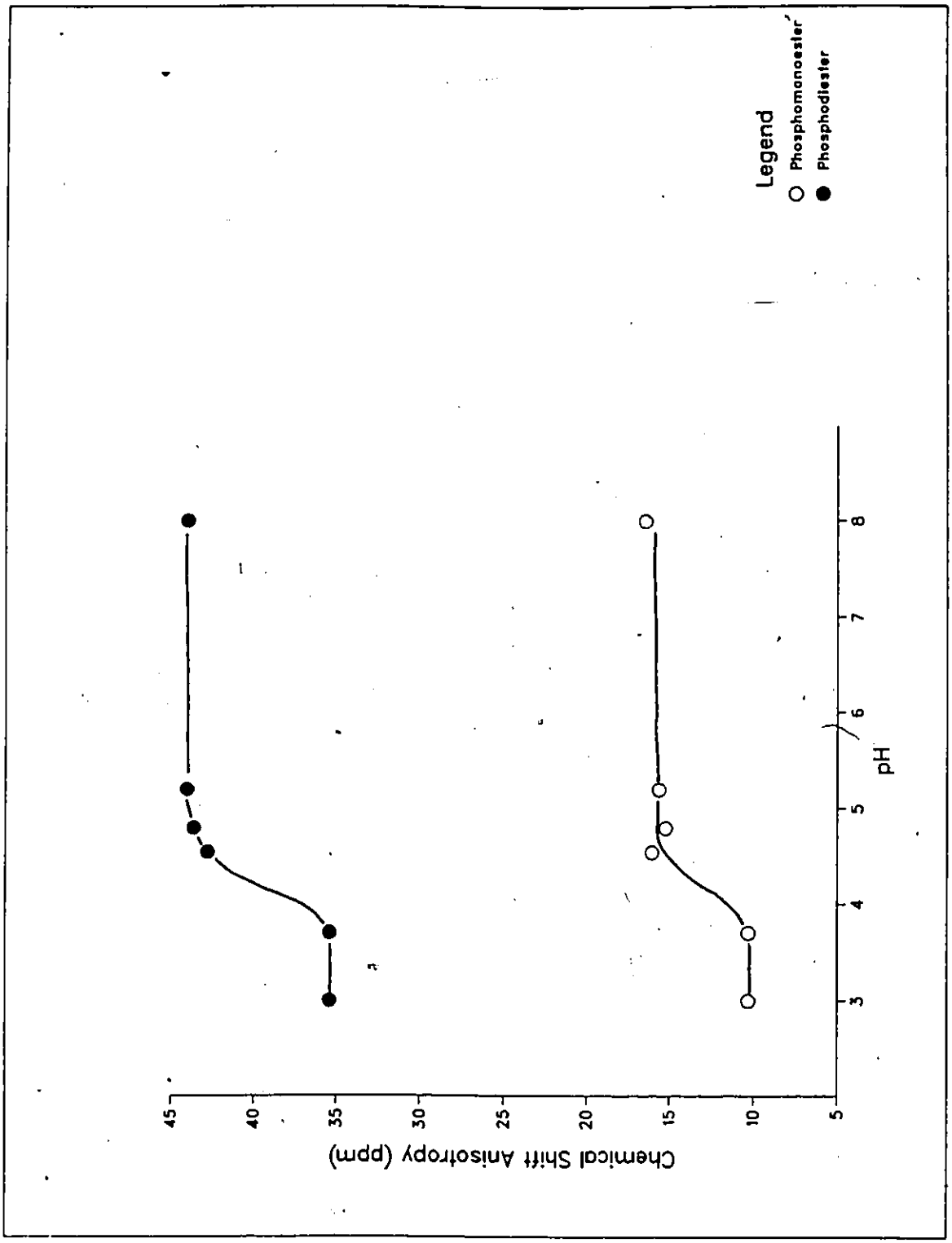
Legend
Phosphomonoester
Phosphodiester
Chemical Shift Anisotropy (ppm)
45
40
35
30
25
20
15
10
5
3
4
5
6
7
8
pH

Table III.13

Comparison of pK values determined by potentiometric and NMR titration of PGP[a]

Method	Solvent	pK_1	pK_2
Potentiometric			
	methanol/water (1:1)[b]	3.25	7.45-7.95
	methanol/water (1:1)[c]	3.55	>11
	aqueous (sonicated)[d]	2.4	>11
High Resolut ion NMR			
	benzene/methanol (1/1:0.2)[e]	2-3.2	>9
	aqueous (sonicated)[f]	<4.5	>11
High Power NMR			
	aqueous (dispersion)[g]	4.25	>8

a. pK_1 and pK_2 refer to the two lower pK values and the higher pK value of the ionizable groups of PGP (see PART III, section 5).
b. Kates et al., 1965.
c. Data taken from Figure III.37.
d. Data taken from Figure III.37.
e. Data taken from Figure III.20; Table III.10.
f. Data taken from Figure III.21; Table III.11.
g. Data taken from Figure III.22; Table III.12

and with appropriate solvent blanks (see PART III, section 5). The pK values were determined to be 2.4 (2 equivalents) and greater than 11 (1 equivalent) which might account for the absence of change of the CSA or chemical shift in the pH range of 5-10.

The pK values determined by high resolution and solid state NMR, and potentiometric titrations in both organic solvents and as aqueous dispersions are summarized in Table III.13. The pK values of the first two groups are probably the same within experimental error (3.2$\pm$ 1 pH unit). The hydrogen of the third ionizable group has a pK greater than 11 (1 equivalent) from potentiometric titrations, which is substantially higher than the second pK of phosphoric acid (7.21).

This high pK can probably be attributed to a combination of a change in the surface-charge density and the presence of intra- and/or intermolecular hydrogen bonding involving at least one of the phosphate groups. As discussed in section I.2, the pK's of ionizable groups of lipids in a bilayer hydrated with distilled water are significantly different from similar water-soluble compounds in solution (Boggs, 1984). The pK of sodium β-glycerophosphate are 3.1 and 6.6 (Trauble and Eibl, 1974) while the values for egg PA in aqueous dispersions are 3.8 and 8.6. In addition, the presence of mono- and divalent cations, charged groups on proteins and the presence of other polar lipids can affect the pK (Boggs, 1984).

A charged surface causes ordering of the electrolytes in a solution into a layer called the Gouy-Chapman-Stern layer. In

the case of a vesicle prepared from anionic lipids such as PGP which is doubly ionized at physiological pH's (6.5-7.5) the double layer is composed primarily of Na^+ and K^+. This high concentration of anions at the vesicle surface may be responsible for the increase in the pK of the third group.

Alternatively, the hydrogen of the third ionizable group may be involved in intramolecular hydrogen bonding.
Evidence for hydrogen-bonding has been shown by FTIR (see PART III, section 4), and would allow for stabilization of the remaining phosphate hydroxyl group and may account for its relatively high pK.

A third alternative is that the terminal phosphate is in the form of a cyclic phosphate.

This would account for the absence of a third pK at approximately pH=7. At very high pH (>11), the cyclic phosphate would be opened and the group ionized. However, the presence of a cyclic phosphate-containing compound is not borne out by the ^{13}C or ^{31}P NMR. Because the CS of the phosphorus is dependent upon the value of the smallest O-P-O bond angle, 5 membered pentacyclic rings exhibit chemical shifts of 11-23 ppm.(i.e., 2',3'-cyclic cytidine monophosphate; CS= 20.3 ppm) (Gorenstein et al., 1984) as compared with the actual values of 1.45 and 0.48 ppm. In addition, the ^{31}P NMR T_1 would be much shorter for a cyclic phosphate. The T_1 values for the phosphate groups of sonicated aqueous dispersions of PGP were similar (1.30 and 1.95 sec).

2.3.3 Effect of counterions

A series of experiments were designed to assess the effects of counterions on the headgroup of PGP. A variety of salt forms of PGP were prepared as described in PART I, section 1. High power ^{31}P NMR showed no change in the CSA (Figure III.23; Table III.14) except for the presence of an isotropic component for the potassium salt form. These experiments indicate that the nature of the counterion associated with the acidic head group has no discernable effect on the phosphate headgroup conformation or packing.

2.3.4 Effect of other membrane components

A comparison of the CSA and T_1 of the ammonium salts of PGP, PGP/GLS (1:1) and total polar lipids indicates that the presence of other lipids has no discernable effect on the amplitudes or rates of motions of the PGP headgroup (See Figure III.24, Table III.15). This also indicates that the CSA difference between purified PGP and the purple membrane is due predominantly to the presence of protein-lipid interactions rather than lipid-lipid interactions.

2.3.5. Effect of Temperature

The effect of temperature on the ^{31}P NMR spectrum of aqueous dispersions of TPL (70 mol % PGP) was determined over the temperature range of -25 to 44°C (see Figure III.25). Previous studies on the effect of temperature on the CSA of PGP and PM (see Fig. III.20) (Ekiel et al., 1981) showed no evidence of an abrupt, first order phase transition over the temperature range 5 to 60°C. At the lower temperatures, approximately -20°C, stopped,

Figure III.23

Effect of counterions on the ^{31}P NMR spectra of PGP.

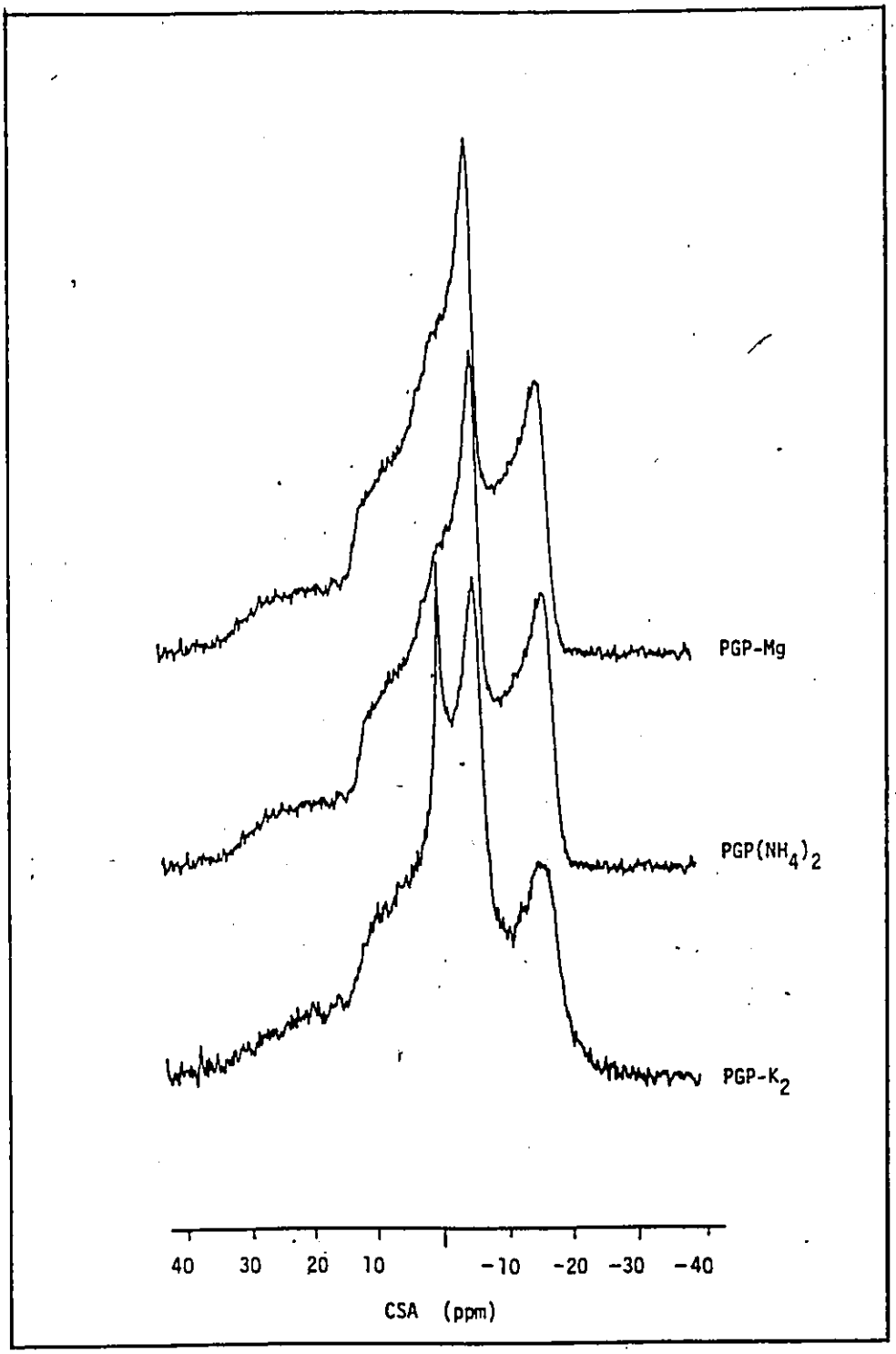
PGP-Mg
PGP(NH4)2
PGP-K2
40
30
20
10
-10
-20
-30
-40
CSA (ppm)

Table III.14

Effect of Counterions on the

^{31}P NMR CSA values of PGP[a]

Compound	conditions	CSA (ppm)
PGP-K_2	tris (25 mM)	18.11, 45.28
	pH 7.0	
PGP(NH_4)$_2$	tris (25 mM)	18.11, 45.28
	pH 7.5	
PGP-Mg	tris (25 mM)	18.11, 45.28
	pH 7.0	

a. Data taken from Figure III.23.

b. Lipid concentration approximately 60-80 mg/ml buffer.

Figure III.24

Effect of other polar lipids on the ^{31}P NMR spectra of PGP.

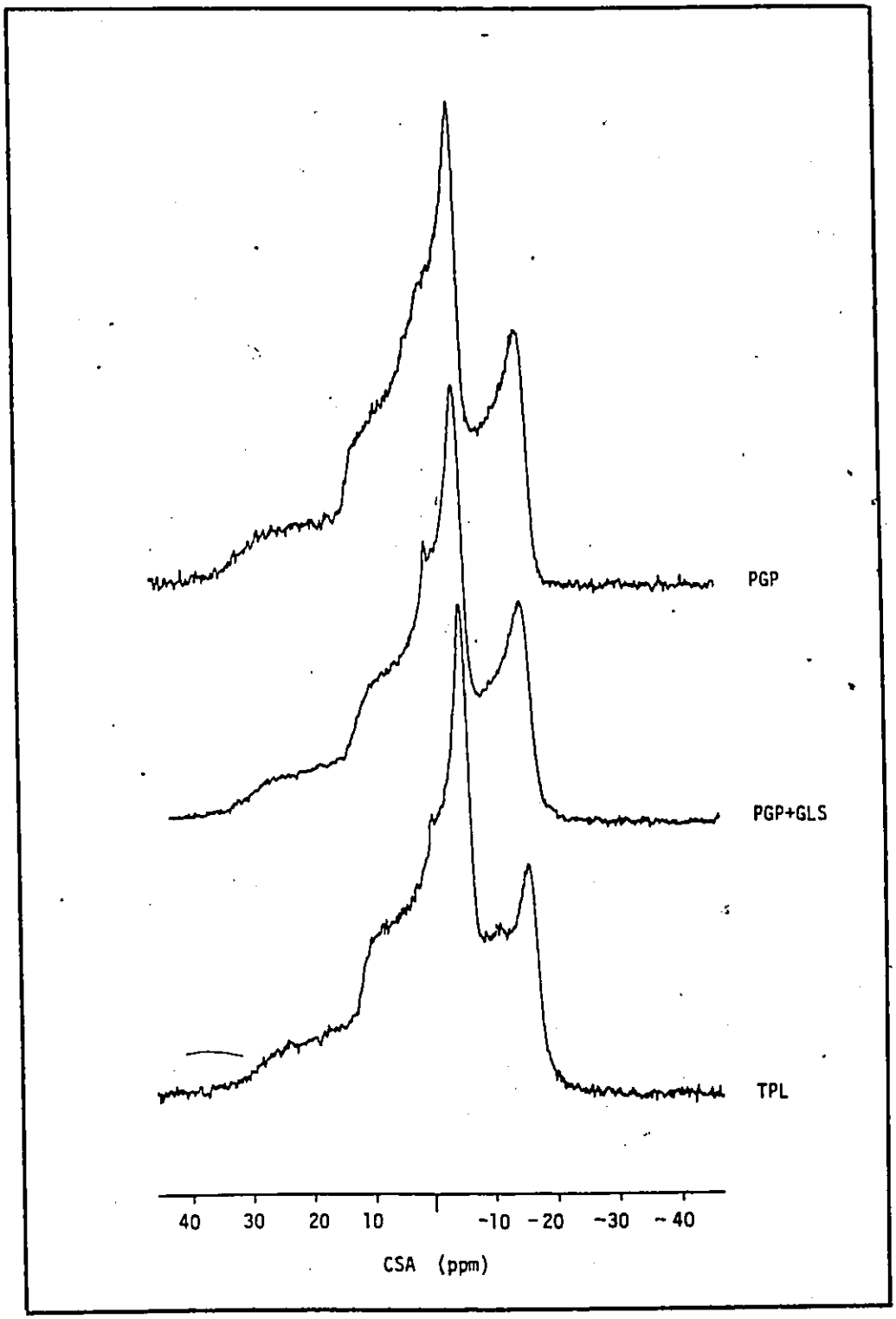
PGP
PGP+GLS
TPL
40
30
20
10
-10
-20
-30
-40
CSA (ppm)

Table III.15

Effect of other polar lipids on the ^{31}P CSA of PGP[a]

Compound [b,c]	conditions	CSA
PGP	Tris (25 mM) EDTA (5 mM) pH 7.5	17.29, 45.69
PGP/GLS[d]	Tris (25 mM) pH 7.8	16.88, 44.87
TPL	Tris (25 mM) pH 7.8	16.88, 44.87

a. Data taken from Figure III.24.

b. Ammonium salt forms.

c. Lipid concentration approximately 60-80 mg/ml.

d. Approximately 1:2 (w/w).

as indicated by the shape of the spectra (see Fig. III.25) (see also Fig. III.5) axial rotation. It may have been this transition which has been incorrectly interpreted by some authors as being indicative of a gel to liquid-crystalline phase transition.

2.4 Summary

^{31}P NMR indicates that there are no significant changes in the values of the chemical shift anisotropies of either phosphate group of PGP in response to pH in the physiological range (7±2 pH units), the nature of the counterion or the presence of other polar lipids. Because the residual CSA is indicative of both the amplitudes of motions and the orientation of the phosphorus headgroup with respect to the magnetic field, it is a sensitive indicator of change in the state of the phosphorus headgroup. The absence of changes in the CSA of either subspectrum indicates the absence of significant changes in the motions or orientations of the headgroup.

The stability of the headgroup may be attributed to the presence of intramolecular interactions between the two phosphate groups and/or a phosphate group and the free hydroxyl group of the headgroup glycerol as has been suggested by FTIR.

Table III.25

Temperature dependence of ^{31}P NMR lineshape and CSA for aqueous dispersions of total polar lipids from *H. cutirubrum*.

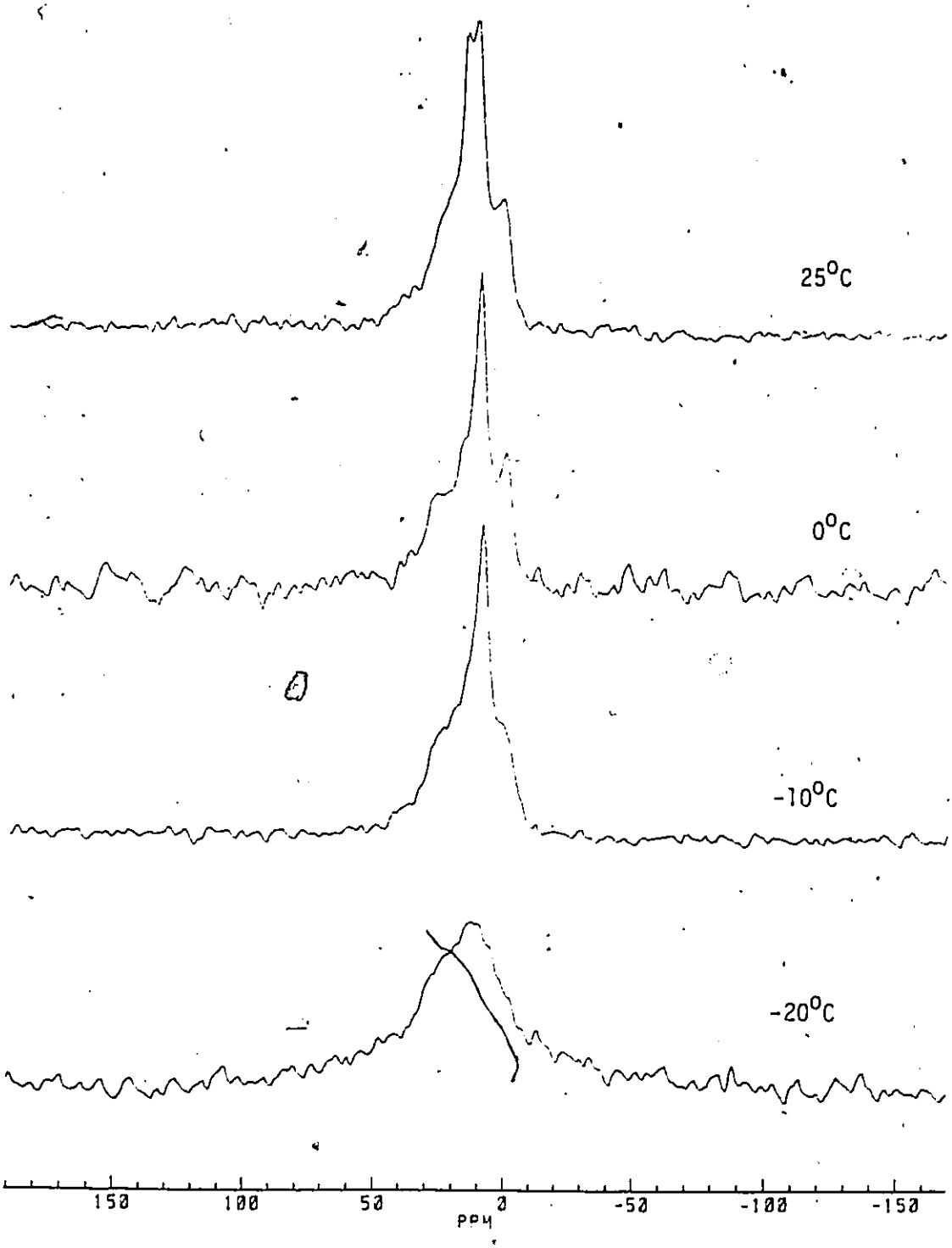
25°C
0°C
-10°C
-20°C
150
100
50
0
-50
-100
-150
ppm

3. Oriented Bilayers

3.1 Introduction and Theory

The analysis of ^{2}H NMR data for labelled lipids in membranes assumes that the axis of molecular motion is oriented perpendicular to the plane of the bilayer. This has been shown to be true by ^{31}P NMR for the headgroup region of DPPC/cholesterol (1:1 mole ratio) (McLaughlin et at., 1975) and, by ^{2}H NMR for PC (Stockton et al., 1974) and glucosyl dialkylglycerol (Jarrell and Smith, 1986) . The question then arises as to whether this is a phenomenon characteristic of all membrane lipids.

The total polar lipids of the archaebacterium Halobacterium cutirubrum are essentially a binary mixture of sn-2,3-diphytanylglycerol derivatives of phosphatidylglycerol phosphate and a glycolipid sulfate (Kates, 1978). These lipids are sufficiently different from the lipids used in previous studies, with respect to charge, glycerol-hydrocarbon linkage and nature of the hydrocarbon chain, to justify the determination of the molecular axis for comparison. In addition, the use of both ^{31}P and ^{2}H NMR allows for the comparison of the director for the headgroup and hydrocarbon regions - which can, in principle, have different orientations.

For a rigid, immobile phospholipid, the value of the ^{31}P NMR chemical shift is determined primarily by the orientation of the phosphate group with respect to the external magnetic field (see section 2). For solid, powdered samples, the spectrum is the weighted sum of the subspectra from all the orientations and is characterized by a broad (190 ppm) spectrum. In membranes or

liposomes, the phospholipid molecule is not immobile but undergoes rapid, axially symmetric rotation leading to a spectrum which is again the weighted average of all orientations of the rotation axis with respect to the magnetic field. If the lipid bilayers are aligned in a specific orientation through the use of glass slides, the resultant ^{31}P NMR spectrum from a stack of lipid/glass multilayers is characterized by a single, narrow peak whose position is dependent upon the orientation of the bilayer (as defined by the glass slides) with respect to the static magnetic field.

The chemical shift (σ) has a $(3\cos^2\theta - 1)/2$ dependence, with CS values varying from the $\sigma_{//}$ and $\sigma_{\perp}$ extremes of the high power spectrum and having a value of θ at 54.7° .

The angle between the axis of motional averaging and the magnetic field is designated as and the angle between the normal to the glass slide and the magnetic field as β . By varying the orientation of the multilayers as defined by the normal to the glass slides, with respect to the magnetic field and comparing the results to the calculated values, it is possible to determine if the axis of motional averaging and the bilayer normal are coincidental (See Figure III.26).

This theory holds true for ^{2}H NMR of deuterium-labelled molecules as well. The value of the quadrupole splittings varies as $(3\cos^2\theta - 1)/2$, collapsing to a narrow, isotropic line when the angle, θ , is 54.7°.

By comparing the angular dependencies (β) of the phosphorus and deuterium signals, it is possible to determine and compare the motional axes of both the headgroup and the hydrocarbon

Figure III. 26

A. Schematic representation of oriented multilayers in a magnetic field indicating the angle, β, between the normal to the glass slide and B_o.

B.i. The lipid molecule is undergoing rapid axial rotation about an axis (the director) which is perpendicular to the plane of the bilayer.

ii. The molecule is undergoing rapid, axial rotation as well as motion (disorder) of the axis about the bilayer normal.

iii. The axis about which the motion of the molecule is centered is not normal to the plane of the bilayer ($\beta \neq \theta$).

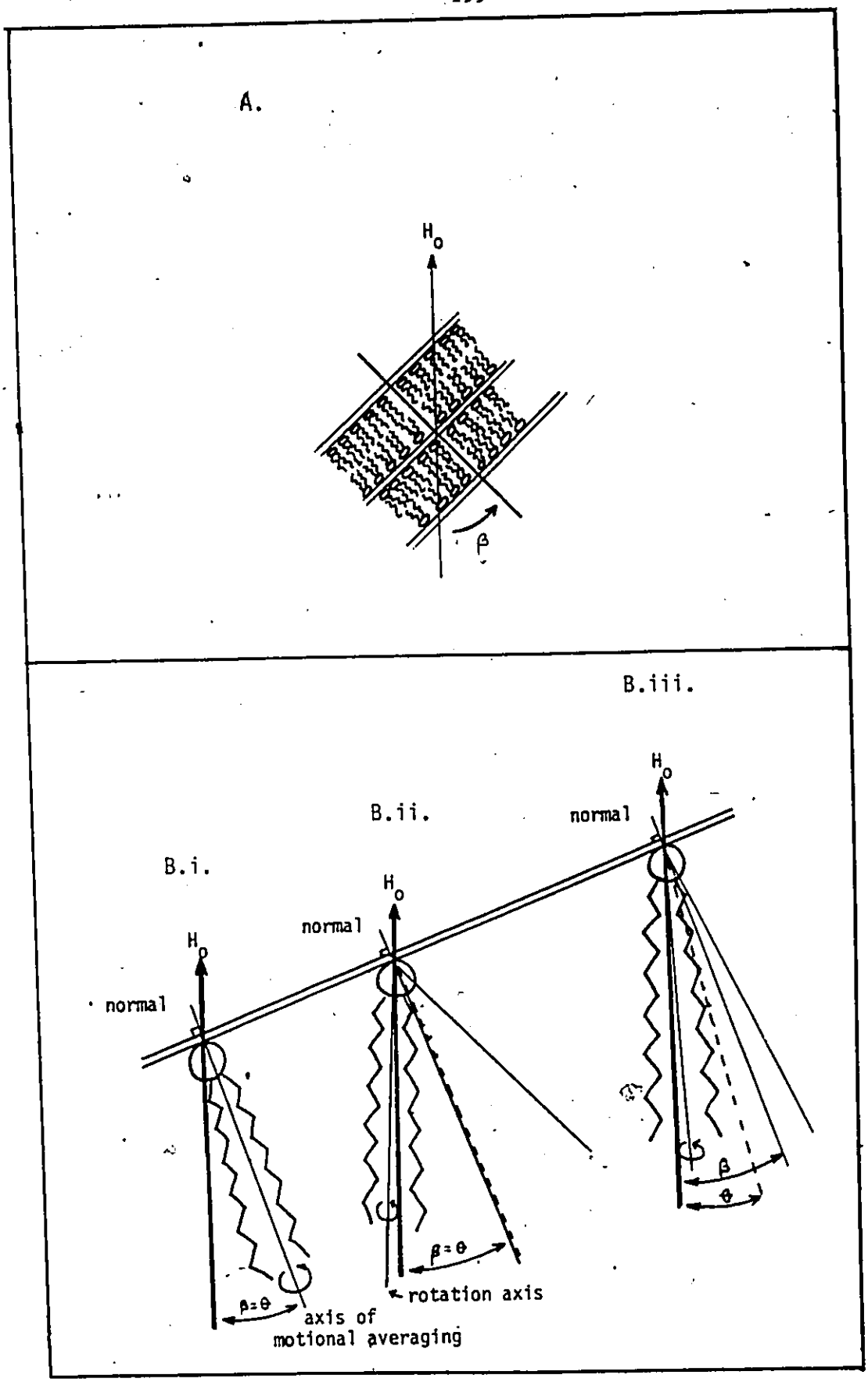
A.
H_o
β
B.iii.
B.ii.
B.i.
normal
normal
normal
H_o
H_o
H_o
β
θ
β=θ
β=θ
rotation axis
axis of
motional averaging

chains.

3.2 Materials and Methods

Halobacterium cutirubrum cells were grown in standard medium supplemented with deuterated sodium acetate (1 gram/litre) and the total polar lipids were extracted and purified according to established procedures (see PART I, section 1). A solution of total polar lipids (containing approximately 70% PGP; 30 mg in 1 ml chloroform) was spotted on 30-35 glass plates (22x7x0.15 mm) and dried under a stream of nitrogen. The plates were stacked in a 10 mm O.D. NMR tube, dried in vacuo and hydrated in a humid atmosphere of deuterium-depleted water overnight at 65°C. A drop of deuterium-depleted water was added and the tube was sealed.

^{31}P NMR spectra were acquired with standard Hahn-echo techniques (90°_{x} -τ-180°_{y} -τ-acquire; 90° pulse, 4-5 μs; recycle time, 2.5 sec) on a Bruker MSL-300 operating at 121.466 MHz. Spectra were not proton-decoupled.

^{2}H NMR spectra were acquired with quadrupolar spin-echo techniques (90°_{x}-τ-90°_{y}-τ-acquire; 90° pulse, 3.95 μs; recycle time 0.15 sec) on a home-built spectrometer operating at 30.70 MHz.

The estimated accuracy of the angular settings is ± 5 as determined by multiple settings of a particular orientation.

3.3 Results and Discussion

Figure III.27 shows the rotation diagram of the phosphorus groups of PGP in a mixture of total polar lipids as determined from the ^{31}P NMR spectra of oriented multilayers. The chemical shifts arising from both phosphate moieties vary from 27 and 11 ppm to -14.1 and -3.6 ppm, which correspond well to the chemical

Figure III.27

Orientational dependence of the ^{2}H NMR quarupolar splittings and ^{31}P NMR chemical shift values for oriented, biosynthetically-deuterated total polar lipids.

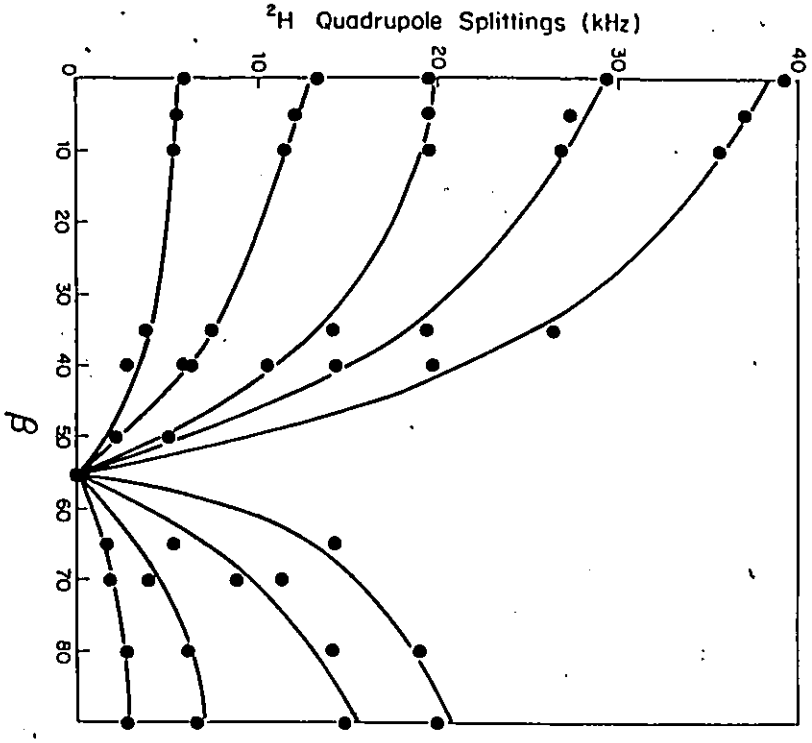
^{2}H Quadrupole Splittings (kHz)
0
10
20
30
40
β
0
10
20
30
40
50
60
70
80

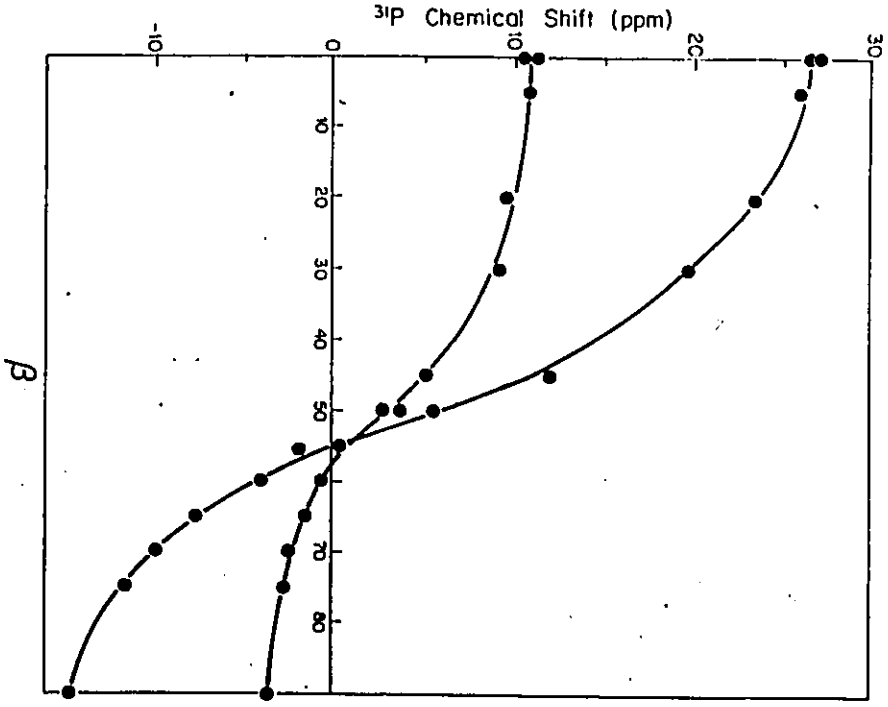
^{31}P Chemical Shift (ppm)
-10
0
10
20
30
β
10
20
30
40
50
60
70
80

shift anisotropy values of non-oriented dispersions of total polar lipids (18 and 41 ppm) (See Table III.16). This implies, as was shown to be true for DPPC/cholesterol (1:1 mole ratio) (McLaughlin et al., 1975) that the conformation and amplitude of motion of the headgroup is the same for both oriented and non-oriented samples. In addition, both subspectra have a chemical shift of zero at $\beta = 55^{\circ}$ which indicates that the axis about which the headgroup undergoes motional averaging is normal to the glass plates. Figure III.25 shows the corresponding ^{2}H NMR rotation diagram for biosynthetically deuterated total polar lipids. The quadrupole splittings for all positions collapse to zero at $\beta = 55^{\circ}$. This indicates that the axis of motional averaging is again normal to the plane of the bilayer; i.e., that the molecule has only one axis of motional averaging. In addition, the quadrupole splittings seen for the $\theta = 90^{\circ}$ orientations correspond within experimental error to the splittings seen for non-oriented samples (see Table III.16).

It should be noted that the molecular axes are the same for all the molecules in the system. This is of particular interest in view of the fact that the total polar lipids of H. cutirubrum are virtually a binary mixture of PGP and glycolipid which have very different headgroup sizes (see Figure III.26). These results are not in agreement with the hypothesis put forward by a number of groups (Plachy et al., 1974; McFarland and McConnell, 1971) stating that the hydrocarbon chains of the phytanyl lipids are not perpendicular to the bilayer surface but are tilted 20° from the bilayer normal. This discrepancy probably arises due to interactions between the branched-chain phytanyl chains and the

Table III.16

Comparison of chemical shift anisotropies and quadrupole splittings from aqueous dispersions and hydrated, oriented bilayers of diphytanylglycerol lipids

nucleus	aqueous dispersions	oriented bilayers
^{31}P	41 ppm	41.1 ppm
	18 ppm	14.4 ppm
^{2}H	18.55 kHz	$\theta = 90^{\circ}$ 19.6 kHz
	13.87	14.2
		10.8
	6.45	5.6
	~~2.54~~	2.9
	1.76	
	0.20	
		$(\theta = 0^{\circ})/2$ 18.2
		14.8
		9.9
		5.9
		2.8

ω_o = 30.70 MHz; T = 25°C.

Figure III.28

CPK models of PGP (on the left) and GLS (on the right).

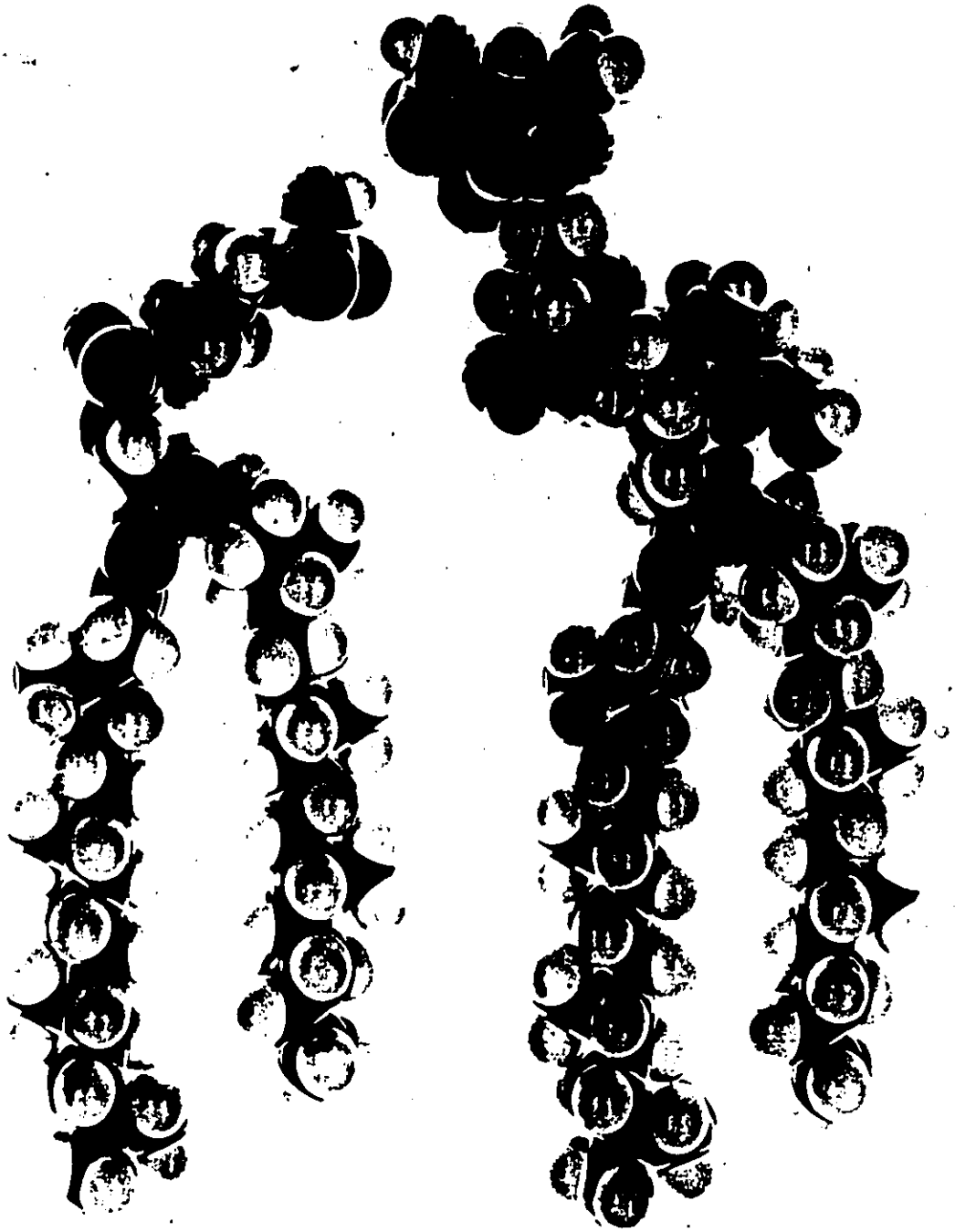

spin-labelled ESR probe which could lead to a shift in the axis of the probe.

The hydrocarbon chains of phospholipids have been shown by ^2H NMR and other physical techniques to undergo extensive gauche-trans isomerization at frequencies of approximately 10^9 to 10^{12} sec^{-1}. In addition, there may be other types of motion, such as chain wagging, or flexing of the molecules, which may be slower than the chain gauche-trans isomerization but which are still fast enough to be averaged on the NMR timescale (40 kHz = 10^5 sec^{-1}). In addition, the headgroup may be undergoing motions independently of the chains. Despite the presence of these internal motions, the resultant motional axis for both the hydrophobic and hydrophilic regions are coincidental and perpendicular to the plane of the bilayer. This has also been shown to be the case for diacyl PC and glycosyl dialkylglycerol (Jarrell and Smith, 1986 Smith et al., unpublished). It implies that the molecular motional axes for all lipid types, whether phospho- or glycolipid, ester- or ether-linked, straight or branched chains, are essentially identical as determined by this technique. While this may seem unlikely, it may arise as a consequency of rapid overall molecular motion, which masks subtle differences in the character of the local motions.

4. Fourier Transform Infrared Spectroscopy

4.1 Introduction

It has been postulated that, in addition to their structural role, anionic lipids may function as proton-conductance pathways across the plane of mitochondrial and chloroplast membranes (Haines, 1983).

This proton-conductance pathway may be of particular interest for the membranes of the extremely halophilic bacteria such as H. cutirubrum. The polar lipids of this organism are almost exclusively (>98%) anionic lipids (Kates, et al., 1982), primarily sn-2,3-diphytanylglycerol-1-phosphoro-3'-glycerol-1'-phosphate (PGP). In addition, the integral membrane protein, bacteriorhodopsin, which functions in light-driven proton translocation, is located within the purple membrane patches, whereas the ATPase, through which the pH gradient is dissipated during ATP production, is located within the adjacent red membrane. Thus, a lipid-mediated proton-conductance pathway involving PGP would be an efficient method of transferring protons from bacteriorhodopsin to ATPase.

Phospholipids such as PG and PC are able to form hydrogen-bonds with neighbouring headgroups (Boggs, 1984; Papahadjopoulos and Weiss, 1969; Jendrasiak and Hasty, 1974; Hauser and Phillips, 1976; Cèvc et al., 1981; Ruocco et al., 1981). This may allow the lipids to function as a proton-conductance pathway along the membrane surface (Haines, 1983). Hence, the study of the conformation of the headgroups of these anionic lipids may

provide information on the role of PGP in proton-conductance.

^{2}H NMR has been used to determine molecular order and dynamics in the hydrocarbon and glycerol backbone region of phospholipids (see PART III, section 1), but application of this technique to the study of the headgroup region of the diphytanylglycerol phospholipids is hampered by the fact that the orientation of the headgroup with respect to the axis of motional averaging is not known. The use of X-ray crystallography is not possible because of the unavailability of single crystals of diphytanylglycerol lipids.

In the past decade, FTIR and, in particular, diffuse reflectance infrared spectrometry (DR-IR) has been applied to the study of a variety of samples due to the ease of sample preparation and to the high signal-to-noise ratio relative to standard IR spectral techniques. The IR spectrum of PGP is complex, particularly in the region from 900 to 1800 cm^{-1}, because of the presence of overlapping bands and changes in the frequency and intensity of the phosphate bands with varying degrees of ionization and inter- and intramolecular hydrogen-bonding. Although the conventional IR spectra of PGP and related compounds have been reported (Kates et al, 1965a; Goni and Arrondo, 1986), the complexity of the spectra precluded precise assignment of the bands.

In this chapter, it is demonstrated that the use of model compounds such as deoxy and methylated derivatives of PGP (see Figure III.29), and PA and PGP molecules of differing degrees of

ionization simplifies the DR-IR spectra and allows for complete assignment of the major spectral bands of PGP.

4.2 Materials and Methods

PG and PGP were isolated from the total polar lipids of H. cutirubrum as described in PART I, section 1. Mono-, di- and tri-potassium salt forms of PA and PGP were prepared by titration of the free acid form with one, two or three equivalents of methanolic KOH as described in PART I, section 1.

PA, dPG, dPGP, proPG and methylated derivative of PGP were synthesized and characterized as described in PART II (see Figure III.29).

Measurement of DR-IR Spectra

The isolated, natural PGP and the synthetic analogues were dissolved in CCl_4 to yield a concentration of approximately 4 % by weight. High purity KCl crystals (Optavac, North Brookfield, MA) were ground in a Wig-L-Bug for five minutes and the powder was used as the matrix to support the sample as well as the reference. Pure KCl powder was first loaded into a special copper sampling cup (6mm in diameter and 4mm in depth), the top was flattened with a spatula and the DR-IR reference spectrum measured. After the collection of the reference spectrum, one drop (approximately 50 µl) of the solution to be examined was loaded onto the top of the KCl powder. The sample was then dried in vacuo for one hour in order to remove the solvent. The final

sample concentration was 0.5 wt% in KCl.

The DR-IR spectra were measured using a 296 interferometer (Digilab Div. of BioRad, Cambridge, MA) and a home build DR-IR accessory based on an on-axis geometry (Yang et al., 1986). An optical retardation of 0.25 cm was used, which results in a digitization interval of 2 cm^{-1} after the interferogram was Fourier transformed into the frequency domain with a zero-filling factor of 2 to increase the resolution. In each case, 500 interferograms were signal-averaged to obtain spectra with a signal-to-noise ratio of better than 1000.

All spectra were normalized to the methylene CH stretching vibration band at approximately 2950 cm^{-1}.

4.3 Results and Discussion

In view of the complicated head group structure of PGP molecules and the similarities of constituents of the hydrogen-bonding groups in a variety of lipids, detailed infrared band assignments will be based on the previous work in this area (Parker, 1983; Thomas and Chittenden, 1964a,1964b,1970; Sen et al., in press).

4.3.1 PA and Corresponding Potassium Salts

DR-IR spectra of the ionized forms of PA ($-H_2$, -KH and $-K_2$), from 800 to 3200 cm^{-1}, are shown in Figures III.30 and 31. Frequencies of the bands along with their tentative assignments are given in Table III.17. A number of bands are of constant

Figure III.30

FTIR spectra of PA-H_2, -KH and K_2

A. PA-H_2

B. PA-KH

C. PA-K_2

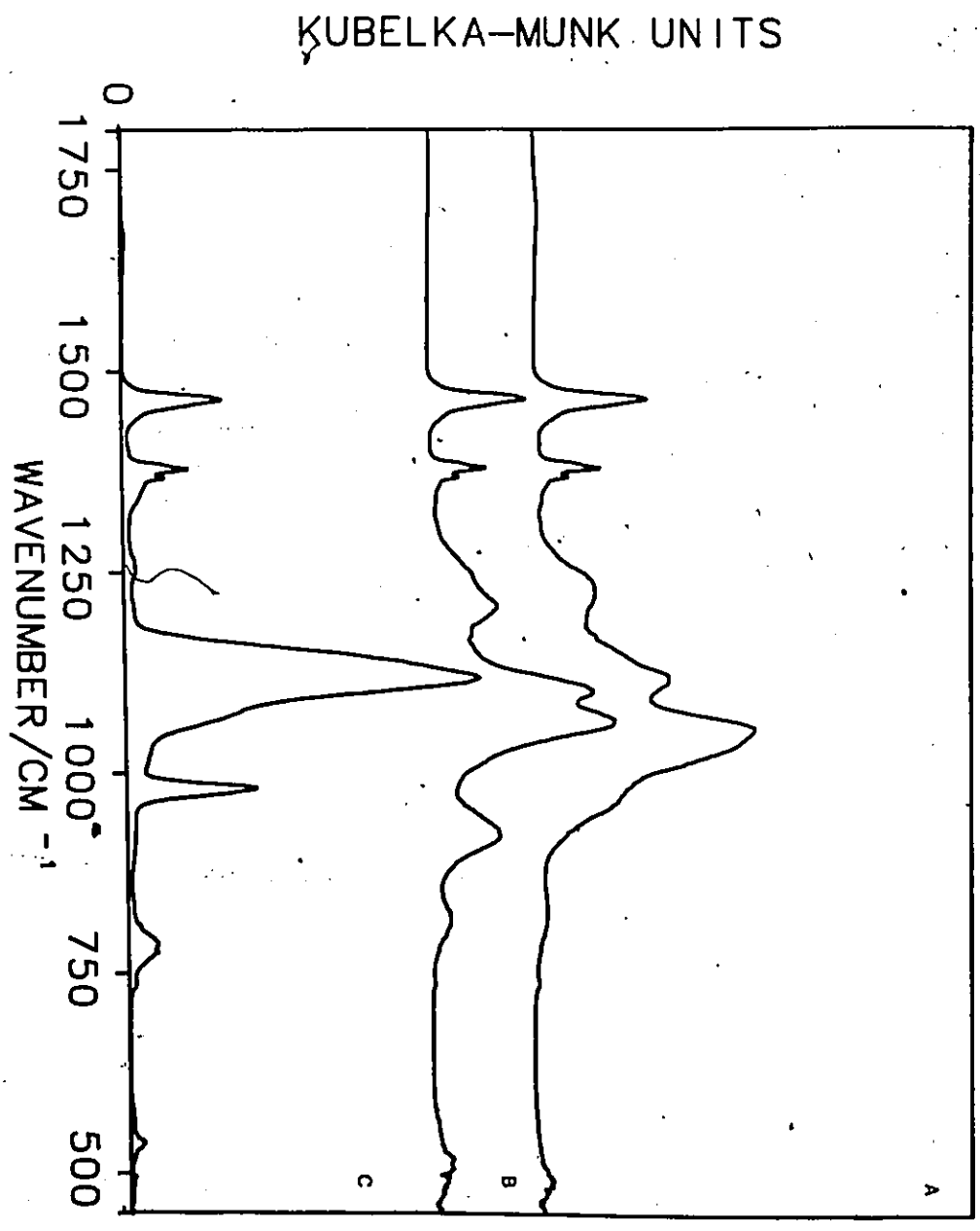
KUBELKA–MUNK UNITS
0
1750
1500
1250
1000
750
500
WAVENUMBER/CM -1
C
B
A

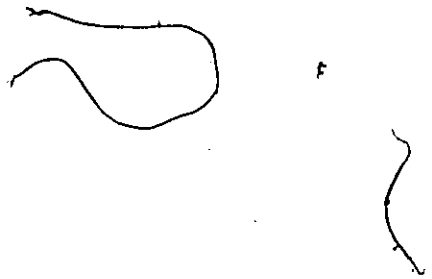

Figure III.31

FTIR spectra of PA-H_2 and PGP-H_3.

A. PA-H_2

B. PGP-H_3

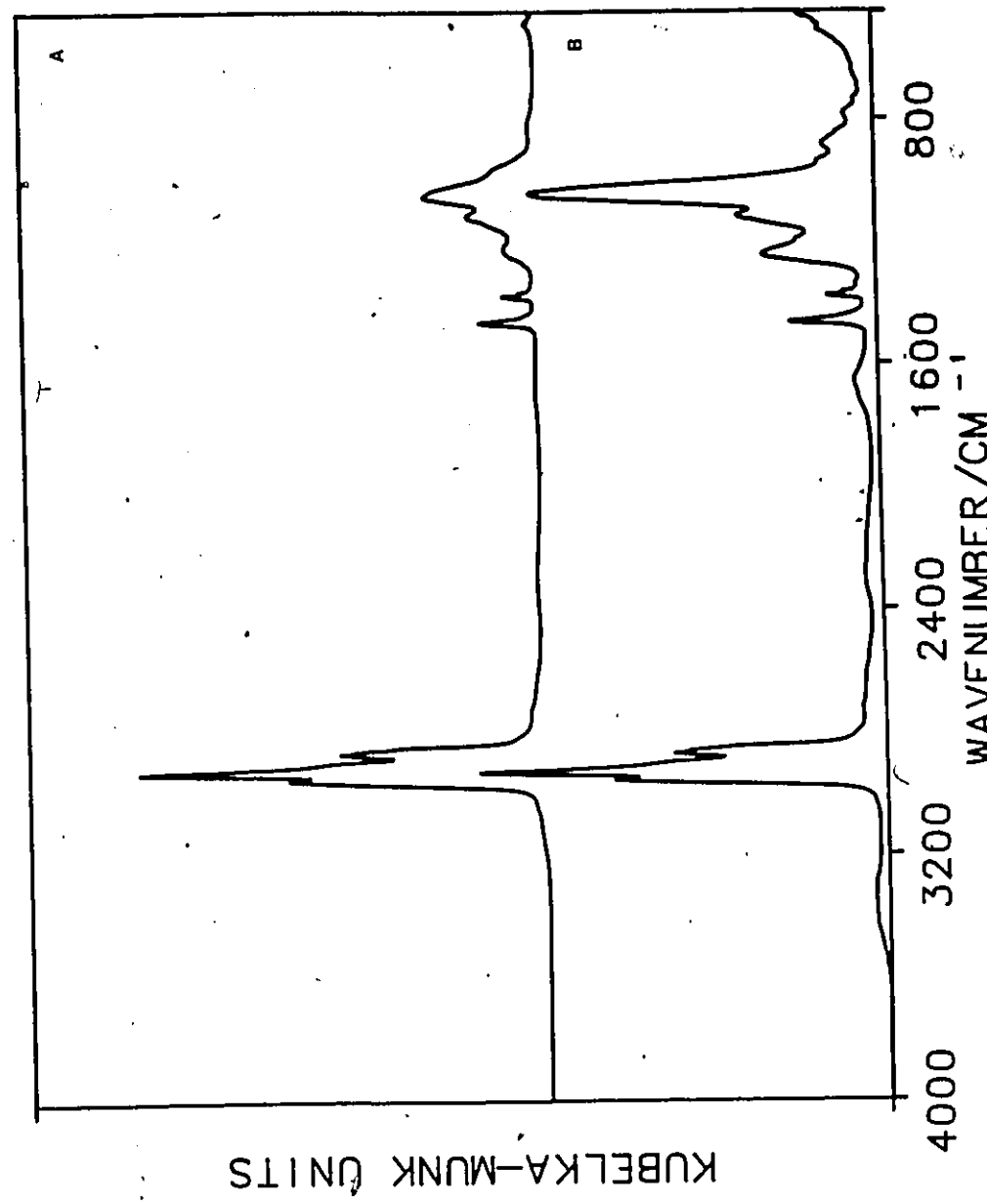
A
B
4000
3200
2400
1600
800
WAVENUMBER/CM⁻¹
KUBELKA-MUNK UNITS

Table III.17

Frequencies and tentative assignments for diphytanylglycerol phosphatidic acid

compounds and FTIR frequencies (cm^{-1})			tentative assignments
PAH_2	PA-HK	$PA-K_2$	
2500-3300	2500-3300	-	hydrogen-bonded P-OH
2318	2372	-	in-plane P-OH def. + P-O-C stretching
1698	1756	1664	P-OX in-plane def. + $P(OX)_2$ wagging
-	-	1252	ν_{as} $P(OX)_2$
1215	1205	-	P-OH in-plane def.
1118	1118	1117	P-O-C stretching
1038	1064	1101	C-O-C stretching
-	1101	1118	ν_s $P(OX)_2$
965	925	980	ν_{as} P-OX stretching
567	511	466	$P(OX)_2$ wagging

shape and intensity in all of these compounds. These correspond to the methyl deformation vibrational band (1360 to 1380 cm^{-1}), the methylene scissoring band (1450 to 1480 cm^{-1}) and the methyl and methylene C-H vibrational stretching bands (2830 to 2980 cm^{-1}).

There are also infrared bands which are indicative of strong H-bonding capabilities. For example, the P-OH in-plane deformation vibration at 1215 cm^{-1} for PA-H_2 narrows and red shifts to 1205 cm^{-1} for PA-HK and is absent in PA-K_2. The P-OH out-of-plane deformation vibration (1050 to 1080 cm^{-1}) is not observable due to its relatively small absorptivity. The band arising from asymmetrical P-O stretching in P-OX , which is usually seen from 920 to 990 cm^{-1} (Suehla, 1976) is observed at 965 cm^{-1} (shoulder) in PA-H_2, at 925 cm^{-1} in PA-HK and 980 cm^{-1} in PA-K_2. In PA-H_2, the P-O-C stretching vibration is at 1118 cm^{-1} and the C-O-C stretching vibration is at 1038 cm^{-1}. In PA-HK, the 1038 cm^{-1} band shifts to 1064 cm^{-1} and a new band at 1101 cm^{-1}, due to the $P(OX)_2$ symmetric stretching, can be observed now. The 1118 cm^{-1} P-O-C stretching vibration is now overlapped with the strong $P(OX)_2$ symmetric stretching mode (1101 cm^{-1}) and can only be observed in the deconvolved spectrum. With further ionization, (PA-K_2), the 1101 cm^{-1} band is further blue shifted to 1117 cm^{-1} and is completely convoluted with the P-O-C stretching mode. The usually very weak ν_{as} $P(OX)_2$ mode can now be observed at 1252 cm^{-1}. $P(OX)_2$ is defined as arising from one or more of the following groups: $P(OH)_2$, $P(OK)_2$, $P(OCH_3)_2$ or a combination such as HO-P-O-K.

There is a broad band (2500-3300 cm^{-1}) under the strong CH stretching band in the spectra of PA-H_2 and PA-HK which can be attributed to the hydrogen-bonded P-OH vibrational mode. Another broad band centered at 2318 cm^{-1} in the spectrum of PA-H_2 and is shifted to 2372 cm^{-1} in PA-KH and is not observable in the spectrum of PA-K_2. This band can be assigned to the combination of the in-plane P-OH deformation and the P-O-C stretching modes. It is clear that this shift is due to the inductive effect imposed by the presence of the K^+ ion in the headgroup. Also, the fact that there is no possibility for the PA molecules to form intramolecular hydrogen-bonding indicates that the PA molecules interact via intermolecular hydrogen-bonding.

The $P(OX)_2$ wagging mode decreases in intensity and red shifts from PA-K_2 (567 cm^{-1}) to PA-HK (511 cm^{-1}) to PA-H_2 (466 cm^{-1}). Combinational overtones of this vibrational mode and the P-OX (with X= H or K) deformational vibration can be observed at 1698 in PA-H_2 and at 1756 cm^{-1} for PA-KH and is at 1664 cm^{-1} for PA-K_2.

4.3.2 Deoxy analogues of PG and PGP

DR-IR spectra of PGP, dPGP, dPG and proPG are shown in Figures III.32 and III.33 and the tentative assignments of the major absorption bands are given in Table III.18. A number of bands (e.g., between 700 and 1600 cm^{-1}) reflect the hydrogen-bonding capabilities of these compounds. The hydrogen-bonded C-OH is seen for dPG at 3200-2500 cm^{-1} in comparison with 3240 cm^{-1} for

Figure III.32

FTIR spectra of dPG and proPG.

A. proPG

B. dPG

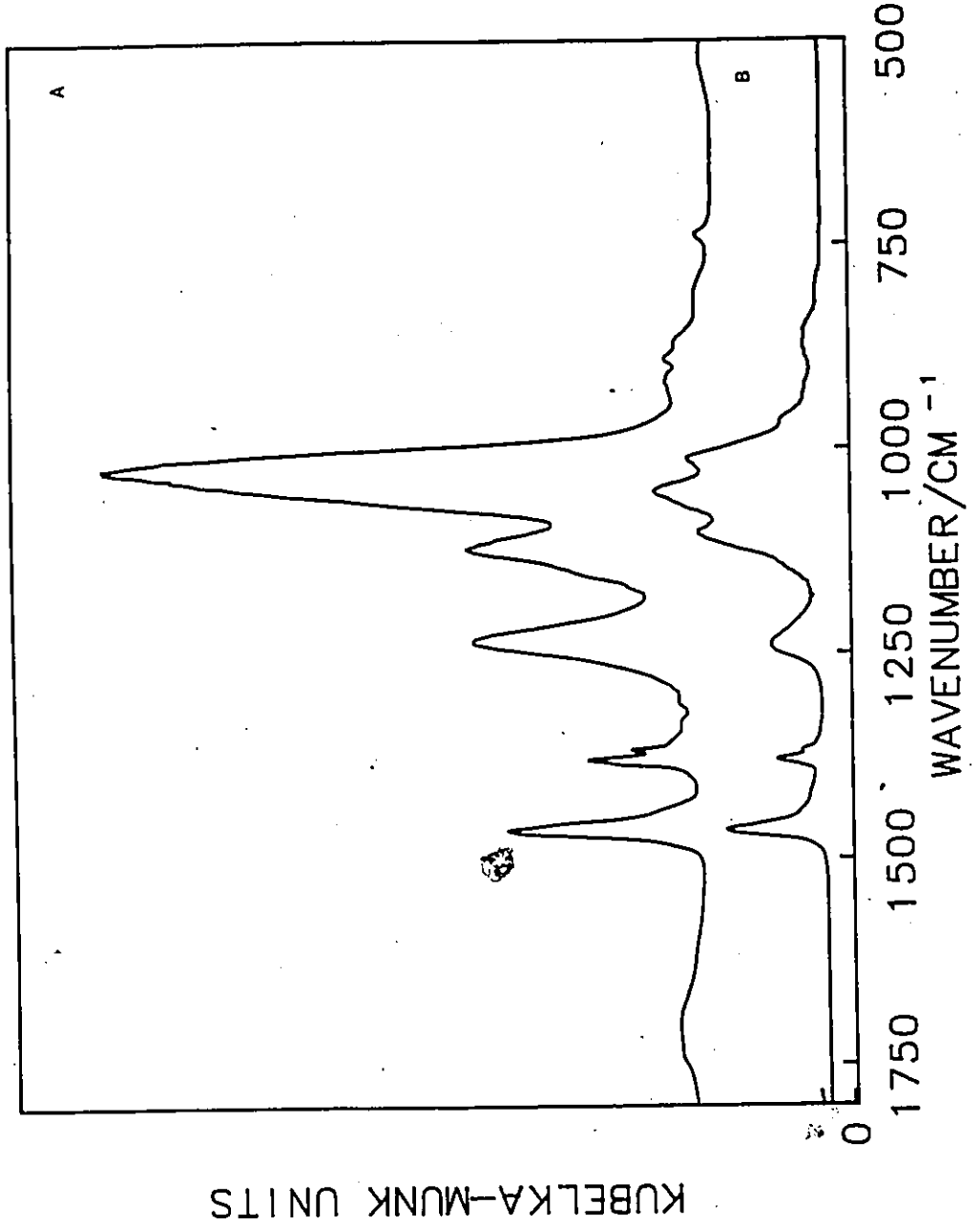
A
B
1750
1500
1250
1000
750
500
0
WAVENUMBER/CM⁻¹
KUBELKA-MUNK UNITS

Figure III.33

FTIR spectra of PGP and dPGP

A. $dPGP(NH_4)_2H$

B. $PGP\text{-}K_2H$

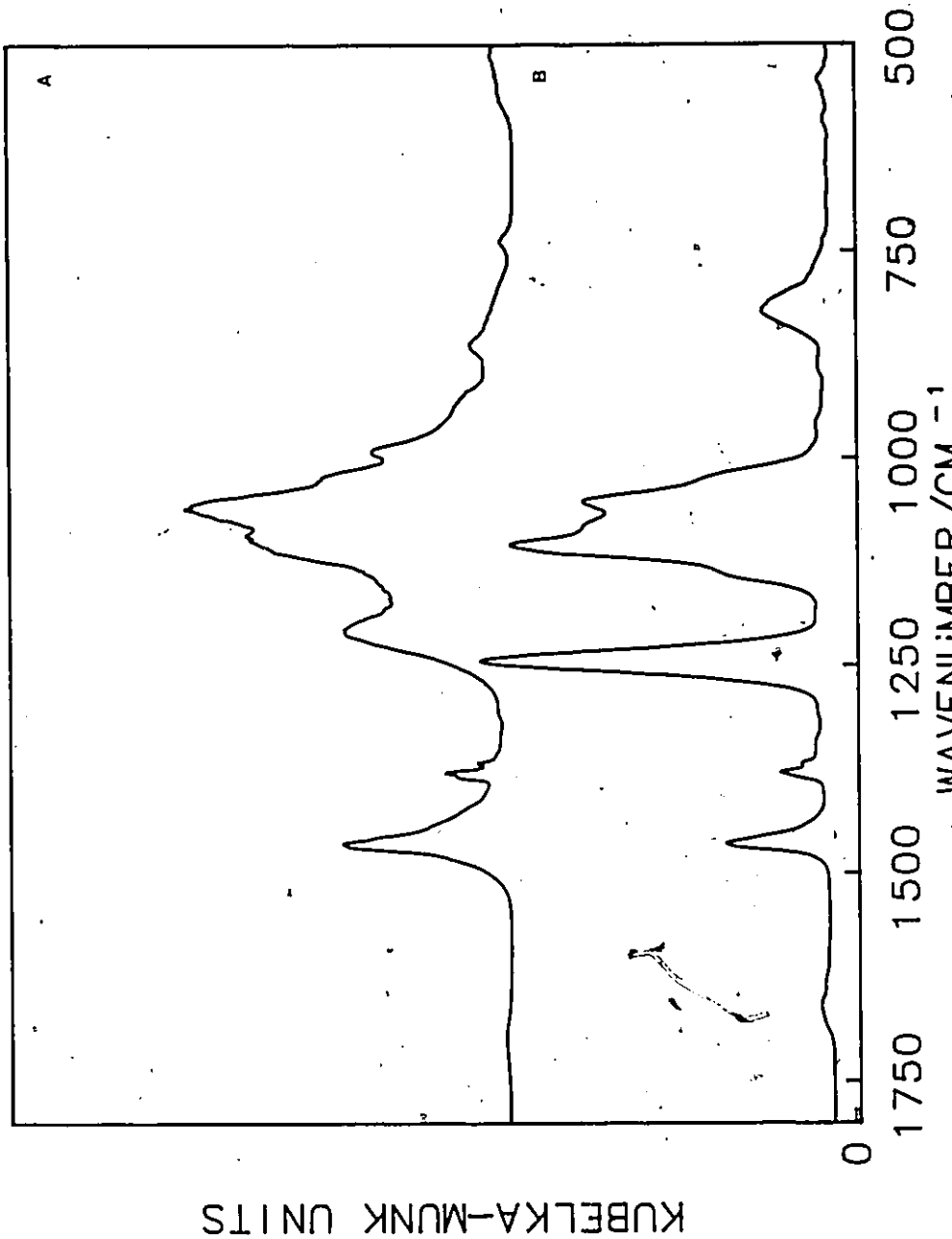
A
B
0
1750
1500
1250
1000
750
500
WAVENUMBER/CM $^{-1}$
KUBELKA-MUNK UNITS

Table III.18

Frequencies and tentative assignments

of PGP and deoxy analogues of PGP

compounds and FTIR frequencies (cm^{-1})				tentative assignments
proPG	dPG	dPGP	$PGP-K_2H$	
3200-2500	3200-2500	3200-2500	3240	C-OH
2316	2310	2341	-	P-OH in-plane deformation + $\nu_{as}\ P(OX)_2$
1711	1738	1695	1660	$\nu_{as}\ P(OX)_2$ + $P(OX)_2$ wagging
1233	1239	1209	1247	$\nu_{as}\ P(OX)_2$
1120	1113	1108	1104	$\nu_{s}\ P(OX)_2$ + P-O-C stretching
1025	1035	1055	1055	P-OH, P-O-C, C-O-C, $\nu_{s}\ P(OX)_2$
-	1012	1021	-	$\nu_{as} P(OX)_2$
-	967	994	-	P-OX stretching
-	-	-	824	ν_{as} O-P-O stretching
515	494	509	505	$P(OX)_2$ wagging

PGP-K_2H. The combinational band from the P-OH in-plane deformation and the ν_{as} $P(OX)_2$ modes is also seen for all deoxy compounds at 2316, 2310 and 2341 cm^{-1} (proPG, dPG and dPGP, respectively). This band and $P(OX)_2$ wagging (1660 cm^{-1} in PGP-K_2H), decreases in frequency from proPG to dPG and increases to dPGP (1711, 1738 and 1695 cm^{-1}, respectively).

Infrared bands from 1233 to 1247 cm^{-1} in the spectra of PGP, proPG and dPG, have been attributed to ν_{as} $P(OX)_2$ and is convoluted with the second ν_{as} $P(OX)_2$ stretching mode. In the spectrum of dPGP, this band shifts to a substantially lower wavenumber (1209 cm^{-1}). The magnitude of the shift is indicative of the formation of a hydrogen bonding involving the P-OH groups. The band at 1120 cm^{-1} in proPG is a combination of P-O-C stretching and ν_s $P(OX)_2$ modes and increases in intensity relative to the 1460 cm^{-1} scissoring mode and decreases in frequency (1113-1108 cm^{-1}) with increasing probability of hydrogen bonding (proPG < dPG < dPGP < PGP). The overlapping bands of the P-OH out-of-plane deformation, ν_{as} $P(OX)_2$ and C-O-C stretching modes, which appeared at 1025-1055 cm^{-1}, increase in intensity and frequency from proPG to dPG and dPGP. The $P(OX)_2$ symmetric mode decreases frequency from 1012 cm^{-1} for proPG to 1021 cm^{-1} for dPG. Similarly, the ν_{as} P-OX mode which is found at 987 cm^{-1} in dPG, shifts to 994 cm^{-1} for dPGP. The $P(OX)_2$ wagging mode (at 515 cm^{-1}) decreases slightly in intensity from proPG to dPG (494 cm^{-1}) and increases again for dPGP (509 cm^{-1}) and PGP (505 cm^{-1}).

The spectrum of dPGP also shows a broad band at 2341 cm^{-1},

approximately 22 cm^{-1} higher than previously observed in PA-H_2 and approximately 32 cm^{-1} less than that in PA-HK. It is clear from the presence of this band, together with the band at 1209 cm^{-1} band, that hydrogen-bonding involving the P-OH moiety of dPGP exists. This could arise from an intra- or intermolecular hydrogen bonded P-OH moeity and will be discussed in detail later.

4.3.3 Methylated PGP

The spectra of di-, tri- and tetramethylated PGP are shown in Figure III.34 and the tentative assignments are given in Table III.19. Again, the bands corresponding to the hydrocarbon bending and stretching modes are invariant with respect to frequency and intensity but significant changes are seen between methylated and non-methylated PGP.

The $P(OX)_2$ mode (1247 cm^{-1}) in PGP-K_2H is shifted to a higher frequency (1268, 1275 and 1288 cm^{-1} for di-, tri- and tetra-methylated compounds, respectively) and is narrower for all three methylated derivates due to decreased hydrogen bonding capabilities. The convoluted band at 1104 cm^{-1} (ν_{as} $P(OX)_2$ and C-O-C modes) for PGP-K_2H, decreased in intensity and shifted to slightly lower frequencies in the methylated compounds (1115-1109 cm^{-1}), again due to the decreasing hydrogen bonding capabilities. This type of shift is also seen in the ν_s $P(OX)_2$ band (1055 cm^{-1}) which narrows and decreases in frequency from PGP-K_2H (1055 cm^{-1}) to the methylated derivates (1045 cm^{-1}), and the

Figure III.34

FTIR spectra of methylated derivatives of PGP.

A. $PGP(CH_3)_2$

B. $PGP(CH_3)_3$

C. $PGP(CH_3)_4$

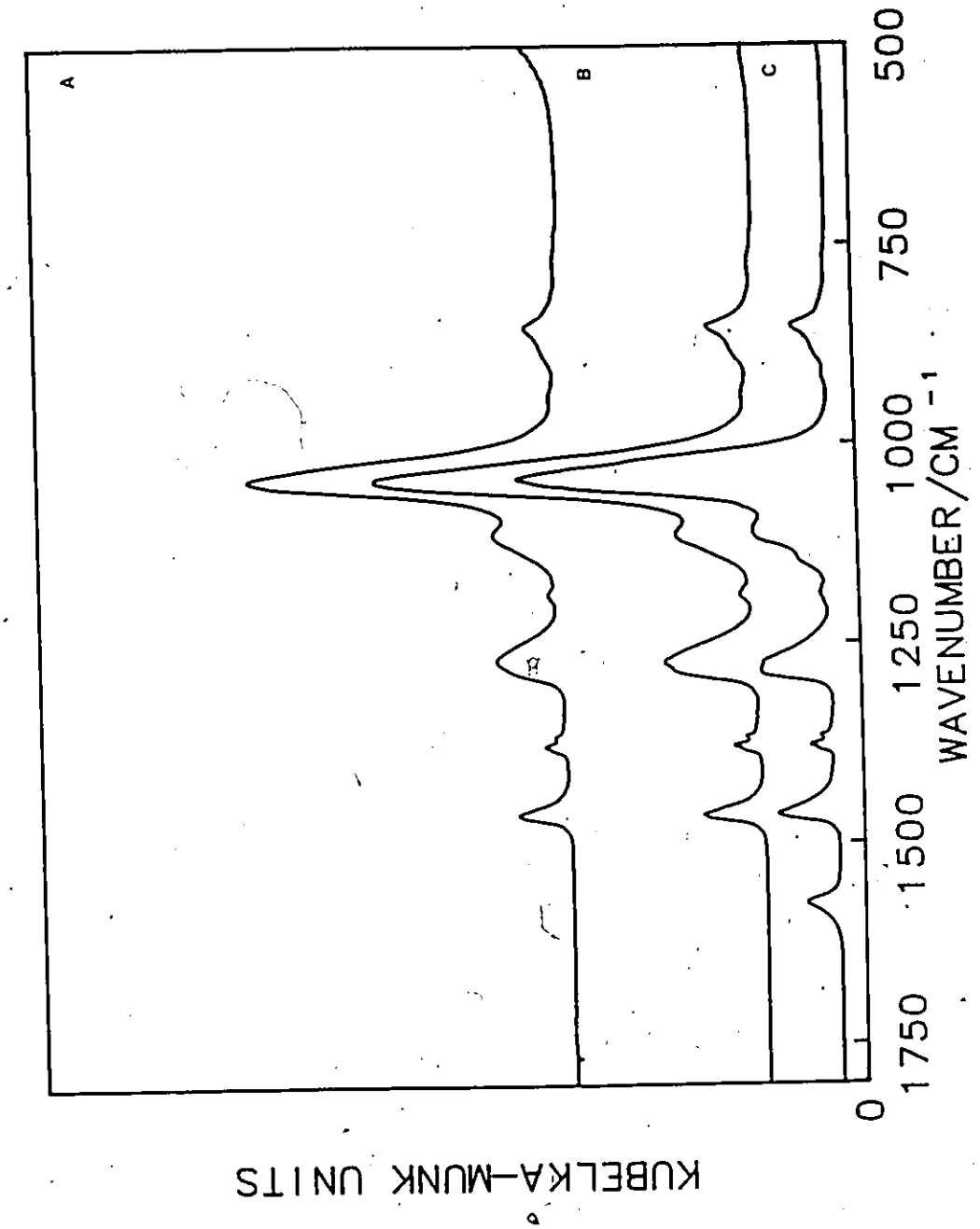
A
B
C
1750
1500
1250
1000
750
500
0
WAVENUMBER/CM⁻¹
KUBELKA-MUNK UNITS

Table III.19

Frequencies and tentative assignments for

PGP and methylated PGP derivatives

compounds and FTIR frequencies (cm^{-1})				tentative assignments
$PGP-K_2H$	$PGP-Me_2$	$PGP-Me_3$	$PGP-Me_4$	
3354	3374	3368	-	C-OH
1247	1268	1275	1288	ν_{as} $P(OX)_2$
1104	1115	1115	1109	ν_{as} $P(OX)_2$ + C-O-C
1055	1045	1045	1045	ν_{s} $P(OX)_2$
824	853	853	853	ν_{as} O-P-O stretching

ν_{as} O-P-O stretching band which narrows and shifts from 824 cm^{-1} for PGP to 853 cm^{-1} for the methylated derivatives.

The band at 1207 to 1286 cm^{-1} is usually assigned to ν_{as} PO_2^- (Thomas and Chillenden, 1964a, b; 1970; Kates et al., 1965; Goni and Arrondo, 1986). The fact that this band is present in PGP-H_3 as well as all three methylated derivatives argues against this assignment. Instead, this band has been assigned to ν_{as} $P(OX)_2$ where X=H or CH_3 (or K in the salt forms of PA and PGP) and can be seen to increase in frequency with increased methylation.

The C-OH band of PGP-K_2H (3354 cm^{-1}) increases in frequency for di- and trimethylated PGP (3374 and 3368 cm^{-1}) and is absent in tetramethylated PGP, as expected.

4.3.4 PGP and corresponding potassium salt forms

The spectrum of PGP-H_3 (Figure III.35, Table III.20) is similar to that of PA-H_2. The methyl deformation vibrational band (1380 cm^{-1}), methylene scissoring band (1460 cm^{-1}), methyl and methylene C-H vibrational stretching bands (2800-3000 cm^{-1}) and C-OH (3360 cm^{-1}) bands are present and virtually invariant with the degree of ionization.

The band at 2200-2300 cm^{-1}, previously attributed to intermolecular hydrogen bonding between the phosphate groups of two PA molecules (vide infra) is seen for PGP-H_3 but not PGP-K_2H or PGP-K_3. The ν_{as} $P(OX)_2$ mode at 1247 cm^{-1} sharpens markedly and increases in intensity with increasing degree of ionization but does not change in frequency. The second ν_{as} $P(OX)_2$ band (1117 cm^{-1} in PGP-H_3) also sharpens and shifts slightly in frequency (1104 cm^{-1}) with increasing degree of ionization. The

Figure III.35

FTIR spectra of PGP-H_3, -K_2H and K_3.

A. PGP-H_3

B. PGP-K_2H

C. PGP-K_3

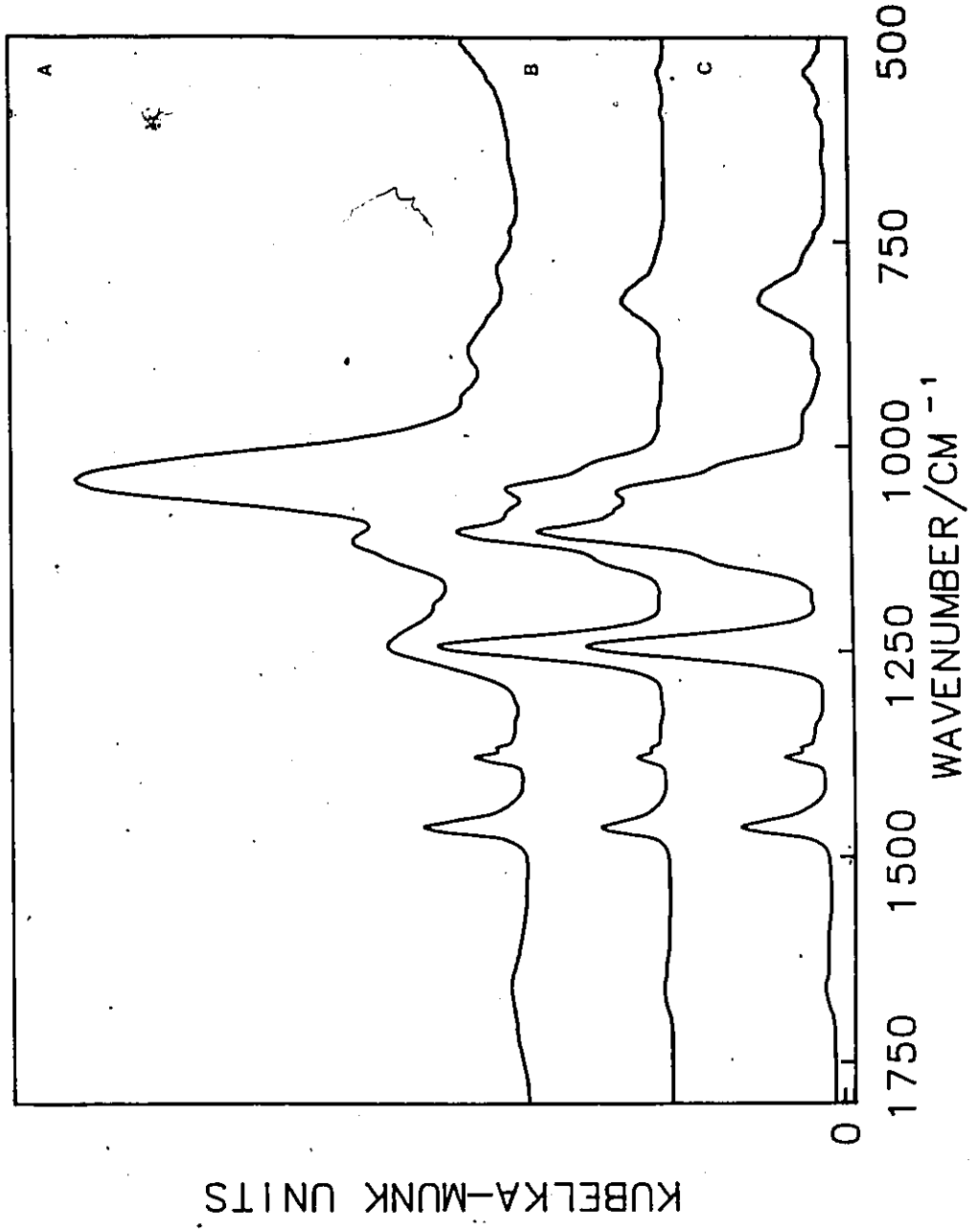
A
B
C
0
1750
1500
1250
1000
750
500
WAVENUMBER/CM⁻¹
KUBELKA-MUNK UNITS

Table III.20

Frequencies and tentative assignments for

PGP of varying degrees of ionization

compounds and FTIR frequencies			tentative assignments
$PGP-H_3$	$PGP-K_2H$	$PGP-K_3$	
3354	3240	3240	C-OH str. (broad)
2200-2300	-	-	hydrogen-bonded P-OH
1660	1660	1660	combinational overtone $\nu_{as}\ P(OX)_2$ + $P(OX)_2$ wagging
1247	1247	1247	$\nu_{as}\ P(OX)_2$
1117	1104	1104	$\nu_{as}\ P(OX)_2$
-	1080	1080	
1054	1053	1055	P-OH, P-O-C, C-O-C, $\nu_s\ P(OX)_2$
1042	-	-	
883	824	824	ν_{as} O-P-O stretching
-	510	540	$P(OX)_2$ wagging

shoulder at 1080 cm^{-1} and the strong band at 1053 to 1055 cm^{-1} in PGP-K_2H and PGP-K_3 are due to overlapping P-OH, P-O-C, C-O-C and $_s$ $P(OX)_2$ bands. In PGP-H_3, the 1054 cm^{-1} band is present but the 1080 cm^{-1} band is absent and is replaced by a band at 1042 cm^{-1}.

The ν_{as} O-P-O band (883 cm^{-1}), which is broad in PGP-H_3 due to both hydrogen bonding and molecular asymmetry (Sen et al., in press), sharpens, increases in intensity and red shifts to 824 cm^{-1} with increasing degree of ionization. The $P(OX)_2$ wagging mode is also seen for PGP-K_2H (510 cm^{-1}) and PGP-K_3 (540 cm^{-1}) but is absent in PGP-H_3 as expected.

In the solid spectrum of PGP-H_3, the broad band at 1247 cm^{-1}, together with the presence of the 2300 cm^{-1} band, is consistent with the formation of an eight-membered inter- and/or intramolecular ring between two phosphate moeities similar to the one proposed for PA:

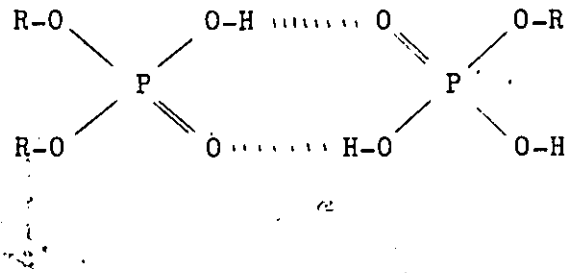

The absence of the 2300 cm^{-1} band in PGP-K_2H, PGP-K_3 and the methylated compounds indicates that this type of hydrogen bonding is not present in these compounds.

The intensity of the 2340 cm^{-1} band in dPGP-$(NH_4)_2$ and its absence in PGP-K_2, despite the presence of a P-OH in both

compounds, indicates that the presence of the free hydroxyl in the glycerol group of PGP prevents the strong intramolecular association between the phosphate groups. The C-OH stretching band is broad in all PGP samples but is shifted from 3354 cm^{-1} for PGP-H_3 to 3240 cm^{-1} for both PGP-K_2H and PGP-K_3 corresponding to free and hydrogen-bonded hydroxyl groups, respectively. This is consistent with the idea of hydrogen-bonding occurring between two phosphate groups in PGP-H_3, and is most likely to be intermolecular as there is no observable intensity at 2300 cm^{-1} in PGP-K_2H.

The band at 1660 cm^{-1} for PGP-H_3, -K_2H and -K_3 has been assigned to the combinational overtone of ν_{as} $P(OX)_2$ (1104-1117 cm^{-1}) and $P(OX)_2$ wagging (510-540 cm^{-1}). This is also the region in which water absorbs (H-O-H stretching; 1610 to 1790 cm^{-1}; Wong and Mantsch, in press) but this assignment has been ruled out for a number of reasons.

Firstly, the ratio of the intensities of the 3240-3400 cm^{-1} band (which contains contributions from CH-OH as well as water) and the 1660 cm^{-1} band is too low to assign the latter band to associated water. Secondly, the low frequency of the 3240 -3400 cm^{-1} band indicates that the moieties contributing to this absorbance are hydrogen-bonded. This is inconsistent with the assignment of the 1660 cm^{-1} band to water as the bandwidth is narrow, particularly for PGP-K_2H and -K_3 (approximately 50 cm^{-1}).

Thirdly, a 40 cm^{-1} decrease in the ν_{as} PO_2^- band of DPPC between anhydrous and completely hydrated samples has been reported (Wong and Mantsch, in press). A similar shift is seen

for PGP-K_2H which decreases from 1247 cm^{-1} to 1221 cm^{-1} (26 cm^{-1}) on hydration (see Table III.21).

The absence of a frequency shift in the υ_{as} $P(OX)_2/P(OX)_2$ wagging overtone from PGP-H_3 (1660 cm^{-1}), in which the P-OH groups are thought to be hydrogen bonded, to PGP-K_2H and -K_3 may indicate that the P-OH bands in these compounds are also hydrogen-bonded.

4.3.5 Inter- or Intramolecular Hydrogen bonding

In order to differentiate between inter- and intramolecular hydrogen bonding in dPGP and PGP, spectra from solids, solutions (in CCl_4 or $CHCl_3$) and aqueous dispersions were compared. The results of both solid and solution samples were then compared with results determined from aqueous dispersions of PGP to ascertain whether there were any gross conformational changes between solid and bilayer samples (See Table III.21).

In the DR-IR spectra of PA-K_2, the $P(OX)_2$ band was found at 1252 cm^{-1} and is not observable in either PA-K_2 or PA-KH because of the strong P-OH in-plane deformation mode. The frequency of this band indicates the presence of hydrogen bonding of the P-OH groups. In PA, this interaction must be intermolecular due to the absence of any other potential hydrogen bonding groups.

The frequency of the $P(OX)_2$ band in solid PGP (1247 cm^{-1}) was significantly higher than dPGP or PA, indicating the absence of strong hydrogen bonding in the solid (Wong and Mantsch, in press). The band did not shift in frequency for concentrated CCl_4 solutions (60 mg/ml) but did decrease to 1213 cm^{-1} for

Table III.21

Comparison of FTIR data for solid, solution and aqueous dispersions of diphytanylglycerol phospholipids

compound	FTIR frequency (cm^{-1})				
	solid	solution[a]		aqueous dispersions[b]	
		conc.	dilute	10°C	40°C
PA-K_2	1252				
dPGP-$(NH_4)_2H$	1209		1207		
PGP-K_2H, -$(NH_4)_2$	1247	1247	1213	1209	1212
	3240		3200		

a. Concentrated solutions were approximately 60 mg/ml; dilute solutions were approximately 5-10 mg/ml in CCl_4 or $CHCl_3$.

b. Aqueous dispersions were approximately 25 mg/ml.

dilute solutions (5-10 mg/ml). Again, the relatively low frequency of the $P(OX)_2$ band in dilute solutions is indicative of hydrogen bonding of the P-OH groups. This value was comparable to the values for aqueous solutions of PGP at 10°C (1209 cm^{-1}) and 40°C (1212 cm^{-1}). The virtual absence of a frequency change with increasing temperature (3 cm^{-1} over 30°C) (which would be expected to affect primarily intermolecular hydrogen bonds) implies that the headgroup structure of PGP in aqueous dispersions is stabilized primarily via the intramolecular hydrogen bonds, possibly with minor contributions from intermolecular bonding.

This is further supported by the results of the deoxy analogue. The frequency of the corresponding band in dPGP-$(NH_4)_2H$ was 1209 cm^{-1}, which is also indicative of strong P-OH hydrogen bonding. When dPGP was dissolved in CCl_4 at a concentration of 5-10 mg/ml, this band shifted to a slightly lower frequency (1207 cm^{-1}). The presence of this shift indicates that the interaction may have intermolecular contributions; however, the magnitude of the shift (2 cm^{-1}) indicates that intramolecular rather than intermolecular hydrogen bonding predominates. Therefore, steric hinderance introduced from the hydroxy group of the glycerol moiety in PGP prevents intramolecular hydrogen bonds from forming.

The proposed picture of inter- and intramolecular hydrogen bonding in PGP is consistent with the frequency shift seen in the headgroup CH-OH (from 3240 $^{-1}$ in the solid to 3200 cm^{-1} in CCl_4).

The CH-OH group could be hydrogen-bonded to water in the solid phase since elemental analysis shows the presence of one water of hydration per PGP molecule and it is unlikely that dissolving the PGP in CCl_4 would lead to a substantial increase in this interaction. However, the presence of a water molecule does not seem to be reflected in the DR-IR spectra. Thus, the hydrogen-bonded CH-OH band, together with the large frequency shift in the $P(OX)_2$ band, indicates stronger intramolecular hydrogen bonding between the P-OX and CH-OH bands of PGP in CCl_4 and aqueous dispersions than is present in the solids.

4.4 Summary

Evidence for intramolecular hydrogen bonding has been shown previously by FTIR in studies of n-acyl PE (Sen et al., in press).

The spectra of protonated or partially ionized PGP and analogues such as dPGP and PA exhibit bands characteristic of inter- and intramolecular hydrogen bonding involving the phosphate group(s).

The spectra of PA-H_2 and -KH show evidence of hydrogen bonded P-OH at 2500-3300 cm^{-1}, 1205-15 cm^{-1} (P-OH in plane deformation) and 2318-2372 cm^{-1} (overtone of P-OH in-plane deformation and P-O-C band). These bands are absent in the spectrum of PA-K_2 since there is no possibility for P-OH hydrogen bonding.

The $P(OX)_2$ band at 1243 cm^{-1} for proPG and dPG is shifted to a substantiallly lower wavenumber (1209 cm^{-1}) for dPGP, indicating the formation of stronger hydrogen bond involving the P-OH

groups. The similarity between the 1243 cm^{-1} bands in proPG and dPG probably indicate that the hydrogen bonding is intermolecular in both cases as no possibility exists in proPG for intramolecular interactions. The spectrum of dPGP also shows P-OH/P-O-C combinational overtones at 2341 cm^{-1} similar to that seen in PA-H_2 and -KH.

In the methylated compounds, the P-OH in-plane deformation band is shifted to a higher frequency and is narrower in comparison with PGP.

In PGP-H_3, the hydrogen bonded P-OH band is seen at 2300 cm^{-1} and the C-OH band is observed at 3240 cm^{-1}. The frequencies of these bands are indicative of the formation of hydrogen bonds. For solid PGP-K_2H samples, the hydrogen bonded C-OH, together with the presence of a band at 1660 cm^{-1}, the absence of the band at 2340 cm^{-1} (P-OH/P-O-C overtone) and the absence of a blue shift in the 1247 cm^{-1} band is consistent with the fact that the P-OH groups are hydrogen-bonded to the C-OH group of the headgroup rather than to other phosphate groups via the intermolecular interactions.

In comparison with the solid samples, CCl_4 solutions or aqueous dispersions of PGP show significant shifts in the frequency of both the CH-OH (3240 to 3200 cm^{-1}) and the $P(OX)_2$ band (1247 to 1213 cm^{-1} in CCl_4 and 1209 - 1212 cm^{-1} in aqueous dispersions). These frequency shifts from solid to solution or dispersion, and the weak temperature dependence of the $P(OX)_2$ band in aqueous systems, indicates the presence of strong intramolecular hydrogen bonding between the phosphate groups and

between the phosphate and CH-OH groups in aqueous dispersions of PGP-K_2H (Figure III.36).

The presence of both inter- and intramolecular hydrogen-bonding involving the P-OH and C-OH groups of the PGP headgroup is necessary for the formation of a proton-conductance pathway along the surface of the membrane. This pathway would facilitate the movement of protons from the PM, where they accumulate following light-induced proton translocation, to the red membrane, where they drive the ATPase-catalysed phosphorylation of ATP.

Figure III.36

Proposed structures for intramolecular hydrogen bonding in $PGP\text{-}K_2$ and $dPGP(NH_4)_2$

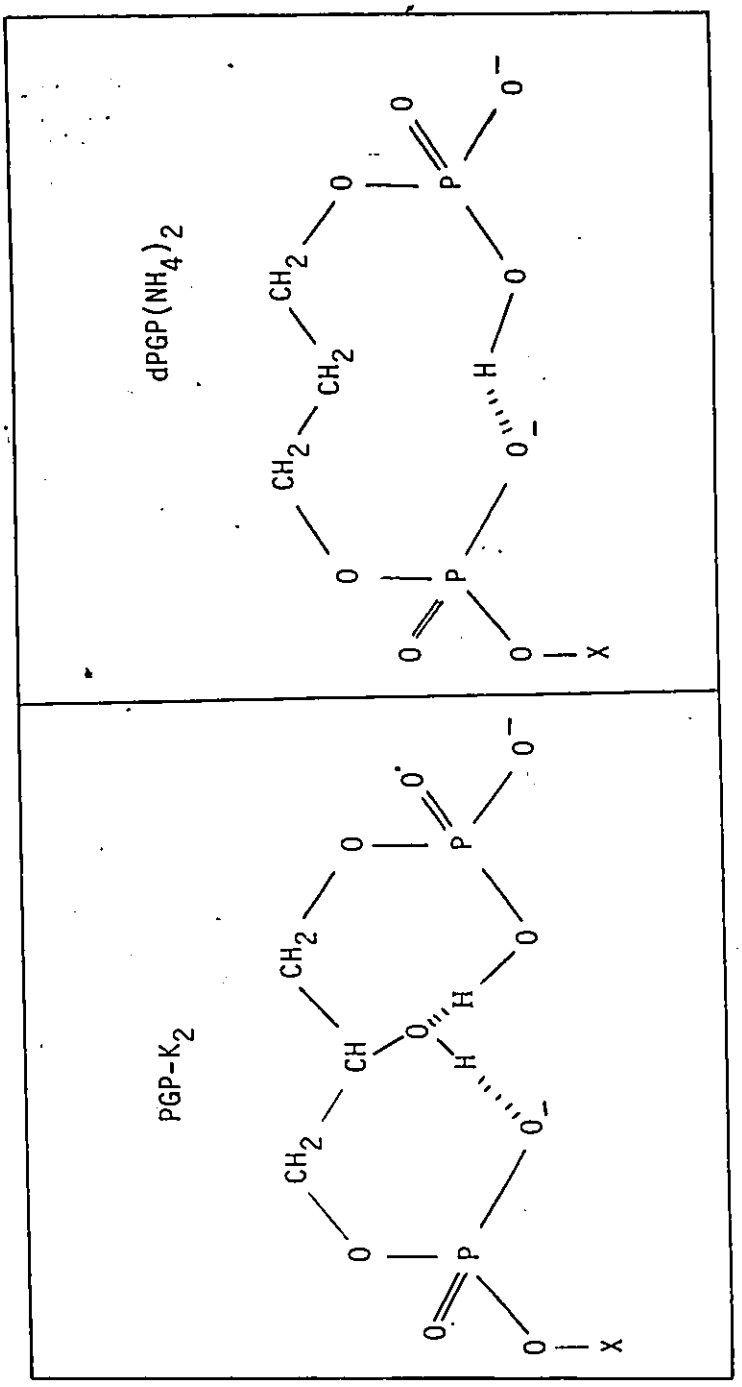
dPGP(NH4)2
PGP-K2

5. Potentiometric Titrations

5.1 Introduction

The major phospholipid of H. cutirubrum has been shown by degradative and analytical procedures (Kates et al., 1965) and synthesis (Joo et al., 1969) to be the diphytanylglycerol analogue of phosphatidylglycerol phosphate (PGP).

Previous potentiometric titrations of the free acid form of PGP in 1:1 methanol/water (Kates et al., 1965) indicated that the pK value for two of the three groups was 3.25 (2.0 eq/mole PGP) and the third was 7.95 (0.38 eq/mole PGP). However, the presence of three free phosphate groups was demonstrated unambiguously by the formation of a trimethyl derivative on treatment with diazomethane (Hancock and Kates, 1971). However, the salt of PGP isolated after titration of a chloroform solution of the free acid with NaOH or KOH to the phenolphthalein end point (pH 8-9) has a cation to phosphate ratio of 1:1 (Smallbone, 1981). Furthermore, high resolution and solid state ^{31}P NMR of aqueous sonicated and unsonicated samples showed neither the presence of a titratable group between pH 4 and 8.5 (see PART III, section 2) nor the presence of a cyclic phosphate group.

Therefore, potentiometric titration of PGP was repeated on methanol/water solutions as well as sonicated, aqueous dispersions. The deoxy analogue (sn-2,3-diphytanylglycerol-1'-(1,3-propane-diol)-3'-phosphate, dPGP) was also titrated (both in methanol/water and as sonicated, aqueous dispersions) and the results compared with PGP. The difference in pK_2 for PGP and dPGP was anticipated on the basis of different R_f values on TLC

run in chloroform/methanol/acetic acid (65:35:5) and chloroform/methanol/NH_4OH (65:35:5). The R_f values for PGP are 0.45 and 0.14 for acid and alkaline, respectively but 0.35 and 0.0 for dPGP. This behaviour is similar to that of PA which has an R_f value of 0.10 in the basic solvent but significantly higher in the acidic solvent (R_f= 0.6).

5.2 Experimental

PGP-K_2 was isolated and purified as described in section 2. dPGP was synthesized as described in PART II, section 7. Samples were sonicated in 0.1 N aqueous KCl for 45 minutes (20% power) at room temperature with a needle tip sonicator (Sonic Dismembrator, Quigley-Rochester Inc.) The samples were transparent over the period of the experiment, except for dPGP which became translucent at low pH values. Methanol/water solutions of PGP or dPGP were prepared by suspending PGP-H_3 in methanol and diluting with an equal volume of 0.1 N aqueous KCl.

Aliquots (containing 5- 10 mg) were titrated under a nitrogen atmosphere with either aqueous HCl or KOH (0.1 - 0.2 N) using a titration system accurate over the pH range of 2 - 12 (Radiometer, Copenhagen). Following the addition of acid or base, samples were equilibrated for 60 seconds prior to obtaining a pH reading.

Aliquots of the 0.1 N KCl solution were also titrated and the titration curves of the samples were corrected for the buffering of this solution. Both samples and solvent blanks were titrated

in duplicate.

5.3 Results and Discussion

The corrected titration curves for PGP and dPGP in sonicated aqueous dispersons and in methanol/water are shown in Figure III.37 and the values of the pK's are given in Table III.22.

In methanol/water, the lower pK values of PGP and dPGP (pK_1, accounting for two equivalents of acid) are the same within experimental error (3.5 and 3.6, respectively) and are comparable to those previously determined (Kates et al., 1965). The highest pK value for PGP (pK_2, > 11) is significantly higher than for the deoxy analogue (8.6) indicating an effect of the free headgroup hydroxyl.

In aqueous, sonicated dispersions of PGP the value of pK_2 of PGP (> 11) is again considerably higher than that of aqueous, sonicated dispersions of dPGP (8.85). The pK_1 of aqueous, sonicated dispersions of PGP (pK_1= 2.4) is slightly lower than that found for PGP dissolved in methanol/ water (pK_1= 3.5). This may be due, in part, to the high dielectric constant of water, in comparison with methanol/water, which would stabilize the charged form and lower the pK. The value of pK_1 of dPGP could not be accurately determined as the compound did not remain suspended at low pH values.

The pK values of sonicated dispersions of dPGP (pK_2=8.85) compare well with the values previously determined for PA (3-4 and 8-9) and PG (3-4) (Boggs, 1984). Boggs attributed the

Figure III.37

Potentiometric titration curves of PGP and dPGP in

A. methanol/water (1:1)

B. 0.1 M aqueous KCl.

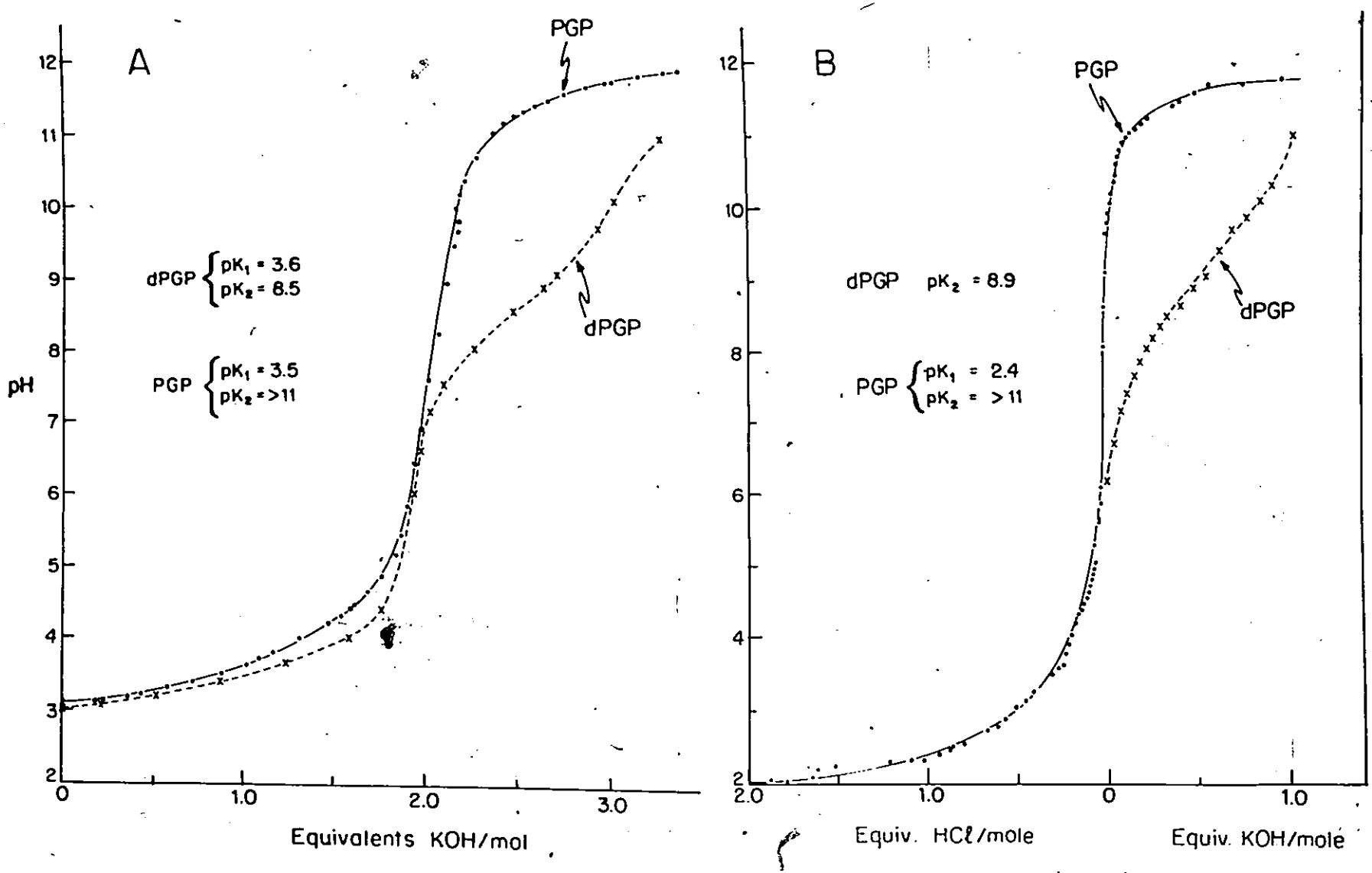
A
B
PGP
dPGP
dPGP $\begin{cases} pK_1 = 3.6 \\ pK_2 = 8.5 \end{cases}$
PGP $\begin{cases} pK_1 = 3.5 \\ pK_2 = >11 \end{cases}$
dPGP $pK_2 = 8.9$
PGP $\begin{cases} pK_1 = 2.4 \\ pK_2 = >11 \end{cases}$
pH
Equivalents KOH/mol
Equiv. HCℓ/mole
Equiv. KOH/mole

Table III.22

Comparison of pK values determined from potentiometric titrations of PGP and dPGP

Compound	solvent	pK_1	pK_2
PGP[a]	methanol/water	3.25	7.95
PGP[b]	methanol/water	3.5	>11
PGP[c]	water	2.4	>11
dPGP[b]	methanol/water	3.6	8.5
dPGP[c]	water	-	8.85
egg PA[d]	water	3.8	8.6
β-glycerophosphate[d]	water	3.1	6.6

a. Kates et al., 1965; methanol/water (1:1)
b. methanol/0.1 N aqueous KCl (1:1)
c. 0.1 N aqueous KCl
d. Abramson et al., 1964.

abnormally high pK value of the last ionizable group in bilayer lipids to charged-surface effects. The magnitude of the effect can be seen from the comparison of the pK values of β-glycerophosphate and sonicated vesicles of egg PA (Abramson et al., 1964). The pK_1 values of the compounds are similar: 3.1 for β-glycerophosphate and 3.8 for egg PA. However, the pK of the second group of the bilayer lipids is 2 pK units greater than that of the water soluble analogue (8.6 and 6.6, respectively). No difference is seen between the respective pK_2 values of PGP and dPGP in water and methanol/water. This may indicate that the lipids form micelles in the methanol/water mixture where charged-surface effects would still be evident.

However, the pK_2 value of PGP is substantially higher than that of either PA or dPGP. This increase may be attributed to the presence of hydrogen-bonding between one P-OH group of the phosphomonoester and either the P=O of the phosphodiester or the C-OH of the headgroup glycerol. Hydrogen-bonding would stabilize the protonated form, resulting in an increase in the pK value. Increases in the pK values of groups implicated in hydrogen-bonding structures have been reported previously in the field of protein biochemistry (Ghélis and Yon, 1982; Scheraga, 1963; Tanford and Wagner, 1954). For example, the formation of a hydrogen-bond between tyrosyl and glutamyl groups resulted in an increase in the pK of the tyrosyl group from 9.6 to 10.6; a difference of 1.0 pK unit. Thus, the increase in pK_2 of dPGP to PGP of over 1 pK unit is not unreasonabe.

Although comparison of the pK values of PGP with the deoxy analogue shows that the free hydroxyl group does affect the pK values, it is not possible to differentiate between these two possible hydrogen-bonded structures using this technique. The absence of the headgroup hydroxyl may simply result in a conformational change which prevents the close association of the phosphate groups rather than participating directly in the hydrogen-bonding. FTIR experiments (PART III, section V) shows evidence of inter- or intramolecular hydrogen-bonding involving the phosphate groups and the headgroup hydroxyl of PGP.

6. Osmometry

6.1 Introduction

Initial rates of osmotic swelling following the suspension of liposomes in hypertonic non-electrolyte solutions, such as urea, are indicative of the rates of penetration of solutes through the bilayer assuming that the permeability constant of the penetrating solute is much lower than that of water (Bangham, 1967). Liposomes suspended in hypertonic non-electrolyte solutions first shrink under osmotic forces then swell due to movement of the permeable solute (and water) across the bilayer. The initial rate of volume change is proportional to the light scattering measured by the absorbance at 450 nm ($1/A_{600}$) and is given by the following equation:

$$\frac{d(1/A_{600})}{dt} = \left(\frac{-1}{A_i^2}\right)\frac{dA}{dt}$$

where A_i is the initial absorbance value as shown in Figure III.38. It has been found experimentally that the initial decrease in the absorbance is linear with time as shown in Figure III.38.

Comparison of swelling rates for PC liposomes of varying chain lengths (dimyristoyl, distearoyl, stearoyldecanoyl and stearoylmyristoyl) (Bittman et al., 1981) showed that an increase in chain length considerably reduces the permeiability of solutes through the bilayer. A strong increase in the rate of solute penetration was also seen with increasing degree of unsaturation (stearoyloleoyl-, dioleoyl- and dilinoleoylPC) (Demel and De

Figure III.38

Changes in the light scattering of a lipid suspension following the addition of a hypertonic urea solution:

i. initial, constant value of 1/A;

ii. shrinking due to initial osmotic pressure; and,

iii. swelling due to influx of electrolytes (and water).

The line, X-Y, fitted to the initial, linear portion of the swelling curve is used to measure d(1/A)/dt.

The arrow indicates the time at which liposomes are added to the hypertonic nonelectrolyte solution.

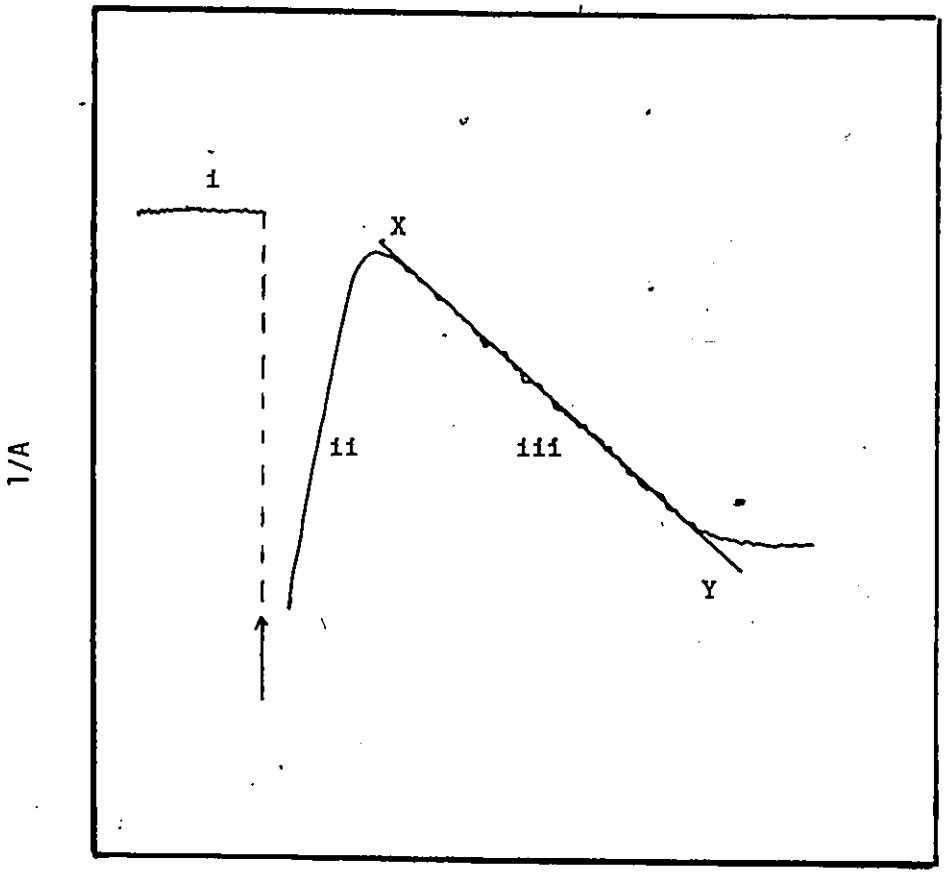
i
X
ii
iii
Y
1/A
time (min)

Kruyff, 1976). Demel and de Kruyff attributed decreased permeability to tighter packing and decreased mobility of the fatty acyl chains.

Furthermore, the presence of cholesterol causes a strong reduction in the rate of solute penetration (Bittman et al., 1981). Positive correlations have been demonstrated between the ability of sterols to modify the permeability behaviour of phospholipid bilayers and their ability to reduce the motional freedom of the fatty acyl chains (Demel and De Kruyff, 1976; Jain, 1975). These studies thus show that a high degree of permeability has been correlated with highly "fluid" bilayers as defined by T_c (short chains, high degree of unsaturation and low cholesterol content).

Osmometry has now been applied to the study of diphytanylglycerol lipids in order to provide information on the physical characteristics of the unusual hydrocarbon region. These studies supplement previous osmometric studies of liposomes prepared from diphytanylglycerol lipids (Chen et al. 1974) which measured the initial rates of swelling rather than steady-state values.

In the present studies, comparisons were made of the initial rates of osmotic swelling of liposomes of DPPC, DPPC/cholesterol mixtures and diphytanylglycerol lipids from H. cutirubrum. Studies with the polar lipids of H. cutirubrum, in which the composition of the hydrocarbon region is identical for all polar lipids, should provide information on the extent to which the hydrocarbon chains are influenced by the packing of the head-

groups. In addition, the polar lipids were studied in the presence and absence of varying concentrations of neutral lipids, comprised primarily of squalenes and bacterioruberins, to determine the influence of the neutral lipids on the packing of the hydrocarbon region.

6.2 Materials and Methods

All swelling experiments were done in collaboration with Dr. R. Bittman, University of New York, Flushing, New York.

Liposomes were prepared from both individual and total polar lipids of H. cutirubrum in the presence and absence of neutral lipids, as well as from DPPC and DPPC/cholesterol (25 mol% cholesterol). Lipids were suspended, with vortexing, in buffer (5 mM Na_2HPO_4 and 60 mM KCl pH 7.4) to a final concentration of 1.0-1.5 mM. Liposomes (0.5 ml) were added rapidly to urea (2.5 ml, 400 mM in buffer). Experiments were performed at 25°C for diphytanylglycerol lipids and 47°C for DPPC and DPPC/cholesterol mixtures. The initial rate of osmotic swelling of the liposomes (after the initial osmotic shrinking), caused by the influx of solute and water, was deterimined by spectrophotometric analysis of light scattering (Perkin-Elmer Model 320) at 600 nm and is proportional to d(1/A)/dt. As described in the introduction, this rate of change of absorbance is calculated from the product of d(A)/dt and $-1/A^2_i$, where dA/dt is the inital rate of absorbance change due to the swelling of the liposomes and A_i is the initial absorbance.

Table III.23

Osmometry studies of liposomes of diphytanylglycerol lipids [a] in urea solution

Sample	d(1/A)/dt ($x10^3$) (sec^{-1})	
PGP	61.0 ± 2.4	(n=8)
PGP + neutral lipids (w/w)		
90:10	78.0 ± 4.0	(n=5)
80:20	127.0 ± 6.0	(n=4)
PGP/GLS (1:1, w/w)	11.9 ± 0.6	(n=7)
PGP/GLS (1:1, w/w) + neutral lipids (w/w)		
90:10	43.0 ± 3.0	(n=5)
80:20	75.0 ± 5.0	(n=6)
TPL	98.2 ± 7.4	(n=5)
DPPC [b]	94.8 ± 6.2	(n=6)
DPPC/cholesterol (3:1 mol/mol)[b]	28.8 ± 1.6	(n=5)

a. 25°C.

b. 47°C. DPPC and DPPC/cholesterol liposomes contained 4 mol% dicetyl phosphate.

6.3 Results and Discussion

The results of the osmotic experiments are summarized in Table III.23.

All samples examined (PG, PGS, PGP and GLS, alone or in mixtures) formed closed bilayers in 60 mM KCl as indicated by the appreciable rate of swelling in 0.4 M urea. This is in contrast to previous studies in which PGP was reported to form closed bilayers only in the presence of GLS (Chen et al., 1974).

The initial swelling rate for PGP [$(61.0 \pm 2.4 \times 10^{-3}$ sec$^{-1})$] is significantly higher than that for a mixture of PGP and GLS [$(11.9 \pm 0.6 \times 10^{-3}$ sec$^{-1})$], indicating that the presence of the sulfated glycolipid leads to substantial decrease in the PGP bilayer permeability. This is particularly interesting in view of X-ray diffraction studies of ferritin/avidin/biotin-labelled PM (Henderson et al., 1978) which showed that the glycolipid is found exclusively on the outer membrane leaflet. Calculations using the compositional data given in Table 1 show that the outer leaflet is 56 mol% glycolipid and 44 mol% PGP while the inner leaflet is almost exclusively PGP. (The other phospholipids, PGP and PGS, are presumably oriented in a manner similiar to that of PGP.)

The addition of 10 or 20% (w/w) neutral lipids (comprised predominantly of mono-, di- and tetrahydrosqualene (73 mol%) with smaller amounts of C_{50} bacterioruberins (16 mol%) and vitamin MK-8 (8 mol%)) to PGP liposomes leads to a marked increase in the swelling rate [$(78.0 \pm 4.0) \times 10^{-3}$ and $(127.0 \pm 6.0) \times 10^{-3}$ sec^{-1})]. The same trend is seen for PGP/GLS liposomes although the

this is unlikely, since the neutral lipids would have to be present in concentrations greater than 20% to account for the observed values.

The permeability value for PGP has been compared with the values from the corresponding n-acyl phospholipid. The value for PGP [$(61 \pm 2.4) \times 10^{-3}$ sec^{-1}] is substantially lower than that for DPPC [$(94.8 \pm 6.2) \times 10^{-3}$ sec^{-1}], indicating a marked effect of the branch methyl groups and/or the anionic headgroups on the bilayer permeability characteristics. This difference is particularly significant in view of the different reduced temperatures at which the lipids were studied. Ideally, comparison of the values derived from diphytanylglycerol lipids and n-acyl lipids should be done at the same reduced temperature, θ, defined by $\theta = (T - T_c)/T_c$ (Seelig and Browning, 1978); however, there is no detectable phase transition temperature for diphytanylglycerol lipids in the temperature range -120 to 120°C (Chen et al., 1974; Jackson and Sturtevant, 1978; Hiraki et al., 1981, Ekiel et al., 1981). However, the transition, if present, is expected to be low as shown by studies of lipids containing iso- and anteiso-branch methyl groups where there is a reduction in the phase transition temperature of 16-23°C, in comparison with the corresponding straight chain lipids (Keough and Davis, 1984). Thus, the temperature at which the diphytanylglycerol lipids were studied (25°C) is considerably higher than the putative gel to liquid-crystalline phase transition temperature whereas the n-acyl lipids were studied at only 3-6°C above the phase transition temperature, T_c= 41-44°C. Based on DSC studies, the branched chain lipids should therefore be in a more fluid

values are lower overall than for PGP liposomes [(PGP/GLS, (12.0 ± 1.0) x 10^{-3} sec^{-1}; plus 10% neutral lipids, (43.0 ± 3.0) x 10^{-3} sec^{-1}; plus 20% neutral lipids, (75.0 ± 5.0) x 10^{-3} sec^{-1})].

These results are consistent with previous fluorescence studies of total lipids and TPL of H. cutirubrum (Lanyi et al., 1974) which indicated a higher value for the rotation relaxation time of perylene in TPL (4.5 ns) than in total lipids (0.9 ns). In addition, studies of 8-anilinonaphthalenesulphonic acid in vesicles prepared from either total lipids or TPL suggest that the presence of the neutral lipids allow for the penetration of more water molecules into the hydrophobic region of the bilayer. Lanyi attributes these effects to the fact that although the neutral lipids are assumed to span the bilayer, the length of a bacterioruberin molecule (28 Å) is shorter than that of a bilayer comprised of the diphytanylglycerol polar lipids (38 Å). This difference may result in local perturbations as the bilayer accomodates the neutral lipids.

The value for TPL, which is essentially a binary mixture of PGP and GLS (3:1, mol/mol), then seems anomalously high [(98.2 ± 7.4) x 10^{-3} sec^{-1})]. Although the presence of PG, PGS and other minor components could be responsible for the high swelling rates, this is not likely because of their low concentrations (see Table 1). According to Table III.23, the presence of neutral lipids leads to an increase in the rates of swelling of the lipid bilayers. It is also possible that the presence of trace neutral lipid impurities in the polar lipid sample might be responsible for erroneously high permeability values; however,

state than the corresponding straight chain lipids. This contrasts markedly with osmometric data which indicate that the bilayers comprised of diphytanylglycerol phospholipids are less permeable than those of n-acyl phospholipids.

Because the swelling experiments were done at 47°C for n-acyl lipids which is well above the gel to liquid-crystalline phase transition temperatures (T_c) for DPPC (T_c=41-43°C), the addition of cholesterol to DPPC would be expected to have an ordering effect on the phospholipid chains (Dufourc et al., 1987), thereby reducing the degree of water penetration. This is reflected in a decrease in the initial rates of shrinking of DPPC in the presence of cholesterol [$(94.8 \pm 6.2) \times 10^{-3}$ sec^{-1} for DPPC; $(28.8 \pm 1.6) \times 10^{-3}$ sec^{-1} for DPPC/cholesterol) (See Table III.23).

The permeability value of PGP bilayers to urea is therefore comparable to that of DPPC/bilayers containing approximately 10-15% cholesterol. (This is an approximate value only, extrapolated from data in Table III.23, assuming a linear relationship between permeability and cholesterol content).

6.4 Summary

As discussed above, solute permeability through lipid bilayers has been attributed to the formation of transient defects in the hydrocarbon region due to the formation of gauche-trans isomers and has been correlated with a high degree of permeability has been correlated with highly "fluid" bilayers as defined by T_c.

were measured at only 3-6°C above the T_c.

Thus, the combination of branch methyl groups and polar heads capable of stabilizing the membrane through intermolecular hydrogen-bonding results in the formation of a lipid bilayer which is relatively non-permeable to urea.

These results contrast with ^2H NMR studies of synthetically and biosynthetically labelled diphytanylglycerol phospholipids (see PART III, section 1) which indicate that the diphytanylglycerol phospholipids are more disordered than DPPC, although the rates of motions are much lower. This implies that it is the rates of motions of the hydrocarbon chains rather than the extents of motions which determine the bilayer permeability (see General Discussion).

The cause of the apparent discrepancy between the swelling values for the total polar lipids and mixtures of PGP and GLS is unknown and additional studies are underway.

PART IV

General Discussion

The aim of this project was to apply the physical techniques of NMR and FTIR to the study of diphytanylglycerol phospholipids in order to obtain information on their molecular conformation and dynamics. A combination of techniques was necessitated by the ability of each of the techniques to probe limited regions within the phospholipid molecule. ^{31}P NMR and FTIR have been used to study the headgroup region and ^{2}H NMR the hydrocarbon regions. The use of both chain and headgroup analogues aided in the interpretation of the data and allowed for comparison with previously published data for other lipid types.

"Fluidity"

A major problem with interdisciplinary fields such as biophysics is correlating a physical concept, such as ^{2}H NMR order parameters or spin-lattice relaxation times, with biologically relevant molecular characteristics such as conformation and dynamics. The temperature dependence of T_1, for example, provides a measure of τ_c^{-1}, the frequency of motion which contributes most efficiently to the relaxation of the spin system following excitation. Physically and mathematically, the parameter is well defined. In molecular terms, the value of the frequency of molecular motion may provide an indication of the

type of motion or motions which the molecule is undergoing; axial rotation, additional motion of the headgroup about the axis of rotation etc. However, because this technique monitors molecular motion only in a limited frequency window, the type of motion measured may not be the predominant motion nor the most important to the membrane's functions.

Another difficulty with data interpretation is extrapolating from molecular characteristics, such as order and dynamics, to concepts such as "fluidity" which are commonly used to describe membrane characteristics. This is due, in part, to the fact that terms such as fluidity, although commonly used, are not well defined for complex systems. In isotropic systmes, fluidity is defined as the tendency of a solution to flow (i.e., the reciprocal of the viscosity). In non-isotropic systems such as membranes, fluidity is predominantly a property , or the sum of a number of properties, of the hydrocarbon chains and is measured, and therefore operationally defined, by many different techniques including ESR, NMR, fluorescence, DSC, laser photobleaching and osmometry. Clearly, a correlation exists between these different parameters but the correlation is complex as the techniques provide information on different regions within the molecule and on different time scales.

The apparent lack of correlation between the results of different physico-biochemical studies is seen in the comparison of DSC data with the results of osmometric studies (see Table 23) and ^{2}H NMR studies (see Table III.6) of diphytanylglycerol-

lipids. Osmometry, which measures the rate of trans-membrane diffusion of an electrolyte via transient defects within the hydrocarbon region of bilayers, has been correlated with membrane fluidity in the conventional sense of low T_c (Keough and Davis, 1984). However, osmometry indicates that the bilayers composed of diphytanylglycerol phospholipids are relatively impermeable to solutes [$(61.0 \pm 2.4) \times 10^{-3}$ sec-1], comparable to DPPC bilayers containing significant amounts of cholesterol [DPPC, $(94.9 \pm 6.2) \times 10^{-3}$ sec^{-1}, DPPC/cholesterol, 3:1, $(28.8 \pm 1.6) \times 10^{-3}$ sec^{-1}]. Although ^2H NMR has shown that the degree of order of these two systems (diphytanylglycerol phospholipids and DPPC/cholesterol) is markedly different, the dynamics are similar as the temperature dependence of the spin-lattice relaxation times for both labelled phytanyl chains and cholesterol show a minimum above 0°C (see Figures III.15 and III.16).

Therefore, the molecular dynamics, rather than solely the molecular order, must play a role in determination of the bilayer permeability characteristics.

The phase transition temperature has traditionally been used as an indicator of the fluidity of lipid bilayers (Boggs, 1984; Keough and Davis, 1984) and the fluidity is thought to increase (as reflected by a decrease in T_c) with decreasing chain length and/or increasing degree of unsaturation. The phase transition temperature of isobranched and anteisobranched lipids is lowered by 13 and 23°C, respectively, from the corresponding n-acyl lipids (DPPC, T_c= 41°C) (Keough and Davis, 1984) In contrast,

diphytanylglycerol phospholipids, which presumably have a low phase transition temperature due to the presence of multiple branch methyl groups, have been shown by ^2H NMR to be more disordered (D_q <24 kHz for all labelled positions) (see Table III.6) and to undergo lower frequency motion ($\tilde{\tau}_c = 3.5 \times 10^{-9}$ sec) (see Figure III.15) than n-alkyl or n-acyl lipids.

These results may be rationalized by comparison of DSC and ^2H NMR data from saturated and unsaturated lipids. Comparison of the ^2H NMR molecular order parameter profiles for the saturated systems (DPPC, T_c= 41-44°C) with the more "fluid" cis-unsaturated system (DOPC, T_c= -9°C) shows that the degree of molecular order actually increases slightly for unsaturated lipids at the position of the double bond, but there is a decrease in the rates of motions in this region as measured by T_1's. These results are consistent with the hypothesis that fluidity is determined by a combination of both molecular order and dynamics.

Structure-Function Relationship in Diphytanylglycerol Lipids

Once the molecular and macromolecular characteristics of the diphytanylglycerol lipid bilayers have been determined, the question still remains as to the relationship between the structure and dynamics of the lipids and their function in the membranes of Archaebacteria such as H. cutirubrum. Perhaps a clue to the structure-function relationship lies in the similarity between the characteristics of the diphytanylglycerol lipids and of cholesterol in cholesterol-phospholipid mixtures (Dufourc and Smith, 1986).

One similarity is that the frequencies of motions which the molecules undergo is significantly lower than for the n-acyl lipids alone . Both TPL labelled in the phytanyl chains and [2,2,3,4,4,6-$^2H_6$]cholesterol exhibit a minimum in the temperature dependence of the spin-lattice relaxation times at 46.5 MHz, corresponding to effective correlation times of 3.5×10^{-9} sec (see Figure III.15 and III.16)

In comparison, the temperature dependence of the T_1 for n-acyl lipids is linear indicating that the frequency of motion is much higher (approximately 10^{-10} to 10^{-11} sec). In addition, the T_1 values for the first labelled position of n-acyl chains ([2,2-$^2H_2$]DPPC, 15.14 - 18.61 ms) or n-alkyl chains (18.14 - 20.93 ms) are significantly higher than those of the first labelled position of phytanyl chains ([1,1-$^2H_2$]DPhPA, T_1=6.06 ms) or the biosynthetically labelled positions (5-18 ms).

Another similarity between membranes high in cholesterol and membranes or liposomes comprised of phytanyl lipids is the absence of a detectable phase transition in either system (Keough and Davis, 1984; Jackson and Sturtevant, 1978; Ekiel et al., unpublished). For the cholesterol-phospholipid system, it has been suggested (Dufourc and Smith, 1986) that the role of cholesterol is to maintain the membrane in a liquid-crystalline state in response to external perturbations such as temperature and pressure gradients. Because the motion of the cholesterol molecule is relatively temperature-independent, it increases the motion of the acyl chains below the T_c and restricts it above the T_c, therefore eliminating the abrupt gel to liquid-crystalline phase transition.

The role of the branched chains lipids may be similar to that of cholesterol in mammalian membranes. The cell membrane of the H. cutirubrum contains a relatively high percentage of neutral lipids (12% w/w) but this is predominantly squalene (9%) and bacterioruberins (3%) and no cholesterol or cholesterol analogues. In addition, the cell membranes of the Archaebacteria are characteristically exposed to harsh environmental conditions including high salinity (Halobacteria), extremes of pH and/or temperature (Thermoacidophiles and Alkalinophiles) and high pressures (Woese and Wolfe, 1985). Thus, the role of the branched chain lipids may be to maintain the membrane in the liquid crystalline state in response to external perturbations in a manner similar to cholesterol.

Headgroup stability

^{31}P NMR of PGP indicates no change in the value of the residual chemical shift anisotropy of either phosphate group of PGP in response to pH (in the physiological range of 7 ± 2 pH units) (see Figures III.20-22; Tables III.10-13), the nature of the counterion (see Figure III.23; Table III.14) or the presence of other polar lipids (see Figure III.24; Table III.15). Because the residual chemical shift anisotropy is indicative of both the amplitudes of motions and the orientation of the phosphorus tensor with respect to the the magnetic field, it is a sensitive indicator of the state of the phosphate headgroup. The absence of a change in the CSA of either sub-spectrum in response to these perturbations indicates the absence of a significant

change in the motions or orientations of the headgroup.

Despite the difference in the size of the phospho- and glycolipid headgroups (see Figure III.28) and the high concentration of glycolipid in the membrane, the conformation and dynamics of PGP is virtually unaffected by the presence of the glycolipid. This has been shown by the comparison of the quadrupole splittings of biosynthetically deuterated PGP and TPL (see Table III.8), comparison of the axis of motional averaging of oriented TPL (see Figures III.26 and III.27; Table III.16) and by comparison of ^{31}P NMR CSA values of PGP, PGP/GLS and TPL (see Figure III.24; Table III.15). These techniques, which report on both the hydrophobic and headgroup regions have shown that pure PGP and PGP/GLS mixtures are virtually indistinguishable with respect to conformation and dynamics.

The apparent insensitivity of PGP to the presence of high concentrations of glycolipids may be due to the inherent headgroup conformational stability provided by the presence of intramolecular hydrogen bonds as has been suggested by FTIR studies of natural diphytanylglycerol phospholipids and headgroup analogues (see PART III, section 4). Both ^{31}P NMR titrations (Table III.13) and potentiometric titrations (Table III.22) have confirmed that PGP is in the diionized form over a large pH range (4.5 to > 11). This may be important in the maintenance of structural integrity of the membranes in response to the large pH gradient produced on light-induced proton translocation (3.5 pH units, Kouyama et al., 1987).

It therefore appears that the structure of both the phosphate headgroup and the phytanyl chains of the major polar lipids of H.

cutirubrum have been selected in such a way as to produce a membrane which is remarkably stable to external perturbations such as temperature, pH and pressure encountered in the natural environment of the Archaebacteria such as the halophiles.

References

Abramson, M.B., Katzman, R., Wilson, C.E., Gregor, H.P. (1964) Ionic properties of aqueous dispersion of phosphatidic acid, J.Biol Chem. 239, 4066.

Aneja, R., Chadha, J.S., Davies, A.P. (1970) A general synthesis of glycerophospholipids, Biochim. Biphys. Acta 218, 102-111.

Aneja, R., Chadha, J.S. (1971) A total synthesis of phosphatidylcholine, Biochim. Biphys. Acta 248, 455-7.

Ansell, G.B., Hawthorne, J.N. (1973) Form and Function of Phospholipids, Elsevier Press, Amsterdam.

Bangham, A.D., de Grier, J., Greville, G.D. (1967) Osmotic properties and water permeability of phospholipid liquid crystals, Chem. Phys. Lipids 1, 225-46.

Bittman, R., Leventhal, A.M., Karp, S., Blau, L., Tremblay, P.A., Kates, M. (1981) Osmotic behavior of liposomes of PS and PSC as a function of lipid concentration,

Blaurock, A.E. (1975) Bacteriorhodpsin: A trans-membrane pump containing α-helix., J. Mol. Biol. 93, 139-158.

Blaurock, A.E., Stoeckenius, W. (1971) Structure of the purple membrane, Nature (London) New Biol. 233, 152-154.

Bligh, E.G., Dyer, W.J. (1959) A rapid method of total lipid extraction and purification, Can. J. Biochem. Phys. 37, 911-7.

Boggs, J.M. (1984) Intermolecular hydrogen bonding between membrane lipids, in "Membrane Fluidity" (Kates, M., and Manson, L.A., eds), pp 3-53, Plenum Pub. Co., N.Y.

Brown, M.F. (1982) Theory of spin-lattice relaxation in lipid bilayers and biological membranes. ^{2}H and ^{14}N quadrupolar relaxation, J. Chem. Phys 77, 1576-99.

Brown, M.F., Seelig, J., Haeberlen, U. (1979) Structural dynamics in phospholipid bilayers from deuterium spin-lattice relaxation time measurements, J. Chem. Phys. 70, 5034-53.

Brown, M.F., Ribeiro, A.A., Williams, G.D. (1983) New view of lipid bilayer dynamics from ^{2}H and ^{13}C NMR relaxation time measurements, Proc. Nat. Acad. Sci. USA 80, 4325-9.

Bruno, S., Cannistraro, S., Gliozzi, A., De Rosa, M., Gambacorta, A. (1985) A spin label ESR and saturation transfer ESR study of archaebacteria bipolar lipids, Eur. Biophys. J. 13, 67-76.

Buldt, G., Seelig, J. (1980) Conformation of PE in the gel phase as seen by neutron diffraction, Biochemistry 19, 6170-5.

Buldt, G., Gally, H.U., Seelig, A., Seelig, J., Zaccai, G. (1978) Neutron diffraction studies on selectively deuterated phospholipid bilayers, Nature (London) 271, 182-7.

Butler, K., Smith I.C.P., ESR studies PM and liposomes prepared from purple membrane lipids, unpublished.

Cevc, G., Watts, A., Marsh, D. (1981) Titration of the phase transition of phosphatidylserine bilayer membranes. Effects of pH, surface electrostatics, ion binding and head-group hydration, Biochemistry 20, 4955-65.

Chaudhary, S.K., Hernandez, O. (1979) A simplified procedure for the preparation of triphenylmethyl ethers, Tetr. Lettr 2, 95-8.

Chen, J.S., Barton, P.G., Brown, D., Kates, M. (1974) Osmometric and microscopic studies on bilayers of polar lipids from the extreme halophile, H. cutirubrum, Biochim. Biophys. Acta 352, 202-17.

Chignell, C.F., Chignell, D.A. (1975) A spin label study of purple membrane from H. halobium, Biochem. Biophys Res. Comm. 62, 136-143.

Davis, J. (1983) The description of membrane lipid conformation, order and dynamics of ^{2}H- NMR, Biochim. Biophys. Acta 737, 117-171.

Degani, H., Danon, A., Caplan, S.R. (1980) Proton and C-13 NMR studies of the polar lipids of H. halobium, biochem. 19, 1626-31.

Demel, R.A., De Kruyff, B. (1976) The function of sterols in membranes, Biochim. Biophys. Acta 457, 109-32.

Dluhy, R., Cameron, D.G., Mantsch, H.H., FTIR studies of intermolecular hydrogen-bonding in carboxylic acid, unpublished.

Dufourc, E.J., Parish, E.J., Chitrakorn, S., Smith, I.C.P. (1984) Structural and dynamical details of cholesterol-lipid interaction as revealed by deuterium NMR, Biochemistry 23, 6062-71.

Dufourc, E.J., Smith, I.C.P. (1986) A detailed analysis of the motions of cholesterol in biological membranes by ^{2}H NMR relaxation, Chem. Phys. Lipids 41, 125-135.

Ekiel, I.H., Marsh, D., Smallbone, D.W., Kates, M., Smith, I.C.P. (1981) The state of the lipids in the purple membrane of H. cutirubrum as seen by 31-P NMR, Biochem. Biophys. Res. Comm 100, 105-110.

Ekiel, I.H., Sprott, D., Smith, I.C.P. (1986) Mevalonic Acid is partially synthesized from amino acids in H. cutirubrum. A ^{13}C NMR study, J. Bact. 166, 1-5.

Ekiel, I.H., Moire, D., Smith, I.C.P., ^{2}H NMR studies of biosynthetically deuterated diphytanylglycerol lipids, unpublished.

Engle, A.K., Cowburn, D. (1981) The origin of multiple quadrupolar couplings in the deuterium NMR spectra of the 2 chain of 1,2-dipalmitoyl-sn-glycero-3-phosphatidylcholine, FEBS Lett. 126, 169-70.

Esser, A.F., Lanyi, J.K. (1973) Structure of the lipid phase in cell envelope vesicles from H. cutirubrum, Biochemistry 12, 1933-9.

Farrar, T.L., Becher, E.D. (1976) Pulse and Fourier transform NMR techniques: a practical approach, Elsevier, Amsterdam.

Fox, G.E., Stackebrandt, E., Hespell, R.B., Gibson, J., Maniloff, J., Dyer, T.A., Wolfe, R.S., Balch, W.E., Tanner, R.S., Magrum, L.J., Zablen, L.B., Blackemore, R., Gupta, R., Bonen, L., Lewis, B.J., Stahl, D.A., Luehrse, K.R., Chen, K.N., Woese, C.R. (1980) The phylogeny of prokaryotes, Science 209, 457-63.

Fukushima, E., Roeder, S.B. (1981) Experimental Pulse NMR. A Nuts and Bolts Approach, Reading Addison-Wesley Pub. Co. Inc., M.A.

Gally, H.U., Pluschke,G., Overath, P., Seelig, J. (1981) Structure of Escherichia coli membranes. Glycerol auxotrophs as a tool for the analysis of the phospholipid headgroup by deuterium magnetic resonance, Biochemistry 20, 1826-1831.

Ghelis, C., Yon, C. (1982) Protein Folding, Academic Press, New York, NY.

Goodman, R.A., Oldfield, E., Allerbrand, A. (1973) Assignment of the natural abundance C-13 NMR spectrum of chlorophyll a and a study of segmental motion in neat phytol, J. Am. Chem. Soc. 95, 7553-8.

Goni, F.M., Arrondo, J.L.R. (1986) A study of phospholipid phosphate groups in model membranes by Fourier transform IR spectroscopy, Faraday Discuss. Soc. 81, 117-26.

Gorenstein, D.G. (1975) J. Am. Chem. Soc. 97, 898-900.

Gorenstein, D.G., Kar, D. (1975) Biochem. Biophys. Res. Comm. 65, 1073-80.

Gorenstein, D.G. (1984) Phosphorus-31 chemical shifts and spin-spin coupling constants. Principles and emperical observations, in Phosphorus-31 NMR: Principles and Applications, Acad. Press, Inc., NY.

Griffin, R.G. (1981) Solid state nuclear magnetic resonance of lipid bilayers, Meth. Enz. 72, 108-23.

Haines, R. (1983) Anionic lipid headgroups as a proton-conducting pathway along the surface of membranes: A hypothesis, Proc. Nat. Acad. Sci. U.S.A. 80, 160.

Hahn, E.L. (1950) Spin-echoes, Phys. Rev. 80, 580-94.

Hancock, A., Kates, M. (1971) Determination of ionizable acid groups in phosphatidyl glycerophosphate (diphytanyl ether analogue) by proton magnetic resonance spectroscopy, Biochim. Biophys. Acta 248, 254-62.

Hauser, A., Phillips, M.C. (1974) Prog. Surf. Membr. Sci 14, 297-131.

Hauser, H., Pascher, I., Pearson, R.H., Sundell, S. (1981) Preferred conformation and molecular packing of PE and PC, Biochim. Biophys. Acta 650, 21-51.

Henderson, R., Unwin, P.N.T. (1975) Three-dimensional model of purple membrane abtained by electron microscopy, Nature (London) 257, 28-32.

Henderson, R. (1975) The structure of the purple membrane from H. halobium: Analysis of the X-ray diffraction pattern, J. Mol. Biol. 93, 123-38.

Henderson, R., Jubb, J.S., Whytock S. (1978) Specific labelling of the proteins and lipids on the external surface of purple membrane, J. Mol. Biol. 123, 259-74.

Hessel, C.W., Morton, I.D., Todd, A.R., Verkada, P.E. (1954) Phosphatidic acid and derivatives. IV. synthesis of α-glycerophosphatidic acids starting from glycerol α-iodohyride, Rec. Traiv. Chim. 73, 105-6.

Hiraki, K., Hamanaka, T., Mitsui, T., Kito, Y. (1981) Phase transition of the purple membrane and the brown membrane. X-ray diffraction, circular dichroism spectrum and absorption spectrum studies, Biochim. Biophys. Acta 647, 18-28.

Hitchcock, P.B., Mason, R., Thomas, K.M., Shipley, G.G. (1974) Structural chemistry of 1,2-dilauroyl-D,L-phosphatidylethanolamine: molecular conformation and intramolecular packing of phospholpids, Proc. Natl. Acad. Sci. USA 71, 3036-40.

Jackson, M.B., Sturtevant, J.M. (1978) Phase behavior of lipids from H. halobium, Biochemistry 17, 4470-4.

Jain, M.K. (1975) Curr. Topics Membr. Transp. 6,1.

Jarrell, H.C., Tulloch, A.P.,Smith, I.C.P. (1983) Relative roles of cyclopropyl-containing and cis-unsaturated fatty acids in determining membrane properties of Acholeplasma laidlawii: A deuterium NMR study, Biochem 22, 5611-19.

Jarrell, H.C., Giziewicz, J.B., Smith, I.C.P. (1986) Structure and dynamics of a glyceroglycolipid: A ^{2}H NMR study of headgroup orientation, ordering and effect of lipid aggregate structure, Biochemistry 25, 3950-7.

Jendrasiak, G.L., Hasty, J.H. (1974) The hydration of phospholipids, Biochim. Biophys. Acta 337, 79-85.

Joo, C.N., Kates, M. (1969) Synthesis of the naturally occuring phytanyl diether analogs of PGP and PG, Biochim. Biophys. Acta 176, 278-97.

Kanemasa, Y., Yoshioka, T., Hayashi, H. (1972) Alteration of the phospholipid composition of S. aureus cultered in medium containing NaCl, Biochim. Biophys. Acta 280, 444-50.

Kates, M. (1978) The phytanyl ether-linked polar lipids and isoprenoid neutral lipids of extreme halophilic bacteria, Prog. Chem. Fats Other Lipids 15, 301-8.

Kates, M. (1986a) Influence of salt concentrations on membrane lipids of Halophilic bacteria, Eur. Fed. Micro. Review, in press.

Kates, M. (1986b) Techniques of lipidology, 2nd edition (Burdon, R.H., van Knippenberg, P.H., eds), Elsevier, N.Y.

Kates, M., Chan, T.H., Stanacev, N.Z. (1963) Aliphatic diether analogs of glyceride-derived lipids. I. Synthesis of C-, β-dialkylglycerol ethers, Biochemistry 2, 394-7.

Kates, M., Palameta, B., Yengoyan, L.S. (1965a) Aliphatic diether analogs of glyceride-derived lipids. I. Synthesis of naturally occuring L-3-di-O-3',7',11',16-tetramethylhexadecyl-glycerol and its D isomer, Biochemistry 4, 1595-99.

Kates, M., Yengoyan, L.S., Sastry, P.S. (1965b) A diether analogue of phosphatidyl glycerophosphate, Biochim. Biophys. Acta 98, 252-68.

Kates, M., Park, C.E., Palameta, B., Joo, C.N. (1971) Synthesis of diphytanyl ether analog of PA and cytidine diphosphate diglycerol, Can. J. Biochem. 49, 275-81.

Kates, M., Kushwaha, S.C., Sprott, G.C. (1982) Lipids of purple membrane from extreme halophiles and of methanogenic bacteria, Meth. Enz. 88: 98-111.

King, G.I., Schoenborn, B.P. (1982) Neutron scattering of bacteriorhodopsin, Meth. Enz. 88, 241-78.

Kushwaha, S.C., Kates, M., Martin, W.G. (1975) Characterization and composition of the purple membrane and red membrane from Halobacterium cutirubrum, Can. J. Biochem. 53, 284-92.

Lanyi, J.K. (1974) Irregular bilayer structure in vesicles prepared from H. cutirubrum lipids, Biochim. Biophys. Acta 356, 245-56.

Lanyi, J.K., Plachy, W.A., Kates, M (1974), Lipid interaction in membrane of extreme halophilic bacteria. II. Modification of the bilayer structure by squalene, Biochemistry 13, 4914-20.

Letcher, J.H., Van Waxer, J.R. (1967) Top. Phosphorus Chem. 5, 175-266.

Lindsey, H., Peterson, N.O., Chan, S.I. (1979) Physicochemical characterization of 1,2-diphytanoyl-sn-glycero-3-phosphocholine in model membrane systems, Biochim. Biophys. Acta 555, 147-67.

Lowry, O.H., Rosenbrough, N.J., Farr, A.L., Randall, R.J. (1951) J. Mol. Biol 193, 265.

Malthaner, M., Seelig, J., Johnston, N.C., Goldfine, H. (1985) Glycerol acetals of plasmalogens of Clostridium butyricum and beijerinkii, Biochemistry 26, 5826-33.

McLaughlin, A.C., Cullis, P.R., Hemminga, M.A., Hoult, D.I., Radda, G.A., SEeley, P.J., Richards, R.E. (1975) Application of ^{31}P NMR to model and biological membrane systems, FEBS Lettr. 57, 213-8.

Mehlhorn, R.J., Probst, I. (1982) Light induced pH gradients measured with spin-labeled amine and carboxylic probes: Application to H. halobium cell envelope vesicles, Meth. Enz. 88, 334-49.

Michaelson, D.M.,Horwitz, A.F., Klein, M.P. (1974) Headgroup modulation of membrane fluidity in sonicated phospholipid dispersions, Biochem 14, 2605-12.

Milburn, M.P., Jeffrey, K.R., Dynamics of the phosphate group in phospholipid bilayers. A ^{31}P NMR relaxation time study, submitted.

Morris, G.A., Freeman, P. (1978) Selective excitation in FT NMR, J. Mag. Res 29, 433-62.

Nagle, J.F. (1975) J. Membr. Biol. 27, 233-50.

Ogilvie, K.K., Beaucage, S.L., Theriault, N., Entwistle, D.W. (1977) A general transesterification method for the synthesis of mixed trialkylphosphates, J. Am. Chem. Soc. 99, 1277-8.

Pake, G.E. (1948) Nuclear resonance absorption in hydrated crystals: Fine structure of the proton line, J. Chem. Phys. 16, 327-36.

Papahadjopoulos, D., Weiss, L. (1969) Amino groups at the surfaces of phospholipid vesicles, Biochim. Biophys. Acta 183, 417-26.

Parker, F.S., Applications of Infrared, Raman and Resonance Raman Spectroscopy in Biochemistry, Chapter 11, pages 421-79, Plenum Press, NY, 1983.

Pearson, R.H., Pascher, I (1977) The molecular structure of lecithin dihydrate, Nature 281, 499-501.

Peterson, N.O., Chan, S.I. (1977) More on the motional state of lipid bilayer membrane: Interpretation of order parameters obtained from NMR experiments, Biochemistry 16, 2657-66.

Phillips, M.C., Finer, E.G., Hause, H. (1972) Differences between conformations of lecithin and phosphatidylethanolamine polar groups and their effects on interactions of phospholipid bilayer membranes, Biochim. Biophys. Acta 290, 397.

Plachy, W.Z., Lanyi, J.K., Kates, M. (1974) Lipid interactions in membranes of extreme halophilic bacteria. I. Electron spin resonance and diatometric studies of bilayer structure, Biochemistry 13, 4906-13.

Rance, M., Jeffrey, K.R., Tulloch, A.P., Butler, K.W., Smith, I.C.P. (1980) orientational order of unsaturated lpids in the membrane of Acholeplasma laidlawii observed by ^{2}H-NMR, Biochim. Biophys. Acta 600, 245-62.

Rance, M., Byrd, A. (1983) Obtaining high fidelity spin-1/2 powder spectra in anisotropic media: Phase-cycled Hahn-echo spectroscopy, J. Mag. Res. 52,221-40.

Ruocco, M.J., Makriyannis, A., Siminovitch, D.J., Griffin, R.G. (1985) Deuterium NMR investigation of ether- and ester-linked phosphatidylcholine bilayers, Biochemistry 24, 4844-51.

Ruocco, M.J., Atkinson, D., Small, D.M., Skarjune, R.P., Oldfield, E., Shipley, G.G. (1981) X-ray diffraction and colorimetric study of anhydrous and hydrated n-palmitoyl-galactosylsphingosine (cerebroside), Biochemistry 20, 5957-66.

Scheiner, S., Hillenbrand, E.A. (1985) Modification of pK values caused by change in hydrogen bond geometry, Proc. Nat. Acad. Sci. (USA) 82, 2341-5.

Scheraga, H.A. (1963) Intramolecular bonds in protein. II. Non-covalent, in The Proteins, Vol. 1, (ed. H. Neurath), p 478, Academic Press.

Schreier, S., Polnaszek, C.F., Smith, I.C.P. (1978) Spin-labels in membranes. Problems in practice, Biochim. Biophys. Acta 515, 375-436.

Seelig, J. (1977) Deuterium magnetic resonance: Theory and application to lipid membranes, Quart. Rev. Biophys. 10, 353-418.

Seelig, J. (1978) ^{31}P NMR and the head group structure of phospholipids in membrane, Biochim. Biophys. Acta 515, 105-40.

Seelig, J., Seelig, A. (1974) The dynamic structure of fatty acyl chains in a phospholipid bilayer measured by deuterium magnetic resonance, Biochemistry 13, 4839-45.

Seelig, J., Gally, H.U. (1976) Investigation of PE bilayers by deuterium and phosphorus NMR, Biochemistry 19, 5199-5204.

Seelig, J., Seelig, A. (1977) Effect of a single cis-double bond on the structure of a phospholipid bilayer, Biochem 16, 45-50.

Seelig, J., Tamm, L., Hymel. L., Fleisher, S. (1981) Deuterium and phosphorus NMR and fluorescence depolarization studies of functional reconstituted sarcoplasmic reticulum vesicles, Biochemistry 20, 3922-32.

Sen, A., Yang, P.W., Mantsch, H.H., Hui, S.W., Extended hydrogen bonded structures of PE, submitted.

Shaka, A.J., Keeler, J., Freeman, R. (1983) Evaluation of a new broadband decoupling sequence: WALTZ-16, J. Mag. Res. 53, 313-40.

Sherman, W.V., Korenstein, R., Caplan, S.R. (1976) Biochim. Biophys. Acta 430, 454-58.

Singer, S.L., Nicolson, G.L. (1972) The fluid mosaic model of the structure of cell membranes, Science 175, 72-6.

Smallbone, B.S., Chemical and physical studies of polar lipids in extremely halophilic bacteria, Ph D thesis, Univeristy of Ottawa, 1982.

Smith, I.C.P. (1984) Conformational and motional properties of lipids in biological membranes as determined by deuterium magnetic resonance, in "Biomembranes, Vol 12" (Kates., M., Manson, L.A., eds) Plenum Press, N.Y.

Smith, I.C.P., Ekiel, I.H. (1984) Phosphorus-31 NMR of phospholipids in membranes, in "Phosphorus-31 NMR Principles and Application" (Gorenstein, D.G. ed) pp 447-75, Adacemic Press, Inc., Toronto.

Solomon, I. (1958) Phys. Rev. 100, 61.

Sternin, E., Bloom, M., MacKay, A.L. (1983) De-Pake-ing of NMR spectra, J.Mag. Res 55, 274-82.

Stoeckenius, W. (1976) The purple membrane of salt-loving bacteria, Sci. Am. 234, 38-46.

Stoeckenius, W., Bogomolni, R.A., Loxier, R.H. (1975) in "Molecular Aspects of Membrane Phenomena", (Kabach, H.R., Neurath, H., Radda, G.K., Schwyzer, R., Wiley, W.R., eds), page 306, Springer-Verlag, Berlin.

Stoeckenius, W., Lozier, R.H., Bogomolni, R.A. (1979) Bacteriorhodopsin and the purple membrane of Halobacteria, Biochim. Biophys. Acta 505, 215-78.

Stockton, G.W., Johnson, K.G., Butler, K.W., Tulloch, A.P., Boulanger, Y., Smith, I.C.P., Davis, J.H., Bloom, M. (1976) Deuterium NMR study of lipid organization in Acholeplasma laidlawii membranes, Nature 269, 267-8.

Svehla, G. (1976) Comprehensive Analytical Chemistry, Volume VI Analytical Infrared Spectra, Elsevier Sci. Pub. Co., New York, N.Y.

Tanford, C., Wagner, M.L. (1954) . Hydrogen ion equilibria of lysozyme, J. Am. Chem. Soc. 76, 3331-6.

Tattrie, N.H., Bailey, R.A., Kates, M. (1958) The action of pancreatic lipase on steroisomeric triglycerides, Arch. Biochem. Biophys. 78, 319-27.

Taylor, M.G., Smith, I.C.P. (1980) The fidelity of the response by nitroxide spin probes to changes in membrane orgainization. the condensing effect of cholesterol, Biochim. Biophys. Acta 599, 140-9.

Thomas, L.C., Chittenden, R.A. (1964a) Characteristic infrared absorption frequencies of organophosphorus compounds-I. The phosphoryl (P=O) group, Spectrochim. Acta 20: 467-87.

Thomas, L.C., Chittenden, R.A. (1964b) Characteristic infrared absorption frequencies of organophosphorus compounds-II. The P-O-(X) bonds, Spectrochim. Acta 20: 489-502.

Thomas, L.C., Chittenden, R.A. (1970) Characteristic infrared absorption frequencies of organophosphorus compounds-VII. Phosphorus ions, Spectrochim. Acta 26A: 781-800.

Thomas, L.C., Chittenden, R.A. (1970) Infrared absorption bands associated with the POH group, J. Opt. Soc. Am. 52: 829-36.

Träuble, H., Eibl, H. (1974) Electrostatic effects on lipid phase transitions: Membrane structure and ionic environment, Proc. Nat. Acad. Sci 71, 214-9.

Tristam-Nagle, S., Yang, C.P., Nagle, J.F (1986) Thermodynamic studies of PM, Biochim. Biophys. Acta 854, 58-66.

Tulloch, A.P. (1977) Preparation of specifically dideuterated octadecanoates and oxooctadecanoates, Lipids 12, 92-8.

Tulloch, A.P. (1979) Synthesis of deuterated and carbon-13 labelled lipids, Chem. Phys. Lipids 24, 391-406.

Vold, R.L., Waugh, J.S., Klein, M.P., Phelps, D.W. (1968) Measurement of spin-relaxation in complex systems, Chem. Phys 48, 4831-1.

Woese, C.R., Wolfe, R.S. (1985) The Bacteria, Volume 84, The Archaebacteria, Academic Press, Inc., Toronto.

Yang, P.W., Mantsch, H.H., Baudais, F (1986) A critical evaluation of three types of diffuse reflectance infrared accessories, Appl. Spectrosc. 40, 974-9.

Zaccai, G., Buldt, G., Seelig, A., Seelig, J. (1979) Neutron diffraction studies on PC model membranes. II. Chain conformation and segmental disorder, J. Mol. Bio. 134, 693-706.

Appendix A

^{13}C and ^{1}H NMR Spectra

Spectrum Number	Nucleus	Compounds
A1	^{13}C	A. PGP
		B. PG
		C. PA
		D. diphytanylglycerol
A2	^{1}H	A. PGP
		B. PG
A3	^{13}C	A. rac-2,3-[1,1,1',1'-$^{2}H_4$]diphytanyl-glycerol
		B. rac-2,3-diphyanylglycerol-[3,3-$^{2}H_2$]-glycerol
		C. diphytanylglycerol
A4	^{13}C	A. [1,1,1',1'-$^{2}H_4$]DPhPA
		B. [2,3,2',3'-$^{2}H_4$]DPhPA
A5	^{13}C	A. [1,1-$^{2}H_2$]hexadecanol
		B. [2,2-$^{2}H_2$]hexadecanol
A6	^{1}H	A. [1,1-$^{2}H_2$]hexadecanol
		B. [2,2-$^{2}H_2$]hexadecanol
A7	^{13}C	A. [2,2-$^{2}H_2$]DHPA
		B. [1,1-$^{2}H_2$]DHPA
A8	^{1}H	A. [1,1-$^{2}H_2$]DHPA
		B. [2,2-$^{2}H_2$]DHPA

A9	^{13}C	sn-1,2-dipalmitoyl-[1,1-$^{2}H_2$]glycerol + sn-1,3-dipalmitoyl-[1,1-$^{2}H_2$]glycerol
A10	^{13}C	A. sn-1,2-diphytanylglycerol-1-phosphoro-2'-[1,1-$^{2}H_2$]glycerol B. sn-1,2-diphytanylglycerol-1-phosphoro-3'-[1,1-$^{2}H_2$]glycerol
A11	^{1}H	A. PGP B. dPGP
A12	^{1}H	A. PG B. dPG
A13	^{13}C	A. proPG B. dPG C. dPGP
A14	^{13}C	A. $PGP(CH_3)_3$ B. $PGP(CH_3)_4$

Figure A1

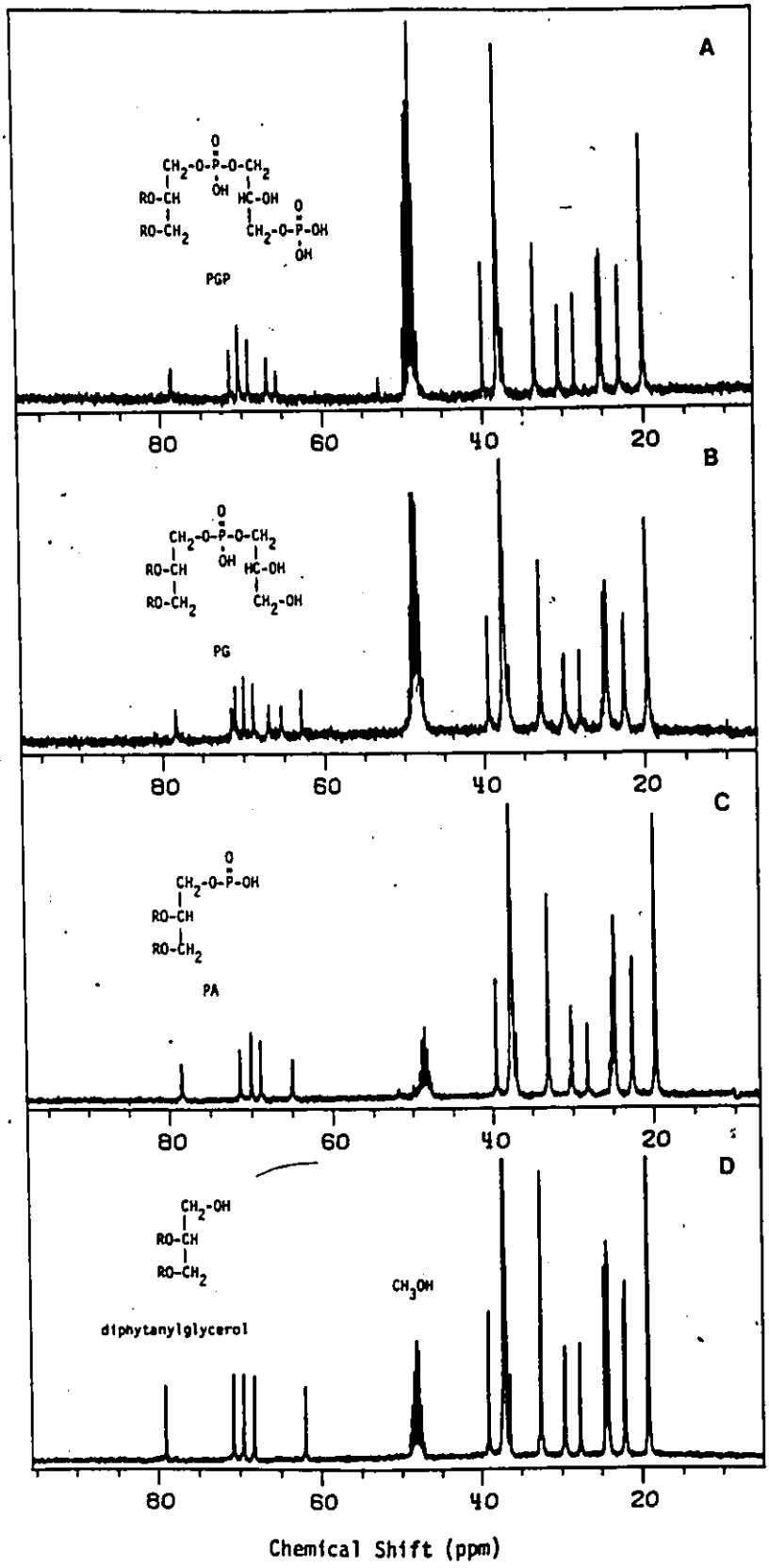
A
PGP
80
60
40
20
B
PG
80
60
40
20
C
PA
80
60
40
20
D
diphytanylglycerol
CH3OH
80
60
40
20
Chemical Shift (ppm)

Figure A2

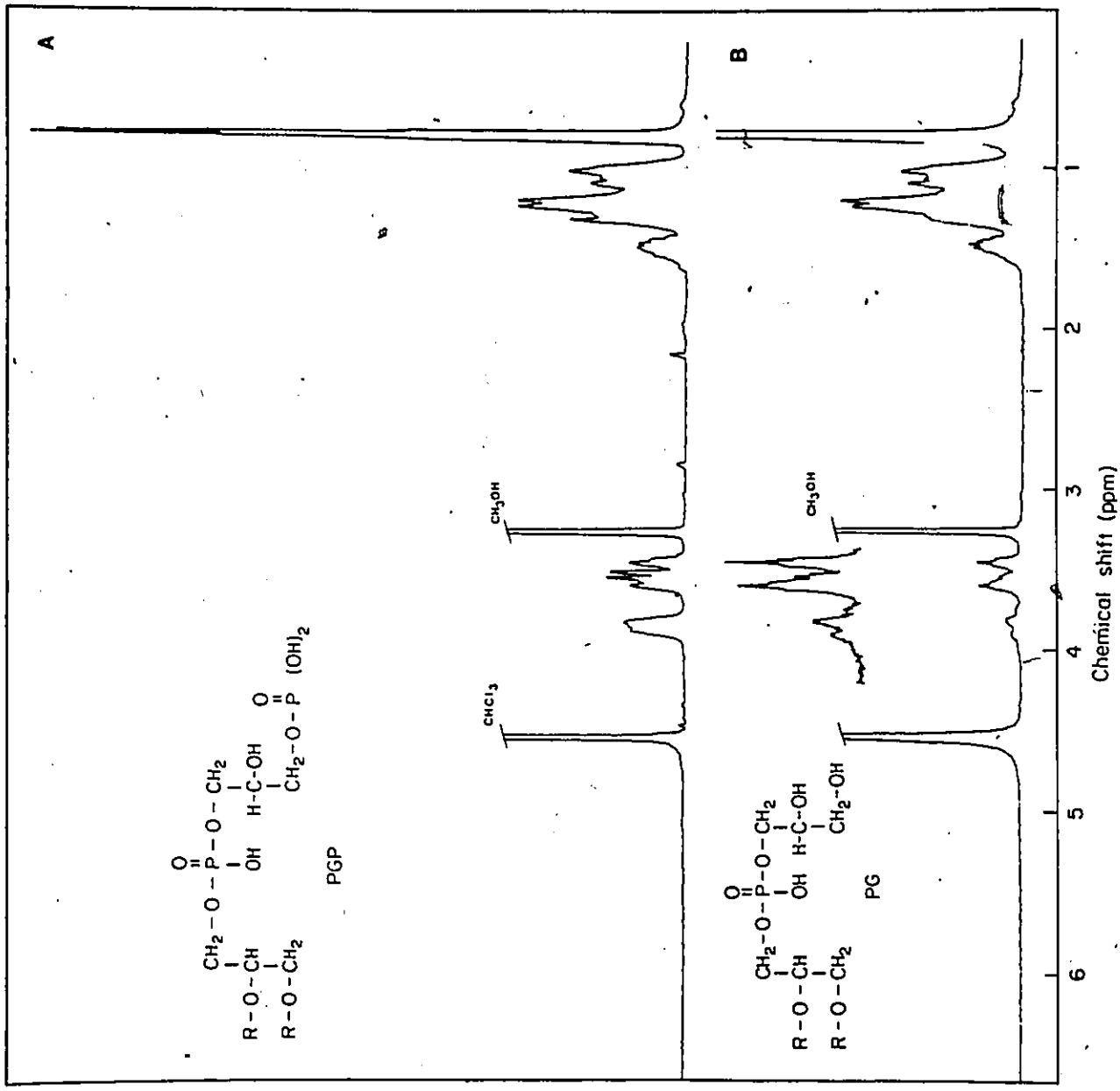

Figure A3

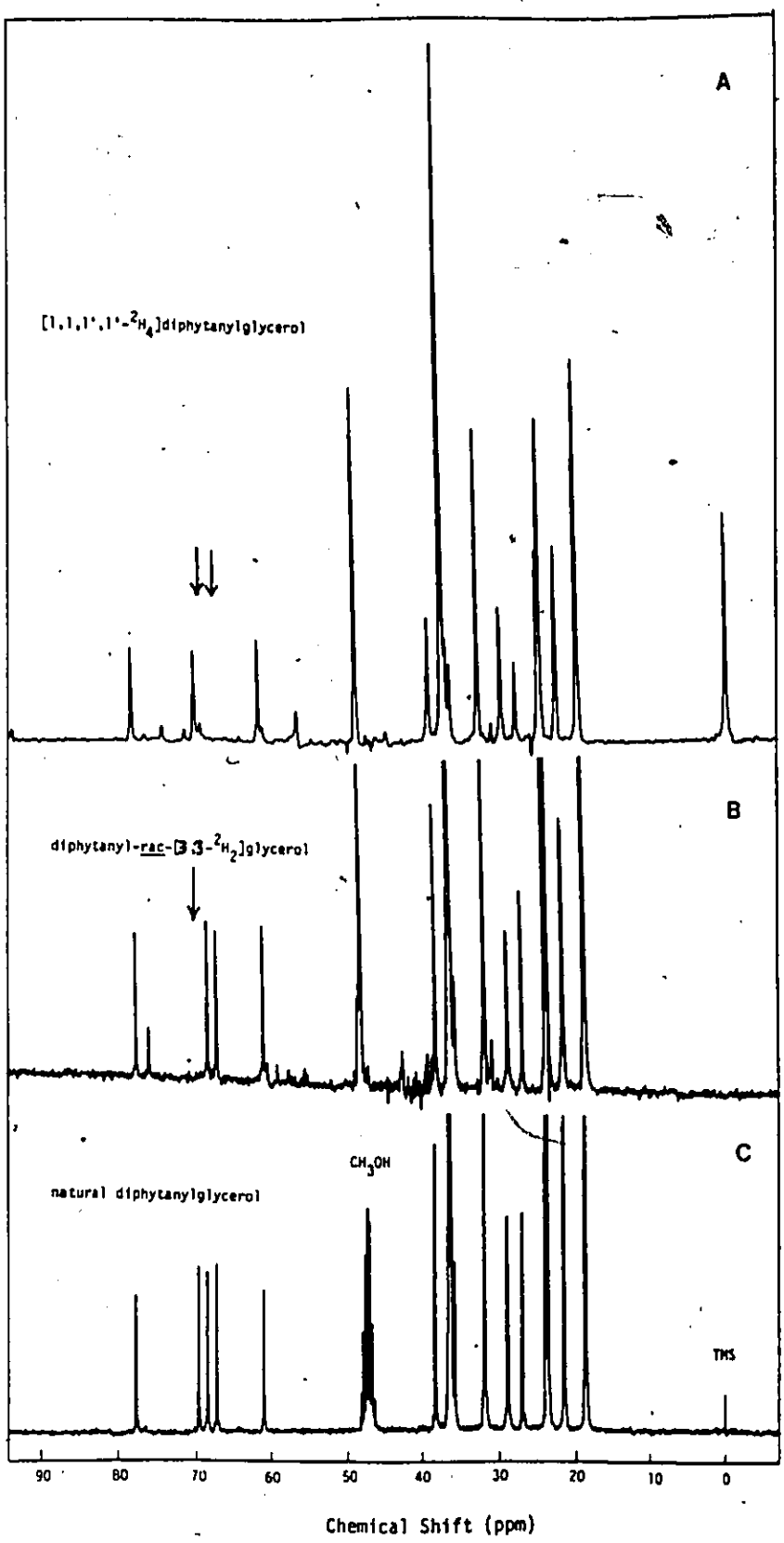
A
[1,1,1',1'-$^2H_4$]diphytanylglycerol
B
diphytanyl-rac-[3,3-$^2H_2$]glycerol
C
CH_3OH
natural diphytanylglycerol
TMS
90
80
70
60
50
40
30
20
10
0
Chemical Shift (ppm)

Figure A4

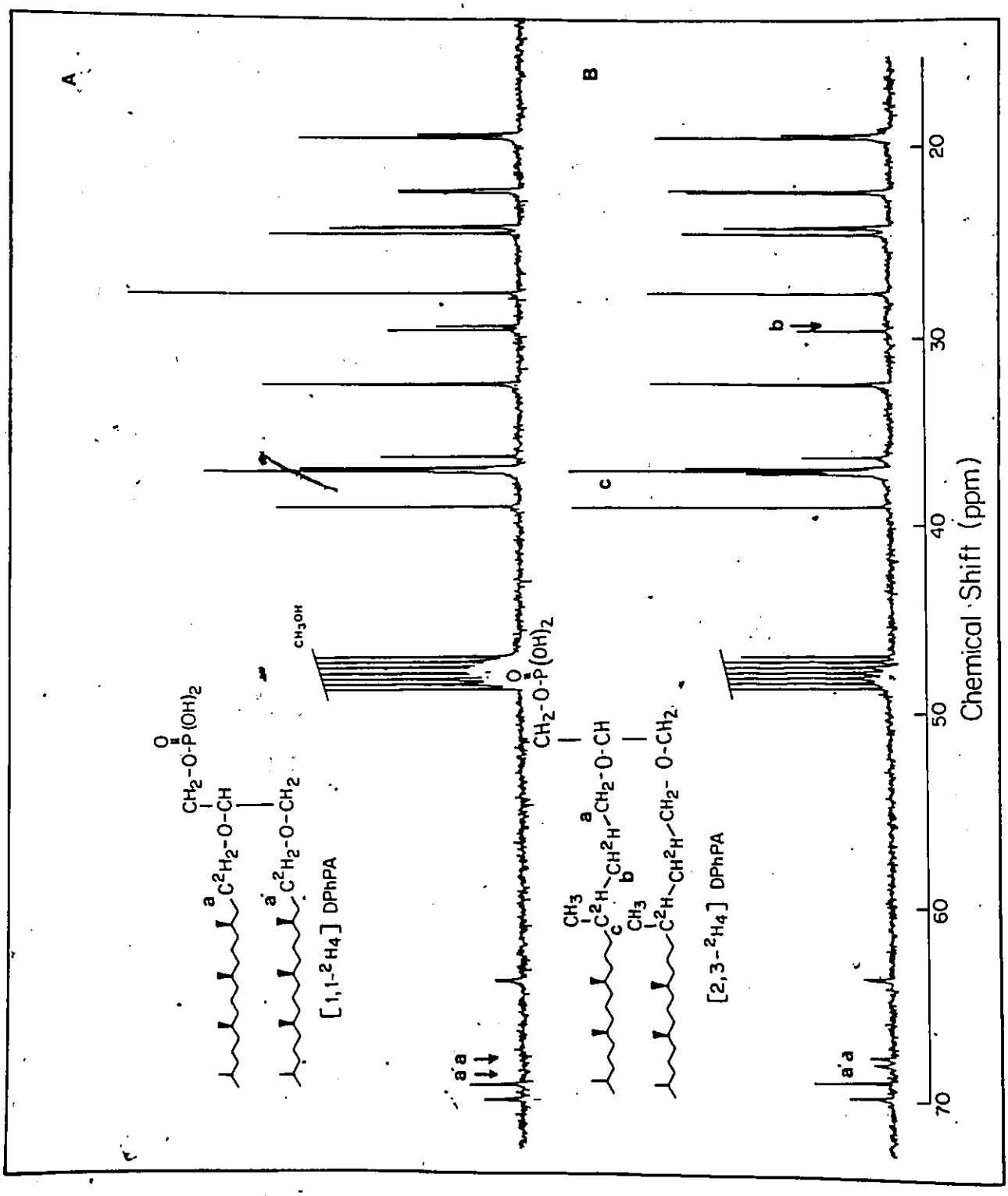
A
B
[1,1-$^2H_4$] DPhPA
[2,3-$^2H_4$] DPhPA
CH_3OH
Chemical Shift (ppm)
20
30
40
50
60
70

Figure A5

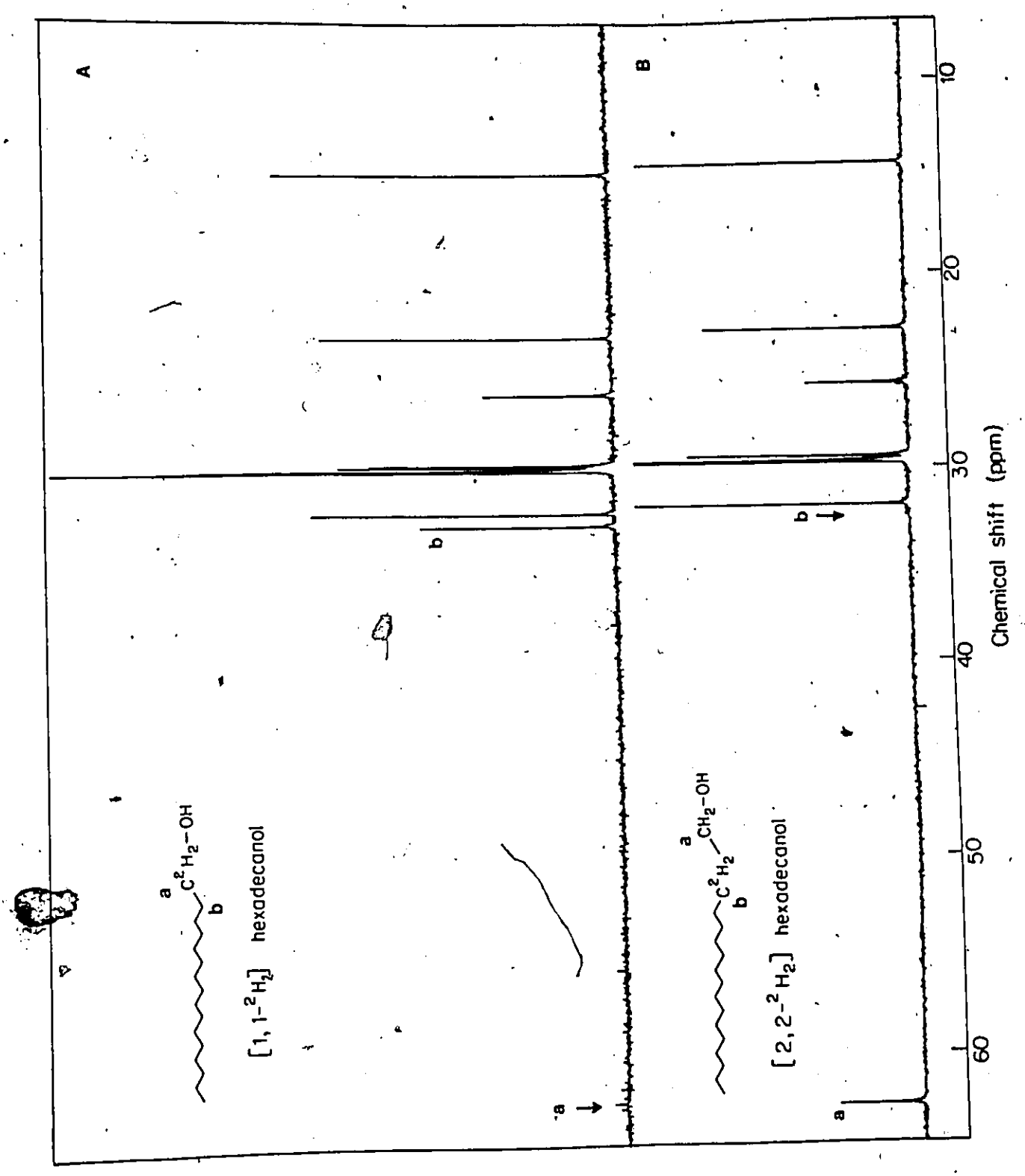
A
B
a
b
C^2H_2—OH
[1, 1-$^2H_2$] hexadecanol
CH_2—OH
[2, 2-$^2H_2$] hexadecanol
10
20
30
40
50
60
Chemical shift (ppm)

Figure A6

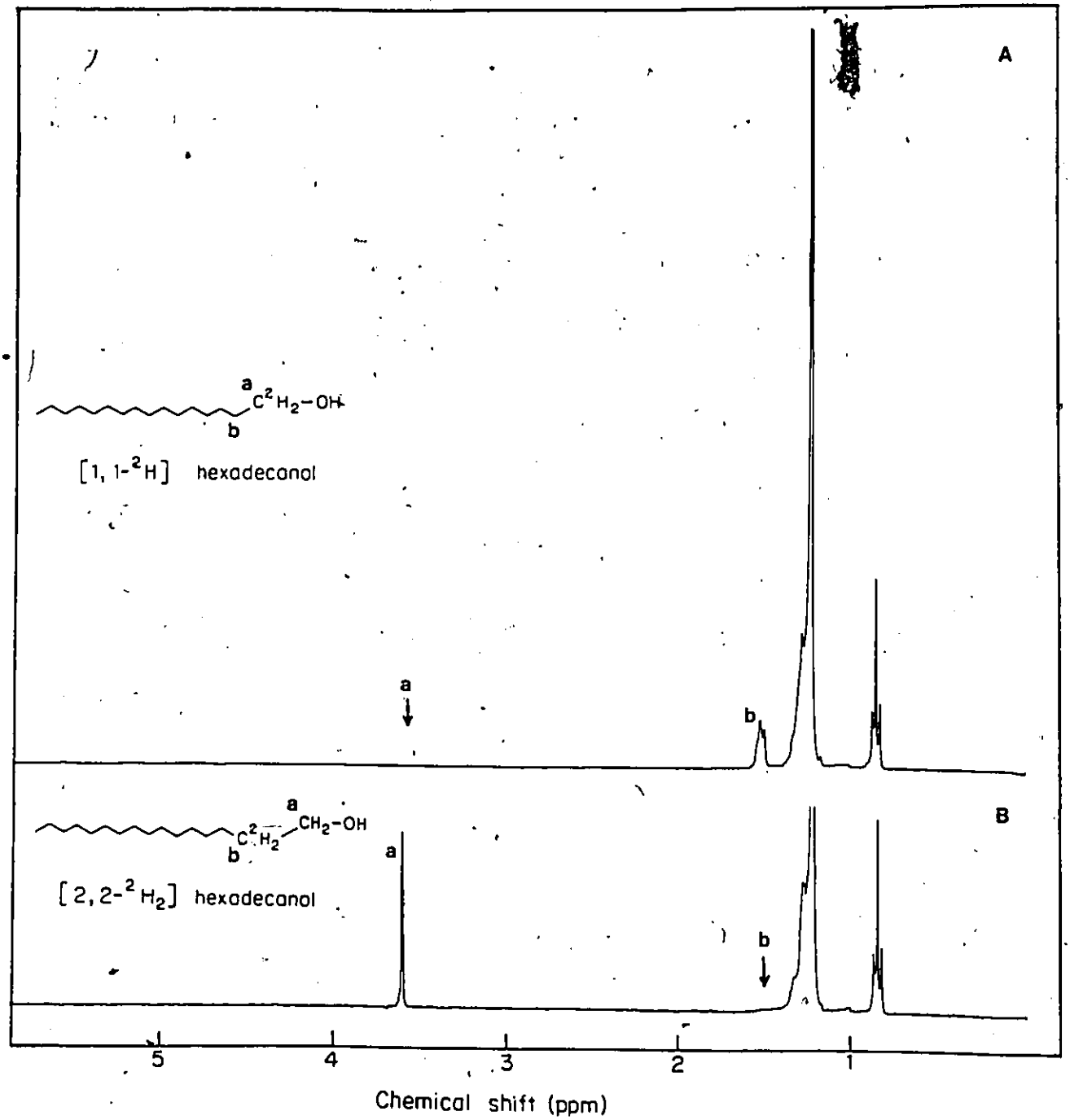
A
a
C^2H_2–OH
b
[1, 1-^{2}H] hexadecanol
a
b
B
a
CH_2–OH
C^2H_2
b
[2, 2-$^2H_2$] hexadecanol
a
b
5
4
3
2
1
Chemical shift (ppm)

Figure A7

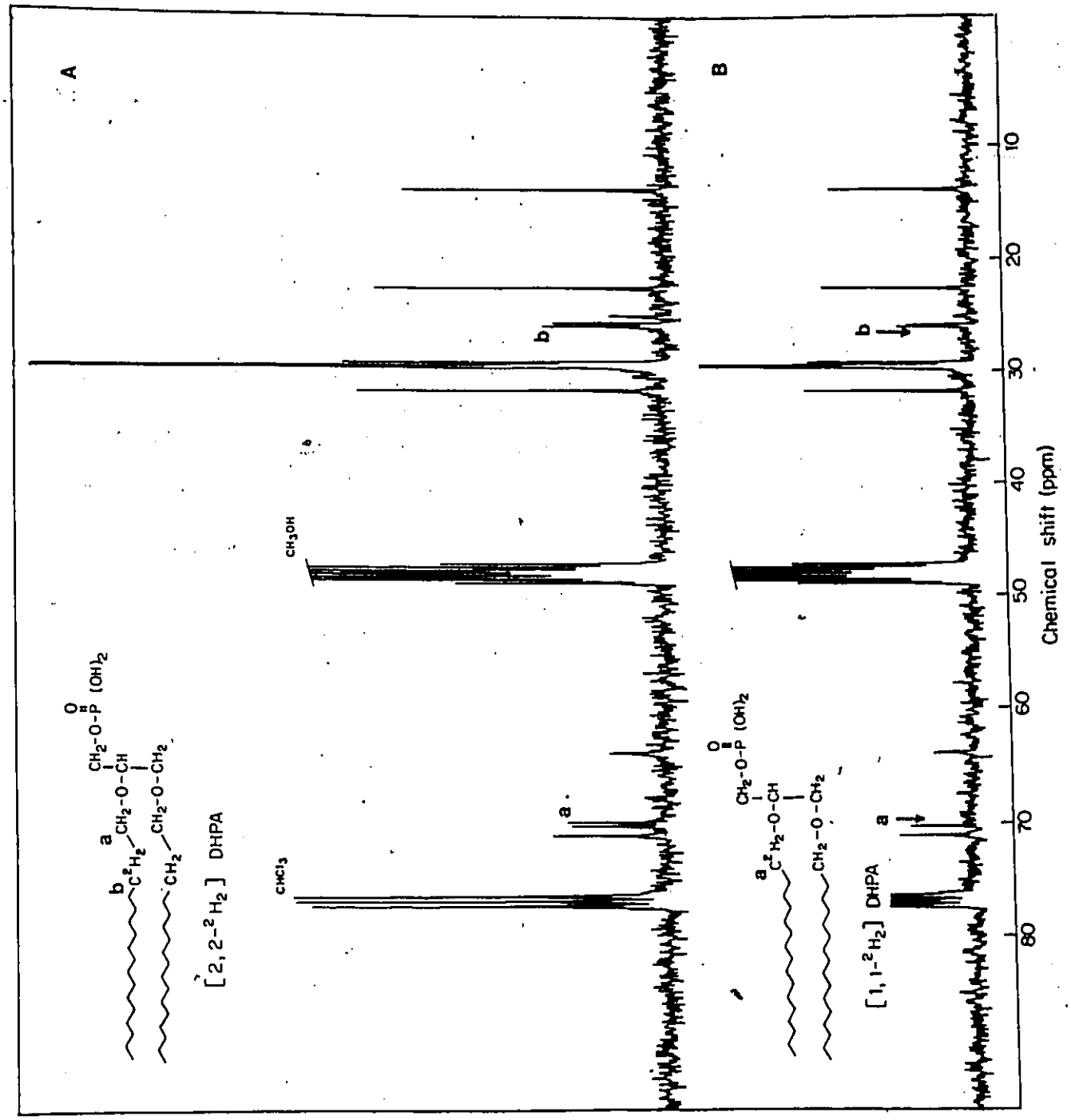
A
B
a
b
CHCl3
CH3OH
[2,2-2H2] DHPA
[1,1-2H2] DHPA
Chemical shift (ppm)
10
20
30
40
50
60
70
80

Figure A8

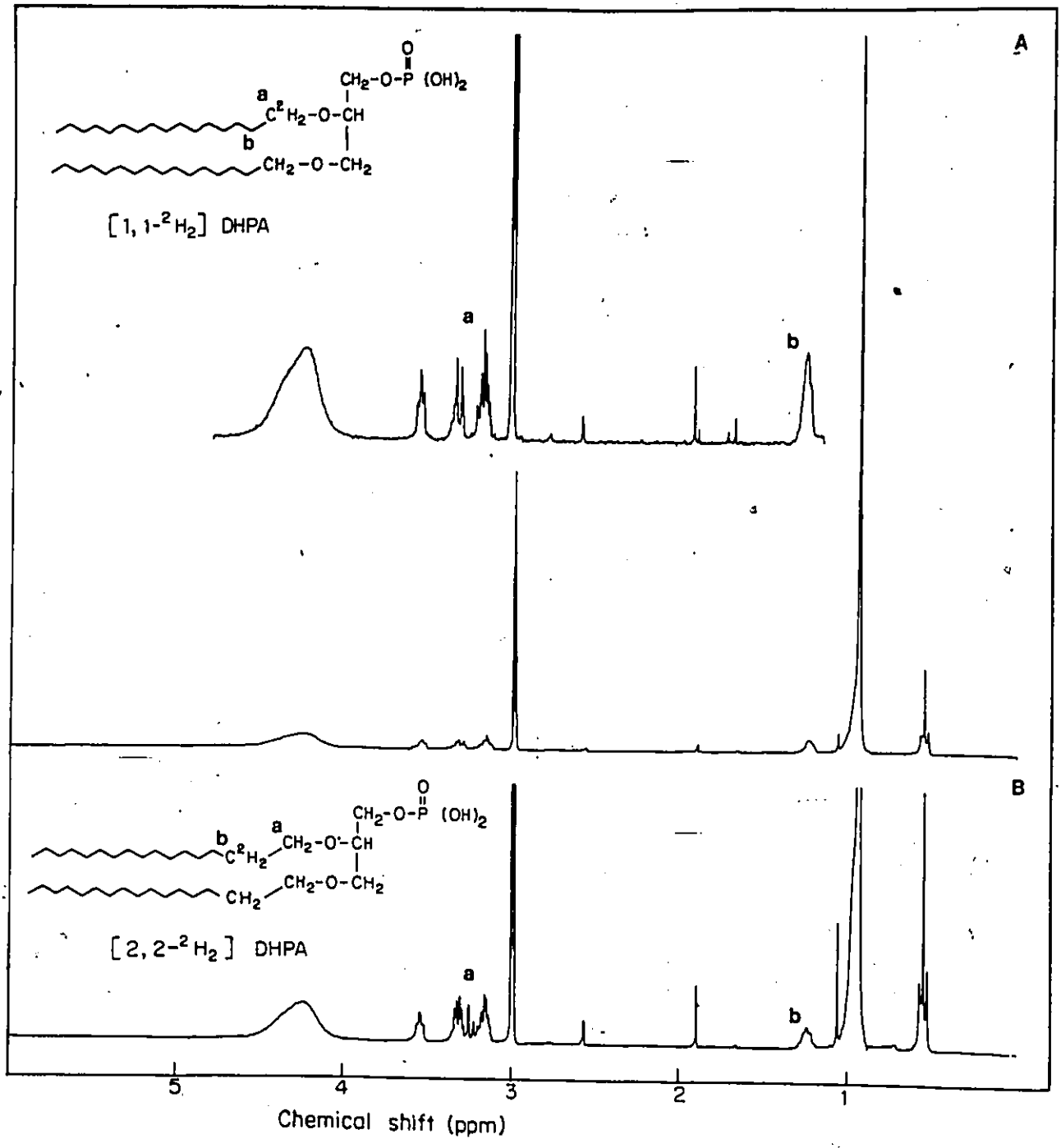

Figure A9

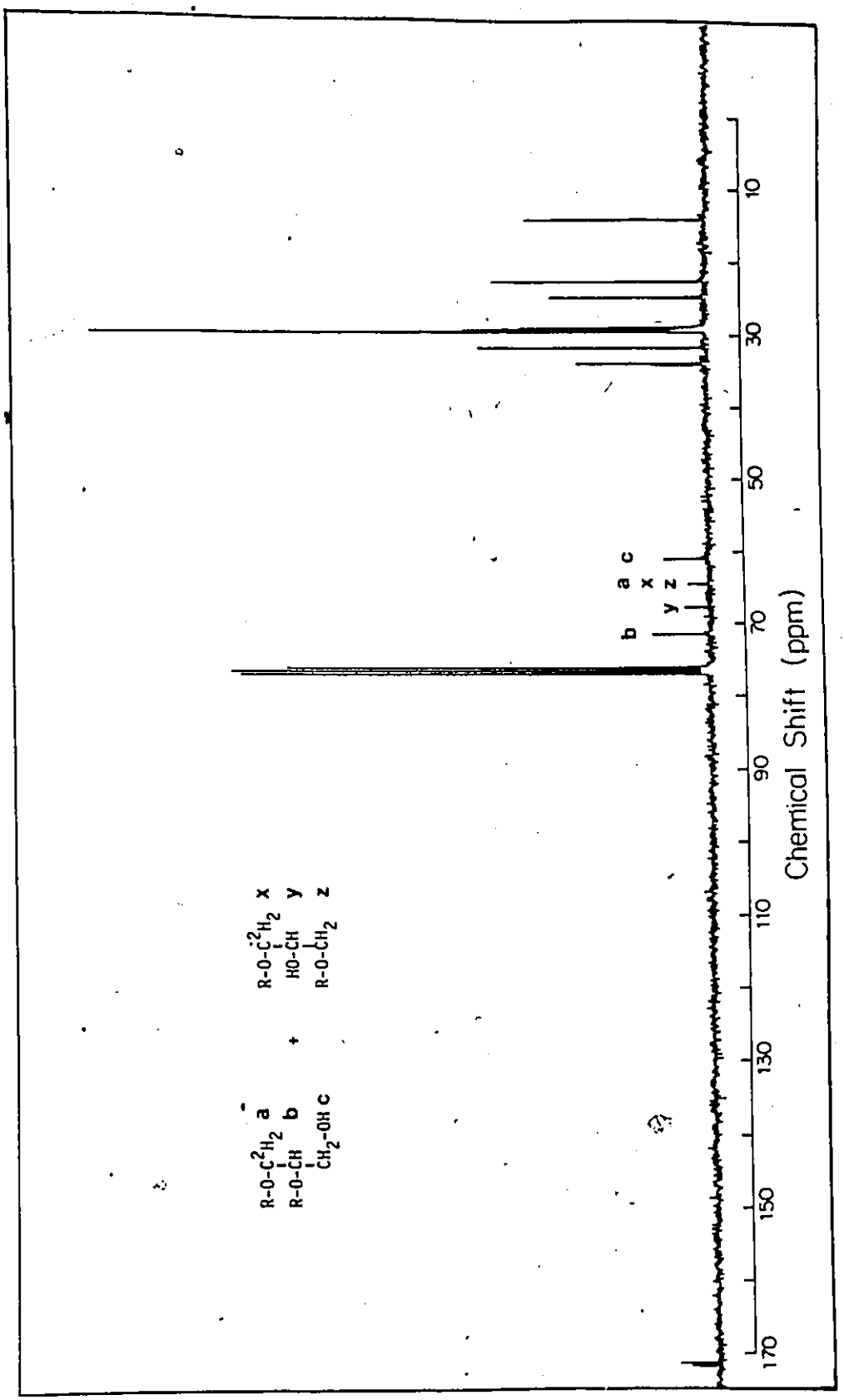
R-O-C²H₂ a
R-O-CH b
CH₂-OH c
+
R-O-C²H₂ x
HO-CH y
R-O-CH₂ z
b a c
x
y z
10
30
50
70
90
110
130
150
170
Chemical Shift (ppm)

Figure A10

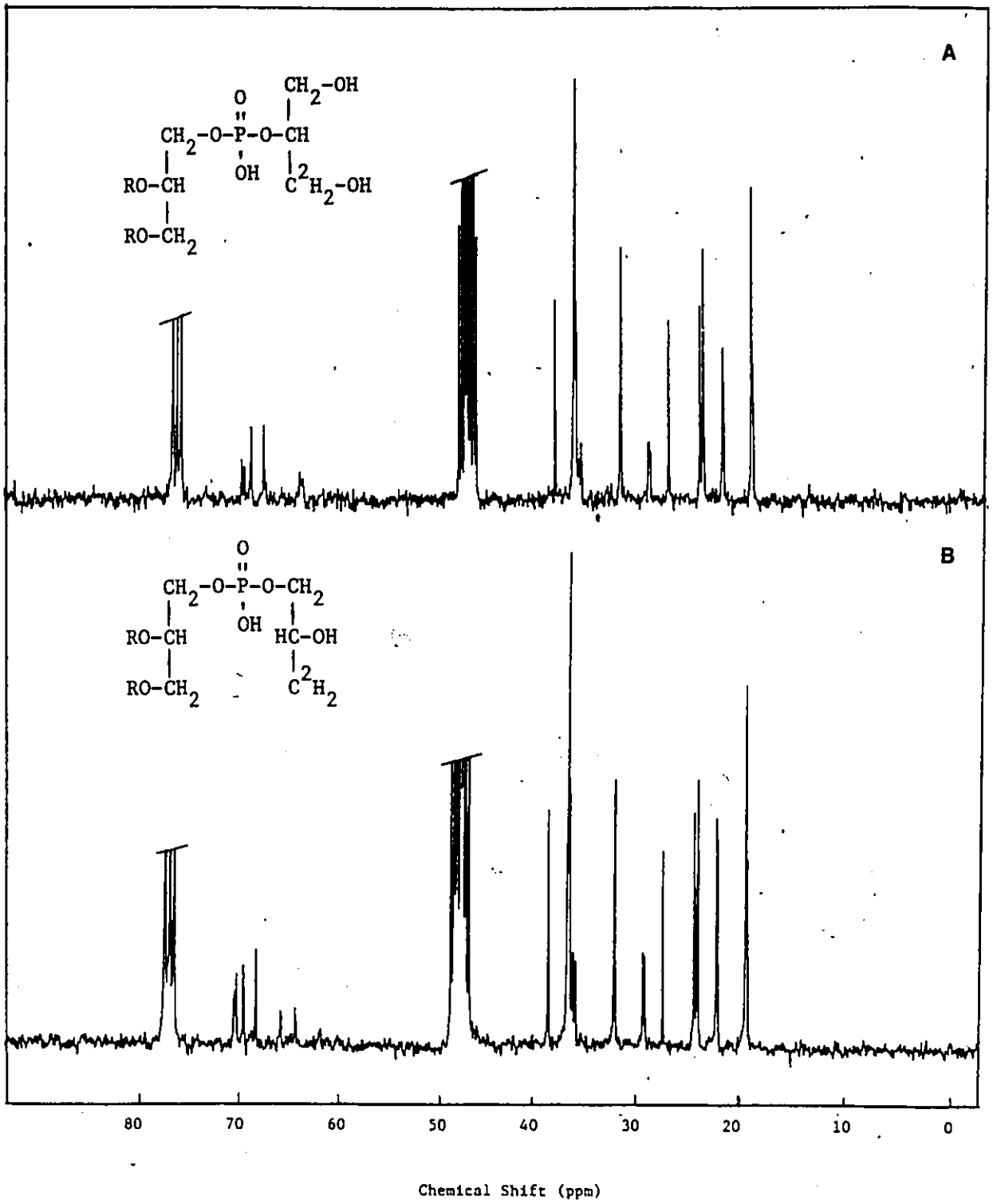

Figure A11

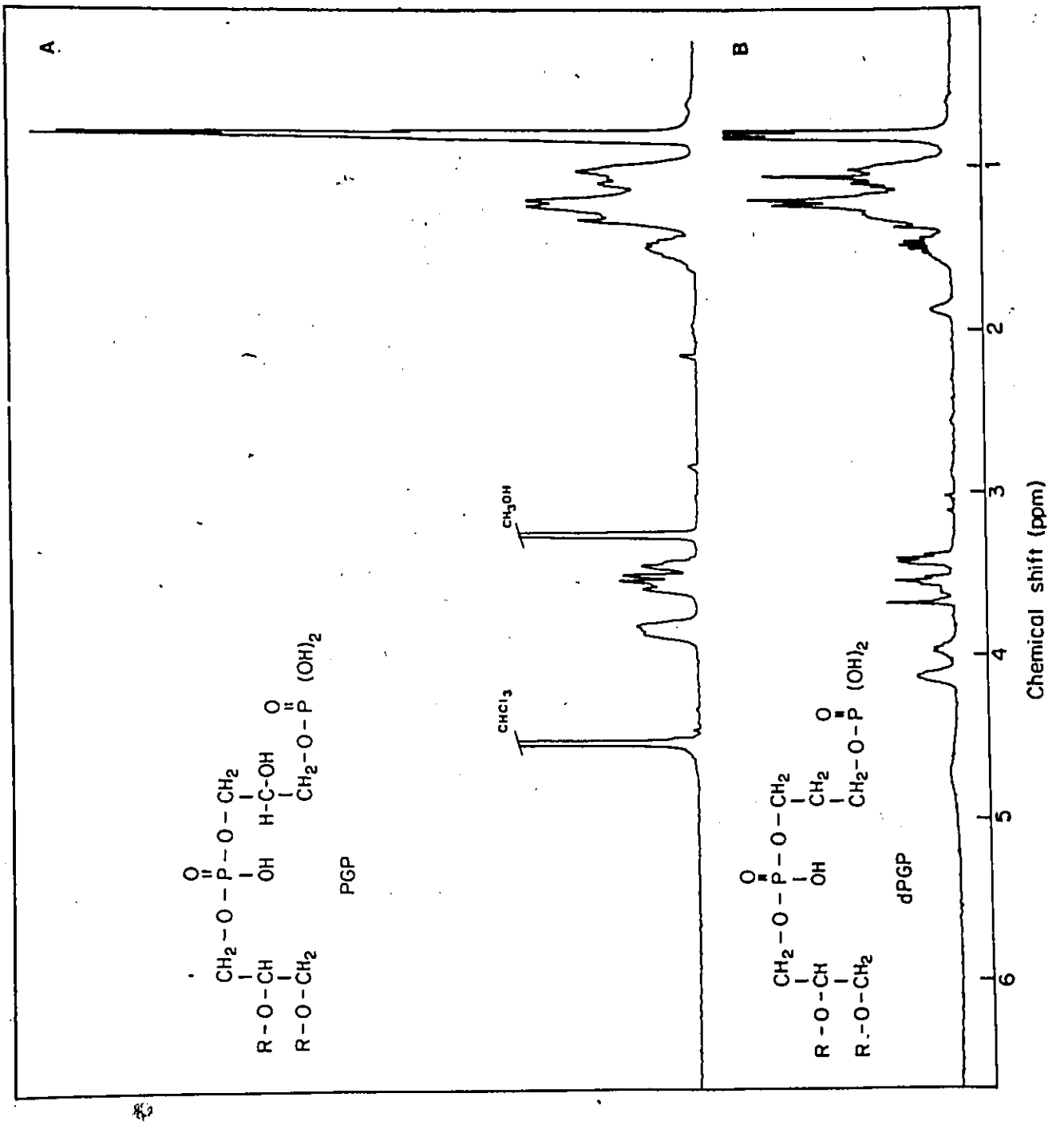

Figure A12

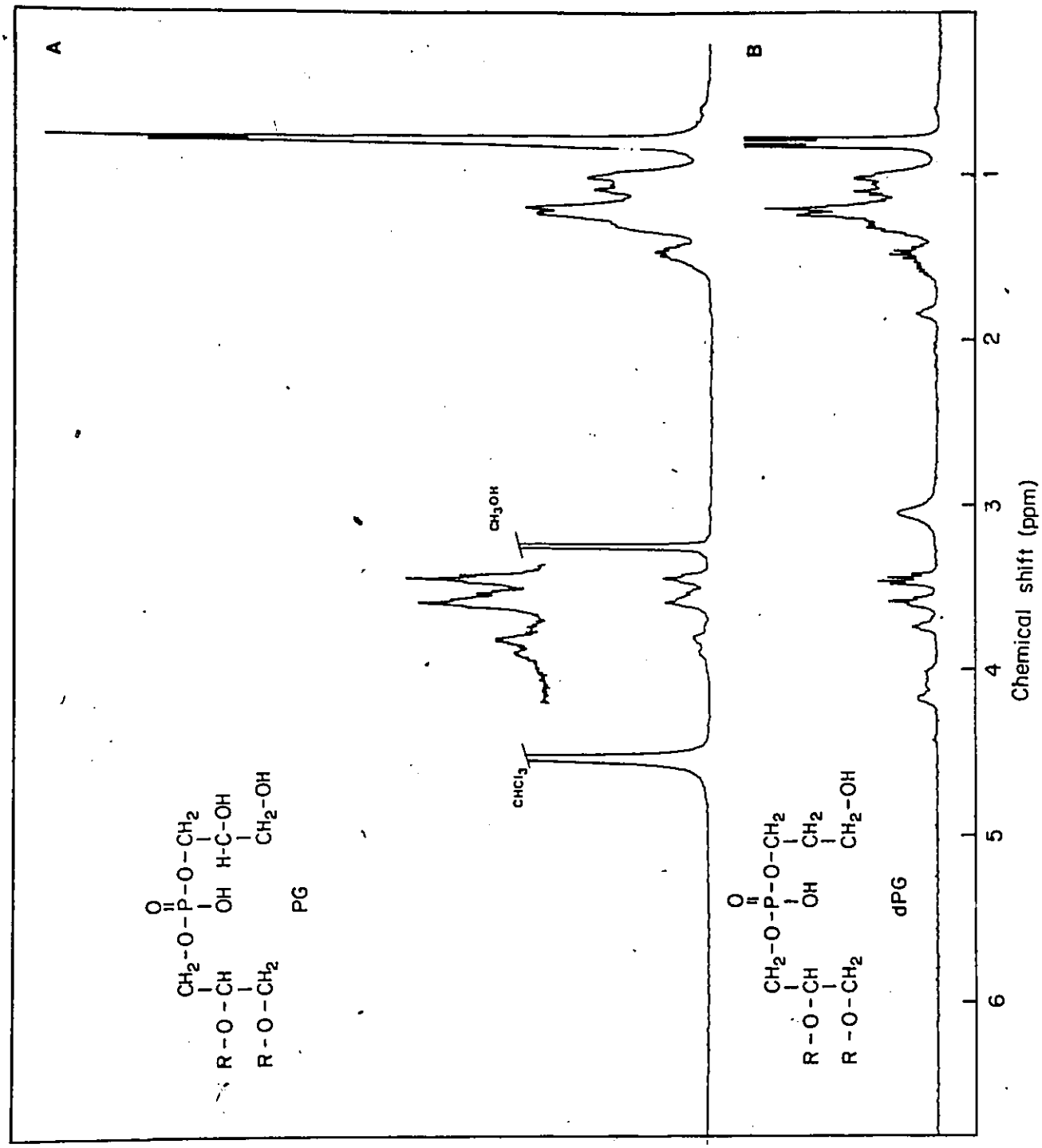

Figure A13

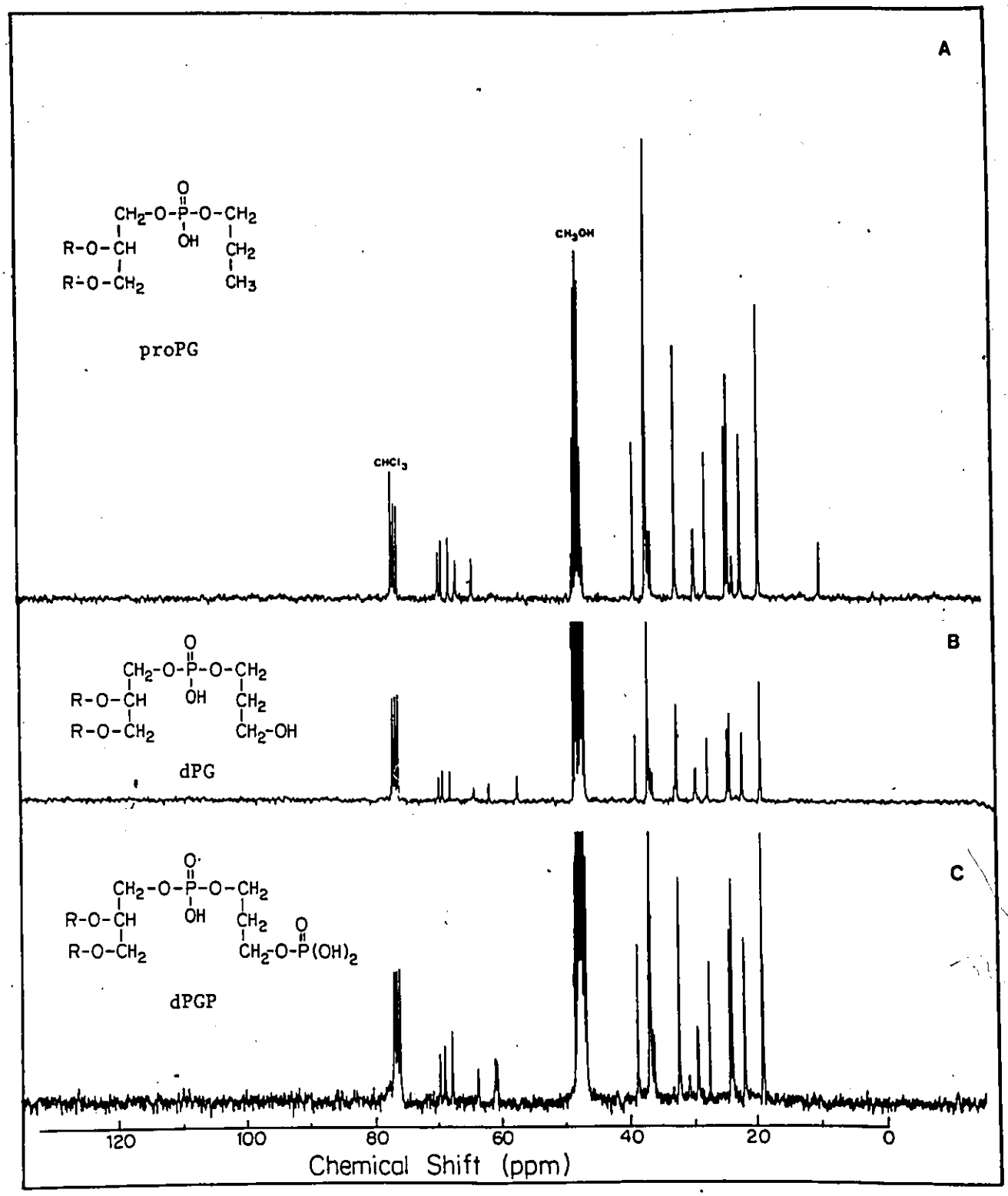
A
B
C
proPG
dPG
dPGP
CHCl3
CH3OH
120
100
80
60
40
20
0
Chemical Shift (ppm)

Figure A14

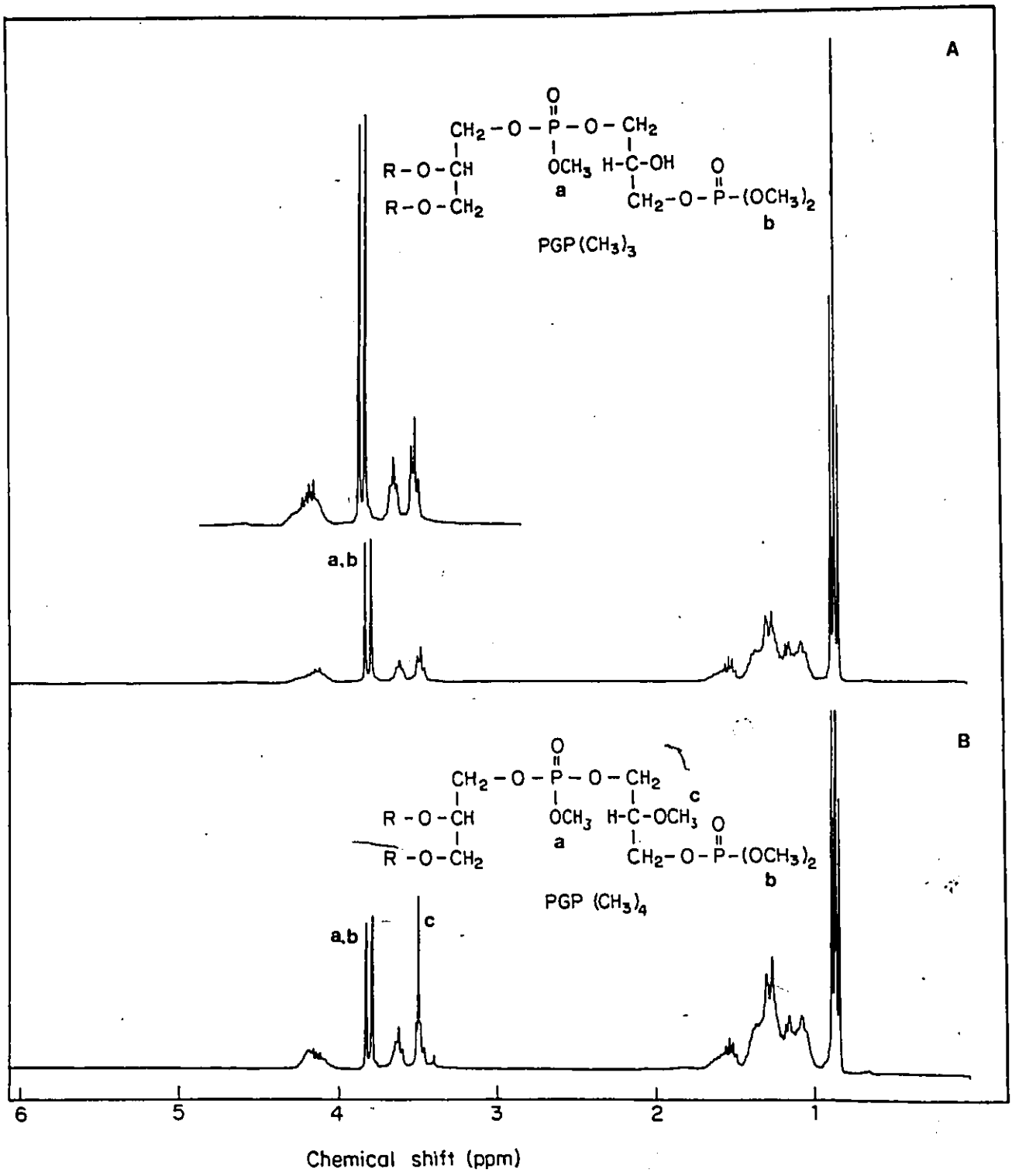

Appendix B

LAURA CHRISTINE STEWART

Department of Biochemistry
University of Ottawa
40 Somerset St. E.,
Ottawa, Canada
K1N 6N5

(613) 564-2958

Division of Biological Sciences
National Research Council
100 Sussex Ave.,
Ottawa, Canada
K1A OR6
(613) 990-0897

EDUCATION

Ph. D. (Biochemistry) University of Ottawa
September 1982 - present
Thesis topic: Physical Studies of Diphytanylglycerol Phospholipids
Supervisors: Dr. Ian C.P. Smith, Division of Biological Sciences, National Research Council of Canada; and, Dr. M. Kates, Department of Biochemistry, University of Ottawa.

B. Sc. (Biochemistry) University of Toronto
September 1979 - May 1982
Thesis topic: Preparation, Purification and Characterization of N-3-(pyrene)maleimide-Conjugated Bovine Pancreatic Ribonuclease
Supervisor: Dr. M.A. Winnik, Department of Chemistry, University of Toronto.

EMPLOYMENT HISTORY

Post-doctoral Fellow

Harvard Medical School NMR Laboratory
November 1987 Cardiac physiology using <u>in vivo</u> NMR techniques

Supervisor: Dr. J.S. Ingwall

Laboratory Demonstrator

University of Ottawa (Department of Biochemistry)
Sept 1982 - present
Supervised Experimental Biochemistry and Physical Biochemistry courses.

Course Coordinator: Dr. H. Kaplan

Laura Stewart

Summer Research Assistant

National Research Council (Chemical Physics)
May - Sept 1981; May - Sept 1982
Laser flash photolysis and ultraviolet/visible spectroscopic studies of photochemical processes in molecules, macromolecules and organized assemblies.

Supervisor: Dr. J.C. Scaiano

AWARDS AND SCHOLARSHIPS

Medical Research Council of Canada Post-doctoral Fellowship, 1987.

Natural Science and Engineering Research Council of Canada Post-doctoral Fellowship, 1987 (declined)

Natural Science and Engineering Research Council of Canada Postgraduate Scholarship, 1984 - 86.

Scholarship awarded by the International Conference of Magnetic Resonance in Biological Systems to defray registration, travel and accomodation expenses, 1986.

CONFERENCES ATTENDED

International Conference on Magnetic Resonance in Biological Systems; Todtmoos, Germany, Sept 1986.

Canadian Federation of Biological Societies, 29th Annual Meeting; Guelph, Canada, June 1986.

Canadian Federation of Biological Societies, 28th Annual Meeting; Toronto, Canada, June 1985.

The Physics of Monolayers, Biolayers and Biological Membranes; Montreal, Canada, June 1983.

MEMBERSHIPS IN SCIENTIFIC ORGANIZATIONS

Canadian Federation of Biological Societies:

Biophysical Society of Canada
Canadian Biochemical Society

Laura Stewart

REFERENCES

Dr. I.C.P. Smith, Director, Division of Biological Sciences, National Research Council of Canada.

Dr. M. Kates, Professor, Department of Biochemistry, University of Ottawa.

Dr. H. Kaplan, Professor, Department of Biochemistry, Univeristy of Ottawa.

Publications (Effective Aug 1987) Laura Christine Stewart

1. Stewart, L.C., Kates, M., Synthesis and Physical Studies of Headgroup Analogues of Diphytanylglycerol Phospholipids, in preparation.

2. Stewart, L.C., Kates, M., Synthesis of Deuterated Dihexadecylglycerol and Diphytanylglycerol Phospholipids, in preparation.

3. Stewart, L.C., Ekiel, I.H., Kates, M., Smith, I.C.P., ^{2}H NMR Study of Synthetically and Biosynthetically Deuterated Dihexadecylglycerol and Diphytanylglycerol Lipids, in preparation.

4. Stewart, L.C., Yang, P, Mantsch, H.H., Evidense for Intra- and Intermolecular Hydrogen Bonding in Diphytanylglycerol Phospholipids: An Infrared Spectroscopic Investigation, in preparation.

5. Bittman, R., Stewart, L.C., Kates, M., Osmometric Studies of Liposomes Prepared from Diphytanylglycerol Lipids, in preparation.

6. Neckers, D.C., Sindler-Kulyk, M., Scaiano, J.C., Stewart, L.C., Weir, D., Excited State Properties of 2-Phenylbenzthiazole and 3-Phenyl-1,2-Benzisothiazole, in press.

7. Yang, P.W., Stewart, L.C., Mantsch, H.H., Polarized Attenuated Total Reflectance Spectra of Oriented Purple Membrane, Biochem. Biophys. Res. Comm. 145, 298-302 (1987).

8. Quinn. P.J., Brain, A.P.R., Stewart, L.C., Kates, M., The structure of membrane lipids of the extreme halophile, H. cutirubrum, in aqueous systems: A freeze fracture study, Biochim. Biophys. Acta 863: 213-220 (1986).

9. Scaiano, J.C., Stewart, L.C., Livant, P., Majors, A.W., Transient Spectroscopy and Kinetics of the Reactions of Mesocyclic Diamines with tert-Butoxyl and with Ketone Triplets. Effects of Ring Conformation, Can. J. Chem. 62: 1339-43 (1984).

10. Scaiano, J.C., Lissi, E.A., Stewart, L.C., Quenching of Triplet Macromolecules. The Role of Energy Migration, J. Am. Chem. Soc. 106: 1539-45 (1984).

11. Scaiano, J.C., Encinas, M.V., Lissi, E.A., Stewart, L.C., Photochemistry of Alkyl Esters of Benzoyl Formic Acid, Can. J. Chem. 62: 386-91 (1984).

Publications (Continued) Laura Christine Stewart

12. Baignee, A., Howard, J.A. Scaiano, J.C., Stewart, L.C., Absolute Rate Constants for Reactions of Cumyloxyl in Solution, J. Am. Chem. Soc. 105: 6120-3 (1983).

13. Scaiano, J.C., Stewart, L.C., Phenyl Radical Kinetics, J. Am. Chem. Soc. 105: 3609-13 (1983).

14. Stewart, L.C., Carlsson, D.J., Wiles, D.M., Scaiano, J.C., Triplet Quenching by tert-Butyl Hydroperoxide, J. Am. Chem. Soc. 105: 3605-09 (1983).

15. Scaiano, J.C., Abuin, E.B., Stewart, L.C., Photochemistry of Benzophenone in Micelles. Formation and Decay of Radical Pairs, J. Am. Chem. Soc. 104: 5673-8 (1982).

16. Mendenhall, G.C., Stewart, L.C., Scaiano, J.C., Laser Photolysis Study of the Reactions of Alkoxyl Radicals Generated in the Photosensitized Decomposition of Organic Hyponitrites, J. Am. Chem. Soc. 104: 5109-14 (1982).

17. Scaiano, J.C., Stewart, L.C., The Triplet Lifetime of Poly(Phenyl vinyl ketone). A Laser Flash Photolysis Study, Polymer 23: 913-6 (1982).